ACTIVIDAD DEL SISTEMA NORADRENERGICO- LOCUS COERULEUS EN EL DOLOR NEUROPATICO A LO LARGO DEL TIEMPO

Tesis Doctoral

María del Carmen Camarena Delgado

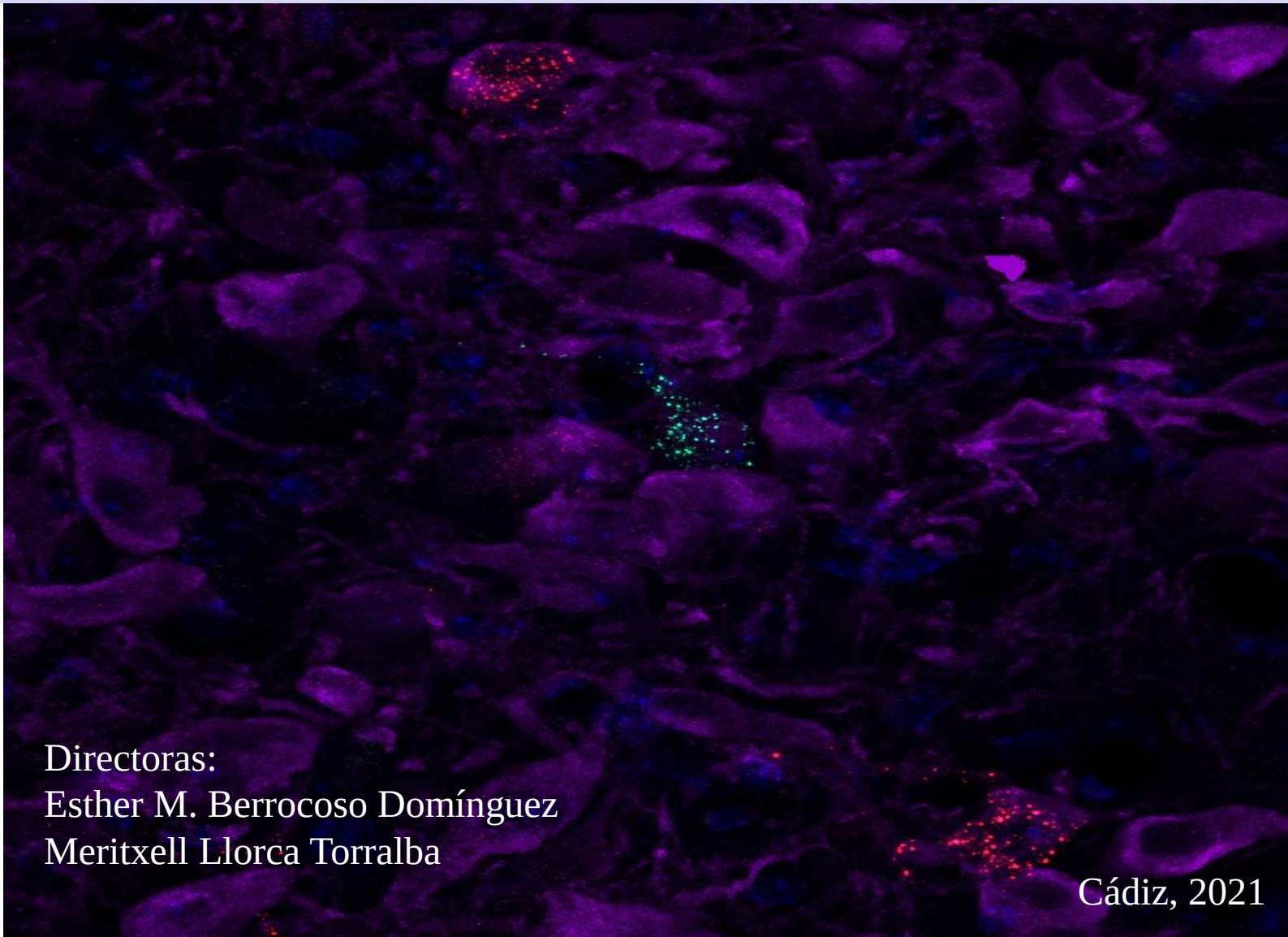

Directoras:
Esther M. Berrocoso Domínguez
Meritxell Llorca Torralba

Cádiz, 2021

ACTIVIDAD DEL SISTEMA NORADRENERGICO- LOCUS COERULEUS EN EL DOLOR NEUROPATICO A LO LARGO DEL TIEMPO

Tesis Doctoral presentada por

María del Carmen Camarena Delgado

Universidad de Cádiz, 2021

Esta Tesis Doctoral, titulada "Actividad del Sistema noradrenérgico-Locus Coeruleus en el dolor neuropático a lo largo del tiempo", se presenta como Compendio de Publicaciones, y cumple con todos los requisitos emitidos por el artículo 23 del reglamento UCA/CG06/2012, de 27 de junio de 2012, sobre la organización de los estudios de doctorado en la Universidad de Cádiz.

La Tesis Doctoral está compuesta por las siguientes publicaciones académicas:

ESTUDIO I: Nerve injury induces transient locus coeruleus activation over time: role of the locus coeruleus–dorsal reticular nucleus pathway

ESTUDIO II: Pain and depression comorbidity causes asymmetric plasticity in the locus coeruleus neurons

De acuerdo con la misma normativa, ambos trabajos originales se incluyen en el presente documento, en la sección de resultados. Los permisos editoriales para la reutilización de la totalidad de los trabajos en esta tesis y la declaración de conformidad de todos los demás coautores para la misma y su renuncia formal a reutilizarlos en otra tesis en cualquier otra universidad, se incluye en los sitios correspondientes en la sección de resultados.

FINANCIACIÓN

La presente Tesis Doctoral ha sido realizada gracias a la financiación obtenida de:

Ayudas para contratos predoctorales para a formación de doctores (2016) del Programa Estatal de Promoción del Talento y su Empleabilidad en I+D+i. Del subprograma Estatal de Formación. (REF: BES-2016-077422).

La adquisición de recursos y la utilización de servicios para las actividades de investigación han sido financiados con cargo a los proyectos:

- Estudio del Sistema Noradrenérgico en la Comorbilidad Dolor-Depresión: una Vía de innovación Farmacológica. Plan Estatal y de Innovación. Ministerio de Economía y Competitividad. Duración: enero 2016- diciembre 2018. Investigador principal: Esther Berrocoso Domínguez.

AGRADECIMIENTOS

En primer lugar, me gustaría demostrar mi más sincero agradecimiento a mis directoras de tesis, las doctoras Esther Berrocoso y Meritxell Llorca, por estos años de formación; académica y personal. En especial, me gustaría agradecer a la Dra. Berrocoso la posibilidad de realizar mi Tesis Doctoral y formar parte de este grupo de investigación tan maravilloso. Gracias por darme la oportunidad de aprender de vosotros, sin duda cada día que he pasado por allí ha sido una lección. Gracias por tus consejos, por mostrar tu parte exigente pero siempre humana, por tu cariño y consejos de mejora en cada reunión y por apoyarme en malos momentos.

Tampoco puedo dejar de agradecer de manera personal a mi codirectora, la Dra. Mertixell Llorca, que desde el minuto uno ha estado conmigo. Por tu enorme paciencia y cariño depositada en mi cada año. Gracias por enseñarme todo lo que hoy día sé sobre los experimentos. Has sido una persona clave en mi formación desde el primer momento. Gracias por todo lo vivido y por tu incansable apoyo.

Por supuesto, agradecer también la oportunidad de formar parte de este grupo de investigación y realizar mi Tesis Doctoral al Prof. Juan Antonio Micó. Me siento afortunada de haber podido compartir tiempo con él durante estos años, por su apoyo, sus consejos, sus anécdotas y por sus esfuerzos por mantener a este grupo siempre a flote. También agradezco su sentido del humor y su incansable lucha por que “me peinara cada día para venir al laboratorio”. Siempre le recordaré como un referente en la farmacología, pero también como una persona fantástica llena de historias que contar, risas y buenos momentos. Al igual que al profesor Juan Gibert, que, con su cariño, amabilidad e inteligencia nos hizo los días mejores. En memoria a ellos, dos grandes personas y profesionales.

In these last years of chaos, in which we have been hit by the COVID-19 pandemic, I have to thank Dr. Fani Neto enormously for the possibility of doing a stay in "online" format, for adapting to the situation with such good predisposition, for helping me in every experiment and in every meeting. Thank you for your kind words and for teaching me that patience and good work are very necessary skills for this world of science. I would also like to dedicate a word of thanks to Dr. Isabel Martins, who has always altruistically helped and guided me during my stay. Thanks also to you for your advice and your kind words. Undoubtedly, if I had gone to your laboratory I would have felt as much at home as I did during this period.

A mi gente de Farma, todos/as me habéis aportado a mi formación, primero como “pollito” con mis chicas postdocs, Lidia, María, Sonia, Laura, Carmeluchi, Irene y nuestra última incorporación, Clara. Gracias a todas, por hacerme sentir que formo parte de todo esto, porque habéis sido mi gran apoyo en los momentos de incertidumbre, gracias por el aprendizaje, los

momentos de risas, cariño y por ser mis mejores consejeras y “hermanas mayores científicas” en mis años más solitarios como predoctoral. Mira que pedí veces “hermanitos predocs”… y fueron llegando, pero poco a poco, mis chic@s predocs, Carolina, Alejandra, Patri, Adri y Alejandro. Con los que he vivido momentos muy divertidos, pero también estresantes “como pollito grande”. Sin duda, trabajar mano a mano con vosotros es una de las cosas más gratificantes de mi experiencia en el laboratorio. También agradecer a mi “compi trueno” José, por estar siempre, desde el principio. Siempre con tu positivismo y por tu insistencia en que hablemos en inglés en el laboratorio. A Elena, por tu paciencia, cariño y mimo en hacer todas las cosas, gracias por estar siempre, en las buenas y en las malas. Gracias también a Santi y Paula, que sin ellos nada podría haber sido posible, por vuestro apoyo y su cuidado porque todo estuviera disponible y a Loli, por tu preocupación porque todo funcione correctamente y por preocuparte, incluso más que yo, por mi postura corporal cuando estoy en el pc, je je je

Mención especial a mi familia, por haberme dado la oportunidad de poder estudiar fuera y dentro de Cádiz. Agradecer a mi madre y mi padre, que lucharais siempre porque fuésemos personas educadas, responsables, trabajadoras y cultas, pero sobre todo por todo el cariño que habéis puesto en ese proceso. A mis hermanos, Juan Antonio y Jesús, habéis sido mis “padres prematuros” desde hace muchos años. Por vuestro apoyo incondicional y por enseñarme a luchar siempre por mis sueños y deseos. A mi hermana Yaye, mi mejor amiga, la persona que mejor me entiende del mundo. A mis cuñadas; Ruth que me ha cuidado como a su hija siempre y a Vero por tu apoyo incondicional. A Rafita, mi cuñado, pero también amigo, me has ayudado y apoyado siempre en lo personal, pero también académicamente con tus consejos y tus explicaciones, gracias. También a mis sobrinos Joan, Xavi y el/la que está en camino, porque nos dais luz y amor cada día. Por su puesto a mis yayos, Maribel y Vicente, que tanto me han cuidado como a una hija o como a una nieta, depositando vuestra confianza y cariño en mí. A Javi, por ser un pilar importante en mi vida, por darme el abrazo que monta los trocitos y reír conmigo cuando todo sale bien. Os quiero a todos. Agradecer a mis amigas, Cristina y Montse, las de siempre, las “nos tomamos un café y nos lo cuentas con detalles”. Sin vosotras, mi vida hubiese dolido el doble (vosotras sabéis a que me refiero). Gracias por hacerme reír cada día y hacerme sentir especial. Os quiero mucho.

Por supuesto me gustaría hacer un reconocimiento a todos los animales que han formado parte de este estudio, espero que podamos contribuir en mejorar la calidad de vida de las personas que sufren dolor y trastornos mentales en un futuro no muy lejano.

“El dolor es para la humanidad un tirano más terrible que la misma muerte” - Albert Schweitzer.

A mi padre,

ABREBIATURAS

A: Test de Acetona

BLA: Basolateral Amygdala

CCA: Corteza Cingulada Anterior

CCAr: Corteza Cingulada Anterior rostral

CCI: Chronic Constriction Injury

CeA: Central Amygdala

CL: Climbing

CNO: Clozapine-N-Oxide

CP: Cold plate test

CPFm: Corteza Prefrontal medial

CREB: elemento de unión de respuesta al AMPc

DAB: Diaminobencidina

DBH: Dopamina Beta hidrixilasa

DREADD: Designer Receptors Exclusively Activated by Designer Drugs

DRt: subnucleus reticularis dorsalis

DNP: Dolor nuropático

FG: Fluorogold

HCN: Hyperpolarization-activated cyclic nucleotide–gated (HCN) channel

HPA: Eje Hipotalámico-Adrenal

IASP: International Association of Study of Pain

IM: Immobility

i.p.: intraperitoneal

fMRI: Imagen por Resonancia Magnética funcional

i.t.: intratecal

LC: Locus Coeruleus

LC_{contra}: LC contralateral

LC_{ipsi}: LC ipsilateral

LE-TH-Cre: Long-Evans Cre-dependiente en neuronas TH

LT: Long-term (Largo plazo de la neuropatía)

L5: Lumbar 5

L6: Lumbar 6

mFST: modified forced swimming test

MT: Mid-term (Medio plazo de la neuropatía)

NA: Noradrenalina

NAT: Noradrenergic transporter

NMDA: N-methyl-D-aspartate receptor

PVDF: polyvinylidene fluoride

RVM: rostral ventromedial medulla

SC: spinal cord

SD: Sprague Dawley

SEPA: Servicios centrales de Experimentación y Producción Animal

SP: Spontaneous pain test

ST: Short-term (Corto plazo de la neuropatía)

SNC: Sistema Nervioso Central

SNI: spared nerve injury

SNL: Spinal Nerve Ligation Model

SW: Swimming

TH: Tiroxina Hidroxilasa

TNT: Tibial nerve transection

VF: Von Frey test

VL: Vértebra lumbar

VTA: Ventral Tegmental Are

INDICE

1. RESUMEN

El proceso por el que el dolor agudo pasa a ser crónico provoca una remodelación cerebral disfuncional, que se caracteriza por una hipersensibilidad sensorial y la posible aparición de trastornos emocionales, provocando la comorbilidad de ambas patologías (dolor-trastorno emocional). Aunque exista una fuerte comorbilidad entre el dolor crónico y la depresión, el mecanismo por el cual una patología precipita la aparición de la otra sigue sin estar claros. Algunos estudios parecen indicar que el dolor y la depresión inducida por dolor crónico comparten mecanismos neurobiológicos comunes. Por tanto, conocer las bases biológicas que subyacen a esta comorbilidad podría establecer un avance en el diagnóstico y el tratamiento de los pacientes, así como en el desarrollo de futuros enfoques terapéuticos. El locus coeruleus (LC) es la fuente principal de noradrenalina del Sistema Nervioso Central y se conoce en el campo del dolor su papel en la inhibición descendente de la transmisión dolorosa de tipo aguda y por su participación en el proceso atencional ante un estímulo bilógicamente relevante como sería el dolor. Además, su actividad parece estar implicada en la conducta pro-depresiva. Sin embargo, aún se desconoce su papel o el papel de sus proyecciones descendentes y ascendentes en condiciones de dolor crónico, así como su relación con la comorbilidad. Utilizando la lesión unilateral por constricción crónica del nervio ciático como modelo de dolor neuropático, en el **estudio I** se utilizaron ratas Sprague Dawley macho. En este estudio se han identificado una serie de cambios plásticos en las neuronas del LC dependiente del tiempo desde el inicio de la lesión y en relación con el lugar de la lesión, LC ipsilateral (LC_{ipsi}; mismo sitio de la lesión) o LC contralateral (LC_{contra}; lado contrario de la lesión) en la evaluación de la dimensión sensorial y la sintomatología depresiva. Para modular la actividad del LC se utilizaron aproximaciones farmacológicas convencionales y de farmacogenética mientras los animales eran sometidos a test de conducta nociceptivos durante tres puntos temporales de la neuropatía: corto plazo (2 días después de la lesión), medio plazo (7 días después de la lesión) y largo plazo (28 días después de la lesión) y de evaluación de la sintomatología depresiva a largo plazo (28 días después de la lesión). Los resultados obtenidos mostraron que la inactivación del LC_{ipsi} mediante la administración intra-LC de lidocaína aumentó la alodinia al frío 2 días después de la lesión nerviosa, pero no luego. Sin embargo, el bloqueo del LC_{contra} (siguiendo la misma metodología) redujo la alodinia al frío 7 y 30 días después de inducir neuropatía, pero no antes. Además, el bloqueo con lidocaína del LC_{ipsi} o del LC_{contra} revirtió la conducta pro-depresiva inducida por dolor 30 días después de la neuropatía. Una de las áreas involucradas en el mantenimiento y la amplificación de la señal dolorosa a lo largo del tiempo es el núcleo reticular dorsal (DRt). En este estudio se reportó en animales con dolor a largo plazo un aumento de la expresión de pCREB en el DRt_{contra}, pero no en el DRt_{ipsi}. Además, la inhibición

de las proyecciones noradrenérgicas del LC_{contra} hacía el DRt_{contra} mediante farmacogenética tuvo un efecto analgésico provocó analgesia 30 días después de la lesión. Aunque la inhibición de esta proyección (neuronas noradrenérgicas del LC_{contra} que proyectan al DRt_{contra}) si efectuó cambios en la dimensión sensorial no provocó cambios en la conducta pro-depresiva en animales con dolor a largo plazo. Sin embargo, si indujo un comportamiento depresivo en animales sanos (Sham). Los resultados obtenidos mostraron que la lesión nerviosa activa el LC_{ipsi}, que amortigua por un corto periodo de tiempo el fenotipo de dolor neuropático. Por otro lado, en el dolor crónico hay una activación de la vía LC_{contra}- DRt_{contra} que contribuye a la facilitación del dolor y mantiene el dolor a lo largo del tiempo. En cambio, ambos LC (LC_{ipsi} y LC_{contra}) se activan de manera global contribuyendo así su actividad en el fenotipo depresivo asociado.

De igual manera, en el **estudio II**, utilizando el mismo modelo de dolor neuropático, pero en ratas Long-Evans wild-type y transgénicas TH-CRE, se evaluó la función del LC en relación con el lugar de la lesión (LC_{ipsi} o LC_{contra}) y los diferentes puntos temporales en la conducta sensorial y pro-depresiva. Mediante el uso de la tecnología DREADD y el uso de farmacología convencional se moduló la actividad del LC en los diferentes test conductuales. De esta manera, la inhibición global del LC ipsi aumentó la sensibilidad al dolor a corto plazo, pero no después. Sin embargo, bloqueo global de ambos LC de manera unilateral alivió la conducta pro-depresiva inducida por dolor crónico. En ambos estudios se ha demostrado una contribución asimétrica por parte de los módulos del LC a medida que se desarrolla la neuropatía. Posteriormente, se estudió el papel de las proyecciones del LC hacia la SC en la conducta sensorial (de manera unilateral). Se ha demostrado que la vía noradrenérgica LC_{ipsi}-SC esta activa en animales con dolor a corto plazo mediante un aumento de los niveles de c-Fos. Por tanto, la inhibición de la vía LC_{ipsi}- médula espinal provocó una disminución del umbral del dolor a corto plazo. Por otra parte, la activación quimiogenética de la vía LC_{ipsi}-SC si produjo un efecto analgésico en todos los puntos temporales de la neuropatía. Por otro lado, una de las áreas supraespinales que recibe proyecciones noradrenérgicas del LC es la corteza cingulada anterior rostral (CCAr). La CCAr es una de las áreas implicadas en la aparición de la sintomatología pro-depresiva inducida por dolor crónico. En este estudio se ha demostrado que la vía noradrenérgica del LC a la CCAr está activa en animales con dolor a largo plazo mediante a un aumento de los niveles de c-Fos. En consecuencia, la inactivación quimiogenética de la vía noradrenérgica del LC hacia la CCAr revierte la depresión inducida por el dolor a largo plazo, sin afectar a la conducta sensorial evocada. Además, este efecto parece estar mediado por los receptores α1 y α2 de la CCAr. Estos resultados demuestran que el dolor provoca una activación asimétrica de módulos específicos

del LC promoviendo un efecto analgésico temprano (dolor agudo) y la aparición del comportamiento depresivo se produce de manera tardía (dolor crónico). Estos datos demuestran que la vía analgésica deja de ser funcional a medida que el dolor se cronifica. Sin embargo, la activación exógena de esta vía produce analgesia en todos los puntos de la neuropatía.

1. SUMMARY

The process by which acute pain becomes chronic causes dysfunctional brain remodelling, which is characterized by sensory hypersensitivity and the possible appearance of emotional disorders, can lead to comorbidity of both pathologies (pain-emotional disorder). Although there is, in fact, a strong comorbidity between chronic pain and depression, the mechanism by which one pathology precipitates the onset of the other remains unclear. Some studies indicate that chronic pain and chronic pain-induced depression share common neurobiological mechanisms. Therefore, understanding the biological basis underlying this comorbidity could suppose a breakthrough in the diagnosis and treatment of patients, as well as in the development of future therapeutic approaches. The locus coeruleus (LC) is the main source of noradrenaline in the central nervous system, and itis known in the field of pain for its role in the descending inhibition of acute pain transmission and its participation in attentional processes related to facing biologically relevant stimuli, such as pain. In addition, its activity seems to be involved in pro-depressive behaviour. However, its role and that of its descending and ascending projections in chronic pain conditions, as well as its relationship with depression comorbidity, remains unknown. Using unilateral chronic constriction injury of the sciatic nerve as a model of neuropathic pain, male Sprague Dawley rats were used in **Study I**. In this study, we have identified a series of lesion time- and site-dependent plastic changes in LC neurons, differentiating, with regards to lesion site, between ipsilateral LC (LC_{ipsi}; same lesion site) and contralateral LC (LC_{contra}; opposite side of lesion), related to the assessment of sensory dimension and depressive-like behavoiur Conventional pharmacological and pharmacogenetic approaches were used to modulate LC activity while animals were subjected to nociceptive behavioural tests at three time points after neuropathy induction: short term (2 days post lesion), mid-term (7 days post lesion) and long term (28 days post lesion) accompanied by assessment of pro-depressive behaviours. Results showed that inactivation of LC_{ipsi} by intra-LC administration of lidocaine increased cold-induced allodynia 2 days after nerve injury, but had no effect 7 or 30 days after neuropathy induction. However, LC_{contra} blockade (following the same methodology) reduced cold-induced allodynia 7 and 30 days after neuropathy induction, but not before. In addition, lidocaine blockade of LC_{ipsi} or LC_{contra} reversed pain-induced pro-depressive behaviour 30 days after neuropathy. One of the areas involved in the maintenance and amplification of the pain signal over time is the dorsal reticular nucleus (DRt). In this study, we report an increase of pCREB expression in the DRt_{contra}, but not in the DRt_{ipsi}, in animals

experiencing long-term pain. Furthermore, pharmacogenetic inhibition of noradrenergic LC-DRt projections contralateral to the lesion site had an analgesic effect 30 days after neuropathy induction. Although inhibition of this projection elicited changes in the sensory dimension, it did not cause changes in pro-depressive behaviour in animals experiencing long-term pain. However, it did induce depressive-like behaviour in healthy animals (Sham). To sum up, the results from this first study showed that nerve injury activates the LC_{ipsi}, which dampens for a short period of time the neuropathic pain phenotype. Furthermore, in animals experiencing chronic pain, there is an activation of the LC_{contra}-DRt_{contra} projectionthat contributes to pain facilitation and maintains pain over time. In contrast, both LCs (LC_{ipsi} and LC_{contra}) are globally activated thus contributing their activity to the associated depressive phenotype.

Similarly, in **study II**, using the same model of neuropathic pain in Long-Evans wild-type and TH-CRE transgenic rats, LC function was evaluated in relation to the same temporal points in the neuropathy of Study I. Using DREADD technology as well as conventional pharmacology, LC activity was modulated during the different behavioural tests. Global inhibition of the LC_{ipsi} increased pain sensitivity 2 days after neuropathy induction, but not afterwards. However, global blockade of both LCs, (unilaterally LC_{ipsi} and LC_{contra}) alleviated chronic pain-induced pro-depressive behaviour. As a whole, both studies demonstrate an asymmetric contribution by LC modules as neuropathy develops. Subsequently, the role of unilateral LC projections to the spinal cord in sensory behaviour was studied. Results showed the noradrenergic LC ipsi-spinal cord projection to be active in animals experiencing short-term pain, as indicated by increased cfos levels. Inhibition of the LC_{ipsi}-spinal cord projection decreased short-term pain threshold. However, chemogenetic activation of the LC_{ipsi}-spinal cord projection did produce an analgesic effect at all time points after neuropathy induction. On the other hand, one of the supraspinal areas that receives noradrenergic projections from the LC is the rostral anterior cingulate cortex (rACC). The rACC is one of the areas involved in the appearance of pro-depressive symptomatology induced by chronic pain. In this study, we have shown that the noradrenergic LC-rACC projection is active in animals experiencing long-term pain, as shown by increased cfos levels. Accordingly, chemogenetic inactivation of the noradrenergic LC-rACC projection reverses long-term pain-induced depressive-like behaviour, but had no effect in sensory behaviour. Moreover, this effect appears to be mediated by α1 and α2 adrenergic receptors in the rACC. These results demonstrate that pain elicits an asymmetric activation of

specific LC modules promoting an early analgesic effect (acute pain) and a later onset of pro-depressive behaviour (chronic pain). These data demonstrate that the analgesic projection ceases to be functional as pain becomes chronic. However, exogenous activation of this projection produces analgesia at all the experimental time points studied after neuropathy induction.

2. INTRODUCCION

2.1. Aspectos generales del dolor

El dolor es un proceso fisiológico encargado de informar al organismo ante un estímulo peligroso y desencadenar mecanismos para evitar o amortiguar los daños. De hecho, los individuos que no tienen la capacidad de detectar estímulos nocivos o dolorosos ponen en riesgo su bienestar y su supervivencia ya que no adoptan las conductas de protección adecuadas (Basbaum y cols., 2019). La Asociación Internacional para el Estudio del Dolor (en inglés International Association for the Study of Pain; IASP) revisó la última definición del dolor en julio del 2020 y lo define como "una experiencia sensorial y emocional desagradable asociada o similar a la asociada a un daño tisular real o potencial" (Raja y cols., 2020). Esta definición considera, respecto a definiciones anteriores, que el dolor no es solo una experiencia exclusivamente sensorial, sino que además integra componentes emocionales y subjetivos y que puede darse sin causa somática que la justifique.

La experiencia dolorosa está compuesta por tres dimensiones: la dimensión sensorial, afectivo-emocional y cognitivo (figura 1). La dimensión sensorial es objetiva y nos proporciona información acerca de la localización e intensidad que provoca el estímulo nocivo produciendo una respuesta temprana del dolor. Esta dimensión es procesada por las cortezas somatosensoriales primarias y secundarias (S1 y S2) (Bushnell y cols., 1999; Plonner y cols., 2002). Por otro lado, la dimensión emocional del dolor es subjetiva e incluyen los aspectos negativos de las emociones (desagrado, miedo y angustia) asociados a futuras patologías (Price y cols., 1980; Price y cols., 2000). En la percepción e interpretación consciente del dolor intervienen varios factores además del biológico y son los factores biopsicosociales y psicológicos (Birket-Smith, 2001; Campbell y cols., 2003). Estos factores formarían la dimensión emocional provocada por el dolor. Existen estudios que han demostrado que la dimensión emocional del dolor es procesada en la corteza cingulada anterior (CCA) (Rainville y cols., 1997; Xiao y Zhang, 2018) y la amígdala, principalmente el núcleo central y basolateral (Veinante y cols., 2013; Corder y cols., 2019). Por último, la dimensión cognitiva, por el cual se evalúa la capacidad de aprendizaje ante una sensación dolorosa. Se ha descrito con anterioridad que ciertas tareas relacionadas con la dimensión cognitiva son procesadas por diferentes áreas cerebrales. En el caso de la memoria es destacable el procesamiento que lleva a cabo el hipocampo, que tiene un papel importante en el control de la formación de la memoria explícita a largo plazo. Por otra parte, aunque ya es conocido que la amígdala principalmente se encarga del manejo de estímulos emocionales, también se la ha relacionado con el procesamiento del aprendizaje. Específicamente, su núcleo basolateral parece estar involucrada en la consolidación

de la memoria (Roozendaal y cols., 2006; Zaletel y cols., 2016; Sawangjit y cols., 2018). Por otra parte, las funciones como el procesamiento de los estímulos, la función ejecutiva y la toma de decisiones parecen estar procesadas en áreas del lóbulo frontal, entre las que destacan: la corteza prefrontal dorsolateral, corteza cingulada anterior o la corteza orbitofrontal (Verdejo-García y cols., 2006).

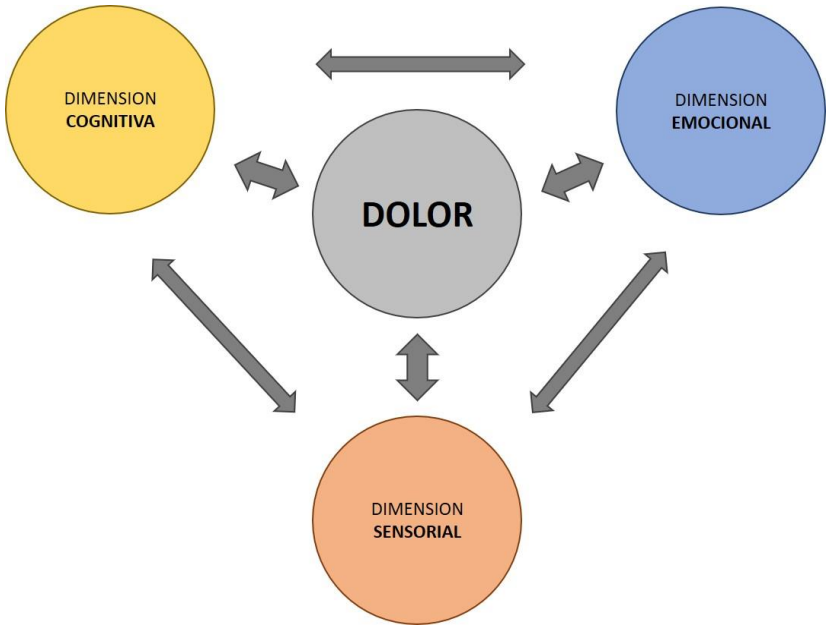

Figura 1: Dimensiones del dolor. La imagen muestra las tres dimensiones que se ven influidas ante la experiencia dolorosa; la dimensión sensorial, emocional y cognitiva. Estas dimensiones, a su vez, influyen entre sí de manera reciproca, provocando un empeoramiento e interfiriendo en el tratamiento del dolor.

En el procesamiento del dolor intervienen diferentes áreas del Sistema Nervioso Central (SNC). Cuando se produce una respuesta de dolor, se activan las vías ascendentes, de esta forma se transmite la información nociceptiva hacía áreas supraespinales como el tálamo y la corteza. Aquí el dolor se hace consciente y de manera inmediata nuestro sistema endógeno regulador responde produciendo analgesia a través de la activación de las vías descendentes del dolor (Lee and cols., 2020). Se ha descrito previamente que la activación de las vías descendentes del dolor actúa como función protectora ante un estímulo de dolor agudo (de poca duración) (figura 2). Sin embargo, cuando el dolor se vuelve persistente en el tiempo sin causa justificable se produce un incremento en la excitabilidad neuronal de las vías nociceptivas, llevando a un estado de sensibilización central, caracterizado por una disminución de los umbrales sensoriales (Millan, 1999; Latremoliere y Woolf, 2009). En esta condición las vías descendentes no son efectivas en su función analgésica y por tanto no cumplen la función protectora. En

consecuencia, se da la aparición del "dolor crónico", uno de los principales problemas de salud en el mundo.

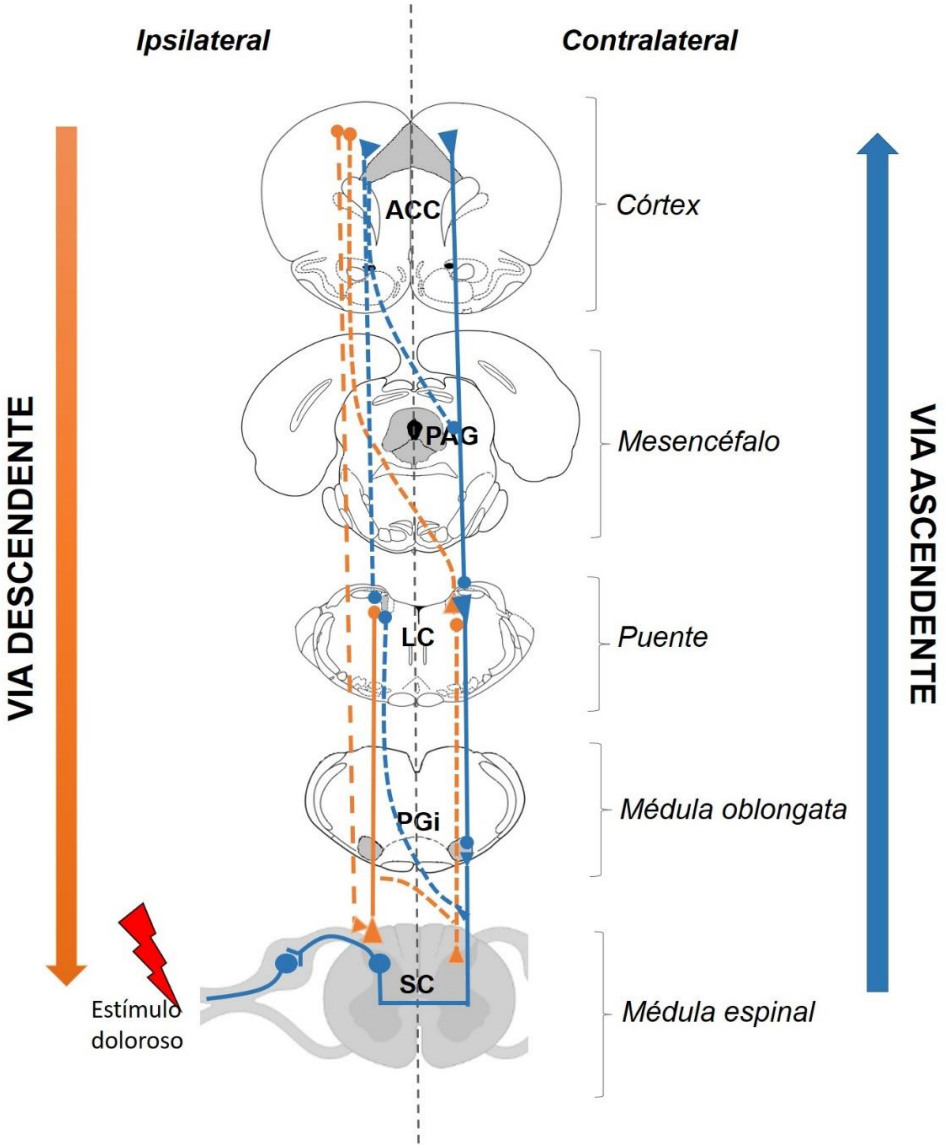

Figura 2: Esquema de las proyecciones ascendentes y descendentes ante una respuesta dolorosa. La imagen muestra las vías ascendentes (en azul) una vez recibe el estímulo nocivo/doloroso que viaja hacía áreas supraespinales, donde se vuelven consciente la experiencia de dolor. Consecuentemente el organismo emite una respuesta analgésica a través de la vía descendente (en naranja) hacía la médula espinal (Modificado Llorca-Torralba y cols., 2016; Algunas imágenes se han creado utilizando BioRender: www.BioRender.com).

Una de las formas en la que se puede clasificar el dolor es según su duración; el dolor agudo es un tipo de dolor adaptativo, puesto que este tipo de dolor nos protege de peligros potenciales y permite así la supervivencia del organismo. Sin embargo, cuando el dolor se experimenta durante un periodo de más de tres meses, deja de ser adaptativo para convertirse en dolor

patológico. Como afirma Apkarian la transición del dolor agudo al dolor crónico implica también un cambio en la condición de procesar una percepción dolorosa como una amenaza externa a un estado de enfermedad internalizado (Apkarian y cols., 2009).

2.2. Dolor crónico

El dolor crónico afecta alrededor del 20% de la población adulta en Europa (van Hecke y cols., 2013). Estudios publicados por el Observatorio del Dolor muestran que el dolor crónico afecta a un 16.6% de la población española, de los cuales más del 50% están limitados en sus actividades diarias, el 30% se sienten tristes y/o ansioso y un 42.2% ven afectada su vida familiar (Dueñas y cols., 2016). Además, existe una mayor prevalencia en mujeres (37.6%) que en hombres (20.9%) y esta va incrementando con la edad (42.6% en personas mayores de 65 años) (Catalá y cols., 2002). El dolor crónico es uno de los motivos más frecuentes para acudir a atención primaria y puede ser la causa o consecuencia del desarrollo de otras enfermedades en el futuro (Gureje y cols., 1998; Smith y cols., 2001). Al año supone un coste económico de 16.000 millones de euros (lo que supone el 2,5 del PIB) en el sistema sanitario español (Torralba y cols., 2014).

El manual sobre la Clasificación Internacional de las enfermedades, edición 11 (CIE-11; en inglés: “International Classification of Diseases 11th”), ha establecido una clasificación de dolor crónico en 7 grupos: dolor crónico primario, oncológico, de tipo neuropático, postraumático o postquirúrgico, dolor de cabeza u orofacial, dolor visceral y dolor musculoesquelético (Tredee y cols., 2019).

Independientemente del subtipo, el dolor crónico se caracteriza por la presentación de sintomatología diversa; dolor espontáneo, hiperalgesia y alodinia (Tredee y cols., 2019). El dolor espontáneo es el dolor que aparece sin estimulación nociceptiva. La hiperalgesia es un estado de dolor que conduce a una respuesta exagerada ante un estímulo doloroso y la alodinia es un estado de dolor que conlleva una respuesta dolorosa ante un estímulo normalmente inocuo (Scholz y cols. 2019).

Además, es importante tener en cuenta que muchos factores socio-demográficos como pueden ser la edad, estatus socio-económico, cultura y geografía, empleo, experiencias de abusos o violencia y estrés contribuyen al empeoramiento del curso del dolor crónico (Hasset y Clauw, 2010; van Hecke y cols., 2013), y probablemente al desarrollo de otras patologías afectivas asociadas al dolor crónico, como pueden ser la ansiedad y la depresión. Es importante destacar que las condiciones de emoción negativa agravan aún más la sensibilidad al dolor, la duración y

la experiencia de vida en condiciones de dolor, convirtiéndolo en un desafío clínico importante en la actualidad para tratar eficazmente el dolor crónico (Wilson y cols., 2001; Micó y cols., 2006; Wiech y Tracey, 2009; Bushnell y cols., 2013). Por lo tanto, cuando los pacientes desarrollan dolor crónico, desafortunadamente es muy difícil su tratamiento ya que están implicados múltiples factores que varían enormemente de un paciente a otro.

2.2.1. Dolor neuropático

La presente tesis doctoral se centra en el dolor neuropático (DNP) como tipo de dolor crónico, el cual es provocado por una lesión o enfermedad del sistema nervioso somatosensorial (Scholz y cols., 2019). El DNP se trata de una condición discapacitante que afecta entre el 7-10% de la población general (7-8% en la población europea (Haanpaä y cols., 2011)) y se trata de una patología notoriamente resistente a los tratamientos analgésicos disponibles en la actualidad (Bouhassira y cols., 2008; Finnerup y cols., 2015).

Además, cabe destacar el considerable gasto económico que conlleva el tratamiento y cuidado de personas con dolor neuropático. Un estudio de Liedgens y sus colaboradores detallan que los costes directos e indirectos por paciente de DNP en España son de 10.597€ (67%) (Liedgens y cols., 2016). Esto es una pequeña parte de la proporción del cuidado total, ya que la mayoría de los cuidados son proporcionados por familiares o amigos y los costes indirectos son los que afectan directamente al entorno laboral.

Actualmente, se desconocen gran parte de los mecanismos fiosiopatológicos que subyacen a los signos y síntomas que presentan los pacientes con DNP (dolor punzante, dolor paroxístico, parestesias, disestesias, hiperalgesia, alodinia, etc.) (Dworkin y cols., 2003; Baron, 2006; Truini y Crucu, 2006). El DNP es un trastorno difícil de tratar, lo que afecta a la calidad de vida de muchos pacientes. Por esta razón, es importante continuar con investigaciones que permitan conocer las bases fisiopatológicas de esta enfermedad y es fundamental identificar nuevas dianas farmacológicas para desarrollar nuevos agentes farmacéuticos (Cavalli y cols., 2018).

Además, se ha de tener en cuenta otras patologías afectivas y cognitivas que aparecen cuando el dolor neuropático es persistente a lo largo del tiempo. Este fenómeno provoca una dificultad adicional a la hora de proponer un tratamiento en estos pacientes.

2.2.2. Consecuencias emocionales del dolor neuropático

El dolor crónico de tipo neuropático es a menudo un factor precipitante a desarrollar otras patologías como la ansiedad o la depresión, así como déficit cognitivo (McWilliams y cols.,

2003; Dueñas y cols., 2015; de Sola y cols., 2016). Se estima que aproximadamente el 50% de los pacientes con dolor crónico de cualquier categoría sufrirá depresión (Bair y cols., 2003) y entre el 20 y el 30% experimentarán trastornos relacionados con la ansiedad (McWilliams y cols., 2003). Pero algo que resulta de suma importancia atender es que, alrededor del 20% de los pacientes con dolor refieren ideación suicida, con una prevalencia de en torno al 5% (Hooley y cols., 2014; Tang y Crane, 2006; Calati y cols., 2015). Aunque el dolor crónico pueda ser considerado un tipo de estrés crónico (Blackburn y Blackburn, 2001), existen estudios clínicos y preclínicos que han demostrado que no existen alteraciones neuroendocrinas en el eje hipotalámico hipofisario adrenal (HPA) (Yalcin y cols., 2011; Ulrich-Lai y cols., 2006). El dolor también es considerado como un trastorno de síntomas somáticos ya que a menudo pacientes con enfermedades psiquiátricas reportan sintomatología dolorosa, y en un alto porcentaje (15-100%) lo hacen los pacientes con depresión (Bair y cols., 2003). Por lo tanto, se podría plantear la existencia de un mecanismo subyacente que provocaría ambas patologías por separado y/o como consecuencia una de otra (Sheng y cols., 2017).

Teniendo en cuenta los eventos acontecidos en los últimos dos años (2019- hasta la actualidad) relacionados con la pandemia por COVID-19, resulta imperativo mencionar el impacto que esta ha tenido en la atención médica y en los pacientes con dolor. Como consecuencia, las medidas de seguridad que se han tomado para evitar la propagación del virus COVID-19 conlleva al retraso o interrupción del tratamiento de los pacientes con dolor crónico severo. Este hecho tendrá consecuencias nefastas para los pacientes y puede repercutir de manera significativa en un empeoramiento de la salud mental, así como en provocar un mayor gasto sanitario (El-Tallawy y cols., 2020; Shantanna y cols., 2020).

Sin embargo, aunque en la clínica ha sido demostrada esta comorbilidad de dolor crónico y trastornos afectivos, sigue siendo necesario estudiar los mecanismos fisiopatológicos subyacentes al dolor crónico para poder realizar una prevención adecuada y un óptimo tratamiento. En la actualidad existen modelos animales de dolor neuropático que mimetizan la sintomatología nociceptiva observada en pacientes con dolor y la comorbilidad con trastornos de tipo depresivo, ansioso y alteraciones cognitivas (Alba-Delgado y cols., 2013; Leite-Almeida y cols., 2015; Hirschberg y cols., 2017; Llorca-Torralba y cols., 2019; Bravo y cols., 2020). Además, demuestran que la aparición de la sintomatología ansiosa y/o depresiva en modelos de dolor crónico dependen del punto temporal de la neuropatía (Narita y cols., 2006; Yalcin y cols., 2011; Alba-Delgado y cols., 2013). Por tanto, el uso de animales de investigación nos dota de una herramienta fiable y válida para estudiar la fisiopatología de estos trastornos que frecuentemente aparecen de manera comórbida (Kremer y cols 2021).

2.3. Sistema noradrenérgico: Locus Coeruleus como modulador del dolor

Existen varias áreas noradrenérgicas clasificadas desde A1 hasta A7 (Dahlstrom y cols., 1964) en el SNC. Pero la fuente principal de noradrenalina (NA) del SNC se encuentra en el lado ventrolateral del cuarto ventrículo en la protuberancia cerebral (prosencéfalo), se tratan de las neuronas situadas en el tallo cerebral, A6, conocidas como Locus Coeruleus (LC).

Tradicionalmente se pensaba que las neuronas noradrenérgicas del LC proyectaban conjuntamente a otras áreas cerebrales a través de una arborización axonal altamente ramificada, que trabajan de forma coordinada y uniforme ante estímulos relevantes o estímulos sensoriales (Fuxe y cols., 2010). Sin embargo, existen evidencias de que las neuronas del LC trabajan en subconjuntos según sus proyecciones a otras áreas, tanto espinales como cortico-límbicas (Jones y cols., 1977; Westlund y cols., 1980; Chandler y cols., 2019; Poe y cols., 2020) y según sus propiedades moleculares o eléctricas (figura 3) (Chandler y cols., 2014; Schwarz y Luo, 2015).

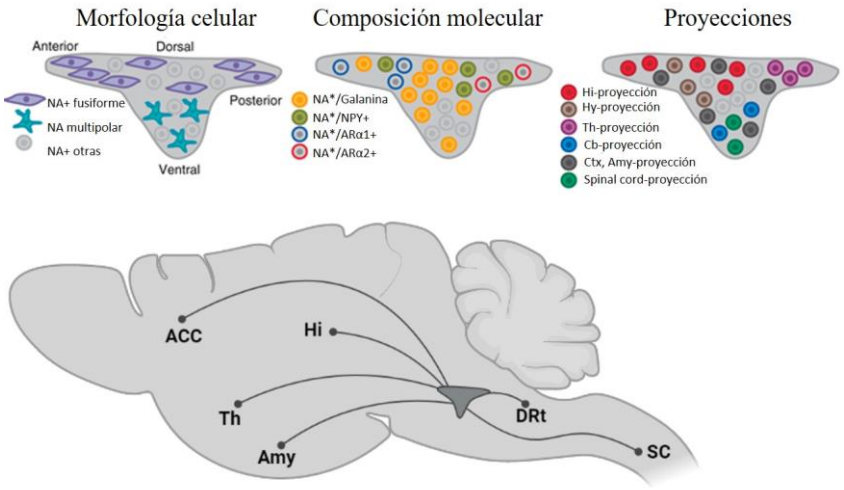

Figura 3: Heterogeneidad de las proyecciones del LC hacía áreas ascendentes supraespinales y descendentes espinales. La imagen muestra las diferencias morfológicas, moleculares y de proyección existentes entre las neuronas noradrenérgicas que componen el núcleo locus coeruleus. Adicionalmente se observa un corte sagital del cerebro de rata que muestra áreas de proyección del locus coeruleus (modificado de Schwartz y Luo, 2015; Algunas imágenes se han creado utilizando BioRender: www.BioRender.com).

2.3.1. Funciones del locus coeruleus

A través de estudios preclínicos y clínicos, se conoce su papel crucial en diferentes funciones biológicas del SNC, como el arousal, estrés, aprendizaje emocional, flexibilidad conductual, toma de decisiones y la percepción (Berridge y Waterhouse, 2003; Aston-Jones y Cohen, 2005; Valentino y Bockstaele, 2008; Arnstern. 2009; Sara y Bouret, 2012; McCall y cols., 2015; Maren y Holmes, 2016). Además, en el estudio de patologías como depresión, ansiedad y dolor se han reportado alteraciones en las neuronas noradrenérgicas del LC (Fortress y cols., 2015; Isingrini y cols., 2016; Llorca-Torralba y cols., 2016; Weinshenker y cols., 2018; Bangasser y cols., 2019).

La implicación del LC en el campo del dolor es centro de estudio debido a su situación anatómica estratégica, pues se encuentra entre la médula espinal (en inglés *spinal cord*; SC) y áreas supraespinales. Estudios anteriores en nuestro laboratorio sugieren que el LC actúa como nexo entre estas áreas en la transmisión y facilitación del dolor de tipo neuropático, así como en la aparición de patologías mentales asociadas. De esta manera, estudios electrofisiológicos han demostrado un aumento de la respuesta del LC_{contra} a la lesión, cuando se realizan estimulaciones dolorosas en la pata dañada o pata ipsilateral en animales con DNP a corto y medio plazo (2 y 7 días tras la implantación del modelo de dolor por constricción crónica del nervio ciático, en inglés; Chronic constriction injury (CCI)) (Alba-Delgado y cols., 2012a). Además, en el modelo de CCI también se ha observado que a los 14 días después de la cirugía y después de someterse a estrés por aislamiento social, el LC presenta una ratio de actividad tónica baja y actividad evocada alta ante una estimulación dolorosa, lo que se correlacionaría con una hiperactivación de este núcleo ante un estímulo doloroso. De manera complementaria, estudios comportamentales demostraron un aumento de la aversión ante la experiencia dolorosa en el test de evitación de plaza (Bravo y cols., 2013).

En cambio, en animales con DNP a largo plazo (30 días después de la cirugía CCI), se ha observado un aumento de la actividad tónica en burst, un aumento de la expresión de la enzima tirosina hidroxilasa (TH) (enzima limitante en la síntesis de NA), un aumento del transportador de NA (NAT) y un aumento de la expresión de los receptores α2 adrenérgicos en el LC. Además de estos hechos, en este punto temporal de la neuropatía también aparece la sintomatología ansiosa-depresiva (Alba-Delgado y cols., 2013).

El LC tiene numerosas proyecciones descendentes y ascendentes hacía diferentes áreas que están implicadas en diferentes funciones del dolor y de la sintomatología afectiva. Aunque es bastante conocido el papel de las proyecciones noradrenérgicas descendentes hacia la SC en el efecto analgésico. Por otro lado, aunque se conoce el papel relevante de áreas supraespinales

como la CCA o la amígdala en aspectos afectivos (depresión y/o ansiedad), existen muy pocos estudios que analicen el rol de estas vías ascendentes en el dolor neuropático y los aspectos afectivos inducidos por dolor neuropático. Por este motivo, en esta tesis doctoral profundizamos en el estudio de las diferentes vías noradrenérgicas descendentes (LC-SC y LC-núcleo reticular dorsal) y ascendentes (LC-corteza cingulada anterior y LC-Amígdala) y su papel en la conducta sensorial y afectiva.

2.4. Vías noradrenérgicas descendentes del dolor

Estudios dónde utilizan marcaje retrógrado mediante inyecciones bilaterales en la SC lumbar, han proporcionado información importante sobre la organización anatómica del sistema noradrenérgico, indicando que núcleos están implicados en la vía descendente del dolor. Algunas áreas supraespinales surgieron como objetivos importantes del árbol axonal de las neuronas noradrenérgicas que proyectan hacia la SC (las llamadas pontoespinales), entre ellas encontramos el neocórtex (incluyendo las cortezas cingulada y frontal) varios núcleos del tálamo, como el núcleo reticular y el ventrolateral, el núcleo gris periacueductal (PAG), la oliva inferior y el cerebelo (Howorth y cols., 2009). Como se ha sugerido, esta organización anatómica puede indicar que las neuronas pontospinales también controlan e influyen en otras áreas que están implicadas en el dolor y, por tanto, comparten cierta especificidad funcional.

Utilizando un vector adenoviral (AAV) retrógrado con una proteína fluorescente eGFP, capaz de transfectar neuronas noradrenérgicas que se proyectan a la SC bajo el control de un promotor catecolaminérgico específico se evaluó la vía noradrenérgica descendente pontoespinal (Hwang y cols., 2001; Lonergan y cols., 2005). Se administró este AAV en los segmentos L4-L5 de la SC y se observó la expresión de la proteína eGFP en las áreas: LC (en un 80%), A5 (en un 12%) y A7 (en un 8%) (Howorth y cols., 2009). Pero una de las informaciones más importantes obtenidas en este estudio fue que la microinyección espinal unilateral de este AVV produjo una distribución bilateral de las neuronas marcadas en LC. Sin embargo, existe un predominio en el lado ipsilateral (63%). Lo que indica que la vía noradrenérgica descendente que parte desde el LC hacia la SC es principalmente ipsilateral, aunque otra parte de la información también cruza la línea media para inervar el lado opuesto al asta dorsal. Estos datos concuerdan con otros estudios anteriores en los que se utilizaron otros neurotrazadores (Proudfit y Clark, 1991).

2.4.1. Función de los receptores noradrenérgicos de la SC

Se ha sugerido que el A5, LC y A7 liberan NA mediante sus proyecciones descendentes hacía la SC y produce una inhibición de los receptores noradrenérgicos α2A presinápticos (aferencias

nociceptivas primarias o de segundo orden) y receptores α1 (interneuronas inhibidoras) que suprimen la señal nociceptiva ascendente. Por otra parte, los receptores α2C de los terminales axónicos de las interneuronas excitadoras del asta dorsal espinal podrían contribuir al control espinal del dolor y podrían estar atenuando las señales nociceptivas (Pertovaara 2006). Sin embargo, este último mecanismo de acción antinociceptivo está aún por estudiar (Duflo y cols., 2002; Fairbanks y cols., 2002).

En la SC encontramos receptores noradrenérgicos de dos tipos: α1y α2. De los cuáles también disponen de diferentes subtipos. Entre los receptores α1, existen tres subtipos: α1A, α1B y α1D y entre los receptores α2, existen tres subtipos también: α2A, α2B, α2C. Aunque los receptores α1 parecen estar también involucrados en la vía descendente, aún existen muchas controversias sobre su función. Por este motivo, en esta tesis doctoral nos centraremos en la función de los receptores α2 y su función en la vía descendente del dolor. La distribución de los receptores noradrenérgicos α2 en la SC (figura 4) indican que lo receptores α2A se encuentran en mayor parte en el hasta dorsal, en el núcleo lateral y en el hasta ventral espinal. Los receptores α2B se encuentran en menor cantidad y sólo en el hasta dorsal superficial y los receptores α2C, también en menor número en varias capas del hasta dorsal espinal (Shi y cols., 1999).

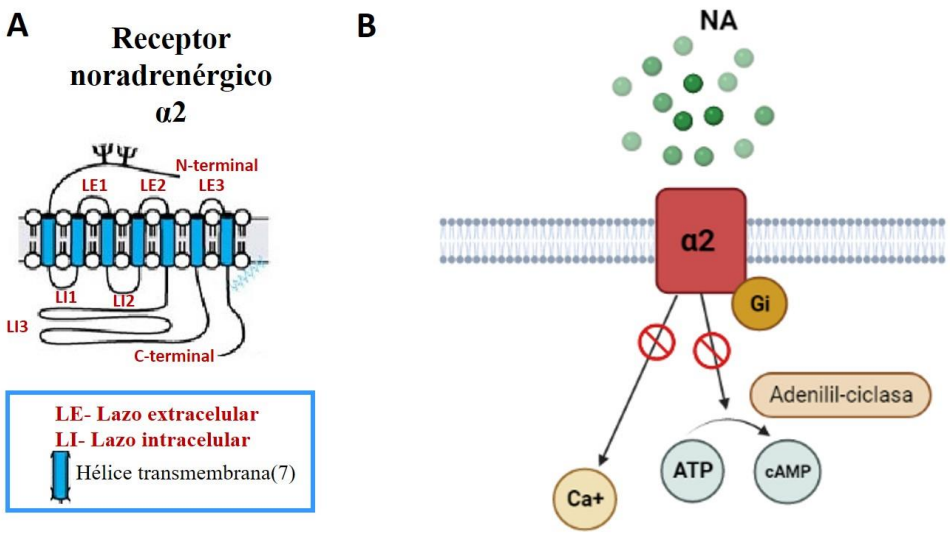

Figura 4: Estructura y mecanismo de acción de los receptores α2. A. Muestra la estructura general de los receptores noradrenérgicos α2 compuesta por siete dominios transmembranas, tres lazos intracelulares y extracelulares, un extremo N-terminal extracelular y un extremo C-terminal intracelular. **B.** Mecanismo de acción de los receptores α2. Los receptores adrenérgicos α2 son miembros de una familia de receptores asociados a la proteína G. Con su activación, una proteína heterotrimérica G, llamada Gi inactiva a la adenilil ciclasa, que a su vez produce una disminución del segundo mensajero intracelular AMPc y una disminución de Ca2+ intracelular. Algunas imágenes se han creado utilizando BioRender: www.BioRender.com) NA; Noradrenalina.

2.4.2. Efecto de la NA en la SC ante una situación dolorosa

Es posible que después de una lesión nerviosa el fenotipo de DNP en animales dependa de la cantidad de NA disponible en áreas pontoespinales (Xu y cols., 1999; Nakajima y cols., 2012). Existen estudios que para demostrar el efecto de la NA en la SC han utilizado dos metodologías; una mimetizando la activación descendente mediante el uso de inhibidores de la recaptación de NA intratecal y otra mecanística mediante el uso de usando el bloqueo de los receptores α2 de la SC (Hughes y cols., 2015). En este sentido, la adminintración intramedular de reboxetina o clonidina provocó una preferencia de lugar en animales con DNP (Hughes y cols., 2015). Por el contrario, la administración sistémica de reboxetina no demuestra preferencia de lugar en animales con dolor neuropático (Hughes y cols., 2015). Esto podría ser debido a que la administración sistémica de un inhibidor de la recaptación de NA a nivel general esté provocando un aumento de la disposición de NA en otras áreas cerebrales con efectos aversivos y que podrían estar contrarrestando el efecto analgésico producido en la SC.

La vía descendente del dolor la componen varios núcleos de los cuales tres envían NA directamente hacia la SC: A5, LC y A7. Sin embargo, en esta tesis doctoral, nos centraremos en la función del LC, como núcleo noradrenérgico que envía de manera predominante proyecciones noradrenérgicas a la SC. En este sentido, esta tesis doctoral se centrará en el estudio de la función de las neuronas específicas (módulo de neuronas) del LC que proyectan hacia la SC.

2.4.3. Vía LC-SC y su función en el dolor

Se conoce bien la conexión del LC con la SC y su implicación con el control de la transmisión dolorosa (Taylor y Westlund, 2017). Sin embargo, hasta ahora existían controversias en cuanto a los estudios que analizaban esta vía noradrenérgica descendente, desde el LC hacia la SC. Hay trabajos que han demostrado que la gabapentina activa las neuronas noradrenérgicas del LC e induce liberación de NA espinal que, a su vez, estimula a los receptores noradrenérgicos α2 y esto conduce a la analgesia (Hayashida y cols. 2007a; Hayashida y cols., 2008b; Hayashida y cols., 2007b; Takasu y cols., 2006). La gabapentina disminuye el GABA extracelular y aumenta el glutamato extracelular en el LC a través del transportador del glutamato 1

(GLUT-1), de esta manera se estimula la inghibición noradrenérgica descendente en ratas con DNP (Suto y cols., 2014; Yoshizumi y cols., 2012). Más tarde, se descubrió que la expresión de GLUT-1 disminuye varias semanas después de la lesión del nervio periferico (Kimura y cols., 2015). Esto en cierta medida, podría explicar la pérdida de la eficacia de la gabapentina tiempo después de provocar el DNP (Kimura y cols., 2016). En cambio, existen otros estudios que no están de acuerdo con que la lesión nerviosa sea lo único que regula el control noradrenérgico descendente para inhibir el dolor. Algunos estudios reportan que existe un déficit del control noradrenérgico descendente en los modelos de DNP. Por ejemplo, en un estudio, la estimulación eléctrica del LC produjo una antinocicepción significativamente más débil en animales con lesiones nerviosas que en los animales control (Viisanen y Pertovaara 2007). Otro estudio demostró que la lesión del nervio periférico provoca la supresión de la inhibición noradrenérgica espinal mediada por los receptores α2 del hasta dorsal de la SC ante estímulos mecánicos de baja intensidad. Sugiriendo así que la lesión nerviosa podría aumentar la inhibición del LC, suprimiendo la inhibición noradrenérgica del dolor y promoviendo el DNP (Rahman y cols. 2008). De manera alternativa, utilizando la administración del antagonista de los receptores α2, yoimbina, demostraron que suprime la hiperalgesia si se inyectaba en los primeros días de la neuropatía (días 3-5) pero no en momentos posteriores (días 10-17) de la neuropatía. En este caso, la contribución del control noradrenérgico descendente podría ser transitoria, restringida a los primeros periodos de DNP (Hughes y cols., 2013). Por lo tanto, teniendo en cuenta los resultados de estudios anteriores se ha propuesto que el efecto de la activación noradrenérgica del LC en el DNP cambia con el tiempo (Taylor y Westlund, 2017). Por este motivo, en la presente tesis doctoral nos centramos en el estudio de los diferentes módulos de neuronas noradrenérgicas que proyectan a áreas posiblemente involucradas en la vía descendente inhibitoria del dolor en las diferentes fases de la neuropatía. De esta manera contribuir a dilucidar el mecanismo por el que se da la facilitación del dolor y provoca la transición del dolor agudo al crónico. En este caso, se estudian la vía noradrenérgica del LC hacia la SC y hacia el núcleo reticular dorsal.

2.4.4. Núcleo reticular dorsal (DRt) y su función en el dolor

El núcleo DRt es un área que *per se* pertenece al sistema endógeno del control del dolor y su función principal reside en facilitar la respuesta de dolor (Lima y Almeida, 2002). Se localiza en

la porción más caudal de la formación reticular dorsolateral de la médula, medialmente al núcleo espinal del trigémino, *pars caudalis,* lateral al núcleo del tracto solitario, ventral al núcleo cuneado y dorsal al núcleo reticular ventral y contiguo.

Las neuronas del DRt se activan de manera selectiva ante una estimulación nociva transmitida por las fibras Aδ y C (Villanueva y cols., 1988; Villanueva y cols., 1989; Lima y Almeida, 2002; Leite-Almeida y cols., 2003). La activación del DRt mediante la administración de glutamato produce un aumento en la capacidad de respuesta de las neuronas espinales (Dugast y cols., 2003). Sin embargo, el bloqueo del DRt ipsilateral mediante la administración de lidocaína induce la supresión de esta capacidad de respuesta después estimular el nervio ciático (Dugast y cols., 2002). Conductualmente se demostró que las lesiones eléctricas o químicas (ácido quinolítico) del núcleo aumentan la latencia en el test de tail-flick y la respuesta a la temperatura en el test de la placa caliente respectivamente (Almeida y cols., 1996). Además, se observó una disminución en la expresión de c-Fos evocada nociceptivamente en las láminas I-II y IV-V del asta dorsal de la SC (Almeida y cols., 1999a). Estos resultados indican que este núcleo se encuentra activo durante la neuropatía y provocando una activación de las neuronas del hasta dorsal de la SC. Este fenómeno se revierte cuando se produce una lesión o una inhibición farmacológica de este núcleo, provocando una disminución de los niveles de c-Fos en la SC.

Existen diferentes evidencias que han demostrado que el núcleo DRt está involucrado en la facilitación de la percepción del dolor en modelos animales de dolor agudo y de dolor crónico, principalmente en modelos de dolor inflamatorios y neuropáticos (Almeida y cols., 1996; Almeida y cols., 1999; Sotgiu y cols., 2008). Este núcleo está modulado por áreas noradrenérgicas como el LC o la A5 y en situaciones de dolor provocan un aumento de la liberación de NA en DRt (figura 5) (Martins y cols., 2010, 2013). De hecho, se produce un aumento de la liberación de NA en el DRt durante la prueba de formalina (Martins y cols., 2013). Este control noradrenérgico se da específicamente a través de la activación de los receptores adrenérgicos α1, ya que se ha observado que la administración de prazosin (antagonista α1) intra DRt produce un decremento de la hiperalgesia en animales con dolor inflamatorio (Martins y cols., 2013). Estos datos sugieren que las proyecciones del LC hacia el DRt ejercen un efecto pronociceptivo y que, por tanto, esta vía noradrenérgica descendente provoca el mantenimiento del dolor a lo largo del tiempo a través de la acción del DRt.

Adicionalmente, se ha encontrado que el asta dorsal de la SC tiene conexiones recíprocas con DRt. Se conoce que la conexión de ambas áreas conforma un circuito reflexivo a través del cual se cree que se amplifica la transmisión dolora en la SC (Lima y Almeida, 2002; Martins y

Tavares, 2017) (figura 5). Estudios con trazadores retrógrados han demostrado que el DRt recibe proyecciones importantes bilaterales de las láminas I, IV-VII y X de la SC con un predominio claro del lado ipsilateral provenientes de la asta dorsal (Lima, 1990; Villanueva y cols., 1991). A su vez, mediante estudios anatómicos y electrofisiológicos se ha demostrado que las neuronas DRt están conectadas de manera recíproca con la lámina espinal I, formando un circuito en bucle excitador (Almeida y cols., 1993, 2000) y ante una señal nociceptiva activa este circuito recíproco que se traduciría finalmente como una amplificación y mantenimiento a lo largo del tiempo de la señal dolorosa. Posiblemente en los pacientes tratados con antidepresivos se produzca una inhibición de la recaptación de NA, y esto esté contribuyendo de manera indirecta a la facilitación del dolor mediante la acción del DRt. Esto podría explicar el efecto incompleto analgésico mediante el tratamiento con antidepresivos en pacientes con dolor crónico (Jasmin y cols., 2002; Vranken, 2012). Por este motivo, en la presente tesis doctoral se propone esta vía noradrenérgica (LC-DRt) como una de las vías de interés para estudiar la amplificación y mantenimiento del dolor a lo largo del tiempo y si el aumento selectivo del control noradrenérgico espinal podría ser una estrategia terapéutica útil.

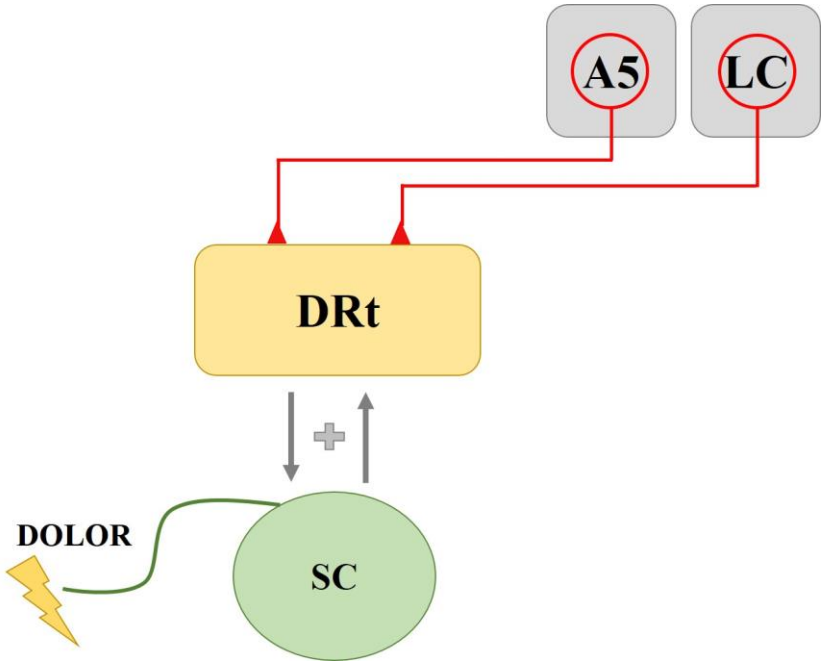

Figura 5. Diagrama que muestra las conexiones del núcleo dorsal reticular (DRt) con la SC y áreas supraespinales noradrenérgicas. El DRt envía y recibe proyecciones de la SC (líneas grises) que están involucradas en la facilitación del dolor. A su vez, el DRt recibe aferencias de varias áreas del tronco encefálico, destacando el locus coeruleus (LC) y el grupo de células noradrenérgicas A5 (modificado de Martins y Tavares y cols., 2017).

2.5. Vías noradrenérgicas ascendentes del dolor

En diversos estudios preclínicos y clínicos de resonancia magnética funcional del inglés; functional magnetic resonance imaging (fMRI) apuntan que diferentes áreas supraespinales podrían ser responsables de la percepción del dolor (Apkarian y cols., 2005). Entre ellas encontramos el tálamo, las cortezas somatosensoriales, la insular y la prefrontal, incluida la CCA, el núcleo lentiforme, el cerebelo, la amígdala y el núcleo accumbens (Bernard y cols., 1996; Becerra y cols., 2001; Apkarian y cols., 2005; Baliki y cols., 2010; Bushnell y cols., 2013). Estas áreas están inervadas por proyecciones del LC que modulan su actividad y cada vez tienen un mayor interés en campo del dolor, especialmente en la comorbilidad dolor crónico y trastornos afectivos asociados.

Es conocido que la información dolorosa asciende de manera contralateral a través de la SC principalmente hacia áreas cortico-límbicas. La misión principal de las vías ascendentes es enviar la información nociceptiva a otras áreas supraespinales que se encargan de procesar los diferentes aspectos del dolor (sensorial, emocional y cognitivo). Las proyecciones ascendentes del LC juegan un papel importante en el arousal y en el proceso atencional, el cual se encarga de la discriminación de los estímulos relevantes (Sara y Bouret, 2012). Estudios electrofisiológicos y conductuales proponen que el LC se activa ante un evento biológicamente relevante, especialmente aquellos que tienen una gran carga emocional, como podría ser una situación peligrosa o ante un estímulo doloroso. De esta manera, el LC aumenta su actividad fásica, liberando NA a otras áreas superiores como la corteza prefrontal y la amígdala, promoviendo la "flexibilidad cognitiva" ejerciendo un control arriba-abajo (en inglés: *top-down*) de la corteza prefrontal sobre la amígdala que permite elaborar una respuesta adecuada ante la situación relevante que se presenta (Aston-Jones y Cohen, 2005; Sara y Bouret, 2012). Entre esas proyecciones noradrenérgicas ascendentes implicadas en el dolor y en trastornos afectivos asociados podemos destacar las áreas de CCA y la amígdala (Koga y cols., 2020; Wang y cols., 2017a/b; Llorca-Torralba y cols., 2019; Veinante y cols., 2013).

2.5.1. Vía LC-Amígdala

2.5.1.1. Funciones de la amígdala en dolor

La amígdala está estrechamente interconectada con numerosas áreas corticales, subcorticales y del tronco del encéfalo. Esta área juega un rol importante en el procesamiento de la sintomatología sensorial, afectiva y cognitiva inducida por el dolor (Ledoux, 2000; Duvarci y cols., 2013; Pereira-Silva y cols., 2020) y existen evidencias anatómicas, neuroquímicas,

electrofisiológicas y conductuales que lo demuestran (Rouwette y cols., 2012; Veinante y cols., 2013; Carr y Zachariou, 2014). En este sentido, la inhibición del núcleo central de la amígdala (CeA) y del núcleo basolateral de la amígdala (BLA) revirtió la hiperalgesia, alodinia y la conducta pro-depresiva en animales con neuropatía periférica (Seno y cols., 2018). Sin embargo, de manera específica, muchos trabajos sobre dolor se han centrado en la CeA o "amígdala nociceptiva". Esto es debido a que recibe información nociceptiva ascendentes proveniente del núcleo para-braquial, y este a su vez de la SC (Veinante y cols.,2013). En esta línea, hay un estudio que demuestra que se produce una disminución de la conducta nociceptiva medida en el test de latencia de retirada de la cola y que este efecto se produce a través de la activación de los receptores α2 de la CeA, pero no de la BLA (Ortiz y cols., 2007).

2.5.1.2. Función de la vía noradrenérgica LC-BLA en aspectos emocionales y cognitivos

En cambio, la BLA ha sido ampliamente relacionada con el procesamiento de trastornos mentales, el miedo y la cognición (Ramos y Arnsten 2007; Boyle, 2013). Se ha de tener en cuenta que la BLA recibe proyecciones del LC y que podría ser una candidata importante para estudiar los comportamientos afectivos provocados mediante la acción del sistema noradrenérgico (Berridge y Waterhouse, 2003; Sara, 2009). La BLA integra información sensorial para codificar y procesar comportamientos como la ansiedad, aversión y recompensa (Robertson y cols., 2013) y como se ha demostrado en estudios anteriores, el LC envía proyecciones noradrenérgicas hacía la BLA. La hiperactivación de esta vía noradrenérgica puede provocar sintomatología ansiosa (Siuda y cols., 2016; McCall y cols., 2017) y aprendizaje aversivo (Uematsu y cols., 2017).

Adicionalmente se ha demostrado que la BLA y su actividad noradrenérgica están involucradas en diferentes funciones de la memoria, entre ellas, la consolidación del miedo. De hecho, la transmisión de orexina del LC hacía la amígdala media el aprendizaje del miedo (amenaza) y más específicamente mientras se da el evento aversivo (Sears y cols., 2013). Además, se ha visto que tanto la activación noradrenérgica de la BLA, como las interacciones de la BLA con otras áreas cerebrales, podrían estar involucradas en la consolidación y en la recuperación de la memoria emocionalmente excitante (Roozendaal y cols., 2006). Por otra parte, también se ha demostrado su papel en el procesamiento de memorias sin contenido emocional, como memorias de reconocimiento de nuevo objeto. En este caso, se ha demostrado que la activación noradrenérgica de la BLA modula la consolidación de este tipo de memoria (Roozendaal y cols., 2008).

Ante el estrés agudo y crónico (olores aversivos, antagonista de receptor α2, exposición crónica al frío, restricción durante 2h) se produce una activación de receptores adrenérgicos de la BLA y

este evento se ha relacionado con un fenotipo de ansiedad y otras conductas relacionadas con el estrés (Miranda y cols., 2007; Buffalari y Grace, 2009a, 2009b; Chang y Grace, 2013). Aunque se ha estudiado en numerosas ocasiones como la transmisión noradrenérgica en la BLA puede alterar la plasticidad sináptica, la codificación del miedo y la consolidación de la memoria, existen pocos estudios que analicen como las neuronas noradrenérgicas del LC modulan a la BLA para provocar conductas de aversión y ansiedad. (Buffalari y Grace, 2007; Buffalari y Grace 2009a, 2009b; Grissom y Bhatnagar, 2011). De manera general, la activación de las células noradrenérgicas del LC aumentan el contexto de estímulos estresantes (Abercrombie y Jacobs, 1987a, 1987b; Mana y Grace, 1997; Aston-Jones y cols., 1999; McCall y cols., 2015). Un estudio de Jordan McCall demostró de manera específica que la fotoestimulación de la vía noradrenérgica del LC hacía la BLA provoca una liberación de NA en la BLA actuando sobre los receptores β-adrenérgicos, observando un aumento de c-Fos (en BLA) que se correlacionaba con un fenotipo aversivo y ansioso en animales sanos (McCall y cols., 2017). En otro estudio, se demostró que tanto la activación quimiogenética como la optogenética de la vía de señalización Gαs en la BLA induce sintomatología ansiosa y de ansiedad social en animales sanos (Siuda y cols., 2016).

2.5.1.3. Función de la vía noradrenérgica LC- BLA en la comorbilidad dolor- ansiedad

En el campo del dolor, se ha demostrado un aumento de los niveles de pERK1/2 en BLA a los 42 días después de inducir dolor inflamatorio que mostraron una conducta ansio-depresiva (Pereira-Silva y cols., 2020). Un estudio reciente realizado en nuestro laboratorio demuestra que la inhibición quimiogenética de la vía LC-BLA revirtieron la ansiedad y el aprendizaje al miedo. Estos resultados fueron replicados cuando se utilizó un antagonista de los receptores β-adrenérgicos intra- BLA y de manera sistémica (intraperitoneal). En cambio, la activación la activación quimiogenética de esta vía provoco un fenotipo ansioso y una mejora tanto en el aprendizaje aversivo como en el índice de memoria en animales sham. Sin ejercer ningún cambio sobre la conducta sensorial o memoria episódica (Llorca-Torralba y cols., 2019). Por lo tanto, estos datos sugieren que las proyecciones noradrenérgicas LC-BLA podrían estar involucradas en la mediación del comportamiento afectivo negativo agudo. Y aunque las proyecciones anatómicas del LC y sus tipos celulares se han estudiado, no se comprenden aún los mecanismos precisos por los que las fibras del LC influyen directamente en la función de BLA para inducir comportamientos afectivos negativos. Se desconoce como el sistema de receptores específicos y la modulación de la actividad celular de las proyecciones de la vía LC-BLA generan sus respuestas conductuales afectivas. Por este motivo el estudio de Llorca-

Torralba es interesante, ya que demuestra la implicación de esta vía (LC-BLA) ante situaciones aversivas sostenidas en el tiempo, como es el dolor crónico. El dolor crónico provoca ansiedad y un aumento del aprendizaje aversivo, pero la inhibición de esta vía específica permite abolir esta sintomatología negativa. Además, es importante destacar, que este efecto está mediado por los receptores β-adrenérgicos de la BLA (Llorca-Torralba y cols., 2019).

2.5.2. Vía LC-Corteza cingulada anterior

2.5.2.1. Anatomía de la Corteza prefrontal

La corteza prefrontal (CPF) se divide en tres partes: corteza prefrontal lateral, orbital y medial. La corteza prefrontal medial (CPFm), a su vez, se divide en tres partes: corteza cingulada anterior (CCA), prelímbica (PL) e infralímbica (IL). Sin embargo, nos centraremos en el estudio de la CCA debido a su implicación en el componente afectivo del procesamiento del dolor (Singer y cols., 2004). Aunque existen muchos trabajos que analizan la implicación del componente afectivo de la CCA en el dolor neuropático de manera general, la CCA tiene dos subregiones; CCA rostral (CCAr), y CCA caudal (CCAc). En esta tesis doctoral nos centraremos en el análisis de la CCAr, ya que, su activación es necesaria y suficiente para codificar la emoción aversiva relacionada con el dolor (Johansen y cols., 2001). Además, el dolor neuropático crónico produce una hiperactivación de esta área (CCAr; 24a/24b) y con cuerda con la aparición de la sintomatología ansio-depresiva inducida por el dolor (Sellmeijer y cols., 2018).

De manera general, la corteza cerebral está compuesta por diferentes capas denominadas del I al VI desde la superficie a la profundidad. Estas capas están formadas por diferentes tipos de neuronas con diferentes propiedades locales y de conectividad hacia otras estructuras del sistema nervioso. Así, la capa I o capa granular, capa II dónde se encuentran neuronas estrelladas o interneuronas, capa III en la que existen interneuronas y neuronas piramidales, capa IV principalmente compuesta por interneuronas, y las capas V, VIa y VIb que se conforman principalmente por neuronas piramidales. Se ha observado que, durante la fase inicial del dolor inflamatorio se produce un aumento de la transmisión glutamatérgica y una debilitación del control inhibitorio en las capas II/III de la CCA provocada por una sensibilización prolongada (Koga y cols., 2018). Además, la plasticidad funcional en la CCA tras la inducción de dolor neuropático se ve afectada en la transmisión sináptica y la excitabilidad neuronal. En este sentido, el modelo de lesión del nervio ciático produjo una modificación a nivel estructural de la capa V de la CCA (Blom y cols., 2014). Otros estudios

han mostrado un aumento de actividad en la ACC en pacientes con lesión nerviosa (Hsieh y cols., 1995). Esta actividad parece ser debida a una pérdida de conectividad entre las neuronas excitadoras e inhibidoras ya que la pérdida de sinapsis inhibidoras en las neuronas piramidales excitadoras y una pérdida de sinapsis excitadoras en las interneuronas inhibidoras conlleva a una desinhibición a nivel local de la red cortical (Blom y cols., 2014).

2.5.2.2. Distribución de los receptores noradrenérgicos en la CCA

La actividad de la CCA está modulada por las proyecciones del LC a través de tres familias de receptores noradrenérgicos (α1, α2 y β). En la categoría de receptor α1 se diferencian tres subtipos: α1A, αB y α1D, que es encuentran principalmente en las capas intermedias (Goldman-Rakic y cols., 1990). Los receptores α1 están acoplados a proteínas Gq y pueden activar la vía de señalización intracelular contralada por la fosfolipasa C produciendo así la activación de la proteína kinasa C y la liberación de calcio intracelular (Duman y Nestler, 1995; Birnbaum y cols., 2004). Respecto a los receptores α2 existen tres subtipos; α2A, α2B y α2C, aunque los α2A son los más comunes en la CPF (Aoki y cols., 1994; Aoki y cols., 1998a). Los receptores α2 están acoplados a proteínas Gi y pueden reducir la producción del monofosfato de adenosina cíclico (cAMP) intracelular inhibiendo algunas isoformas del adenilil ciclasa (Duman y Nestler, 1995; Ramos y cols., 2006). Y finalmente, los receptores β, entre los que se diferencian tres subtipos (β1, β2 y β3) que se encuentran en las capas intermedias de la CPF (Goldman-Rakic y cols., 1990). Los receptores β se encuentras acoplados a proteínas Gs de adenilil ciclasa produciendo un incremento de la vía de señalización cAMP (Duman y Nestler, 1995; Birnbaum y cols., 2004).

2.5.2.3. Función de los receptores noradrenérgicos de la CCA en la modulación del dolor neuropático

Las neuronas de la ACC reciben varias entradas neuromoduladoras de estructuras subcorticales, incluidas las neuronas noradrenérgicas del LC (Koga y cols., 2020). Se ha demostrado que las neuronas del LC liberan NA hacia la corteza prefrontal medial (CPFm) y suprimen la actividad nociceptiva evocada en la CPFm a través de los receptores α2B. De esta manera se atenúa la hipersensibilidad mecánica provocada por el dolor neuropático (Condes-Lara, 1998; Kandel y cols., 2013; Chu y cols., 2015). En la CCA, los receptores α2B parecen estar implicados en los efectos analgésicos provocados en el test de dolor espontáneo después de administrar clonidina. La expresión de los receptores α2B se ve incrementada a los 3 y 7 días de la lesión, sin

embargo, a los 14 días se produce un decremento de la expresión (Wang y cols., 2017b). Por otra parte, los efectos proalgésicos parecen estar mediados por receptores α1 (Kaushal y cols., 2016). La NA liberada induce un disparo persistente en las neuronas piramidales de la CPF a través de los receptores adrenérgicos α1 que se encuentran en las terminales glutamatérgicas de la CPF y facilitan la transmisión sináptica rápida (Zhang y cols., 2013). Por otro lado, un estudio realizado en animales con dolor neuropático a largo plazo se observó un aumento de los niveles de NA en la CPF, que provocó un daño en las funciones de la CPF posiblemente mediado por la acción de los receptores α1 (Suto y cols., 2014).

2.5.2.4. Análisis de la implicación de la CCA en el dolor crónico y en la sintomatología ansio-depresiva asociada

En el campo del dolor neuropático hay estudios clínicos y preclínicos que revelaron cambios en la CCA, los cuales, estaban relacionados con el procesamiento de la información emocional en la experiencia de dolor neuropático (Paulson y cols., 2002; Vartiainen y cols., 2009; Li y cols., 2010; Ning y cols., 2013; Kummer y cols., 2020). La activación selectiva de la CCA mediante estimulación eléctrica o mediante optogenética provoca síntomas nociceptivos y emocionales en monos y roedores (Calejesan y cols., 2000; Vogt y cols., 2005; Kang y cols., 2015; Koga y cols., 2020). De hecho, en roedores se ha demostrado que la estimulación dolorosa provoca activación de neuronas de la CCA (Descalzi y cols., 2013; Lu y cols., 2018). Existen estudios de registros electrofisiológicos realizados en un modelo de ratón con dolor neuropático que muestran una hiperactividad de la CCA durante la estimulación nociceptiva y después de evaluar el comportamiento de tipo ansiodepresivo (Sellmeijer y cols., 2018). Estos datos, están respaldados por resultados obtenidos mediante un registro ex vivo de Patch-Clamp en el que se observa un aumento de la transmisión excitadora postsináptica y aumento de la contribución de los receptores NMDA en la CCA (Sellmeijer y cols., 2018). La estimulación optogenética de la CCA induce comportamiento ansio-depresivo en animales naïve sin afectar al umbral mecánico (Barthas y cols., 2015). Además, se ha demostrado que la activación quimiogenética de la vía LC-CPF provoca dolor espontáneo y sintomatología ansiosa y aversión en animales naive (Hirschberg y cols., 2017 elife). Por el contrario, la lesión (usando ácido iboténico) y la inhibición optogenética de la CCA previene o puede aliviar el comportamiento ansiodepresivo sin afectar a la alodinia mecánica (LaBuda y Funchs, 2005; Barthas y cols., 2015), reduce la aversión producida por la inyección intraplantar de formalina o la estimulación mecánica de la pata dañada (Johansen y cols., 2001; LaGraize y cols., 2004). La inhibición de la CCA produce un bloqueo en el componente aversivo del dolor neuropático en la preferencia condicionada

provocada por fármacos analgésicos y disminuye el tiempo de inmovilidad en el test de natación forzada en animales con dolor neuropático crónico (King y cols., 2009; Qu y cols., 2011). Estos datos demuestran que el dolor provoca la activación de la ACC promoviendo de igual manera al desarrollo de conducta ansiodepresiva en animales.

Estudios de resonancia magnética en animales con dolor neuropático han demostrado cambios bilaterales en la CCA asociados con el dolor y la conducta pro-ansiosa a lo largo del tiempo. Entre estos cambios se destacan, alteraciones morfológicas, en el volumen, incremento de la arborización y en la longitud de dendritas de neuronas piramidales basales de la ACC en animales con dolor neuropático durante una semana (Metz y cols., 2009). Es importante señalar que el decremento del volumen en la corteza prefrontal se da un tiempo después de inducir el modelo de dolor y a menudo coincide con el inicio de conducta ansiosas (Seminowicz y cols., 2009).

Estos estudios demuestran que el dolor provoca una activación de la CCA y que parece correlacionarse con la aparición de la sintomatología afectiva asociada (Sellmeijer y cols., 2018). Sin embargo, se desconocen cuáles son los mecanismos fisiopatológicos que intervienen en la comorbilidad dolor-depresión/ansiedad en relación al LC. Teniendo en cuenta que el DNP produce una disfunción en el sistema monoaminérgico y que el LC envía proyecciones noradrenérgicas hacia la CCA (Koga y cols., 2020), sería importante el estudio de la vía noradrenérgica LC-CCAr y su implicación en la sintomatología sensorial y en la aparición de la sintomatología depresiva en un modelo de DNP.

3. HIPOTESIS Y OBJETIVOS

La hipótesis de la presente Tesis doctoral plantea que el dolor neuropático provoca cambios neuroplásticos en las proyecciones noradrenérgicas del LC que influyen de manera negativa en los aspectos sensoriales y emocionales del dolor y además son responsables del desarrollo de sintomatología afectiva asociada. Específicamente, se realizará un estudio de la función del LC en la conducta sensorial y afectiva. Más tarde y de manera específica, se estudiarán vías descendentes y ascendentes del LC que podrían estar involucradas en la comorbilidad dolor-depresión. Entre estas vías descendentes se estudiará la vía noradrenérgica LC-SC y su función en la conducta nociceptiva en los diferentes puntos temporales. Además, se estudiará la vía noradrenérgica LC-DRt para evaluar su implicación en el mantenimiento del dolor, así como su implicación en el desarrollo de conducta pro-depresiva en animales con DNP a largo plazo. Por otro lado, se realizará un estudio de la vía noradrenérgica ascendente del LC hacia la CCAr, para analizar su implicación en la conducta sensorial y afectiva de animales con DNP a largo plazo. En todos los casos, se tendrá en cuenta que la lesión se realiza de manera unilateral, por lo tanto, será indispensable tener en cuenta la lateralidad de las diferentes vías.

Los objetivos específicos son:

Objetivo 1: Evaluar la implicación del LC en los aspectos sensoriales y emocionales del dolor crónico en un modelo animal de DNP a lo largo del tiempo.

Objetivo 3:- Evaluar la actividad de las proyecciones noradrenérgicas descendentes del LC hacía la SC y el DRt en los aspectos sensoriales y emocionales del DNP.

Objetivo 4: Evaluar la implicación de las proyecciones noradrenérgicas ascendentes del LC hacia la CCAr en los aspectos sensoriales y emocionales del DNP.

Objetivo 5: Estudiar la participación de los receptores noradrenérgicos de la CCAr en los aspectos sensoriales y emocionales inducidos por DNP.

4. ANALISIS CRITICO DE LOS ANTECEDENTES

En esta tesis doctoral nos centraremos en el estudio del LC y su función en el procesamiento del dolor. Este núcleo noradrenérgico, además de ser la fuente principal de noradrenalina en el SNC, procesa diferentes funciones, entre ellas el procesamiento del dolor. Existen estudios que apoyan la idea de que la función principal del LC en el procesamiento del dolor es la de "inhibidor del dolor". En cierta manera no es una idea equivocada, aunque incompleta. Se realizará un análisis crítico acerca de lo que conocemos hasta ahora sobre la función de las neuronas noradrenérgicas del LC en el procesamiento del dolor a lo largo del tiempo.

Existen un conjunto de estudios preclínicos que sugieren que los sistemas inhibidores del dolor, que descienden del tronco cerebral, implican una inhibición noradrenérgica de la transmisión nociceptiva espinal (Fields y cols., 1991; Millan, 2002). Actualmente, los tratamientos de primera línea para el dolor clínico son antidepresivos (amitriptilina y duloxetina) y clonidina espinal, pues se piensa que estos agentes farmacológicos mimetizan el mecanismo analgésico noradrenérgico (Dworkin y cols., 2007). En cambio, por razones que aún se desconocen su eficacia ha sido muy decepcionante. Estudios hechos en animales sugieren que la eficacia analgésica, que es bastante potente después de una lesión, se pierde con el paso del tiempo (Llorca-Torralba y cols., 2016). Este fenómeno podría deberse a que la señalización de los receptores noradrenérgicos α2 en la SC no se limita a reducir las respuestas nociceptivas agudas. En el contexto del dolor neuropático, estos fármacos también ejercen una señalización facilitadora opuesta mediada por los receptores α2 (o activación indirecta) a nivel del tronco cerebral, lo que anula la eficacia de los antagonistas noradrenérgicos durante una lesión nerviosa sostenida en el tiempo (Wei y Pertovaara, 2006). El LC, es el núcleo que mayor número de neuronas noradrenérgicas posee en todo el cerebro (aproximadamente 1600 células (Schwarz y Luo, 2015)), podría ser descrito por muchos autores como un "supresor del dolor" (Pertovaara, 2013; Llorca-Torralba y cols., 2016). Sin embargo, otros estudios utilizan modelos estándar de DNP posicionan al LC como un "generador de dolor" (Brightwell y Taylor, 2009; Kaushal y cols., 2016). Con intención de desenmarañar esta controversia se presenta a continuación un análisis crítico sobre lo que hasta ahora conocemos sobre la función del LC en el procesamiento del dolor.

El organismo dispone de unos mecanismos neurofisiológicos que procesan el DNP y su inhibición. Una lesión nerviosa provoca un aumento de la expresión y/o la activación en el SNC de los canales iónicos activados por voltaje y ligando, los receptores peptídicos y los factores neuroinmunes que luego provocan hiperexcitabilidad neuronal en el asta dorsal de la SC (Taylor, 2009). La hiperexcitabilidad se produce por numerosos factores, como las alteraciones

en la actividad de los neurotransmisores excitatorios e inhibitorios locales, junto con la actividad aferente primaria en curso/ evocada, así como el control supraespinal descendente (Taylor, 2009). Los sistemas inhibitorios endógenos supraespinales sirven como influencias compensatorias opuestas y cada vez están siendo más reconocidos debido a su capacidad para frenar la alodinia y la hiperalgesia (Taylor, 2009). Sin embargo, se propone que la excesiva regulación a la baja o la defectuosa regulación al alza compensatoria de estos sistemas durante un largo periodo de tiempo después de la lesión, contribuye al mantenimiento del DNP. Por lo tanto, una estrategia para desarrollar analgésicos nuevos y eficaces para el dolor neuropático es imitar y potencia la neurotransmisión inhibitoria que surge del cerebro. Inicialmente se prestó mucha atención a la capacidad inhibitoria de la médula rostro-ventral (RVM), pero ha resurgido el interés por otros sistemas cerebrales, incluido el LC.

El LC está preparado anatómica y fisiológicamente para ejercer de modulador del dolor agudo y persistente. Es un núcleo heterogéneo y está compuesto por diferentes subdivisiones (módulos de neuronas) a lo largo del eje rostro-caudal y dorso-ventral que se proyectan a otras áreas cerebrales (Mason y Fibiger, 1979). Las neuronas del LC forman una elaborada red de proyecciones ascendentes y descendentes (Grzanna y Molliver, 1980). Los axones ascendentes de las neuronas LC noradrenérgicas se proyectan a regiones específicas del SNC, incluyendo el tálamo, la corteza prefrontal medial, la corteza cingulada anterior, el hipocampo, el hipotálamo, la amígdala y el cerebelo, mientras que los axones descendentes de los subgrupos de células noradrenérgicas en la protuberancia se dirigen al circuito de la vía del dolor en el asta dorsal espinal (Jones y Moore, 1977; Mason y Fibiger, 1979; Westlund y Coulter, 1980; Loughlin y cols., 1986; Westlund y Craig, 1996; Millan, 2002; Panneton y cols., 2011; Agster y cols., 2013). Como ya se ha explicado anteriormente, la NA que recibe el asta dorsal de la SC se deriva de las terminaciones de los axones descendentes provenientes de las neuronas noradrenérgicas provenientes principalmente del LC, pero también de las áras A5 y A7 (Westlund y cols., 1983). Existen estudios, que hacen evidente la activación del LC ante un estímulo doloroso en animales con DNP (Martins y cols., 2015), demostrando un aumento de pCREB y Fos (Brightwell y Taylor, 2009) y con dolor inflamatorio después de la inyección intraplantar de formalina diluida, este último demostró un aumento de la expresión de c-Fos en las neuronas que proyectan hacia la SC; L4-L5 (Howorth y cols., 2009a). Aunque en ausencia de lesiones, un estímulo nocivo aumenta el disparo de las neuronas del LC (Hickey y cols., 2014).

Se ha demostrado que las proyecciones noradrenérgicas descendentes del LC proporcionan inhibición endógena del DNP. Las proyecciones noradrenérgicas descendentes fueron descritas anatómicamente en ausencia de lesiones (Westlund y Coulter, 1980; Kwiat y Basbaum, 1992) y

fueron caracterizadas neurofisiológicamente como inhibidoras del dolor por Jones y Gebhart (1986, 1987), e informaron que la actividad eléctrica del LC reducía la actividad provocada por el estímulo térmico de las neuronas del asta dorsal en ratas anestesiadas. En estudios realizados posteriormente se ha demostrado que la activación tónica o transitoria de los núcleos cerebrales noradrenérgicos pontoespinales reduce la nocicepción aguda (Martin y cols., 1999; Millan, 2002). Sin embargo, se ha descrito que el agotamiento de NA mediante las lesiones provoca un aumento de las respuestas de estimulación nociva en ratas sin lesión dolorosa. Este fenómeno contradice la idea de que la transmisión noradrenérgica tónica tiene un efecto en estados de dolor no patológico (Jasmin y cols., 2003; Hayashida y cols., 2012).

A pesar de esto, la idea de que el LC es capaz de activar sistemas que promueven la inhibición de la nocicepción persistente que surge tras una lesión tisular o nerviosa, está generalmente aceptada. De hecho, hay evidencias que demuestran que las lesiones del LC y subcoeruleus aumentan la respuesta neuronal del asta dorsal de la SC y el comportamiento inducido por la inflamación a la estimulación térmica (Tsuruoka y Willis, 1996a, b; Wei y cols., 1999; Tsuruoka y cols., 2003). Un estudio realizado en el laboratorio de Pickering demostró que la inhibición quimogenética de las neuronas noradrenérgicas pontoespinales (no se especificó la contribución del LC) aumenta la hipersensibilidad al calor (pero no mecánica) en un modelo de dolor inflamatorio. Además, demostró un aumento de los niveles de c-Fos en el hasta dorsal de la SC después de la inyección intraplantar de formalina diluida (Howorth y cols., 2009b). Martin y cols., (1999) y Taylor y cols. (2000) descubrieron que la destrucción selectiva de las neuronas noradrenérgicas mediante la administración intratecal o intracerebroventricular de la neurotoxina saporina conjugada con la antidopamina-beta-hidroxilasa (anti-DbH-saporina) reducía, en lugar de aumentar, la nocicepción inducida por la formalina. En su momento, estos resultados fueron bastante inesperados, y sugirieron que la LC podría cumplir una función facilitadora del dolor. Aun no se conoce bien la función del LC en la modulación del dolor inflamatorio, pero si existe un consenso en cuanto a la función del LC como inhibidor de la retroalimentación dolorosa en DNP. La lesión de las neuronas noradrenérgicas descendentes mediante la administración intratecal de anti-DbH-saporina produjo un aumento de la hipersensibilidad mecánica tras una lesión nerviosa (Jasmin y cols., 2003; Hayashida y cols., 2012). Además, la administración de agonistas de los receptores noradrenérgicos a2 provocó una reducción de los signos de DNP en animales, pero también en humanos (Baba y cols., 2000; Kawasaki y cols., 2003). La inyección intratecal del antagonista de los receptores adrenérgicos α2 yohimbina produjo hiperalgesia en la extremidad contralateral a la transección del nervio tibial, así como la expresión de Fos en el asta dorsal,de la SC. Lo que sugiere que la inhibición

noradrenérgica pontospinal enmascara la hiperalgesia contralateral (Hughes y cols., 2013). Este mecanismo está probablemente restringido a la SC.

Una lesión nerviosa provoca diferentes cambios a nivel neuroplásticos (como la liberación de BDNF en las fibras noradrenérgicas descendentes) (Hayashida y cols., 2008a) y aumenta la eficacia del acoplamiento de la proteína G a los receptores noradrenérgicos α2 espinales (Bantel y cols., 2005). En este caso y como se ha detallado anteriormente, se ha descubierto que la perdida de eficacia antihiperalgésica de la Gabapentina con el tiempo después del DNP, se debe a una disminución de la expresión de los receptores GLT-1 después de varias semanas de lesión (Kimura y cols., 2016). Sin embargo, no todos los estudios están de acuerdo con el principio de que la lesión nerviosa se asocia necesaria y únicamente con un aumento del control noradrenérgico descendente inhibidor del dolor. Hay estudios que indican la existencia de un déficit en la actividad del sistema noradrenérgico descendente en modelos de DNP. La antinocicepción espinal inducida por la estimulación eléctrica del LC fue significativamente más débil en los animales con lesiones nerviosas que en los de control (Viisanen y Pertovaara, 2007). Además, la lesión del nervio periférico provocó la supresión de la inhibición noradrenérgica espinal mediada por los receptores noradrenérgicos α2 del asta dorsal de la columna vertebral evocada por estímulos mecánicos de baja intensidad (Rahman y cols., 2008). Estos resultados sugieren que la lesión nerviosa puede aumentar la inhibición del LC, suprimiendo así la inhibición noradrenérgica del dolor y promoviendo el DNP. Alternativamente, basado en el hallazgo de que la inyección intratecal del antagonista de los receptores noradrenérgicos α2, la yohimbina, suprimió la hiperalgesia sólo cuando se inyectaba en los primeros de tiempo después de la SNI (días 3-5), pero tuvo poco efecto en la hiperalgesia establecida cuando se administraba en momentos posteriores de tiempo (días 10-17). La contribución del control noradrenérgicos descendentes de inhibición del dolor puede ser transitoria, restringida a los primeros periodos de dolor neuropático (Hughes y cols., 2013).

Por otro lado, aunque la actividad del LC se ha asociado predominantemente a la inhibición del DNP, existen estudios que han demostrado la existencia de otras proyecciones descendentes y ascendentes del LC que contribuyen al mantenimiento o facilitación del DNP, sobre todo en momentos posteriores a la lesión. Un estudio de Brightwell y Taylor evaluaron la respuesta de alodinia en animales dos semanas después de inducir el DNP y después de la microinyección en LC de lidocaína (Brightwell y Taylor, 2009). La lidocaína redujo todos los signos conductuales de dolor neuropático de forma reversible, lo que sugiere que el LC contribuye a la facilitación del dolor. En otro estudio, realizando una inyección intracerebroventricular de anti-DbH-saporina 3 semanas después de inducir DNP, redujo los signos de comportamiento de hipersensibilidad mecánica durante al menos 1 mes después del inicio del tratamiento (Kaushal

y cols., 2016). En conjunto, estos datos indican que la LC facilita tanto el desarrollo como el mantenimiento del DNP tras la lesión de los nervios ciático o trigémino (Brightwell y Taylor, 2009; Kaushal y cols., 2016). Sin embargo, dado que la inyección intracerebroventricular de anti-DbH-saporina interrumpe tanto las vías noradrenérgicas ascendentes (por ejemplo, A1 y A2) como las descendentes (A5, A6, A7), se necesitan más estudios para determinar si el LC contribuye a la alodinia o la hiperalgesia a través de las proyecciones ascendentes, las proyecciones laterales a otros sitios del tronco encefálico o las proyecciones descendentes a la SC. Actualmente, ya hay ciertos estudios que están empezando a contestar a algunas preguntas.

Como ya se ha detallado en el apartado de introducción, un circuito conocido por su importante papel en la facilitación del dolor es el que está compuesto por el LC, DRt y la SC. De hecho, las manipulaciones locales en el DRt que disminuyen los niveles de noradrenalina (con la administración de vectores virales retrógrados de TH) o que aumentan los niveles de noradrenalina (con el inhibidor de la recaptación nomifensina) atenúan o aumentan los comportamientos nociceptivos inducidos por el dolor neuropático, respectivamente (Martins y cols., 2010, 2013). La microinyección del antagonista del adrenoceptor α1 prazosin, pero no del antagonista del adrenoceptor α2, disminuyó la hipersensibilidad inducida por el SNI a la estimulación mecánica o fría nociva, lo que indica que los α1- pero no los α2-adrenorreceptores median la facilitación del dolor desde el DRt (Martins y cols., 2015). Estos datos demuestran que la inervación noradrenérgica está implicada en el desencadenamiento de la facilitación descendente del dolor desde el DRt (Martins y cols., 2010, 2013) y plantean la interesante idea de que el LC ejerce un efecto pronociceptivo indirecto debido a sus proyecciones al DRt (Martins y cols., 2013). Por este motivo, se ha planteado, en esta tesis doctoral el estudio de esta vía, con la intención de dilucidar su función bilateral o unilateral en la respuesta nociceptiva de animales con DNP.

Además, el LC parece provocar la facilitación del dolor a través de las vías noradrenérgicas ascendentes. Una de las principales vías noradrenérgicas ascendentes del LC incluye la proyección a la CPFm (Aston-Jones y cols., 1984; Aston-Jones y Cohen, 2005), un importante sitio de activación en pacientes con dolor crónico. En roedores, la estimulación eléctrica unilateral del LC provoca una activación bilateral y sostenida de la CPFm (Marzo y cols., 2014). En un estudio anterior, para determinar la contribución de las proyecciones del LC hacia mPFC al DNP, se microinyectaron antagonistas de los receptores noradrenérgicos α1 y α2 (benoxathian y clorhidrato de idazoxan, respectivamente) directamente en la CPFm para bloquear los efectos de la entrada noradrenérgica (Kaushal y cols., 2016). El benoxathian, pero no el vehículo ni el idazoxan, aliviaron la hipersensibilidad mecánica asociada al DNP, lo que sugiere que los receptores noradrenérgicos a1 de la CPFm contribuyen al efecto facilitador de

las neuronas noradrenérgicas del LC en el dolor neuropático orofacial crónico (Kaushal y cols., 2016).

El LC regula numerosas funciones interconectadas interrelacionadas, como la atención, los ciclos de sueño y vigilia, el rendimiento cognitivo y la motivación (Berridge y Waterhouse, 2003; Jones, 2003; Sara, 2009). Pickering y sus colegas plantearon la hipótesis de que las acciones pronociceptivas del LC pueden estar mediadas por un subconjunto de neuronas que también son responsables de promover la vigilia y la atención (Carter y cols., 2010), como parte de un sistema para enfocar los recursos cognitivos (Hickey y cols., 2014); de hecho, el circuito LC-CPFm optimiza las funciones cognitivas relevantes para el comportamiento (Aston-Jones y Cohen, 2005; Marzo y cols., 2014). Por ejemplo, los acontecimientos internos o externos destacados pueden alterar la función o "reiniciar" poblaciones neuronales a gran escala. Esto puede estar mediado por la liberación selectiva de noradrenalina en la CPFm y puede cambiar el equilibrio excitatorio/inhibitorio de la CPFm a un estado más excitable. Por lo tanto, especulamos que una lesión cambia la modulación del dolor dentro del circuito noradrenérgico LC-CPFm de la inhibición a la excitación. De tal manera que, para ayudar para ayudar a la recuperación homeostática e inhibición del dolor, el exceso de estrés y la liberación de noradrenalina cambia la unión noradrenérgica a los receptores noradrenérgicos α1, en vez de a los receptores noradrenérgicos α2. Los receptores α1 son de menor afinidad que los α2, lo que provocaría la facilitación del dolor y su cronificación. Por este motivo y como se ha planteado anteriormente, será interesante estudiar la función de los receptores α1 y α2 de la corteza cingulada anterior en animales con DNP en la respuesta nociceptiva pero también en la conducta emocional inducida por el dolor crónico.

Por lo tanto y teniendo en cuenta todo lo comentado anteriormente, se propone que durante la activación intensa o prolongada después de una lesión nerviosa las vías descendentes de modulación del dolor desde el LC hacia el DRt, la SC, así como las vías moduladores del dolor ascendentes del LC a la CPFm se vuelven predominantemente facilitadores promoviendo la cronificación del dolor. En ausencia de lesiones, Pickering y sus colegas utilizaron un enfoque optogenético para revelar una modulación bidireccional de las respuestas neuronales en la LC a los estímulos de calor (Hickey y cols., 2014). Concluyeron que las acciones pronociceptivas y antinociceptivas están mediadas por subpoblaciones distintas de neuronas del LC, y que el efecto antinociceptivo se origina en las neuronas de la región ventral del LC y del subcoeruleus que se proyectan al asta dorsal de la SC (Westlund y cols., 1983; Loughlin y cols., 1986; Howorth y cols., 2009a; Bruinstroop y cols., 2012, Hirschberg y cols., 2017). Esto implica que los efectos pronociceptivos se originarían en neuronas localizadas más dorsalmente en el LC.

Es bien sabido que el LC está compartimentado dentro de su extensión rostrocaudal: las neuronas noradrenérgicas descendentes se localizan principalmente en la LC caudal, mientras que las ascendentes se originan principalmente en la LC más rostral (Jones y Moore, 1977; Millan, 2002). Aunque es muy probable que las neuronas del LC localizadas caudalmente y proyectar espinalmente el LC envíen proyecciones colaterales a sitios supraespinales como la CPFm, o que las neuronas dorsales que proyectan rostralmente envían colaterales a sitios espinales como el asta dorsal (Guyenet, 1980; Leanza y cols., 1989; Howorth y cols., 2009a). Además, como se ha señalado anteriormente la lesión del nervio periférico se asocia con la activación de neuronas localizadas tanto caudalmente como rostralmente dentro del LC (Brightwell y Taylor, 2009). Una comprensión incompleta de las influencias multinivel a lo largo de la extensión rostrocaudal del LC durante el procesamiento del dolor y su impacto multirreceptor resultante en los sistemas del SNC ascendentes y descendente del SNC plantea un problema especialmente interesante, aunque difícil, para futuras investigaciones.

De manera general, entre las proyecciones noradrenérgicas del LC se han encontrado evidencias que demuestran que existen proyecciones noradrenérgicas descendentes del LC que proporcionan inhibición endógena del dolor neuropático y proyecciones noradrenérgicas que facilitan el dolor neuropático. La cuestión que se plantea es, ¿Cómo un mismo núcleo puede realizar dos funciones opuestas?. Pues se ha sugerido la posibilidad de que se den ambas funciones, pero en diferentes momentos de la neuropatía (Taylor y Westlund, 2017). Partiendo de la idea de que, aunque el LC es un núcleo compuesto por una gran cantidad de neuronas noradrenérgicas, trabajaría por módulos neuronales, capaces de trabajar al mismo tiempo efectuando diferentes funciones. Además, se ha de tener en cuenta la sugerencia que se ha hecho anteriormente, en la que se pone de manifiesto que la función inhibitoria del LC en DNP puede desplazarse con el tiempo, provocando en un inicio de una inhibición profunda mediada por proyecciones descendentes del LC ventral al núcleo DRt y las astas dorsales y terminando con la cronicidad del dolor mediada por proyecciones cerebrales del LC dorsal a la CPFm. A este cambio hacia la facilitación del dolor contribuye claramente al mecanismo subyacente de la transición del dolor agudo al dolor crónico (Taylor y Westlund, 2017). La contribución de los sistemas noradrenérgicos centrales a la de la modulación del DNP ha atraído una considerable atención, ya que los inhibidores de la recaptación noradrenérgica, como la duloxetina son a veces eficaces (Brecht y cols., 2007) y se encuentran entre los fármacos más recetados para tratar el dolor crónico (Sindrup y cols., 2005; Attal y cols., 2010). Sin embargo, los receptores noradrenérgicos α2 del LC ya no pueden considerarse una diana "pura" para la modulación inhibitoria del dolor. Las acciones inhibidoras del dolor de los fármacos antidepresivos que se consiguen con concentraciones elevadas de noradrenalina en el asta dorsal de la SC pueden

oponerse a la activación simultánea de los sistemas facilitadores supraespinales dependientes de los receptores noradrenérgicos α1 en el DRt y la CPFm (Kaushal y cols., 2016) y de los receptores noradrenérgicos α2 en el LC (Wei y Pertovaara, 2006). De hecho, estas acciones opuestas pueden explicar, en parte, la limitada eficacia de los antidepresivos tricíclicos y los inhibidores de la recaptación de noradrenalina en el tratamiento del dolor crónico (Finnerup y cols., 2015). El reconocimiento del componente facilitador del dolor del LC acelerará el desarrollo de terapias más eficaces dirigidas a los receptores noradrenérgicos α1 y α2 para el tratamiento del DNP. Por este motivo, en esta tesis doctoral nos centramos en el estudio de los diferentes módulos neuronales del LC que proyectan hacia otras áreas y en su función en el procesamiento del dolor en las diferentes fases temporales. Así como evaluar el papel que juega los diferentes receptores noradrenérgicos en las diferentes áreas diana en la respuesta nociceptiva y afectiva inducida por el dolor crónico.

3. MATERIAL Y MÉTODOS

5.1. Animales de uso experimental

Para realizar los diferentes estudios se utilizaron dos cepas wild-type de ratas macho con un peso de 250-350g, Sprague-Dawley (SD) y Long-Evans (LE) y ratas transgénicas TH-Cre 3.1.Deis (donadas por el Dr. K. Deisseroth; Centro de recursos e investigación de ratas; Rat Resource and Research Center (RRCC, USA)) que expresan la recombinasa Cre en neuronas TH. Los animales estuvieron estabulados en las instalaciones del Departamento de Neurociencias y en las instalaciones de los Servicios centrales de Experimentación y Producción Animal (SEPA) de la Universidad de Cádiz manteniendo condiciones *standard* de laboratorio (disposición de agua y comida *ad libitum*, periodos de luz/oscuridad de 12 horas de duración (luz a partir de las 8a.m.) y temperatura ambiente de 22 ±1 ºC). Todos los procedimientos, así como la manipulación de animales se llevaron a cabo según las directrices de la Directiva de la Comisión Europea (2010/63/ CE) y el Real Decreto español (RD 53/2013) sobre la protección de los animales utilizados en experimentación y otros fines científicos. Además, se siguieron las "recomendaciones éticas en investigaciones de dolor experimental en animales conscientes" de Zimmerman (1983). El Comité de Ética de la Universidad de Cádiz aprobó todos los procedimientos experimentales.

5.2. Modelo de dolor crónico: Constricción crónica del nervio ciático

Se utilizó como modelo de dolor crónico la constricción crónica del nervio ciático o ligadura laxa (en inglés, *Chronic constriction injury*; CCI) descrita previamente por Bennet y Xie (Bennet y Xie, 1988) (Figura 6). Este modelo reproduce muchos de los síntomas sensoriales del dolor neuropático: hiperalgesia (incremento de la sensación de dolor ante un estímulo nociceptivo), alodinia (hipersensibilidad a estímulos mecánicos y térmicos inocuos) y dolor espontáneo. Los síntomas son evidentes desde las 48 horas después de la cirugía y se mantienen alrededor de dos meses. Este modelo es uno de los más utilizados en investigación del dolor crónico ya que guarda una buena relación con el dolor clínico y muestra alta reproducibilidad entre laboratorios.

Por lo que se refiere al procedimiento quirúrgico, las ratas fueron anestesiadas con isofluorano. La inducción anestésica se realizó a una concentración de entre el 3 y 4% y para el mantenimiento se utilizó al 1.5-2.5% de isofluorano. Se realizó una incisión de

aproximadamente 3 cm en el bíceps femoral y el nervio ciático izquierdo se expuso aproximadamente a mitad de muslo, junto a la trifurcación del nervio ciático. Se liberó aproximadamente 7 mm de nervio adherido a tejido contiguo y se procedió a realizar 4 ligaduras con catgut cromado 4/0 (softcat, B.Braun, España) y dejando una distancia próxima a 1mm entre ligaduras, la longitud del nervio afectado fue de entre 5-6 mm (Figura 6). Las ligaduras se realizaron con mucho cuidado, apretando lo suficiente sin cortar la irrigación sanguínea. Finalmente se cerró la incisión por capas. En primer lugar se realizó la sutura del músculo con seda trenzada estéril no absorbible 4/0 (Silkan, B.Braun, España) y la piel con seda 2/0 (Silkan, B.Braun, España). Los animales sham fueron sometidos al mismo procedimiento quirúrgico a excepción de la ligadura del nervio. Los animales que presentaron alguna anomalía, como la autotomía (mutilación) de al menos una falange de la pata operada fueron excluidos de los estudios y posteriormente sacrificados con la intención de cumplir con las normas éticas que impone el estudio del dolor (Berrocoso y cols., 2007). Se utilizará la nomenclatura de "pata ipsilateral" a la pata izquierda que ha sido operada y "pata contralateral" a la que no ha tenido intervención quirúrgica.

En los estudios que componen esta tesis doctoral evaluamos los siguientes puntos temporales después de inducir la neuropatía: corto plazo (2 días: CCI-2d), medio plazo (7 días: CCI-7d) y largo plazo (30 días: CCI-30d).

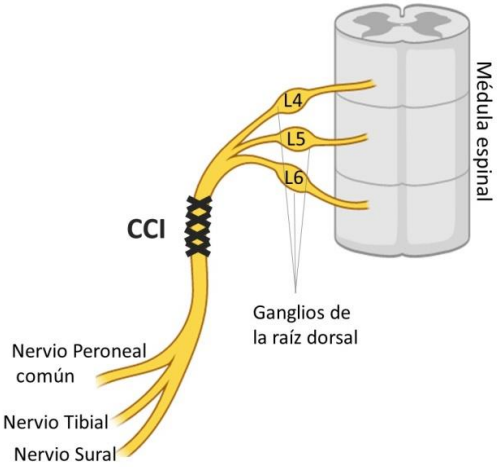

Figura 6. Esquema de la constricción del nervio ciático y sus inervaciones. Ilustración de la colocación de las ligaduras en el nervio ciático en el modelo de CCI, que se encuentra entre las aferencias primarias y las ramas terminales de la zona lumbar de la SC. *Imagen creada en BioRender (www.BioRender.com).*

5.3. Evaluación de la conducta nociceptiva

Antes de comenzar cualquier test de conducta los animales fueron habituados a la sala durante 20 minutos (temperatura ambiente de 22 ±1 ºC).

5.3.1. Test de la acetona

La evaluación de la hipersensibilidad al frío se realizó el test de la Acetona (Bravo y cols., 2012). Los animales fueron individualizados en cajas de Plexiglás (5.5 x 8 cm) (18.5 × 21.0 × 13.5 cm^3) colocadas sobre un suelo de rejilla elevada (9 cm) y fueron habituados durante 20 minutos al paradigma antes de llevar a cabo el test. Una vez habituados, se aplicó una gota de acetona (100 µl) con una pipeta en la superficie plantar de las patas traseras. Se tomaron 4 medidas alternativas en cada pata en intervalos de 5 min y se evaluó la respuesta durante 1 min después de la aplicación. A continuación, se presenta la escala de respuesta: 0. Sin respuesta; 1, retirada brusca; 2, sacudida repetida de la pata; 3, sacudida y lameteo repetido de la pata. El "Acetone Score" para cada pata se calculó a partir de la media de los cuatro ensayos. El aumento de respuesta fue un indicativo de hipersensibilidad al frío. El test de la acetona se realizó antes y después de cualquier tratamiento.

5.3.2. Test de von Frey

Utilizando el mismo paradigma para individualizar y habituar a los animales que en el test de la acetona se evaluó la hipersensibilidad mecánica usando la versión automática del test de von Frey (Modelo 37 450-001, Dynamic plantar Aesthesiometer; Ugo Basile, Italia) (Berrocoso y cols., 2011). Se colocó un filamento de manera perpendicular a la superficie plantar de las patas traseras y se aplicó una fuerza constante y creciente de 0 a 50 g durante un periodo máximo de 20 s. Se tomaron dos medidas en cada pata y posteriormente se hizo la media de ambas. El umbral nociceptivo para cada animal se determinó como la fuerza que produjo una respuesta de retirada de la pata, con un límite de 50g. Se considera hipersensibilidad mecánica a la disminución en la fuerza tolerada por el animal. El test de von Frey se realizó antes y después de los tratamientos farmacológicos.

5.3.3. Test de dolor espontáneo

Para analizar la evaluación del dolor espontáneo se realizó una modificación en el paradigma del test de von frey, en el que se utilizaron compartimentos de dimensiones más grandes (18.5 × 21.0 × 27.5 cm^3) para facilitar el libre movimiento de los animales, y debajo se colocó una

cámara para grabar la sesión. Fueron introducidos en el test durante 20 minutos de los cuales sólo los últimos 5 minutos fueron analizados. Se cuantificó el número de levantamientos y retrocesos de ambas patas traseras. Un incremento en el número de levantamientos y retrocesos de la pata dañada se definió como un aumento del dolor espontáneo (Hirschberg y cols., 2017). El test de dolor espontáneo se realizó después de los tratamientos.

5.3.4. Test de presión de la pata

Esta prueba (Paw pressure) se usó para evaluar la hiperalgesia mecánica (Ugo Basile, Italia) (Randall y Sellito, 1957). Se presionó la superficie lateral plantar de las patas traseras con un cono de metacrilato invertido de punta roma con una fuerza creciente de manera constante de 0 a 250g hasta que el animal retira la pata. Se definió como grado de hiperalgesia mecánica la fuerza registrada de retirada (Berrocoso y cols., 2007). La disminución de la fuerza soportada por los animales indicó hiperalgesia mecánica. El test presión de la pata se realizó antes y después de los tratamientos.

5.3.5. Test de la placa fría

Se utilizó esta prueba para evaluar la hipersensibilidad al frío (Berrocoso y cols., 2007). Los animales se colocaron individualmente sobre una placa de metal (25 x 25 cm) a una temperatura constante de 4ºC ±1 y cubierta por la caja de Plexiglás transparente (25 x 25 x 25 cm) (Panlab S. L., España). Se cuantificó el número de veces que los animales levantaron bruscamente la pata trasera izquierda durante un periodo de 2min. La hipersensibilidad al frío se definió en esta prueba como un aumento del número de retiradas de la pata. El test de la placa fría se realizó después de los tratamientos.

5.3.6. Test de actividad locomotora (actimetría)

Esta prueba se utilizó para evaluar la libre deambulación exploratoria de los animales y si algunos de los compuestos utilizados en los diferentes estudios tenían efecto estimulante, sedante o de deterioro motor. Los animales fueron colocados individualmente durante 40 minutos en cajas de Plexiglás (40 x 4 cm). Para analizar la conducta se utilizó un sistema de

video-tracking; Registro y seguimiento espontáneo de la actividad motora (en inglés, *Spontaneous Motor Activity Recording and tracking*; SMART) (v3.0 Panlab S.L., España). La medida de % de la distancia total recorrida (UA, Unidades arbitrarias) fue el indicador de actividad locomotora (Llorca-torralba y cols., 2019).

5.4. Evaluación de la conducta pro-depresiva.

5.4.1. Test de natación forzada modificado

El comportamiento tipo depresivo se evaluó en la prueba de natación forzada modificada (en inglés modified forced swimming test; mFST). Este test fue desarrollado inicialmente por Porsolt y sus colaboradores (Porsolt y cols., 1978), pero en 1995 fue modificado por Detke y Lucki (Detke y cols., 1995). Debido a su buena validez predictiva, este test se usa como estrategia para identificar mecanismos antidepresivos. En este paradigma se evalúa la respuesta lucha-huida, ya que el animal se somete a una situación problemática sin solución aparente y tiene que elegir entre buscar una solución al problema o rendirse y esperar que se solucione por sí mismo. Después de introducir al animal en el cilindro, por lo general, muestran una conducta activa del tipo escalada o natación y más tarde una conducta pasiva o de inmovilidad (figura 7). El comportamiento de inmovilidad implica un fracaso de la persistencia en el comportamiento de huida después del estrés o desesperación conductual, que se trata de un síntoma característico en pacientes que sufren depresión. En estudios anteriores se ha demostrado que este test puede discriminar cambios catecolaminérgicos y serotoninérgicos basados en si el movimiento predominante de escalada o natación. Así, antidepresivos catecolaminérgicos aumenta selectivamente el comportamiento de escalada, mientras que agentes serotoninérgicos aumentan selectivamente el comportamiento de natación (Detke y cols., 1996; Lucki 1997; Cryan y cols., 2002; Cryan y cols., 2005).

Los animales se colocaron individualmente en un cilindro de plexiglás (altura 40 cm, diámetro 18 cm) lleno a una profundidad de 30 cm con agua a 25 ± 1 ° C durante dos sesiones diferentes. Se realizó un pre-test de 15 min y 24 h después un test de 5 min, ambas sesiones fueron grabadas y en la sesión del test se evaluó el comportamiento predominante (inmovilidad (IM), escalada (CL) o natación (SW)) utilizando un software específico creado en nuestro laboratorio (Red-Mice, España). Este software mide la conducta que predomina cada 5 s en un ensayo de 300s, y proporciona un total de 60 medidas (Figura 7).

La conducta de escalada se definió como movimientos enérgicos de las patas delanteras dentro y fuera del agua y junto a la pared del cilindro. La conducta de natación se consideró movimiento predominante cuando el animal se movía en horizontal, a lo largo del cilindro incluyendo los

cruces de cuadrantes. La conducta de inmovilidad se definió por la ausencia de actividad salvo los movimientos mínimos y necesarios para mantener la cabeza fuera del agua. Un incremento de la conducta de inmovilidad se definió como comportamiento pro-depresivo.

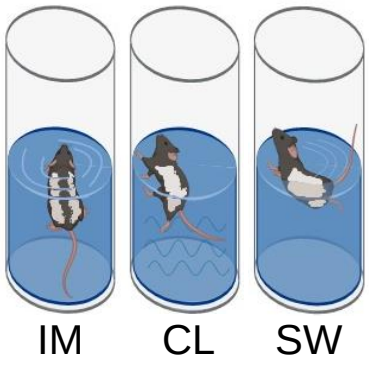

Figura 7: Test modificado de natación forzada.

Ilustración que muestra como las ratas son introducidas en un cilindro llenos de agua hasta 30 cm. Se mide la conducta predominante de: inmovilidad, escalada o natación durante 2 sesiones (pre-test y test) en dos días consecutivos. Ambas sesiones fueron grabadas por una cámara. IM: Immobility, CL: Climbing y SW: Swimming. *Imagen creada en BioRender (www.BioRender.com).*

5.5 Implantación de cánulas en LC y CCAr para estudio farmacológico

Para llevar a cabo la implantación de cánulas de acero inoxidable (22ga, 0.7 x 30 mm) los animales fueron inicialmente anestesiados con un mix de ketamina/xilacina, posteriormente fueron colocados en el aparato estereotáxico (Korpf Instruments, EE.UU.) y se procedió a la implantación de cánulas de manera unilateral en LC o bilateral en CCAr (tabla 1: consultar coordenadas de implantación de cánulas). Las cánulas fueron fijadas al cráneo con cemento poliacrílico y 3 tornillos de acero inoxidable. Posteriormente se introdujo un alambre de acero inoxidable a través de la cánula para evitar la obstrucción y se mantuvo puesto hasta la realización de los test de conducta.

Tabla 1: Coordenadas de implantación de las cánulas y de administración de fármacos

Área	*Lateralidad respecto CCI*	*Coordenadas*	*Coordenadas administración de fármacos*	*Estudio*
LC	Contralateral	AP: +3.2; ML: -1.3; DV: 6.1 (Lambda) α = -15º	DV: 6.2	I y II
LC	Ipsilateral	AP: +3.2; ML: +1.3; DV: 6.1 (Lambda) α = -15º	DV: 6.2	II
CCAr	Bilateral	AP: +3.0; ML: ±1.0; DV: 1.1(Bregma) α = -2º	DV: 1.2	II

3.5.1. ESTUDIO I: Se realizó la administración de lidocaína intra-LC (LC ipsilateral y LC contralateral) para evaluar la implicación del LC en la conducta sensorial y afectiva en ratas SD. Se evaluó la respuesta sensorial durante los diferentes tiempos de la neuropatía y el análisis de la conducta afectiva se realizó solamente durante la fase más tardía del DNP.

3.5.2. ESTUDIO II: Se realizó la administraron de prazosin, idazoxan o propranolol intra-CCAr para evaluar la implicación de los diferentes receptores adrenérgicos (α1, α2 y β1-2 respectivamente) en la conducta sensorial y afectiva de ratas LE con DNP a largo plazo.

Para la administración de los diferentes fármacos (tabla 2: consultar mecanismo de acción, dosis y lugar de administración de los fármacos) se inmovilizaron a los animales, se extrajo el alambre y se introdujo una aguja de administración con una longitud de 1 mm mayor que la cánula guía (16 mm). La aguja de administración se conectó a una jeringa mediante un tubo de polietileno (0,68 mm de diámetro) a una jeringa Hamilton de 10µl y el fármaco se administró durante 30s. Para evitar el reflujo se esperó 1 min para sacar la aguja de administración.

Tabla 2: Mecanismo de acción, dosis y lugar de administración de los fármacos

Fármacos administrados

Fármaco	Mecanismo de acción	Dosis	Lugar administración	Estudio	Casa comercial
Clorhidrato de lidocaína	Bloqueante de los canales de Na+	4% /0.5 µl	LC unilateral	I	
Clozapina-N-Oxidada (CNO)	Ligando exógeno de receptores DREADDs	1mg/kg	Intraperitoneal (i.p.)	I	Carbosynth, Reino Unido
		3µM/20µl	Intratecal (i.t.)	II	
		3µM/0.5µl	CCAr bilateral	II	
Clorhidrato de Clonidina	Agonista selectivo α2	20µg/10µl	Intratecal (i.t.)	I	Sigma-Aldrich, España
Clorhidrato de Prazosin	Antagonista selectivo α1	5µg/0.5µl	CCAr bilateral	II	Sigma-Aldrich, España
Clorhidrato de Idazoxan	Antagonista selectivo α2	9µg/0.5µl	CCAr bilateral	II	Sigma-Aldrich, España
Clorhidrato de Propranolol	Antagonista no selectivo β 1 y 2	1 µg/0.5µl	CCAr bilateral	II	Sigma-Aldrich, España

5.6. Tecnología DREADD (Designer Receptors Exclusively Activated by Designer Drugs)

Esta técnica se basa en un nuevo enfoque farmacogenético que permite controlar de manera selectiva la actividad neuronal en animales en libre movimiento. Esta técnica es una de las mejores herramientas para manipular la actividad de los circuitos cerebrales, así como poblaciones celulares (Gomez y cols., 2017; Dobrzanski y Kossut, 2017).

Los DREADDs “Designer Receptors Exclusively activated by Designer Drugs” son receptores metabotrópicos (muscarínicos) modificados a partir de la proteína original que se acoplan a proteínas G (Gi, Gs, Gq, etc) (Zhu y cols., 2014). Estos receptores responden exclusivamente a ligandos sintéticos. Como ligando exógeno el más utilizado es la clozapina-N-óxido (CNO), metabolito de clozapina inerte e inactivo (Gomez y cols., 2017). Cuando se activan estos receptores se produce un aumento o inhibición de la excitabilidad y tasa de disparo neuronal de

manera específica. Se utilizaron adenovirus asociados dependientes de la recombinasa CRE ya que contienen una secuencia de reconocimiento específica (loxP): AAV2/hSyn-DIO-hM4D(Gi)-mCherry (virus inhibidor), cuyos receptores se acoplan a la vía de señalización Gi-GIRK, precipita la hiperpolarización de la membrana neuronal y con esto la inhibición de la liberación del neurotransmisor (inhibición neuronal) (Arambruster y cols., 2007) y AAV2/hSyn-DIO-rm3D(Gs)-mCherry (virus activador) cuyos receptores se acoplan a la vía de señalización cAMP provocando la despolarización neuronal (*Gene Therapy Center Vctor Core en la Universidad del Norte de Carolina*) (figura 8).

Esta técnica tiene muchas ventajas ya que permite modular selectivamente tipos de células específicas (señalización de receptores acoplados a proteína G; GPCR), no requiere de un equipo específico para poder utilizarla como la optogenética. Se adapta muy fácilmente a la evaluación del comportamiento y es posible disponer de muchos tipos de DREADDs y de animales transgénicos para estudiar diferentes dianas. Actualmente se utilizan nuevos receptores quimiogenéticos que solo responden al ligando exógeno selectivo; como es el CNO, pero no ante los ligandos endógenos como la acetilcolina. Permite, además, realizar diferentes test a lo largo del tiempo (más de un día) debido a que el CNO es soluble en agua y puede ser consumido por el animal sin consecuencias neurotóxicas y permitiendo que no disminuya el efecto en el comportamiento. Las estimulaciones que se realizan mediante el uso de DREADDs son estimulaciones no invasivas (Spangler and Brushas, 2017).

En contraposición, también tiene desventajas, ya que tiene una baja resolución temporal comparada con la optogenética, puesto que se han de esperar al menos 20 minutos después de administrar el CNO para ver los efectos y la optogenética permite activar o dejar de activar mediante el encendido o apagado de la fibra óptica (los efectos son inmediatos). También tiene una resolución espacial baja ya que no permite realizar modulaciones a nivel subcelular de la señalización GPCR (Karunarathne y cols., 2013), aunque si permite la modulación de áreas cerebrales más grandes (Robinson y cols., 2014) o estudiar dos vías simultáneamente con una sola administración de CNO (Aldrin-Kirk y cols., 2016). En la actualidad existe un debate abierto sobre la utilización de CNO como ligando exógeno ya que existen estudios que demuestran que el CNO también ejerce cambios biológicos en animales que no expresaban DREADDs (MacLaren y cols., 2016) o que los DREADDs provocan actividad biológica en ausencia de CNO (Saloman y cols., 2016). Aun así, existen otras alternativas de ligando exógenos de los receptores muscarínicos DREADD que pueden sustituir el uso de CNO, como el componente 21 (Chen y cols., 2015). Estos resultados destacan la importancia que tiene el diseño de un experimento incluyendo los controles adecuados (Spangler and Brushas, 2017). En

los estudios que componen esta tesis doctoral se han planteado los controles oportunos para controlar todas las posibles condiciones.

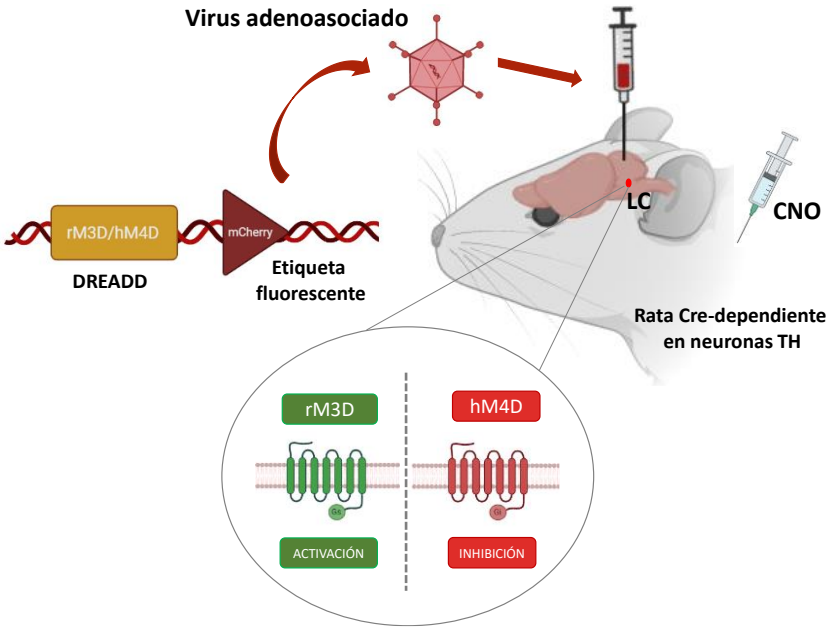

Figura 8. Administración de Virus adenoasociados (AAV) intra LC. La cadena de ADN vírico contiene el vector doblemente floxeada para que sea reconocida por la Cre recombinasa de las neuronas TH del LC. Una vez expresados los receptores (activadores o inhibidores), se podrá modular la actividad de las neuronas TH de manera selectiva mediante la administración de CNO. *Imagen creada en BioRender (www.BioRender.com).*

En los diferentes estudios que componen esta Tesis doctoral se llevaron a cabo diferentes experimentos con la tecnología DREADD para modular selectivamente la actividad del LC y sus vías noradrenérgicas específicas y evaluar la repercusión en la conducta sensorial y afectiva:

5.6.1. ESTUDIO I:

5.6.1.1. Modulación de la actividad de la vía específica LC-DRt

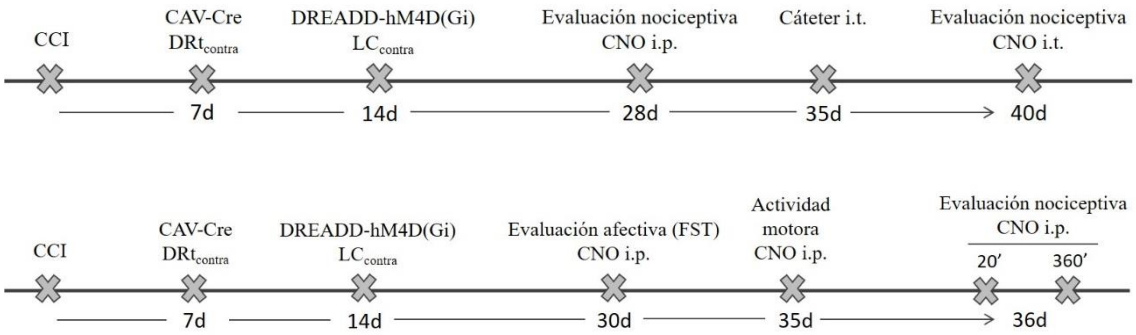

Para evaluar la implicación de la vía específica LC-DRt de ratas Sprague-Dawley en la conducta sensorial y afectiva en primer lugar se administró un adenovirus canino retrógrado (Cre) unilateral intra-DRt contralateral y un adenovirus DREADD inhibidor unilateral intra-LC contralateral.

Las ratas fueron anestesiadas con un mix de ketamina (100 mg/kg: Richter Pharma, España) y xilacina (20 mg/kg: Calier laboratory, S.A., España) y una vez dormidas fueron colocados en un aparato estereotáxico (Korpf Instruments, EE.UU.). Se les rasuró y se desinfectó con iodopovidona el área quirúrgica para evitar infecciones, se les realizó una incisión y se dejó al descubierto el cráneo. Desde lambda se tomaron las coordenadas para DRt y LC teniendo en cuenta la inclinación de la cabeza para cada área y se procedió a la administración de los respectivos vectores virales (Tabla 3: consultar coordenadas, dosis, volumen de administración de los vectores). Después de la inyección, la herida fue limpiada con salino al 0.9% y desinfectada con iodopovidona. Finalmente, se realizó una sutura de la piel con hilo de seda trenzada no absorbible de 4-0 (B.Braun, España).

Las administraciones fueron llevadas a cabo mediante el uso de una bomba de infusión programable (Harvard Apparatus; Pump 11 Elite) y después se esperó un minuto para retirar la jeringa Hamilton para evitar el reflujo de los vectores.

Para esta aproximación experimental, se administró un adenovirus canino retrogrado que contiene una construcción que permite la expresión de Cre-recombinasa fusionada con una proteína verde fluorescente (GFP: CAV2-Cre-GFP). CAV2-Cre-GFP se transporta de forma retrógrada hacia los somas neuronales (tabla 4: consultar vectores virales y trazadores utilizados). Una semana después de la inyección del virus CAV2-Cre en DRt_{contra} se inyectó el virus inhibidor (AAV-Gi-mCherry) o control (AAV-mCherry) en LC_{contra} que es dependiente

de Cre para su expresión (tabla 3). Ambos vectores llevan una proteína fluorescente asociada; mcherry para virus inhibidor o control (587 y 610 nm) y GFP para CAV2-Cre (pico de absorción/emisión 395-475nm) y ambas sirven como control de expresión en la zona de administración (Roth 2017).

Tabla 3: Inyección de vectores virales y trazadores

Área	*Lateralidad respecto CCI*	*Coordenadas*	*Volumen de administración Fluorogold*	*Volumen de administración DREADD*	*Volumen de administración CAV-Cre*	*Estudio*
DRt	Contralateral	AP: 6.2 y 6.6mm, ML: -1.4mm y DV: -8.0 y 8.2mm (Lambda) α = 0º	0.2µl en dos sitios		0.15µl en dos sitios	I
LC	Contralateral	AP: +3.2; ML: -1.3; DV: 6.2 (Lambda) α = -15º		1.4µl		I y II
LC	Ipsilateral	AP: +3.2; ML: +1.3; DV: 6.2 (Lambda) α = -15º		1.4µl		II
LC	Bilateral	AP: +3.2; ML: ±1.3; DV: 6.2 (Lambda) α = -15º		1.4µl/lado		II
CCAr	Ipsilateral	AP: +3.0; ML: -1.0; DV: 1.2 (Bregma) α = -2º	0.2µl			II
CCAr	Bilateral	AP: +3.0; ML: ±1.0; DV: 1.2(Bregma) α = -2º	0.2µl/ lado			II
SC	Ipsilateral	Entre L4 y L6	0.4µl en cuatro sitios (0.1µl/sitio a lo largo de L4-L6)			II

Tabla 4: -Vectores virales y trazadores

Vectores/Trazador	*Información*	*Proteína fluorescente*	*Estudio*	*Casa comercial*
CAV2-Cre-GFP	titer 2.5 x 10^12 pp/m	GFP (Verde)	I	Laboratorio Kremer Montpelier, Francia
AAV-Gi-mCherry (inhibidor)	titer 3 x 10^12 vg/ml	mCherry (rojo)	I y II	Gene Therapy Center Vector Core en la Universidad del Norte de Carolina
AAV-Gi-mCherry (activador)	titer 3 x 10^12 vg/ml	mCherry (rojo)	I y II	Gene Therapy Center Vector Core en la Universidad del Norte de Carolina
AAV-mCherry (control)	titer 5.6 x 10^12 vg/ml	mCherry (rojo)	I y II	Gene Therapy Center Vector Core en la Universidad del Norte de Carolina
Fluorogold	Concentración del 4% en 0.9% (NaCl)		I y II	

Para modular la actividad de la vía específica LC-DRt mediante el uso de DREADDs se administró CNO de manera intraperitoneal (tabla 2). La conducta fue evaluada 20 min después de la administración del CNO.

Para garantizar una buena expresión de los vectores, los estudios comportamentales se realizaron 2 semanas después de la inyección del virus inhibidor o control y 3 semanas después de la inyección del adenovirus canino retrogrado.

5.6.2. ESTUDIO II:

5.6.2.1. Modulación de la actividad global del LC

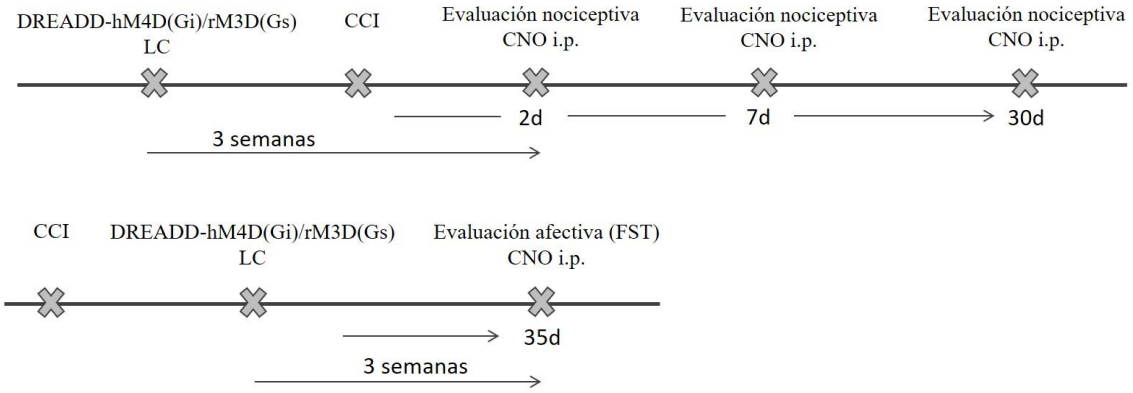

Para evaluar la implicación general del LC en la conducta sensorial y afectiva se utilizó la tecnología DREADD con la administración de diferentes tipos de adenovirus en el LC_{ipsi} o LC_{contra} de ratas LE TH-Cre (inhibidor, activador o control).

Las ratas fueron anestesiadas con un mix de ketamina (100 mg/kg: Richter Pharma, España) y xilacina (20 mg/kg: Calier laboratory, S.A., España) y una vez dormidas fueron colocadas en un aparato estereotáxico (Korpf Instruments, EE.UU.). Se les rasuró y se desinfectó con yodopovidona el área quirúrgica para evitar infecciones, se les realizó una incisión y se dejó al descubierto el cráneo. Desde lambda se tomaron las coordenadas para LC (Tabla 4), teniendo en cuenta la inclinación de la cabeza para cada área para la administración de los vectores virales. Después de la inyección, la herida fue limpiada con salino al 0.9% y desinfectada con iodopovidona. Finalmente, se realizó una sutura de la piel con hilo de seda trenzada no absorbible de 4-0 (B.Braun, España).

La administración fue llevada a cabo mediante el uso de una bomba de infusión programable (Harvard Apparatus; Pump 11 Elite) y después se esperó un minuto para retirar la jeringa Hamilton para evitar el reflujo de los vectores.

Se administraron de manera unilateral en el LC_{ipsi} o LC_{contra} los virus DREADDs inhibidor, activador o control (tabla 4) y fueron activados mediante la administración de CNO de manera intraperitoneal (tabla 2). Los efectos del CNO aparecen 20 minutos después de su administración.

Para garantizar una buena expresión de los vectores, los estudios comportamentales se realizaron 3 semanas después de la inyección del virus inhibidor, activador o control.

5.6.2.2. Modulación de la actividad de la vía específica LC-SC

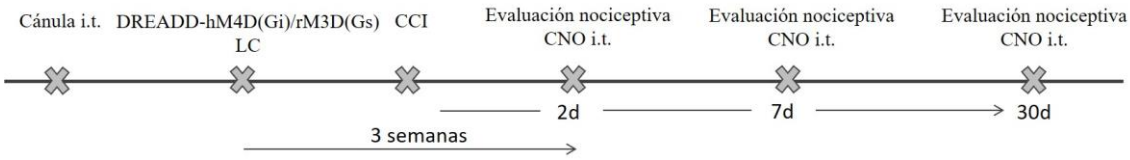

Para evaluar la implicación de la vía específica LC-SC en la conducta sensorial, en primer lugar, se implantó un catéter lumbar en el espacio subaracnoideo espinal y más tarde se administró los virus DREADDs inhibidor o activador de manera unilateral en LC_{ipsi} o LC_{contra} de ratas LE TH:CRE

Tal y como fue descrito previamente por Wei y sus colaboradores en 2014 (Wei y cols., 2014), los animales fueron anestesiados con isofluorano (4% inducción y 2% mantenimiento) y se rasuró y desinfectó el área quirúrgica. A continuación, se realizó una incisión en la piel, a lo largo de la superficie de L6 a L5, unos 5mm laterales a la línea media y 10-15 mm caudal a la línea que une ambas espinas iliacas. Por la incisión, a través de la musculatura dorsolumbar, se introdujo una cánula (20 ga, 0.9 x 40 mm) en dirección craneal ligeramente medial y se desplazó suavemente por la superficie de la vértebra lumbar 6 (VL6) hasta encontrar un aumento de resistencia donde se localiza la vértebra lumbar 5 (VL5). Posteriormente, la punta de la cánula se resituó específicamente en la línea media dorsal y avanzó 3.5 mm por el estrecho espacio intervertebral, entre VL5 y VL6. La colocación correcta de la cánula se confirmó mediante un movimiento de la cola (tail flick), una retracción de la pata o el reflujo de líquido cefalorraquídeo. Se introdujo un catéter de polietileno (0,68 mm de diámetro) por el extremo de la cánula hasta que alcanzó el nivel de la costilla caudal y se retiró la cánula. El catéter se fijó primero en la superficie de la musculatura lumbar y el resto se pasó por vía subcutánea a lo largo de la columna vertebral, apareciendo a través de la piel en la región occipital. Esta forma de colocarlo permitió que se mantuviera intacta durante un largo periodo de tiempo. Después de unos días de recuperación se administró lidocaína (4% / 15 µl) para verificar la correcta colocación de la cánula intraespinal, observando parálisis motora inmediata del tren inferior del animal que duró aproximadamente 10-20 min. Este hecho indicó la correcta colocación del catéter. Los animales que no tuvieron parálisis motora fueron excluidos del estudio.

La administración de los adenovirus se realizó de la misma manera que en el apartado de "**Modulación de la actividad del LC global**". Posteriormente, para modular la actividad de la

vía LC-SC mediante el uso de DREADDs se administró CNO de manera intratecal (tabla 2). Los efectos del CNO aparecen 20 minutos después de su administración.

5.6.2.3. Modulación de la actividad de la vía específica LC-ACC

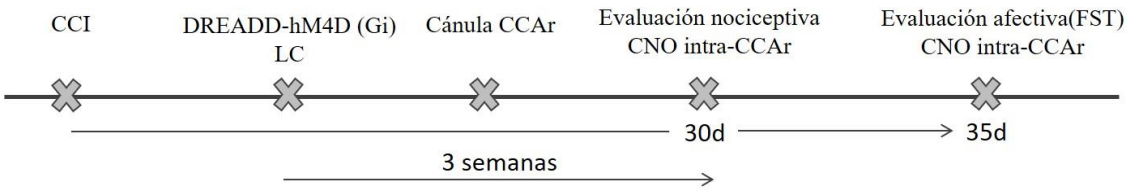

Para evaluar la implicación de la vía específica LC-CCAr en la conducta sensorial y afectiva, en primer lugar se administró el virus DREADD inhibidor de manera bilateral en ambos LC (LC_{ipsi} y LC_{contra}) y más tarde se implantaron cánulas bilaterales en la CCAr de ratas LE TH:Cre.

La administración de los adenovirus se realizó de la misma manera que en el apartado de "**Modulación de la actividad del LC global**". Más tarde, se llevó a cabo la implantación de cánulas en la CCAr (tabla4) siguiendo el procedimiento anteriormente detallado en el apartado **"Implantación de cánulas en LC y CCAr para estudio farmacológico"**.

Para manipular de manera selectiva la actividad de la vía LC-CCAr se administró CNO de manera local intra-CCAr. Para la administración del CNO intra CCAr se inmovilizaron a los animales (tabla 2), se extrajo el alambre y se introdujo una aguja de administración con una longitud de 1 mm mayor que la cánula guía (16 mm). La aguja de administración se conectó a una jeringa mediante un tubo de polietileno (0,68 mm de diámetro) a una jeringa Hamilton de 10µl y el fármaco se administró durante 30s. Para evitar el reflujo se esperó 1 min para sacar la aguja de administración. Los efectos del CNO aparecen 20 minutos después de su administración.

5.7. Estudio neuroanatómico mediante administración de trazador retrógrado

Para evaluar anatómicamente las proyecciones del LC hacía DRt, CCAr y SC se utilizó un trazador retrogrado, Fluorogold (FG) (tabla 4).

5.7.1. Inyección de FG intracerebral

En primer lugar, las ratas fueron anestesiadas con un mix de ketamina (100 mg/kg: Richter Pharma, España) y xilacina (20 mg/kg: Calier laboratory, S.A., España) y una vez dormidas fueron colocados en un aparato estereotáxico (Korpf Instruments, EE.UU.). Se les rasuró y se desinfectó con Yodopovidona el área quirúrgica para evitar infecciones, se les realizó una incisión y se dejó al descubierto el cráneo. Desde lambda se tomaron las coordenadas para las áreas de DRt y CCAr (tablas 3 y 4), para consultar coordenadas, dosis y volumen de administración de trazador) teniendo en cuenta la inclinación de la cabeza para cada área. Después de las inyecciones, la herida fue limpiada con salino al 0.9% y desinfectada con iodopovidona. Finalmente, se realizó una sutura de la piel con hilo de seda trenzada no absorbible de 4-0 (B.Braun, España).

Las administraciones fueron llevadas a cabo mediante el uso de una bomba de infusión programable (Harvard Apparatus; Pump 11 Elite, España) y después se esperó un minuto para retirar la jeringa Hamilton para evitar el reflujo del vector/trazador.

5.7.2. Inyección de FG intracerebral

Las ratas fueron anestesiadas con pentobarbital sódico (50 mg/kg, i.p.: Vetoquinol S.A., España) también se administraron analgésicos locales: Carprofreno (10 mg/kg.: Zoetis, España) y Bupivacaina (2 mg/kg: B. Braun Medical S.A., España). Durante la cirugía fueron necesarias dosis adicionales de pentobarbital para mantener a los animales en el plano analgésico. Para llevar a cabo la administración de FG a nivel lumbar de la SC, se colocaron a las ratas en un aparato estereotáxico y se realizó una laminectomía al nivel de las vértebras T12-L2 para exponer los segmentos L4-L6 de la SC. Se extrajo duramadre y se procedió a la administración de FG (tablas 3 y 4).

El protocolo de administración en este caso se basa en realizar cuatro inyecciones de 0.1µl de volumen total a lo largo del hasta dorsal L4-L6 ipsilateral de la SC. Para ello se utilizó una bomba programable de infusión (Harvard Apparatus; Pump 11 Elite, España) que permitió realizar la administración de manera lenta y controlada a una ratio de de 0.1µl/min. Se esperó un minuto antes de retirar la Hamilton para evitar el reflujo (Revisar tabla 1 para consultar las coordenadas) (David-Pereira y cols., 2017).

Después de la inyección de FG, la piel se cerró con grapas estériles de acero y la herida se limpió con solución salina al 0,9% y se desinfectó con iodopolividona.

En el **estudio I** se analizó las conexiones directas del LC hacía DRt en ratas SD y en el **estudio II** se analizaron las conexiones directas del LC hacía SC y las conexiones del LC hacia CCAr en ratas LE.

5.8 Perfusión y extracción de las muestras

Los animales fueron anestesiados con una dosis letal de pentobarbital sódico (30%) disuelto en salino (NaCl 0.9%). Posteriormente, se realizó una incisión en el abdomen para acceder a la cavidad torácica, exponiendo la cavidad pleural y el corazón. Se insertó una aguja acoplada a un tubo de polietileno a través del ventrículo izquierdo hasta llegar la entrada de la aorta. Seguidamente, a través de la cánula de perfusión conectada a una bomba de infusión, se introdujo 300-400 ml de solución salina (0.9%) en una ratio de 50-55ml/min. Una vez eliminada la sangre del organismo del animal se introdujo una solución de paraformaldehído fría al 4% preparada en tampón fosfato 0.1M (PBS, pH 7.4) para fijar el tejido. Posteriormente, se extrajeron cuidadosamente los cerebros y médulas y se introdujeron en un bote con la misma solución de paraformaldehído durante 2h (post-fijación). Después, se pasaron a una solución crioprotectora compuesta por sacarosa al 30% (p/v) y azida sódica 0.1% en tampón fosfato 0.1M dónde se mantuvieron al menos 2 noches. Finalmente, las áreas de estudio fueron cortadas en secciones de 30 o 40 µm utilizando un criostato (-22ºC) y las diferentes series de secciones fueron conservadas en una solución crioprotectora a -20ºC hasta su procedimiento.

5.9. Inmunohistoquímica

5.9.1. Expresión de mCherry y GFP en las neuronas de LC.

Para verificar la expresión de mCherry y GFP en las neuronas noradrenérgicas que expresan la enzima dopamina beta hidroxilasa (DBH). Todas las secciones de LC fueron incubadas durante 48 horas a 4ºC con un anticuerpo contra la proteína fluorescente roja [5F8] (rat anti-mCherry) y el anticuerpo mouse anti-DBH. Después, los anticuerpos fueron detectados con anticuerpo secundario biotinilado donkey anti-rat el cuál fue visualizado con una estreptavidina 568 o un anticuerpo secundario fluorescente Alexa Fluor donkey anti-mouse 488 (tablas 5-6, para más información sobre los anticuerpos).

Tabla 5: Anticuerpos primarios

Proteína	Especie	Dilución	Casa comercial	Estudio
Anticuerpos Primarios				
5F8 Anti-mcherry	Rat	1:500	Chromotek, Alemania	I y II
Anti-DBH	mouse	1:1000	Merck Chemicals & life science S.A., España	I y II
Anti-TH	Rabbit	1:1000		II
Anti-FG	Rabbit	1:1000	Merck Chemicals & life science S.A., España	I y II
Anti-c-Fos	Rabbit	1:1000	Synaptic System, Alemania	II
Anti- pCREB	Rabbit	1:1000	Millipore, EE.UU.	I
Anti-CREB	Rabbit	1:500	Cell Signaling, EE.UU.	II
Anti-TH	Sheep	1:5000	Abcam, UK	II
Anti-B-actina	Rabbit	1:10000	Sigma-Aldrich Chem., España	II
Anti-α-Tubulina	Mouse	1:10000	Sigma-Aldrich Chem., España	II
Anti-GFP	Rabbit	1:500	Chromotek, Alemania	I
Anti- pCREB	Rabbit	1:1000	Millipore, EE.UU.	I

Tabla 6: Anticuerpos secundarios

Proteína	Especie	Dilución	Casa comercial	Estudio
Anticuerpos Secundarios				
Anti-rat biotinilado	Donkey	1:200	Jackson ImmunoResearch Laboratories, UK	I y II
Anti-rabbit biotinilado	Donkey	1:200	Jackson ImmunoResearch Laboratories, UK	I y II
Anti-mouse biotinilado	Donkey	1:200	Jackson ImmunoResearch Laboratories, UK	II
Anti-mouse Alexa Fluor 488	Donkey	1:1000	Invitrogen™, USA	I y II
Anti-mouse Alexa Fluor 568	Donkey	1:1000	Invitrogen™, USA	I y II
IRdye Anti-rabbit 800 CW	Goat	1:10000	Jackson ImmunoResearch Laboratories, UK	II
IRdye Anti-mouse 680 LT	Goat	1:10000	Jackson ImmunoResearch Laboratories, UK	II
Streptavidina Alexa Fluor 568		1:000	Invitrogen™, USA	I y II
Streptavidina Alexa Fluor 488		1:000	Invitrogen™, USA	I y II

Las secciones fueron lavadas y cubiertas con un medio de montaje acuoso para fluorescencia y las imágenes fueron adquiridas con un microscopio Congocal Zeiss LSM 880 con FAST Airyscan (Carl Zeiss Microscopy GmbH, Alemania).

La expresión selectiva de DREADD también fue evaluada en un núcleo noradrenérgico como A5, otro dopaminérgico (VTA) y un núcleo no noradrenérgico como es el área parabraquial. El núcleo dopaminérgico (VTA) fue incubado con un anticuerpo primario contra la enzima TH (rabbit anti-TH) y visualizado con un anticuerpo secundario donkey anti-rabbit fluorescente 488 (tabla 5).

En **estudio I** se evaluó la expresión de mcherry + GFP + DBH en LC, A5 y área parabraquial en ratas SD. En el **estudio II** se evaluó la expresión de mcherry + DBH en LC, A5 y mcherry + TH en VTA en ratas LE.

5.9.2. Estudio neuroanatómico de las proyecciones del LC hacia DRt, CCAr y SC

Se evaluó la expresión de FG en secciones secuenciales del LC_{ipsi} y LC_{contra} (9 secciones representativas de 30 µm por animal a lo largo del eje rostro-caudal). Se incubaron las secciones durante 48 horas a 4ºC con anticuerpos rabbit anti-FG y mouse anti-DBH. Los anticuerpos fueron posteriormente visualizados con un anticuerpo secundario IgG biotinilado donkey anti-rabbit seguido de una streptavidina verde (488) o un anticuerpo para fluorescencia roja Alexa fluor donkey anti-mouse (568) (tablas 5-6).

Las secciones fueron lavadas y cubiertas con un medio de montaje acuoso para fluorescencia y las imágenes fueron adquiridas con un microscopio Olympus para fluorescencia equipado con una cámara Olympus DP73 (España).

Se cuantificaron manualmente las neuronas en las que colocalizan FG y DBH y el número de neuronas FG positivas a lo largo del eje rostro-caudal en el LC_{ipsi} y LC_{contra}, y se representó en cuanto a la media ±error por sección representativa. Además, se evaluó la distribución de las neuronas FG y DBH positiva en el plano dorso-ventral del LC medial (-9.72 hasta -9.96mm desde bregma, 3 cortes por animal). A media altura respecto a la expresión de DBH fue establecido como criterio para diferenciar entre la parte dorsal y ventral y fue representado como una proporción relativa al número total de las neuronas solapadas (FG +DBH). *Más información sobre los anticuerpos utilizados en **tabla 5.**

En el **estudio I** se realizó el análisis anatómico en LC de las proyecciones del LC hacía el DRt en ratas SD y en el **estudio II** se realizó el análisis anatómico en LC de las proyecciones del LC hacía SC y del LC hacía CCAr en ratas LE.

5.9.3. Expresión de pCREB en las neuronas de DRt.

Para evaluar la expresión de pCREB en DRt en el **estudio I**, las secciones (3-4 animales por grupo) fueron incubados durante dos noches a 4 ºC con un anticuerpo rabbit anti-pCREB. Seguidamente, las secciones fueron incubadas con un anticuerpo secundario biotinilado donkey anti- rabbit (los cuales fueron visualizados con un kit de tinción de peroxidasa ABC ultrasensible (1:1000, Thermo Scientific, España) y 3,3-Diaminobencidina (DAB) (Llorca-torrabla y cols., 2019 Biological psychiatry). Las secciones fueron montadas en portas, lavadas con xilol y cubiertas con DPX. Además, las imágenes se adquirieron en los mismos parámetros de exposición e iluminación en un microscopio Olympus BX40 equipado con una cámara

Olympus DP73 (España). El número de neuronas pCREB positivas se cuantificó manualmente en cada sección (3-4 secciones secuenciales de 30 µm de cada DRt; ipsilateral y contralateral) (tablas 5-6).

5.9.4. Expresión de c-Fos en las neuronas de LC

Se evaluó la activación del LC_{ipsi} y LC_{contra} en dos puntos de la neuropatía; ST y LT mediante la expresión de c-Fos. Estudiando adicionalmente la expresión de c-Fos y FG en proyecciones noradrenérgicas del LC_{ipsi} y LC_{contra} hacia la SC o CCAr. Por otra parte, se evaluó la inhibición mediada por AAV-Gi-mCherry de las neuronas del LC que proyectan hacia CCAr.

Las secciones de LC medial secuencial ipsilateral y contralateral (-9.72 a -9.96 de Bregma, 3 cortes de 30 µm por animal) se incubaron durante 48 horas a 4 ºC con un anticuerpo primario rabbit anti-c-Fos y un anticuerpo mouse anti-DBH. A continuación, los anticuerpos se visualizaron con un anticuerpo biotinilado donkey anti-rabbit, seguido de estreptavidina Alexa Fluor 488. O un anticuerpo secundario Alexa Fluor donkey anti-mouse 568 (tabla 5). Después de lavar y montar en medio acuoso de fluorogel, las imágenes se adquirieron en un microscopio fluorescente Olympus BX40 equipado con una cámara Olympus DP73 (España). El número de neuronas marcadas con c-Fos en el LC medial ipsilateral y contralateral se contó manualmente y se representó como la media ± SEM por corte de LC. El número de neuronas marcadas con c-Fos y FG en el LC medial ipsilateral y contralateral también se contó manualmente mediante la superposición de la expresión de c-Fos y FG utilizando el software Fiji Image (EE. UU.), Representado como la proporción del número total de neuronas c-Fos marcadas. En ambas cuantificaciones, también se estudió la distribución dorso-ventral en el LC medial (-9.72 a -9.96 de Bregma, 3 cortes por animal) del LC ipsilateral y contralateral.

En el **estudio I** se realizó el análisis de c-Fos en LC de las proyecciones del LC hacía el DRt en ratas SD y en el **estudio II** se realizó el análisis de c-Fos en LC de las proyecciones del LC hacía SC y del LC hacía CCAr en ratas LE.

5.9.5. Expresión de DBH en SC

Para evaluar las fibras de DBH en el asta dorsal de la SC (L4-L6) en el **estudio II**, las secciones de 40 µm (3-4 animales por grupo) se incubaron durante 2 noches a 4 ºC con un anticuerpo mouse anti-DBH. Posteriormente, las secciones se incubaron con anticuerpo biotinilado donkey

anti-mouse, y se visualizaron con un kit de tinción de peroxidasa ABC ultrasensible y 3, Tetrahidrocloruro de 3'-diaminobencidina (DAB) (Llorca-Torralba y cols., 2019) (tabla 5). Las secciones se montaron en portaobjetos, se limpiaron con xileno y se cubrieron con un cubreobjetos con DPX, y las imágenes se adquirieron con los mismos ajustes de exposición e iluminación en un microscopio Olympus BX40 equipado con una cámara Olympus DP73. La densidad óptica de expresión de DBH se calculó en la materia gris del asta dorsal de la SC con el software Fiji Image (EE. UU.), Definiendo 5 regiones de interés del mismo tamaño por sección y aplicando la intensidad media, restando el ruido de fondo de cada sección (3 secciones secuenciales de 40 µm de cada lado ipsilateral y contralateral de L4-L6).

5.10. Western Blot

Los animales fueron anestesiados profundamente y posteriormente sacrificados mediante decapitación. El tejido cerebral fue extraído bilateralmente en fresco según las coordenadas estereotáxicas (Paxinos y Watson, 2009), LC_{ipsi} y LC_{contra} por separado (Llorca-Torralba y cols., 2019, Mol. Neurobio). Las muestras de tejido correspondientes al LC se congelaron rápidamente en hielo seco y posteriormente se almacenaron a -80ºC hasta su procesamiento. Se separaron cantidades iguales de proteína de homogeneizados de tejido (LC_{ipsi} y LC_{contra}) mediante SDS-PAGE (electroforesis en gel de poliacrilamida-dodecilsulfato de sodio) y se transfirieron a membranas de difluoruro de polivinilideno (PVDF). Se incubaron las membranas durante una noche a 4°C con anticuerpos primarios contra pCREB, CREB, TH y β-actina. Los anticuerpos primarios se detectaron utilizando el correspondiente anticuerpo secundario hecho en cabra anti-conejo (verde), y otro hecho cabra anti-ratón (rojo). Las señales de proteínas se detectaron utilizando un sistema de imágenes de fluorescencia cuantitativa de dos canales LI-COR Odyssey® (Bonsai Advanced Technologies, España) (tabla 5). Las imágenes digitales de Western blots se analizaron por densitometría utilizando el software de acceso libre ImageJ (National Institutes of Health, EE. UU.). Todas las proteínas fueron normalizadas para la cantidad de la proteína β-actina (que contiene el citoesqueleto de las células).

5.11. Técnicas histológicas

5.11.1. Verificación de la administración de cánulas en LC, ACC y SC

Al finalizar el experimento se administró azul de Pontamina sky blue en el área cerebral o medular en que se había implantado la cánula guía o el catéter lumbar. Posteriormente, se perfundieron a los animales siguiendo el protocolo del apartado **Perfusión animal y extracción de muestras**. Para evaluar la implantación de las cánulas en LC en el **Estudio I** y en CCAr en el **estudio II**, se realizaron cortes de 40 µm en un criostato (Shandon Cryotome, EE.UU.). A continuación, los cortes fueron sometidos a un protocolo de tinción estándar con Rojo Neutro y se observó si la marca azul de Pontamina sky blue se situaba sobre la región del LC o CCAr. mediante el uso de un microscopio óptico (Olympus BX60, España). En el caso de la verificación de la colocación del catéter lumbar **en ambos estudios (I y II)**, también se administró Pontamina sky blue a través de la cánula (10µl) y fue verificado *in situ* antes de extraerla (se tomó una fotografía usando una cámara Leica VARIO-SUMMILUX-H-1:1.6-2.4). Los animales que no tenían bien colocadas las cánulas en el LC o el catéter lumbar fueron excluidos del estudio.

5.11.2. Verificación del lugar de administración de FG (DRt, SC y CCAr)

Al acabar los procedimientos se perfundieron a todos los animales con paraformaldehído al 4% y se verificó el lugar de inyección de FG en DRt (**estudio I**), SC y CCAr (**estudio II**). Las diferentes regiones fueron cortadas en secciones de 40 µm, se montaron con un medio acuoso para fluorescencia y fueron visualizados directamente en un microscopio para fluorescencia Olypus BX40 equipado con una cámara Olympus DP73 (España). Todos los animales que no mostraron expresión de FG en las áreas estudiadas fueron excluidos del análisis.

5.12. Análisis estadístico

Se realizó el análisis estadístico mediante el uso de los programas estadísticos Graphpad Prism (versión 5.0, Graphpad Software, EE.UU.) y Statistica 10.0 (StatSoft, EE.UU.). En primer lugar, se realizó una prueba de normalidad mediante el test de Shapiro-Wilk. Una vez conocida la naturaleza normal o no normal de las muestras de los diferentes estudios se utilizaron tests no paramétricos en el caso de no cumplir la normalidad y tests paramétricos en el caso de que si la cumplieran. Se utilizaron los siguientes tests no paramétricos, para comparaciones entre dos

grupos se utilizó una U de Mann Whitney, para comparaciones entre más de dos grupos se usó el test de Kruskal Wallis y para comparaciones dos a dos se usó la U de Mann Whitney como prueba post hoc. En cuanto a los tests paramétricos se utilizó una t de Student (de dos colas no emparejados o no emparejados) para comparaciones entre dos grupos y análisis de la varianza (ANOVA) de una o dos vías, con o sin medidas repetidas, seguidas de un test post-hoc Tuckey o Newman Keuls para comparaciones entre más de dos grupos. Todos los datos se han representados como la media ± SEM. El grado de significancia aceptado fue $p<0.05$ (límite de confianza mayor del 95%)

STUDY I

Title: Nerve injury induces transient locus coeruleus activation over time: role of the locus coeruleus–dorsal reticular nucleus pathway

Authors: Carmen Camarena-Delgado†, Meritxell Llorca-Torralba†, Irene Suárez-Pereira, Lidia Bravo, Carolina López-Martín, Jose A. Garcia-Partida, Juan A. Mico and Esther Berrocoso.

†These authors contributed equally to this work.

Journal: Pain

DOI: 10.1097/j.pain.0000000000002457

Publisher: PAIN: August 20, 2021 - Volume - Issue – (In press)

ISSN: 1872-6623 (online)/ 0304-3959

Journal of Citations Report 2021 2-year Impact Factor: 6.961

Journal of Citations Report 2021 5-year Impact Factor: 5.674

Category	Rank	Quartile
Anesthesiology	4/33	Q1
Neurosciences	39/273	Q1
Clinical Neurology	23/208	Q1

All co-authors, the undersigned, in order to fulfil the requirements issued by Article 23 of the UCA/CG06/2012 regulation, dated 27 June 2012, on the organisation of doctoral studies at the University of Cádiz, hereby declare that:

- The PhD candidate, María del Carmen Camarena Delgado, contributed to performing the stereotactic microsurgery and behavioural experiments. In addition, she collaborated in the experimental design, data analysis and the writing of the first draft of the manuscript.

- They expressly and formally agree for this scholarly publication to be included as a part of the compendium of publications to be submitted by the PhD candidate.

- They expressly and formally renounce to reuse this scholarly publication as a part of another PhD thesis at any other university.

M. Llorca-Torralba:

LLORCA TORRALBA MARITSELL - 48964174A

Firmado digitalmente por LLORCA TORRALBA MARITSELL - 48964174A
Nombre de reconocimiento (DN): c=ES, serialNumber=IDCES-48964174A, givenName=MARITSELL, sn=LLORCA TORRALBA, cn=LLORCA TORRALBA MARITSELL - 48964174A
Fecha: 2021.11.25 08:47:49 +01'00'

I. Suárez-Pereira:

SUAREZ PEREIRA IRENE - 28809292K

Firmado digitalmente por SUAREZ PEREIRA IRENE - 28809292K
Fecha: 2021.11.19 07:17:45 +01'00'

L. Bravo:

BRAVO GARCIA LIDIA - 53580566L

Firmado digitalmente por BRAVO GARCIA LIDIA - 53580566L
Nombre de reconocimiento (DN): c=ES, serialNumber=IDCES-53580566L, givenName=LIDIA, sn=BRAVO GARCIA, cn=BRAVO GARCIA LIDIA - 53580566L
Fecha: 2021.11.19 10:56:34 +01'00'

C. López-Martín:

LOPEZ MARTIN CAROLINA - 49041195C

Firmado digitalmente por LOPEZ MARTIN CAROLINA - 49041195C
Fecha: 2021.11.24 22:41:49 +01'00'

J.A. García-Partida:

E. Berrocoso:

BERROCOSO DOMINGUEZ ESTHER MARIA - 52928983A

Firmado digitalmente por BERROCOSO DOMINGUEZ ESTHER MARIA - 52928983A
Nombre de reconocimiento (DN): c=ES, serialNumber=IDCES-52928983A, givenName=ESTHER MARIA, sn=BERROCOSO DOMINGUEZ, cn=BERROCOSO DOMINGUEZ ESTHER MARIA - 52928983A
Fecha: 2021.11.24 15:50:54 +01'00'

Estudio I

Nerve injury induces transient locus coeruleus activation over time: role of the locus coeruleus–dorsal reticular nucleus pathway

Carmen Camarena-Delgado†, Meritxell Llorca-Torralba†, Irene Suárez-Pereira, Lidia Bravo, Carolina López-Martín, Jose A. Garcia-Partida, Juan A. Mico and Esther Berrocoso.

†These authors contributed equally to this work.

Pain, 2021

(*Online available*) DOI: 10.1097/j.pain.0000000000002457

F.I.:6.961

La transición del dolor agudo al crónico da lugar a una remodelación cerebral inadaptada, caracterizada por la hipersensibilidad sensorial y la consiguiente aparición de trastornos emocionales. Utilizando la lesión por constricción crónica del nervio ciático como modelo de dolor neuropático en ratas macho Sprague-Dawley, identificamos una plasticidad dependiente del tiempo de las neuronas del locus coeruleus (LC) relacionada con el lugar de la lesión, ipsilateral (LC_{ipsi}) o contralateral (LC_{contra}) a la lesión, con la hipótesis de que la vía LC→núcleo reticular dorsal (DRt) está implicada en la nocicepción patológica asociada al dolor crónico. La inactivación del LC_{ipsi} con lidocaína aumentó la alodinia al frío 2 días después de la lesión del nervio, pero no más tarde. Sin embargo, un bloqueo similar del LC_{contra} redujo la alodinia al frío 7 y 30 días después de inducir la neuropatía, pero no antes. Además, el bloqueo con lidocaína del LC_{ipsi} o del LC_{contra} revirtió la depresión inducida por el dolor 30 días después de la neuropatía. El dolor a largo plazo aumenta la expresión de la proteína de unión al

elemento de respuesta de AMPc fosforilada en el DRt_{contra} pero no en el DRt_{ipsi}. Además, la inactivación quimiogenética de la vía $LC_{contra}→DRt_{contra}$ activada exclusivamente por fármacos de diseño (CNO) produjo una analgesia consistente en el dolor evocado y espontáneo 30 días después de la lesión. Esta analgesia fue similar a la producida por la activación espinal de los adrenoreceptores a2. Además, la inactivación quimiogenética de la vía $LC_{contra}→DRt_{contra}$ indujo un comportamiento depresivo en animales sham, pero no modificó la depresión inducida por el dolor a largo plazo. En general, el daño nervioso activa el LC_{ipsi}, que amortigua temporalmente el fenotipo neuropático. Sin embargo, la consiguiente activación de una proyección facilitadora del dolor $LC_{contra}→DRt_{contra}$ contribuye al dolor crónico, mientras que la activación bilateral global del LC contribuye al fenotipo depresivo asociado.

Nerve injury induces transient Locus Coeruleus activation over time: role of the Locus Coeruleus – Dorsal Reticular Nucleus Pathway

Carmen Camarena-Delgado[1,2]*, Meritxell Llorca-Torralba[1,2,4]*, Irene Suárez-Pereira[2,3,4], Lidia Bravo[2,3,4], Carolina López-Martín[1,2], Jose Antonio Garcia-Partida[2,3], Juan Antonio Mico[2,3,4], and Esther Berrocoso[1,2,4]

1 Neuropsychopharmacology and Psychobiology Research Group, Department of Psychology, University of Cádiz, Cádiz, Spain

2 Instituto de Investigación e Innovación Biomédica de Cádiz, INiBICA, Hospital Universitario Puerta del Mar, Cádiz, Spain,

3 Neuropsychopharmacology and Psychobiology Research Group, Department of Neuroscience, University of Cádiz, Cádiz, Spain,

4 Centro de Investigación Biomédica en Red de Salud Mental (CIBERSAM), Instituto de Salud Carlos III, Madrid, Spain,

* These authors contributed equally to this work

Corresponding author: Esther Berrocoso PhD, Neuropsychopharmacology and Psychobiology Research Group, Psychobiology Area, Department of Psychology, University of Cádiz, 11510 Puerto Real, Cádiz, Spain. Tel.: +34956015224; Email: esther.berrocoso@uca.es.

Abstract

The transition from acute to chronic pain results in maladaptive brain remodeling, as characterized by sensorial hypersensitivity and the ensuing appearance of emotional disorders. Using the chronic constriction injury of the sciatic nerve as a model of neuropathic pain in male Sprague-Dawley rats, we identified time-dependent plasticity of locus coeruleus (LC) neurons related to the site of injury, ipsilateral (LC_{ipsi}) or contralateral (LC_{contra}) to the lesion, hypothesizing that the LC→dorsal reticular nucleus (DRt) pathway is involved in the pathological nociception associated with chronic pain. LC_{ipsi} inactivation with lidocaine increased cold allodynia 2 days after nerve injury but not later. However, similar blockade of LC_{contra} reduced cold allodynia 7 and 30 days after inducing neuropathy but not earlier. Furthermore, lidocaine blockade of the LC_{ipsi} or LC_{contra} reversed pain-induced depression 30 days after neuropathy. Long-term pain enhances pCREB (phosphorylated cAMP-response element binding protein) expression in the DRt_{contra} but not in the DRt_{ipsi}. Moreover, inactivation of the LC_{contra}→DRt_{contra} pathway using dual viral-mediated gene transfer of DREADDs (designer receptor exclusively activated by designer drugs) produced consistent analgesia in evoked and spontaneous pain 30 days post-injury. This analgesia was similar to that produced by spinal activation of α2-adrenoreceptors. Furthermore, chemogenetic inactivation of the LC_{contra}→DRt_{contra} pathway induced depressive-like behaviour in naïve animals but it did not modify long-term pain-induced depression. Overall, nerve damage activates the LC_{ipsi}, which temporally dampens the neuropathic phenotype. However, the ensuing activation of a LC_{contra}→DRt_{contra} facilitatory pain projection contributes to chronic pain, while global bilateral LC activation contributes to associated depressive-like phenotype.

Introduction

The mechanisms underlying the transition from acute to chronic pain and the appearance of comorbid emotional symptoms are still poorly understood. However, these phenomena seem to be caused by the aberrant activation or deactivation of proalgesic and analgesic neural pathways, as well as those related to emotional processing [5,16]. Among the areas thought to be involved in these events, the noradrenergic-locus coeruleus (LC) neurons, bilaterally located in the pontine brainstem, have been implicated in intrinsic analgesia and paradoxically, also with pain and associated anxiodepressive symptoms [24]. In the case of pain, it has been proposed that descending LC projections regulate sensory aspects, while ascending projections regulate both the sensory and emotional aspects of pain [24]. Thus, the nociceptive information following a nociceptive stimulus reaches the spinal cord and ascends to the LC, which in turn sends information to several brain structures mainly involved in the emotional-motivational aspects of pain. At the same time, the descending noradrenergic LC-spinal pain pathway is activated, producing analgesia by blocking the ascending spinal nociceptive information [21,34]. Therefore, this circuit plays an important role in conditions of acute nociception.

By contrast, the role of the LC during chronic pain has been more difficult to define mechanistically. In the case of pain induced by nerve injury (neuropathic pain), it has been reported a functional upregulation of the LC that contributes to endogenous analgesia [25,28], while others propose that a functional deficit, or even aberrant activation, contributes to the initiation and/or maintenance of neuropathic pain [12,36], and even of the secondary affective and cognitive disturbances observed in long-term chronic pain [1,27]. Considering this contrasting evidence, we set out to study the time-dependent LC plasticity in a rat model of neuropathic pain (chronic constriction injury, CCI) relative to the site of injury, ipsilateral (LC_{ipsi}) or contralateral (LC_{contra}) to the lesion. Furthermore, as the LC is apparently composed of modules that might produce targeted neuromodulation [35], we wanted to discern the role of modulating the LC as a whole, and that of modulating just a specific pathway. As such, we assessed the behavior of both the global LC and that of its projections to the dorsal reticular nucleus (DRt), a nucleus that belongs to the endogenous pain control system and that fulfils a unique pain-facilitatory role [23,42]. The DRt is involved in a reciprocal feedback loop with the spinal cord and through its projections to the lateral ventromedial thalamus, it participates in a reticulo-thalamo-cortical ascending nociceptive pathway [33]. Interestingly, the DRt receives afferent inputs from the LC and the A5 noradrenergic cell group. An increase in noradrenaline released in the DRt was previously detected during the formalin test, yet a reduction significantly attenuates pain behavior in this test [32]. In neuropathic pain, the reduction of noradrenaline release at the DRt induces a long-lasting attenuation of pain responses [31]. These data suggest that the DRt is a major relay center for pain facilitatory inputs from noradrenergic areas, even though the direct implication of the LC in neuropathic pain still remains elusive.

Materials and Methods

Animals

Male Sprague-Dawley and Long-Evans rats (weighing 250-350 g) were maintained under standard laboratory conditions (22 ºC, 12 h light/dark cycle, lights on at 08:00 am, food and water *ad libitum*). All animal handling and procedures were carried out in accordance with the European Commission's directive (2010/63/EC) and Spanish Law (RD 53/2013) regulating animal research. Furthermore, all experimental protocols were approved by the Committee for Animal Experimentation at the University of Cadiz (Spain).

Neuropathic pain model

Chronic constriction injury (CCI) of the sciatic nerve was used as a model of neuropathic pain [7,8]. The rats were anesthetized with isoflurane (induction with 3-4% and maintenance with 1.5-2.5%), and the left sciatic nerve was then exposed at the mid-thigh level, proximal to the sciatic trifurcation. Four chrome gut (4–0) ligatures were tied loosely around the nerve, separated by 1.0–1.5 mm so as not to compromise the vascular supply. The overlying layers of muscle were then closed with 4–0 non-absorbable silk thread and the skin was sutured with 2–0 silk thread. Sham operations were performed in the same manner but without nerve ligation.
The experimental procedures were carried out on 2-3 (short-term, ST), 7-8 (mid-term, MT) and 28-30 (long-term, LT) days after CCI.

Vectors and tracer

The following vectors were used: a retrograde canine adenoviral vector carrying a construct encoding Cre-recombinase fused to the green fluorescent protein (GFP: CAV2-Cre-GFP, titer 2.5 10^{12} pp/ml, 0.30 µl/contralateral dorsal reticular nucleus-DRt_{contra}: Kremer laboratory, Montpellier vectorology platform, France) [44]; Designer Receptor Exclusively Activated by Designer Drugs (DREADDs: Virus Vector Core, Gene Therapy Center Vector Core at the University of North Carolina, USA); AAV2/hSyn-DIO-hM4D(Gi)-mCherry (AAV-Gi-mCherry), inhibitor virus, titer 3 x 10^{12} vg/ml, 1.4 µl/LC; and AAV2/hSyn-DIO-mCherry (AAV-mCherry) control virus; titer 5.6 x 10^{12} vg/ml, 1.4 µl/LC) [27]. The control vector contained a mCherry reporter protein without the DREADD reporter. Fluoro-Gold (FG) was used as a retrograde tracer (4%/0.2 µl for DRt_{contra}: Fluorochrome, USA).

Vectors and tracer injection

For virus (CAV2-Cre-GFP, AAV-Gi-mCherry or AAV-mCherry) or FG injections into the LC or DRt, rats were anesthetized with an i.p. injection of ketamine (100 mg/kg: Richter Pharma, Spain) and xylazine (20 mg/kg: Calier laboratory, S. A, Spain), and placed in a stereotaxic frame with the skull level along both the antero-posterior (AP) and medio-lateral (ML) axis for precise targeting. Cranial windows were opened above the target coordinates: LC - AP -3.2 mm, ML ±1.3 mm, DV (dorsal-ventral) 6.2 mm (respect to lambda), with the head oriented at a 15º angle to the horizontal plane; DRt_{contra} - AP -6.2 and -6.6 mm, ML +1.4 and +1.3 mm, DV 8.0 and 8.2 mm, with the head oriented at a 0º angle to the horizontal

plane. After injection, the wound was cleaned with 0.9% saline and disinfected with iodine polyvidone. The skin was sutured with 4–0 non-absorbable silk thread. To enhance vector and tracer expression, the behavioral studies were carried out 3 weeks (AAV-DREADD virus) or 4 days (FG tracer) after injection.

LC cannula implantation

For intra-LC lidocaine administration, a cannula was implanted unilaterally into the ipsilateral (LC_{ipsi}) or contralateral LC (LC_{contra}) under ketamine (100 mg/kg) and xylazine (20 mg/kg) anesthesia, as described in detail elsewhere [26]. The following coordinates were used to situate the cannula, with the head oriented at a 15º angle to the horizontal plane: AP -3.2 mm, ML ±1.3 mm and DV: 6.2 mm (respect to lambda). The cannulas were fixed in place with dental cement and four anchor screws, and they were maintained closed until the test session by inserting a stainless-steel wire. Any animals with an incorrectly placed or obstructed cannula were removed from the analysis.

Intrathecal catheter installation

For intrathecal (i.t.) clonidine injection, a catheter (PE-10) was implanted at the lumbar level of the SC under isoflurane anesthesia, as described in detail elsewhere [45]. An incision was made in the skin and a cannula (20 ga, 0.9 x 40 mm) was introduced in a slightly medial cranial direction along the surface of L6 up to L5. Correct placement of the cannula was confirmed by a tail flick, a retraction of the leg or the reflux of cerebrospinal fluid. A polyethylene catheter (0.68 mm diameter) was introduced from the end of the cannula until it reached the caudal rib level and the cannula was removed. The catheter was first fixed onto the surface of the lumbar musculature and the rest was passed subcutaneously along the spine, appearing through the skin in the occipital region. Lidocaine (4%/15 µl, i.t.) was administered to verify the correct placement of the intraspinal cannula, observing immediate motor paralysis of the posterior third of the animal that lasted for about 10-20 min. Any animals in which motor paralysis was not reversed were excluded from the analysis.

Drugs

The following drugs were administered to awake animals that were well-habituated to handling. Lidocaine hydrochloride (4%/0.5 µl intra-LC, 15 min before testing: Sigma-Aldrich, Spain), clozapine-n-oxide (CNO, 1 mg/kg intraperitoneal -i.p., administered 20 min before the behavioral tests: Carbosynth, UK) or clonidine hydrochloride (20 µg/10 µl i.t., 30 min before testing: Sigma-Aldrich, Spain).

Experimental design

For the pharmacological inhibition of LC_{ipsi} or LC_{contra} by lidocaine (4%), a metal cannula was implanted into the LC_{ipsi} or LC_{contra} of Sprague-Dawley rats 4 days prior to performing the behavioral tests. The behavioral nociceptive tests were performed on parallel, independent groups of CCI-ST (2-3 days), -MT (7-8 days) and -LT (28-30 days) rats, administering lidocaine 15 minutes beforehand. The acetone (day 2,

7 and 28 after CCI) and paw pressure test (day 3, 8 and 29 after CCI) were performed on each experimental group on consecutive days, although the paw pressure test was not performed in all animals with a cannula in the LC_{ipsi} because of cannula obstruction. The forced swimming test was also performed on another set of Sprague-Dawley CCI-LT animals (30 days after surgery), administering lidocaine 15 minutes prior to testing.

For the chemogenetic modulation of noradrenergic LC projections to the DRt (LC_{contra}→DRt_{contra} pathway), CAV2-Cre-GFP was injected into the DRt_{contra} 7 days after inducing CCI in Sprague-Dawley rats. After 14 days of CCI, AAV-Gi-mCherry or AAV-mCherry (control virus) was injected into the LC_{contra} and the behavioral tests were performed on CCI-LT rats (28 days after CCI). CNO was administered i.p. 20 min before performing the nociceptive tests, all on the same day (acetone test, von Frey test and spontaneous pain test). After 7 days, a catheter was inserted (i.t.) to evaluate nociception after clonidine administration, which was administered 30 min before performing the nociceptive tests.

In another set of CCI-LT Sprague-Dawley rats (30 days after surgery), the forced swimming test was evaluated after LC_{contra}→DRt_{contra} pathway inhibition, administering CNO i.p. 20 min before performing the test. In addition, the same animals were tested in the acetone test and von Frey test 20 min and 360 min after CNO administration.

In CCI-LT Long-Evans animals, acetone (day 28 after CCI) and paw pressure tests (day 29 after CCI) were performed administering lidocaine into the LC_{contra} 15 minutes prior to testing.

Nociceptive behavioral tests

Acetone test: the response (score) of the hindpaws to the application of a drop of acetone (100 mL) to the surface in the middle of a hindpaw with a pipette was used as a measure of thermal hypersensitivity [9,11].

Von Frey test: the withdrawal threshold (grams) of a hindpaw when subjected to a force from 0 to 50 g increasing over a period of 20 seconds was used as a measure of mechanical hypersensitivity [11].

Paw-pressure test: the withdrawal threshold (grams) of the hindpaws when subjected to pinching with a graded motor-driven device (250 g cut-off: Ugo Basile, Comerio VA, Italy) was used as a measure of mechanical hypersensitivity [9].

SPONTANEOUS FOOT LIFT: The number of spontaneous foot lifts and flinches was recorded over 5 min as an index of spontaneous pain. The animals were placed into a Plexiglas chamber on a metal grid and a camera (JVCKenwood, Spain) was positioned underneath the chamber [17].

The experimenters were blind to the animal's status in all the nociceptive behavioral tests.

Locomotor activity

Free exploratory ambulation was recorded individually for 40 min in a transparent cage (40 x 40 x 40 cm) using a Spontaneous Motor Activity Recording and Tracking (SMART) video system (v3.0, Panlab S.L., Spain) in a light-attenuated room. The total distance travelled (arbitrary units, A.U.) was measured as an

indicator of locomotor activity [27]. Lidocaine or CNO was administered immediately prior to commencing the test.

Modified Forced Swimming Test

Depressive-like behavior was evaluated in the modified forced swimming test (mFST) [1,15]. Rats were placed individually into a Plexiglas cylinder (height 40 cm, diameter 18 cm) filled to a depth of 30 cm with water at 25 ± 1 °C for two different sessions. A 15 min pre-test was followed by a 5 min test performed 24 hours later. Using a time-sampling technique, the predominant behaviors were recorded (climbing -CL, swimming –SW, or immobility -IM), and scored in each 5 s period of the 300 s test session using customized software (Red-Mice, Spain), providing a total of 60 scores. The predominant behavior was scored blind to the experimental status of the animals. Immobility behavior was determined when no activity was observed other than the movements necessary to keep the animal's head above water. Climbing behavior was measured when the rats made vigorous upward movements with their forepaws in and out of the water. Swimming was considered the predominant behavior when the rats moved around the cylinder. Depressive-like behavior was defined as an increase in the mean immobility behavior.

Immunohistochemistry and histology

Immunohistochemistry was performed to evaluate the expression of DREADD-mCherry, CAV-GFP and the FG tracer in the LC [27]. Animals were perfused with paraformaldehyde (4%) at the end of the experiments. To verify the expression of the GFP and/or mCherry protein in noradrenergic LC neurons, and A5 and parabrachial nuclei, all sections were incubated for 48 hours at 4 ºC with antibody against the red fluorescent protein [5F8] (RFP, 1:500, Chromotek, Germany), rabbit anti-GFP (1:500, Chromotek, Germany) and a mouse anti-dopamine beta hydroxylase antibody (DBH, 1:1000, Merck Chemicals & Life Science S.A., Spain). Subsequently, the antibodies were detected with a biotinylated donkey anti-rat antibody (1:200, Jackson ImmunoResearch Europe, UK), which was visualized with Alexa Fluor 568 streptavidin, donkey anti-rabbit Alexa Fluor 488 (1:1000, Invitrogen™, USA) and donkey anti-mouse Alexa Fluor 647 (1:1000, Invitrogen™, USA). The sections were then washed and coverslipped in fluoro-gel aqueous mounting medium and the images were acquired with Zeiss LSM 880 Confocal microscope with FAST Airyscan (Carl Zeiss Microscopy GmbH, Germany).

For the neuroanatomical study of the LC projections to the DRt, FG was injected into the DRt_{contra} of Sprague-Dawley rats and they were then perfused four days after FG injection. To evaluate the ipsilateral and contralateral projections from the LC, sequential LC sections (9 representative sections of 30 μm per animals along the rostra-caudal axis) were incubated for 48 hours at 4 ºC with a rabbit anti-FG antibody (1:1,000, Merck Chemicals & Life Science S.A., Spain) and a mouse anti-DBH antibody (1:1,000, Merck Chemicals & Life Science S.A., Spain). The antibodies were visualized with a biotinylated donkey anti-rabbit IgG (1:200, Jackson ImmunoResearch Europe, UK) followed by Alexa Fluor 488 streptavidin (1:1,000, Invitrogen™, USA) or a donkey anti-mouse Alexa Fluor 568 (1:1,000, Invitrogen™, USA).

After washing and coverslipping in fluoro-gel aqueous mounting medium, images were acquired on a fluorescent Olympus BX40 microscope equipped with an Olympus DP73 camera (Spain). The number of FG-positive neurons along the rostro-caudal axis in both the ipsilateral and contralateral LC were counted manually, and represented as the mean + SEM per representative slice. In addition, we studied the dorso-ventral distribution of FG labelled neurons in the medial ipsilateral and contralateral LC (-9.72 to -9.96 mm from Bregma, 3 slices per animal). Half height with respect to DBH expression was established as the dorso-ventral criteria and it was represented as the proportion relative to the total number of FG-labelled neurons.

In addition, pCREB expression in the DRt was evaluated in another set of neuropathic Sprague-Dawley and Long-Evans animals (30 days after surgery). The sections (3-4 animals per group) were incubated for 2 nights at 4 ºC with a rabbit anti-pCREB antibody (1:1000, Merck Millipore, Spain). Subsequently, the sections were incubated with biotinylated donkey anti-rabbit antibody (1:500, Jackson ImmunoResearch Europe, UK), which were visualized with an ultra-sensitive ABC peroxidase staining kit (1:1,000, Thermo Scientific, Spain) and 3,3'-diaminobenzidine tetrahydrochloride (DAB) [27]. The sections were mounted on slides, cleared in xylene and coverslipped with DPX, and the images were acquired with the same exposure and illumination settings on an Olympus BX40 microscope equipped with an Olympus DP73 camera (Spain). The number of pCREB positive neurons was counted manually using a selective area of DRt (0.1 mm^2) in each section (3-4 sequential sections of 30 µm from each ipsilateral and contralateral DRt).

Histology

Cannula placement into the LC and lumbar spinal cord was verified by injection of 0.5 µl and 0.3 µl Pontamine Sky Blue at the injection site, respectively, just before the animals were perfused. Sequential LC (30 µm) sections were stained with neutral red, and the images were acquired on an Olympus BX40 microscope equipped with an Olympus DP73 camera (Spain). The location of the injection site was verified to be within the LC in all the animals studied. The location of the FG or CAV-GFP injection site was verified to be within the DRt in all the animals studied. Sequential DRt (30 µm) sections were visualized directly on an Olympus BX40 fluorescent microscope equipped with an Olympus DP73 camera (Spain).

Statistical Analysis

The number of animals analyzed from each group is indicated in the figure legends. The data are presented as the means ± SEM and they were analyzed using STATISTICA 10.0 (StatSoft, USA) or

GraphPad Prism 5 software (GraphPad Software, USA). When data were not normally distributed, the Kruskal–Wallis test was used to compare the means, followed by Mann–Whitney U post hoc test. When the data were normally distributed, the groups were compared with a two-way analysis of variance (ANOVA) with or without repeated measures, followed by a Tukey post-hoc test, or with unpaired Student's T test. Significance was accepted at $p<0.05$. See detailed statistical analysis in supplemental tables (Tables 1-20).

Results

Effect of the pharmacological blockade of LC on nociception

As shown previously [1,27], nerve-injury produces robust cold hypersensitivity immediately after nerve damage, as shown by a consistent reduction in the short-term (ST), mid-term (MT) and long-term (LT) acetone score (CCI-ST 1.50 ± 0.12 vs Sham-ST 0.75 ± 0.11; CCI-MT 2.17 ± 0.12 vs Sham-MT 0.50 ± 0.10; CCI-LT 2.03 ± 0.19 vs Sham-LT 0.22 ± 0.09, $p<0.01$ and $p<0.001$: Fig. 1A). To explore whether the activity of the ipsilateral (side of injury, LC_{ipsi}) and contralateral LC (opposite side to the injury, LC_{contra}) is involved in the sensorial phenotype observed in neuropathic rats, we examined the effect of lidocaine-mediated blockade of LC_{ipsi} or LC_{contra} on the nociceptive threshold in Sprague-Dawley rats (Fig. 1B-D). Blockade of the LC_{ipsi} induced a significant increase in the acetone response of the ipsilateral hindpaw at short-term pain (CCI-ST-Lido 2.31 ± 0.13 vs CCI-ST-Sal 1.56 ± 0.11, $p<0.01$: Fig. 1C). By contrast, no significant changes were observed in the CCI-MT-Lido or CCI-LT-Lido rats relative to their respective controls CCI-MT-Sal and CCI-LT-Sal (CCI-MT-Lido 2.14 ± 0.22 vs CCI-MT-Sal 2.00 ± 0.15; CCI-LT-Lido 1.55 ± 0.24 vs CCI-LT-Sal 1.56 ± 0.19; $p>0.05$: Fig. 1C). These findings were also observed in the paw pressure test, in which there was a decrease in the withdrawal threshold of the ipsilateral hindpaw in the CCI-ST-Lido group relative to the CCI-ST-Sal group (CCI-ST-Lido 112.5 ± 8.66 vs CCI-ST-Sal 151.9 ± 6.40, $p<0.01$: Fig. S1A-B). No effect was observed in the Sham groups or in the contralateral hindpaws after lidocaine administration at any time point.

We then explored the effect of the blocking the LC_{contra} on nociception and we found no changes in the acetone response of the ipsilateral hindpaw in the CCI-ST-Lido group relative to the CCI-ST-Sal rats (CCI-ST-Lido 1.40 ± 0.27 vs CCI-ST-Sal 1.75 ± 0.16, $p>0.05$: Fig. 1D). However, blockade of the LC_{contra} induced a robust decrease in the acetone response of the ipsilateral hindpaw in the CCI-MT-Lido (1.15 ± 0.17, $p<0.01$) and CCI-LT-Lido (0.47 ± 0.10, $p<0.001$) rats relative to their saline controls CCI-MT-Sal (2.05 ± 0.14) and CCI-LT-Sal (1.83 ± 0.22) (Fig. 1D). In addition, the duration of lidocaine analgesia when administered to the LC_{contra} was evaluated in the long-term pain group (CCI-LT-Lido group) in the acetone test (Fig. S2A-B). The analgesia produced by lidocaine in CCI-LT-Lido (CCI-LT-Lido: 0.47 ± 0.10 vs CCI-LT-Sal: 1.83 ± 0.22, $p<0.001$) was abolished 120 min after administration, consistent with the pharmacokinetics of lidocaine (CCI-LT-Lido 1.55 ± 0.18 vs CCI-LT-Sal 1.61 ± 0.24, $p>0.05$: Fig. S2B) [20]. Moreover, no effect of lidocaine was evident in the acetone test in long-term pain (CCI-LT) animals when the cannula was situated outside the LC (Fig. S2B). The effect of lidocaine

administration in the LC_{contra} was also explored in the paw pressure test and like cold allodynia, LC_{contra} significantly increased the withdrawal threshold in CCI-MT-Lido (146.30 ± 5.84, $p<0.05$) and CCI-LT-Lido (174.00 ± 6.50, $p<0.001$) rats relative to their respective CCI-Sal rats (CCI-MT-Sal 128.30 ± 4.93; CCI-LT-Sal 115.00 ± 3.54: Fig. S1C). Finally, lidocaine did not produce any effect on the behavior of the sham group or of the contralateral paws.

We previously demonstrated that chemogenetic blockade of the LC_{contra} did not modify the withdrawal threshold in CCI-LT Long-Evans neuropathic rats [25] and thus, we explored the effect of lidocaine administration into the LC_{contra} in this strain. Accordingly, lidocaine failed to modify the responses in the acetone (CCI-LT-Lido 2.18 ± 0.11 vs CCI-LT-Sal 2.04 ± 0.11, $p>0.05$) or paw pressure tests (CCI-LT-Lido 86.25 ± 8.85 vs CCI-LT-Sal 102.5 ± 6.32, $p>0.05$: Fig. S3A-B).

The effect of pharmacological blockade of the LC on depressive-like behavior

As previously shown, long-term neuropathic pain produces functional changes in the LC that coincide with the development of depressive like behavior [1,2,27]. Accordingly, we explored the influence of LC_{ipsi} and LC_{contra} activity on depressive-like behavior through lidocaine-mediated blockade in long-term neuropathic animals. As expected, the long-term pain rats developed a depressive-like phenotype evident through a significant increase in their immobility in the mFST task (CCI-LT 40.83 ± 0.70 vs Sham-LT 21.50 ± 1.89, $p<0.001$) and a decrease in the climbing behavior (CCI-LT 17.83 ± 0.98 vs Sham-LT 36.50 ± 0.64, $p<0.001$) relative to the sham rats (Fig. 2A). By contrast, there were no changes in the swimming behavior of these animals. Unlike the sensory tests, silencing the LC_{ipsi} or LC_{contra} by administering lidocaine induced a significant decreased in the immobility (LC_{ipsi}-CCI-Lido 25.57 ± 2.95 vs CCI-Sal 41.20 ± 0.86; LC_{contra}-CCI-Lido 18.90 ± 1.68 vs CCI-Sal 35.40 ± 2.63; $p<0.01$: Fig. 2B) and an increase in climbing behavior of the CCI-LT-lido rats relative to the CCI-LT-sal group (LC_{ipsi}, CCI-Lido 31.00 ± 1.99 vs CCI-Sal 16.60 ± 0.93, $p<0.01$; LC_{contra}, CCI-Lido 40.80 ± 1.94 vs CCI-Sal 21.70 ± 2.72; $p<0.001$: Fig. 2B), suggesting bilateral LC activation contributes to depression LT post-CCI. Again, the animal's swimming behavior was not altered. Moreover, blocking either LC_{ipsi} or LC_{contra} had no effect on the sham-animals or on the spontaneous locomotion in any experimental group (Fig. 2B-C).

Role of the LC→DRt pathway in nociception

To study the specific efferent pathways that may modulate the evolution of neuropathy, we explored how the descending LC to the DRt pathway influences the pain-related phenotype. Anatomical studies of this pathway were performed, establishing that the retrograde fluorescent tracer Fluoro-gold (FG) became confined to the boundaries of the DRt after its administration to the LC (Fig. 3A). FG administration to the contralateral DRt produced more FG labeled neurons in the LC_{contra} than the LC_{ipsi} (DRt_{contra} 60.77 ± 2.46% vs DRt_{ipsi} 39.23 ± 2.46%, $p<0.01$), being predominantly located in the medial LC domain considering the rostro-caudal axis (Fig. 3B). This shows that the LC projections to the DRt are partially lateralized, and that they are distributed along the dorso-ventral axis (LCipsi, dorsal 40.86 ± 5.04 vs ventral 59.14 ± 5.04; LCcontra, dorsal 43.15 ± 1.40 vs ventral 56.85 ± 5.40: Fig. 3C).

We next explored the expression of the phosphorylated cAMP response element binding protein (pCREB) in CCI-LT rats. Immunoreactivity for pCREB was significantly enhanced in the contralateral (DRt_{contra} 52.47 ± 3.46, $p<0.01$) but not the ipsilateral DRt (DRt_{ipsi} 29.00 ± 4.10) (Fig. 3D-E). However, these changes were not found in the DRt of CCI-LT Long-Evans rats (DRt_{contra} 35.02 ± 4.72; DRt_{ipsi} 44.68 ± 3.81) (Fig. S3C-D). Since FG tracing showed LC neurons to innervate the DRt profusely (Fig. 3A-C), we specifically blocked the LC_{contra} innervation to the DRt_{contra} using trans-synaptic CAV-Cre and Cre-dependent chemogenetic approaches (DREADD, designer receptor exclusively activated by designer drugs). As such, CAV2-Cre-GFP was injected into the DRt_{contra} and AAV-Gi-mCherry was injected into the LC_{contra} in CCI-LT rats (Fig. 4A and Fig. S4A-F). The selective inhibition of LC_{contra}→DRt_{contra} pathway by hM4D(Gi)-DREADD led to a robust alleviation of injury-induced neuropathic evoked pain, evident as a reduced acetone score (CCI-CNO 0.90 ± 0.13 vs CCI-Sal 2.25 ± 0.07, $p<0.001$) and mechanical withdrawal threshold in the Von Frey test (CCI-CNO 18.01 ± 0.86 vs CCI-Sal 4.67 ± 0.55; $p<0.001$: Fig. 4B). Furthermore, there was a significant decrease in the number of ipsilateral paw flinches following CNO administration (CCI-CNO 8.50 ± 0.81 vs CCI-Sal 17.88 ± 1.87, $p<0.001$: Fig. 4B), an index of spontaneous pain. As expected, subsequent intrathecal clonidine administration produced consistent spinal-mediated analgesia in this group for both evoked and spontaneous pain (acetone test, CCI-Cloni 0.30 ± 0.06 vs CCI-Sal 2.25 ± 0.10, $p<0.001$; von Frey test, CCI-Cloni 21.03 ± 3.67 vs CCI-Sal 5.20 ± 0.60, $p<0.01$; spontaneous pain test, CCI-Cloni 6.78 ± 1.22 vs CCI-Sal 17.88 ± 1.87, $p<0.01$: Fig. 4C). Finally, CNO administration to a control virus group (control-DREADD) did not produce any behavioral change (Fig. S5A-B), yet the intrathecal administration of clonidine consistently relieved pain-induced nerve injury (Fig. S5C-D).

Role of the LC→DRt pathway in depressive-like behavior

We explored the influence of the LC_{contra}→DRt_{contra} pathway on pain-related depressive-like behavior. In contrast to the sensory tests, selective inhibition of the LC_{contra}→DRt_{contra} pathway by hM4D(Gi)-DREADD did not produce any change in the depressive phenotype of CCI-LT rats (Fig. 5A-B). Surprisingly, there was a significant increase in the immobility (Sham-CNO 45.22 ± 2.19 vs Sham-Sal 35.50 ± 1.96, $p<0.01$) and a decrease in climbing behavior (Sham-CNO 14.78 ± 2.19 vs Sham-Sal 24.50 ± 1.96, $p<0.01$) of the Sham-CNO rats relative to the Sham-Sal animals following CNO administration (Fig. 5B). CNO administration did not produce any behavioral change in spontaneous locomotion in any experimental group (Fig. 5C). In addition, the effect of inhibiting the LC_{contra}→DRt_{contra} pathway on nociceptive behavior was also explored, as in Fig 4B. As expected, CNO administration produced an analgesic effect in injury-induced neuropathic evoked pain, evident as a reduced acetone score (CCI-LT-CNO 0.86 ± 0.15 vs CCI-LT-Sal 1.83 ± 0.17, $p<0.01$) and a higher mechanical withdrawal threshold in the Von Frey test (CCI-LT-CNO 16.49 ± 1.99 vs CCI-LT-Sal 7.57 ± 1.04; $p<0.05$: Fig. 5D). This analgesic effect had been lost 360 min after CNO administration, consistent with the pharmacokinetics of CNO (Fig. 5D) [43]. Finally, CNO did not produce any effect on the nociceptive behavior of the sham group or that of the contralateral paws.

Discussion

We have demonstrated time-dependent plastic changes in the noradrenergic-LC system as pain develops from acute to chronic and it becomes associated with behavioral despair. In Sprague-Dawley rats, increasing the tone of the LC_{ipsi} initially dampens injury-induced neuropathic pain, yet this analgesic system fails over time, with endogenous activation of other LC modules aggravating pain and emotional symptoms. Thus, there is over-activation of a contralateral-LC-medulla facilitatory pain pathway that contributes to pain, while global bilateral LC activation contributes to pain-induced depression.

Inactivation of the LC by lidocaine was used to reveal the time-dependent endogenous plasticity in the LC that occurs during the development of neuropathy. Hence, silencing the LC_{ipsi} increases pain sensitivity in the ipsilateral paw of Sprague-Dawley rats for a short period of time (2 days after injury) but not later. This analgesic effect is consistent with earlier data showing that chemogenetic blockade of the LC_{ipsi} in Long-Evans rats or administration of α2-adrenoreceptor antagonists at the lumbar level (LC projection area) in Wistar rats suppress the development of nerve-injured hindpaw sensitization, albeit only at the beginning of nerve injury and not later [19,25]. Therefore, these results would suggest that the LC_{ipsi} projection to the SC is activated by neuropathy, increasing the release of noradrenaline in the SC in recently injured animals and providing endogenous analgesia through spinal α2-adrenoreceptors. However, this effect seems to be lost shortly after nerve injury, suggesting the exhaustion of this endogenous analgesic system, as reported previously. Indeed, microinjection of lidocaine into the LC_{ipsi} 3 weeks after the induction of nerve injury did not affect hypersensitivity in the injured hindpaw of spared nerve injury rats [41]. Hence, LC_{ipsi} neurons lose their ability to become activated when injury persists.
We also assessed the effect of pharmacological inhibition of the LC_{contra} with lidocaine. The administration of lidocaine leads to a clear analgesic effect in the ipsilateral paw in mid- and long-term neuropathy, suggesting a proalgesic role of the LC_{contra}. This result is consistent with previous data in Sprague-Dawley also showing that bilateral microinjections of lidocaine into the LC completely reversed the behavioral signs of neuropathy in a spinal nerve injury (SNI) model after 2 weeks of nerve injury [12]. Therefore, under prolonged painful conditions the spinal anti-nociceptive influence of noradrenaline presumably released from the LC seems to be compromised, by the activation of other pronociceptive LC ensembles, such as those projecting to the DRt [23,33]. Interestingly, nociceptive stimulation 2 or 3 weeks after SNI induction increases noradrenaline release into the DRt of Wistar neuropathic animals [30]. Thus, it is likely that LC activation after long-term neuropathic pain enhances the descending facilitation from the DRt [30,31], as shown by the increase expression of pCREB in the DRt_{contra}. As lidocaine might inhibit input or passage fibers in the LC [29], we evaluated the chemogenetic inhibition of this pathway. DREADDs-mediated inactivation of the $LC_{contra}\rightarrow DRt_{contra}$ pathway produces a clear analgesic effect in evoked and spontaneous pain, unmasking a descending facilitation noradrenergic pathway to the DRt. This activation might contribute to spinal sensitization during neuropathic pain [42]. As CNO was administered systemically, our data do not rule out the possibility that LC neurons projecting to the DRt also project to other regions, an idea supported by previous anatomical work [38]. Furthermore, the subsequent activation of spinal α2-adrenoreceptors in the same animals produces a comparable analgesic effect to that when chemogenetically inhibiting the $LC_{contra}\rightarrow DRt_{contra}$ pathway. This demonstrates that spinal mediated analgesia can be achieved exogenously even after long-term pain

[17,25]. Therefore, the time-dependent evaluation of endogenous LC activity as neuropathy develops reconciles the data available suggesting an analgesic and proalgesic role of the LC in neuropathic pain. Furthermore, our results in Sprague-Dawley rats contrast with the findings in CCI-LT Long-Evans rats, in which chemogenetic [25] or pharmacological inhibition of the LC_{contra} did not modify sensorial hypersensitivity or the pCREB expression in the DRt, suggesting that the long-term LC_{contra} pain plasticity is strain dependent. Accordingly, spinal blockade of α2-adrenoreceptors had no effect on allodynic Sprague-Dawley or Holtzman rats. However, it unmasked allodynia in previously nonallodynic Holtzman rats with spinal nerve ligation (De-Felice-2011-Pain). Thus, rat strain, chronology and the side of the LC relative to the injury are critical factors for dynamic LC plasticity, contributing to opposing behaviors (pain/analgesia). In agreement with previous findings [37,40], lidocaine administration did not modify the sensorial response in sham animals suggesting that LC activity appears to have a minor influence on basal pain sensitivity. Furthermore, we did not see any change in the pain threshold of the contralateral paw of injured animals at any time point, consistent with previous data [12]. However, intrathecal yohimbine was seen to unmask contralateral hindlimb allodynia and hyperalgesia in tibial nerve injured Wistar animals from 3 to 17 days after nerve injury [19]. This discrepancy could be explained by the activation of other noradrenergic nuclei projecting to the SC (e.g. A5 and A7) [18], differences in the rat strain or animal model of neuropathic pain used [13,14,24,39].

A particularly serious consequence of suffering pain is the comorbidity with mental disorders, of which depression seems to be the most common by affecting more than 50% of chronic pain patients [5,16]. Indeed, pain is currently considered a risk factor to suffer psychiatric disorders and as pain is fundamentally unpleasant, it could be considered a potential stress to the organism. However, the mechanisms underlying this comorbidity are not clear. We previously found that long-term pain triggers increased c-fos, pCREB, tyrosine hydroxylase (TH) and noradrenaline transporter expression, and enhanced α2-adrenoceptor expression and sensitivity in the LC of Sprague-Dawley rats, which temporally coincides with the onset of anxiodepressive behavior in such animals [1,2,27]. Furthermore, chemogenetic blockade of the LC_{ipsi} or LC_{contra} reversed pain-induced depression in Long-Evans rats [25]. In agreement, lidocaine-mediated LC blockade of the ipsi- or contralateral LC produces less immobility in Sprague-Dawley rats, suggesting the activity of LC_{ipsi} or LC_{contra} contributes to the behavioral despair phenotype associated with long-term pain. These data agree with in vivo electrophysiological recordings in anesthetized animals showing minor mid-term changes after nerve injury. However, alterations to both spontaneous ipsilateral and contralateral LC activity were found with long-term pain, as witnessed by the higher incidence of burst firing and irregular firing [3]. These data suggest that both sides of the LC are hyperactivated in long-term pain, and such a situation may explain the aberrant LC response to environmental challenges. Furthermore, we also demonstrate that LC inactivation did not modify the mFST responses in sham animals, suggesting that the activity of the LC is required to produce depressive-like behavior in sensitized animals, although the basal activity of the LC itself does not favor depression. Finally, we also explored the effect of selective chemogenetic inhibition of the LC_{contra}→DRt_{contra} pathway in animals submitted to the mFST. The inactivation of this pathway significantly increased the time spent immobile in sham animals, suggesting that the activity of this pathway is relevant in terms of coping with acute stressful situations, probably to trigger alert reactions that generate a protective/defense reaction to

stress [6]. However, the already elevated levels of immobility in long-term neuropathic animals were not modified. Therefore, the inactivation of this pathway leads to analgesia but it does not modify the depressive phenotype in animals experiencing chronic pain.

We demonstrate that there are endogenous time-dependent adaptations induced by nerve injury. Specifically in Sprague-Dawley rats, nerve injury drives endogenous activation of noradrenergic LC_{ipsi} neurons, which dampens the neuropathic pain phenotype for a short period after the lesion. By contrast, the LC_{contra} robustly triggers long-term sensorial hypersensitivity, which seems to be contributed by the specific activation of the $LC_{contra}\rightarrow DRt_{contra}$ pathway. However, the spinal analgesia mediated by the exogenous activation of α2-adrenoreceptors is able to provide consistent pain relief. Furthermore, LC_{contra} activity does not seem involved in sensorial hypersensitivity in long-term pain in Long-Evans rats. This time dependent evaluation of the LC reconciles data demonstrating that the LC is a source of pain inhibition but also, a chronic pain generator. Furthermore, it also explains the limited efficacy of systemic drugs increasing global noradrenaline availability [4,10,22]. Therefore, more specific approaches increasing the noradrenaline restricted to the SC would be able to provide stronger analgesia [17,25], avoiding the activation of other areas that increase sensorial hypersensitivity and an anxiodepressive phenotype, such as the DRt, prefrontal cortex and basolateral amygdala [17,25,27]. Hence, it has been shown that the chemogenetic activation of the LC projections to the prefrontal cortex exacerbated spontaneous pain, produced aversion and increased anxiety-like behavior in neuropathic animals [17]. Furthermore, chemogenetic inhibition of the pathway to the basolateral amygdala or cingulate cortex abolished neuropathic pain-induced anxiety and depression [25,27].

We show that the sensorial threshold is lateralized and pain-induced depression has a bilateral contribution, suggesting that sensorial and emotional behaviors are not controlled internally within the LC and that the activation or lack of its activity is controlled by specific afferents. Hence, the mechanisms underlying the comorbidity of chronic pain and mood disorders are likely to be related to complex alterations in brain networks rather than to changes occurring in a single brain structure.

Acknowledgments

We are very grateful to Mr Santiago Muñoz, Ms Paula Reyes Perez and Ms Elena Marín Álvarez for their excellent technical assistance. This study was supported by grants co-financed by the “Fondo Europeo de Desarrollo Regional” (FEDER)-UE “A way to build Europe” from the “Ministerio de Economía y Competitividad” (MINECO: RTI2018-099778-B-I00) and by the “Ministerio de Salud-Instituto de Salud Carlos III (PI18/01691); the “Consejería de Salud de la Junta de Andalucía” (PI-0134-2018); the “Programa Operativo de Andalucía FEDER, Iniciativa Territorial Integrada ITI 2014-2020 Consejería Salud, Junta de Andalucía” (PI-0080-2017); Instituto de Investigación e Innovación en Ciencias Biomédicas de Cádiz (INiBICA LI19/06IN- CO22); the “Consejería de Economía, Innovación, Ciencia y Empleo de la Junta de Andalucía” (CTS-510); and the “Centro de Investigación Biomédica en Red de Salud Mental-CIBERSAM” (CB/07/09/0033).

Conflict of Interest: The authors declare no conflicts of interests.

References

[1] Alba-Delgado C, Llorca-Torralba M, Horrillo I, Ortega JE, Mico JA, Sanchez-Blazquez P, Meana JJ, Berrocoso E. Chronic pain leads to concomitant noradrenergic impairment and mood disorders. Biol Psychiatry 2013;73(1):54-62.

[2] Alba-Delgado C, Llorca-Torralba M, Mico JA, Berrocoso E. The onset of treatment with the antidepressant desipramine is critical for the emotional consequences of neuropathic pain. Pain 2018;159(12):2606-2619.

[3] Alba-Delgado C, Mico JA, Berrocoso E. Neuropathic pain increases spontaneous and noxious-evoked activity of locus coeruleus neurons. Progress in neuro-psychopharmacology & biological psychiatry 2020;105:110121.

[4] Attal N. Pharmacological treatments of neuropathic pain: The latest recommendations. Rev Neurol (Paris) 2019;175(1-2):46-50.

[5] Bair MJ, Robinson RL, Katon W, Kroenke K. Depression and pain comorbidity: a literature review. Arch Intern Med 2003;163(20):2433-2445.

[6] Barik A, Thompson JH, Seltzer M, Ghitani N, Chesler AT. A Brainstem-Spinal Circuit Controlling Nocifensive Behavior. Neuron 2018;100(6):1491-1503 e1493.

[7] Bennett GJ, Xie YK. A peripheral mononeuropathy in rat that produces disorders of pain sensation like those seen in man. Pain 1988;33(1):87-107.

[8] Berrocoso E, Mico JA. In vivo effect of venlafaxine on locus coeruleus neurons: role of opioid, alpha(2)-adrenergic, and 5-hydroxytryptamine(1A) receptors. J Pharmacol Exp Ther 2007;322(1):101-107.

[9] Berrocoso E, Rey-Brea R, Fernandez-Arevalo M, Mico JA, Martin-Banderas L. Single oral dose of cannabinoid derivate loaded PLGA nanocarriers relieves neuropathic pain for eleven days. Nanomedicine 2017;13(8):2623-2632.

[10] Bravo L, Llorca-Torralba M, Berrocoso E, Mico JA. Monoamines as Drug Targets in Chronic Pain: Focusing on Neuropathic Pain. Front Neurosci 2019;13:1268.

[11] Bravo L, Mico JA, Rey-Brea R, Camarena-Delgado C, Berrocoso E. Effect of DSP4 and desipramine in the sensorial and affective component of neuropathic pain in rats. Progress in neuro-psychopharmacology & biological psychiatry 2016;70:57-67.

[12] Brightwell JJ, Taylor BK. Noradrenergic neurons in the locus coeruleus contribute to neuropathic pain. Neuroscience 2009;160(1):174-185.

[13] Bruinstroop E, Cano G, Vanderhorst VG, Cavalcante JC, Wirth J, Sena-Esteves M, Saper CB. Spinal projections of the A5, A6 (locus coeruleus), and A7 noradrenergic cell groups in rats. J Comp Neurol 2012;520(9):1985-2001.

[14] Clark FM, Yeomans DC, Proudfit HK. The noradrenergic innervation of the spinal cord: differences between two substrains of Sprague-Dawley rats determined using retrograde tracers combined with immunocytochemistry. Neurosci Lett 1991;125(2):155-158.

[15] Detke MJ, Rickels M, Lucki I. Active behaviors in the rat forced swimming test differentially produced by serotonergic and noradrenergic antidepressants. Psychopharmacology (Berl) 1995;121(1):66-72.

[16] Doan L, Manders T, Wang J. Neuroplasticity underlying the comorbidity of pain and depression. Neural Plast 2015;2015:504691.

[17] Hirschberg S, Li Y, Randall A, Kremer EJ, Pickering AE. Functional dichotomy in spinal- vs prefrontal-projecting locus coeruleus modules splits descending noradrenergic analgesia from ascending aversion and anxiety in rats. Elife 2017;6.

[18] Howorth PW, Thornton SR, O'Brien V, Smith WD, Nikiforova N, Teschemacher AG, Pickering AE. Retrograde viral vector-mediated inhibition of pontospinal noradrenergic neurons causes hyperalgesia in rats. J Neurosci 2009;29(41):12855-12864.

[19] Hughes SW, Hickey L, Hulse RP, Lumb BM, Pickering AE. Endogenous analgesic action of the pontospinal noradrenergic system spatially restricts and temporally delays the progression of neuropathic pain following tibial nerve injury. Pain 2013;154(9):1680-1690.

[20] Ikeda Y, Oda Y, Nakamura T, Takahashi R, Miyake W, Hase I, Asada A. Pharmacokinetics of lidocaine, bupivacaine, and levobupivacaine in plasma and brain in awake rats. Anesthesiology 2010;112(6):1396-1403.

[21] Jones SL. Descending noradrenergic influences on pain. Prog Brain Res 1991;88:381-394.

[22] Kremer M, Salvat E, Muller A, Yalcin I, Barrot M. Antidepressants and gabapentinoids in neuropathic pain: Mechanistic insights. Neuroscience 2016;338:183-206.

[23] Lima D, Almeida A. The medullary dorsal reticular nucleus as a pronociceptive centre of the pain control system. Prog Neurobiol 2002;66(2):81-108.

[24] Llorca-Torralba M, Borges G, Neto F, Mico JA, Berrocoso E. Noradrenergic Locus Coeruleus pathways in pain modulation. Neuroscience 2016;338:93-113.

[25] Llorca-Torralba M, Camarena-Delgado C, Suárez-Pereira I, Bravo L, Mariscal P, López-Martín C, Wei H, Pertovaara A, Mico J, Berrocoso E. Neuropathic pain and depression comorbidity causes asymmetric time-dependent platicity in the noradrenergic Locus Coeruleus neurons. Brain (in press) 2021.

[26] Llorca-Torralba M, Mico JA, Berrocoso E. Behavioral effects of combined morphine and MK-801 administration to the locus coeruleus of a rat neuropathic pain model. Progress in neuro-psychopharmacology & biological psychiatry 2018;84(Pt A):257-266.

[27] Llorca-Torralba M, Suarez-Pereira I, Bravo L, Camarena-Delgado C, Garcia-Partida JA, Mico JA, Berrocoso E. Chemogenetic Silencing of the Locus Coeruleus-Basolateral Amygdala Pathway Abolishes Pain-Induced Anxiety and Enhanced Aversive Learning in Rats. Biol Psychiatry 2019;85(12):1021-1035.

[28] Ma W, Eisenach JC. Chronic constriction injury of sciatic nerve induces the up-regulation of descending inhibitory noradrenergic innervation to the lumbar dorsal horn of mice. Brain Res 2003;970(1-2):110-118.

[29] Martin JH. Autoradiographic estimation of the extent of reversible inactivation produced by microinjection of lidocaine and muscimol in the rat. Neurosci Lett 1991;127(2):160-164.

[30] Martins I, Carvalho P, de Vries MG, Teixeira-Pinto A, Wilson SP, Westerink BH, Tavares I. Increased noradrenergic neurotransmission to a pain facilitatory area of the brain is implicated in facilitation of chronic pain. Anesthesiology 2015;123(3):642-653.

[31] Martins I, Costa-Araujo S, Fadel J, Wilson SP, Lima D, Tavares I. Reversal of neuropathic pain by HSV-1-mediated decrease of noradrenaline in a pain facilitatory area of the brain. Pain 2010;151(1):137-145.

[32] Martins I, de Vries MG, Teixeira-Pinto A, Fadel J, Wilson SP, Westerink BH, Tavares I. Noradrenaline increases pain facilitation from the brain during inflammatory pain. Neuropharmacology 2013;71:299-307.

[33] Martins I, Tavares I. Reticular Formation and Pain: The Past and the Future. Frontiers in neuroanatomy 2017;11:51.

[34] Pertovaara A, Hamalainen MM, Kauppila T, Mecke E, Carlson S. Dissociation of the alpha 2-adrenergic antinociception from sedation following microinjection of medetomidine into the locus coeruleus in rats. Pain 1994;57(2):207-215.

[35] Poe GR, Foote S, Eschenko O, Johansen JP, Bouret S, Aston-Jones G, Harley CW, Manahan-Vaughan D, Weinshenker D, Valentino R, Berridge C, Chandler DJ, Waterhouse B, Sara SJ. Locus coeruleus: a new look at the blue spot. Nat Rev Neurosci 2020.

[36] Porreca F, Burgess SE, Gardell LR, Vanderah TW, Malan TP, Jr., Ossipov MH, Lappi DA, Lai J. Inhibition of neuropathic pain by selective ablation of brainstem medullary cells expressing the mu-opioid receptor. J Neurosci 2001;21(14):5281-5288.

[37] Safari MS, Haghparast A, Semnanian S. Effect of lidocaine administration at the nucleus locus coeruleus level on lateral hypothalamus-induced antinociception in the rat. Pharmacol Biochem Behav 2009;92(4):629-634.

[38] Schwarz LA, Miyamichi K, Gao XJ, Beier KT, Weissbourd B, DeLoach KE, Ren J, Ibanes S, Malenka RC, Kremer EJ, Luo L. Viral-genetic tracing of the input-output organization of a central noradrenaline circuit. Nature 2015;524(7563):88-92.

[39] Sluka KA, Westlund KN. Spinal projections of the locus coeruleus and the nucleus subcoeruleus in the Harlan and the Sasco Sprague-Dawley rat. Brain Res 1992;579(1):67-73.

[40] Smith LJ, Shih A, Miletic G, Miletic V. Continual systemic infusion of lidocaine provides analgesia in an animal model of neuropathic pain. Pain 2002;97(3):267-273.

[41] Song Z, Ansah OB, Meyerson BA, Pertovaara A, Linderoth B. Exploration of supraspinal mechanisms in effects of spinal cord stimulation: role of the locus coeruleus. Neuroscience 2013;253:426-434.

[42] Sotgiu ML, Valente M, Storchi R, Caramenti G, Mario Biella GE. Contribution by DRt descending facilitatory pathways to maintenance of spinal neuron sensitization in rats. Brain Res 2008;1188:69-75.

[43] Tervo DGR, Proskurin M, Manakov M, Kabra M, Vollmer A, Branson K, Karpova AY. Behavioral variability through stochastic choice and its gating by anterior cingulate cortex. Cell 2014;159(1):21-32.

[44] Uematsu A, Tan BZ, Ycu EA, Cuevas JS, Koivumaa J, Junyent F, Kremer EJ, Witten IB, Deisseroth K, Johansen JP. Modular organization of the brainstem noradrenaline system coordinates opposing learning states. Nat Neurosci 2017;20(11):1602-1611.

[45] Wei H, Viisanen H, You HJ, Pertovaara A. Spinal histamine in attenuation of mechanical hypersensitivity in the spinal nerve ligation-induced model of experimental neuropathy. Eur J Pharmacol 2016;772:1-10.

Figure legends

Fig. 1. (A) Graphs showing the acetone test response of the ipsilateral and contralateral hindpaw of rats at short-term (ST), mid-term (MT) and long-term (LT) after chronic constriction injury (CCI - Sham n=9, CCI n=9: **p<0.01, ***p<0.001 vs Sham). (**B)** Timeline and representative image of the inhibition of the ipsilateral-LC (LC_{ipsi}) and contralateral-LC (LC_{contra}) by lidocaine (4%) microinjection in Sprague-Dawley rats. (**C)** Representative image of LC_{ipsi} inhibition by lidocaine (4%) microinjection. The graphs show the acetone test response of the Ipsilateral and Contralateral paw in ST-, MT- and LT-CCI rats (ST - Sham-Sal n=9, Sham-Lido n=9, CCI-Sal n=9, CCI-Lido n=8; MT - Sham-Sal n=6, Sham-Lido n=6, CCI-Sal n=8, CCI-Lido n=7; LT - Sham-Sal n=8, Sham-Lido n=8, CCI-Sal n=9, CCI-Lido n=9: **p<0.01, ***p<0.001 vs Sham-Sal; ++p<0.01 vs CCI-Sal). (**D)** Representative image of LC_{contra} inhibition by lidocaine (4%) microinjection. The graphs show the acetone test response of the Ipsilateral and Contralateral paw of ST-, MT- and LT-CCI rats (ST - Sham-Sal n=8, Sham-Lido n=10, CCI-Sal n=8, CCI-Lido n=10; MT - Sham-Sal n=9, Sham-Lido n=10, CCI-Sal n=10, CCI-Lido n=10; LT - Sham-Sal n=7, Sham-Lido n=9, CCI-Sal n=9, CCI-Lido n=10: ***p<0.001 vs Sham-Sal; ++p<0.01, +++p<0.001 vs CCI-Sal). CCI, Chronic constriction injury; A, Acetone test; Sal, Saline; Lido, Lidocaine; Ipsi-paw, ipsilateral paw; Contra-paw, contralateral paw.

Fig. 2. Timeline and representative image of the modified forced swimming (mFST) test long-term (LT) after chronic constriction injury (CCI). The graphs show the predominant behavior in the mFST: immobility, IM; climbing, CL; swimming, SW (Sham n=4, CCI n=6: ***p<0.001 vs Sham-Sal Student's t-test for each predominant behavior). (**B)** Timeline and representative image of ipsilateral-LC (LC_{ipsi}) and contralateral-LC (LC_{contra}) inhibition by lidocaine (4%) in LT-CCI rats. The graphs show the predominant behavior (IM, CL and SW) in the mFST after microinjection of 4% lidocaine (LC_{ipsi} - Sham-Sal n=6, Sham-Lido n=6, CCI-Sal n=5, CCI-Lido n=7; LC_{contra} - Sham-Sal n=10, Sham-Lido n=10, CCI-Sal n=10, CCI-Lido n=10: **p<0.001, ***p<0.001 vs Sham-Sal; ++p<0.01, +++p<0.001 vs CCI-Sal). (**C)** Effect of lidocaine administration on spontaneous locomotor activity (arbitrary units, A.U. - Sham-Sal n=3, Sham-Lido n=3, CCI-Sal n=6, CCI-Lido n=5: ***p<0.001 vs min 5). CCI, Chronic constriction injury; LC, locus coeruleus; mFST, modified forced swimming test; AU, Arbitrary Units; Sal, Saline; Lido, Lidocaine. Some elements of this figure were produced using BioRender (www.BioRender.com).

Fig. 3 (A) Retrograde FG tracer strategy to target LC neurons that project to the DRt nucleus in-Sprague-Dawley rats and a representative image of unilateral FG injection into the contralateral DRt (DRt_{contra}: scale bar 500 µm). FG labeled neurons are shown in the inset. (**B)** Graphs showing the ipsilateral and contralateral distribution of FG labeled LC neurons along the rostral-caudal axis of the ipsilateral (LC_{ipsi}) and contralateral (LC_{contra}) LC after unilateral FG-tracer administration in the DRt . The data represent the mean + SEM of the number of neurons per slice (n= 3 animals: **p<0.01 vs LC_{ipsi}). (**C)** Representative immunofluorescence of the medial LC_{ipsi} and LC_{contra} (-9.96 from Bregma: Paxinos and Watson, 2007) showing the dorso-ventral aspect (half height relative to DBH expression) (scale bar 100 µm). FG labeled neurons are shown in the inset. The graphs show the dorso-ventral distribution of the medial LC_{ipsi} and LC_{contra} projections in the DRt_{contra} (n= 3 animals). (**D)** Quantification of pCREB positive neurons to the

ipsilateral DRt (DRt_{ipsi}) and DRt_{contra} of sham and CCI-LT rats (Sham n=4, CCI n=3: **p<0.01 vs DRt_{ipsi} in CCI-LT animals). (**E)** Representative image of pCREB positive neurons into the DRt_{ipsi} or DRt_{contra} of CCI-LT rats. CCI, Chronic constriction injury; LT, Long-term; LC, locus coeruleus; DRt, dorsal reticular nucleus; FG, Fluoro-Gold; DBH, dopamine beta-hydroxylase; IR, immunoreactivity.

Fig. 4. (A) Timeline and scheme of the retrograde CAV-Cre-GFP injection into the contralateral DRt (DRt_{contra}), and of AAV-Gi-mCherry into the contralateral LC (LC_{contra}) to inhibit the LC_{contra}→DRt_{contra} pathway in Sprague-Dawley rats. Histological verification of CAV-Cre-GFP administration intra-DRt_{contra} (scale bar 200 μm). Representative immunofluorescence of GFP, mCherry and DBH expression in LC neurons (scale bar 20 μm). Green, dopamine beta-hydroxylase; red, mCherry marked with red fluorescent protein; cyan, green fluorescent protein. **(B)** The graphs show the response of the ipsilateral and contralateral hindpaw in the acetone, von Frey and spontaneous pain tests after CNO administration (1 mg/kg, i.p.) to CCI-LT animals (Sham-Sal n=6, Sham-Cloni n=7, CCI-Sal n=8, CCI-Cloni n=10: ***p<0.001 vs Sham-Sal; +++p<0.001 vs CCI-Sal). **(C)** The graphs show the response of the Ipsilateral and Contralateral paw in the acetone, von frey and spontaneous pain tests after clonidine (20 μg, i.t.) administration to CCI-LT animals (Sham-Sal n=5, sham-Cloni n=6, CCI-Sal n=8, CCI-Cloni n=10: ***p<0.001 vs Sham-Sal; ++p<0.01, +++p<0.001 vs CCI-Sal). DBH, dopamine beta-hydroxylase; DRt, dorsal reticular nucleus; GFP, green fluorescent protein; LC, locus coeruleus; CCI, Chronic constriction injury; LT, Long-term; CNO, clozapine-n-oxide; Sal, Saline; Cloni, clonidine; A, acetone test; VF, von Frey test; SP, spontaneous pain test; i.t., intrathecal; i.p., intraperitoneal; Ipsi-paw, ipsilateral paw; Contra-paw, contralateral paw.

Fig. 5. (A-B) Timeline and representative scheme of the retrograde CAV-Cre-GFP injections into the contralateral DRt (DRt_{contra}), and of the AAV-Gi-mCherry into the contralateral LC (LC_{contra}) to inhibit the LC_{contra}→DRt_{contra} pathway in Sprague-Dawley rats. The graph shows the predominant behavior (IM, CL and SW) in the mFST after intraperitoneal CNO (1 mg/kg) administration (Sham-Sal n=10, Sham-CNO n=9, CCI-Sal n=11, CCI-CNO n=9: ***p<0.001 vs Sham-Sal). **(C)** Effect of CNO administration on spontaneous locomotor activity (arbitrary units, A.U. - Sham-Sal n=10, Sham-CNO n=9, CCI-Sal n=11, CCI-CNO n=9). **(D)** The graphs show the duration of the effect of CNO in the acetone and von Frey test, and the response of the ipsilateral and contralateral hindpaw 20 and 360 min after applying acetone or the metal filament (Sham-Sal n=10, Sham-CNO n=9, CCI-Sal n=11, CCI-CNO n=9: ***p<0.001 vs Sham-Sal; +p<0.05, ++p<0.01 vs CCI-Sal). CCI, Chronic constriction injury; DRt, dorsal reticular nucleus; LC, locus coeruleus; CNO, Clozapine-n-oxide; Sal, Saline; LA, Locomotor activity test; d, days; LT, Long-term; mFST, modified forced swimming test; A, Acetone test; VF, Von Frey test; IM; immobility; CL, Climbing; SW, swimming; AU, Arbitrary Units; min, minutes; Ipsi-paw, ipsilateral-paw; Contra-paw, contralateral paw.

Supplemental figures

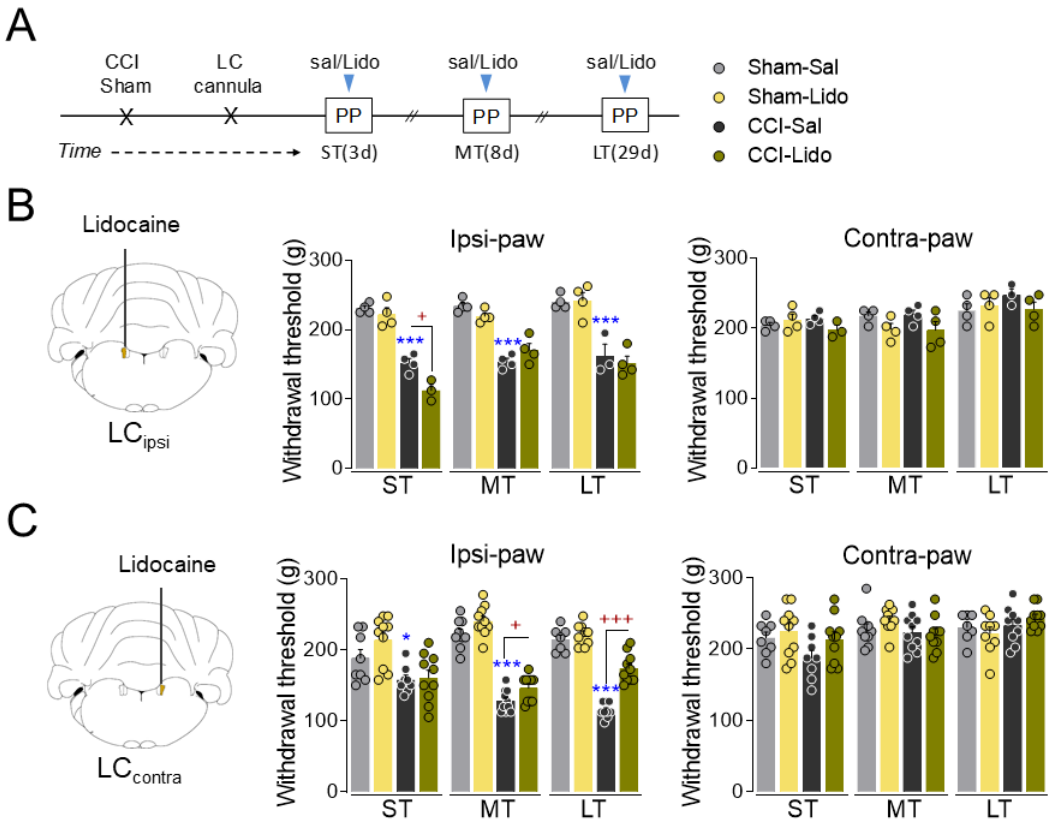

Fig. S1. (**A)** Timeline and representative image of ipsilateral-LC (LC_{ipsi}) and contralateral-LC (LC_{contra}) inhibition with a lidocaine (4%) microinjection in Sprague-Dawley rats. (**B)** Representative image of LC_{ipsi} inhibition by lidocaine (4%) microinjection. The graphs show the withdrawal threshold of the ipsilateral and contralateral paw of ST-, MT- and LT-CCI rats in pressure tests (ST - Sham-Sal n=4, Sham-Lido n=4, CCI-Sal n=4, CCI-Lido n=3; MT - Sham-Sal n=4, Sham-Lido n=4, CCI-Sal n=4, CCI-Lido n=4; LT - Sham-Sal n=4, Sham-Lido n=4, CCI-Sal n=3, CCI-Lido n=4: ***p<0.001 vs Sham-Sal; +p<0.05 vs CCI-Sal). (**C)** Representative image of LC_{contra} inhibition by lidocaine (4%) microinjection. The graphs show response of the Ipsilateral and Contralateral paw of ST-, MT- and LT-CCI rats in the acetone test (ST - Sham-Sal n=8, Sham-Lido n=10, CCI-Sal n=8, CCI-Lido n=10; MT - Sham-Sal n=9, Sham-Lido n=10, CCI-Sal n=10, CCI-Lido n=10; LT - Sham-Sal n=7, Sham-Lido n=9, CCI-Sal n=9, CCI-Lido n=10: ***p<0.001 vs Sham-Sal; +p<0.05, +++p<0.001 vs CCI-Sal). CCI, Chronic constriction injury; PP, paw pressure; Sal, Saline; Lido, Lidocaine; Ipsi-paw, ipsilateral paw; Contra-paw, contralateral paw.

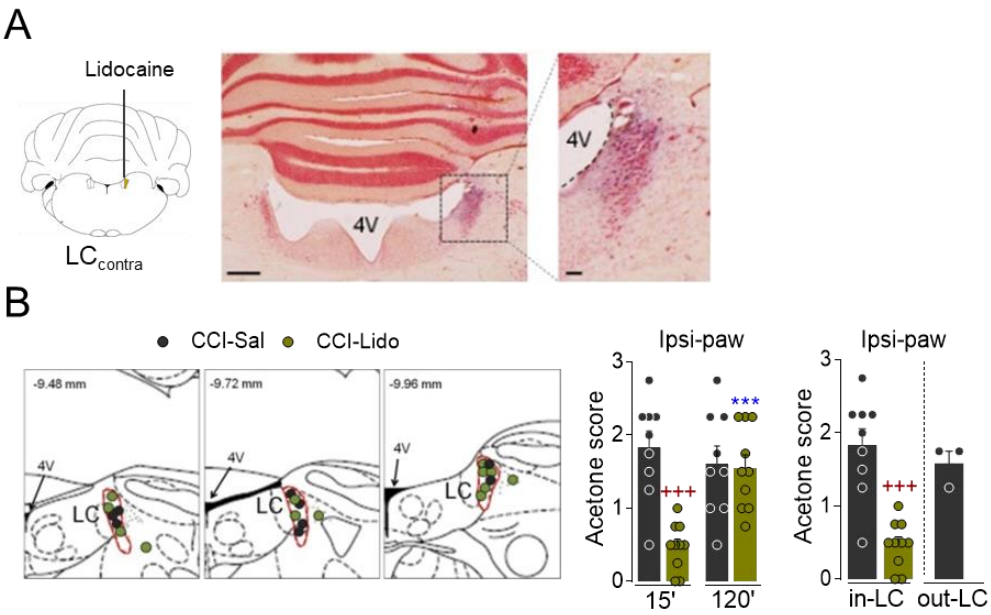

Fig. S2. (A) Representative image of LC_{contra} inhibition by lidocaine (4%) microinjection in Sprague-Dawley rats. Photomicrograph of a coronal section (neutral red stain) of a Sprague-Dawley rat brainstem showing the spread of Pontamine Sky Blue solution after its administration into the LC (scale bar: 250 µm) and a higher magnification of the inset (scale bar 250 µm). (**B)** Schemes adapted from the Paxinos and Watson atlas (co-ordinates relative to bregma: Paxinos and Watson, 2007) to show the lidocaine microinjection sites within (in) and beyond (out) the LC of the LT-CCI rats. The graph shows the duration of the effect of lidocaine in the acetone test, the graph shows the response of the ipsilateral hindpaw 15 and 120 min after applying acetone (CCI-Sal n=9, CCI-CNO n=10: ***p<0.001 vs CCI-Lido (15'); +++p<0.001 vs CCI-Sal (15'). The next graph shows the response of the ipsilateral paw in the acetone test when lidocaine was microinjected outside the LC (CCI-Sal [out-LC] n=3, CCI-Sal [in-LC] n=9, CCI-CNO [in-LC] n=10: +++p<0.001 vs CCI-Sal). CCI, Chronic constriction injury; Lido, lidocaine; Sal, saline; LC, locus coeruleus; 4V, fourth ventricle; Ipsi-paw, ipsilateral paw; Contra-paw, contralateral paw.

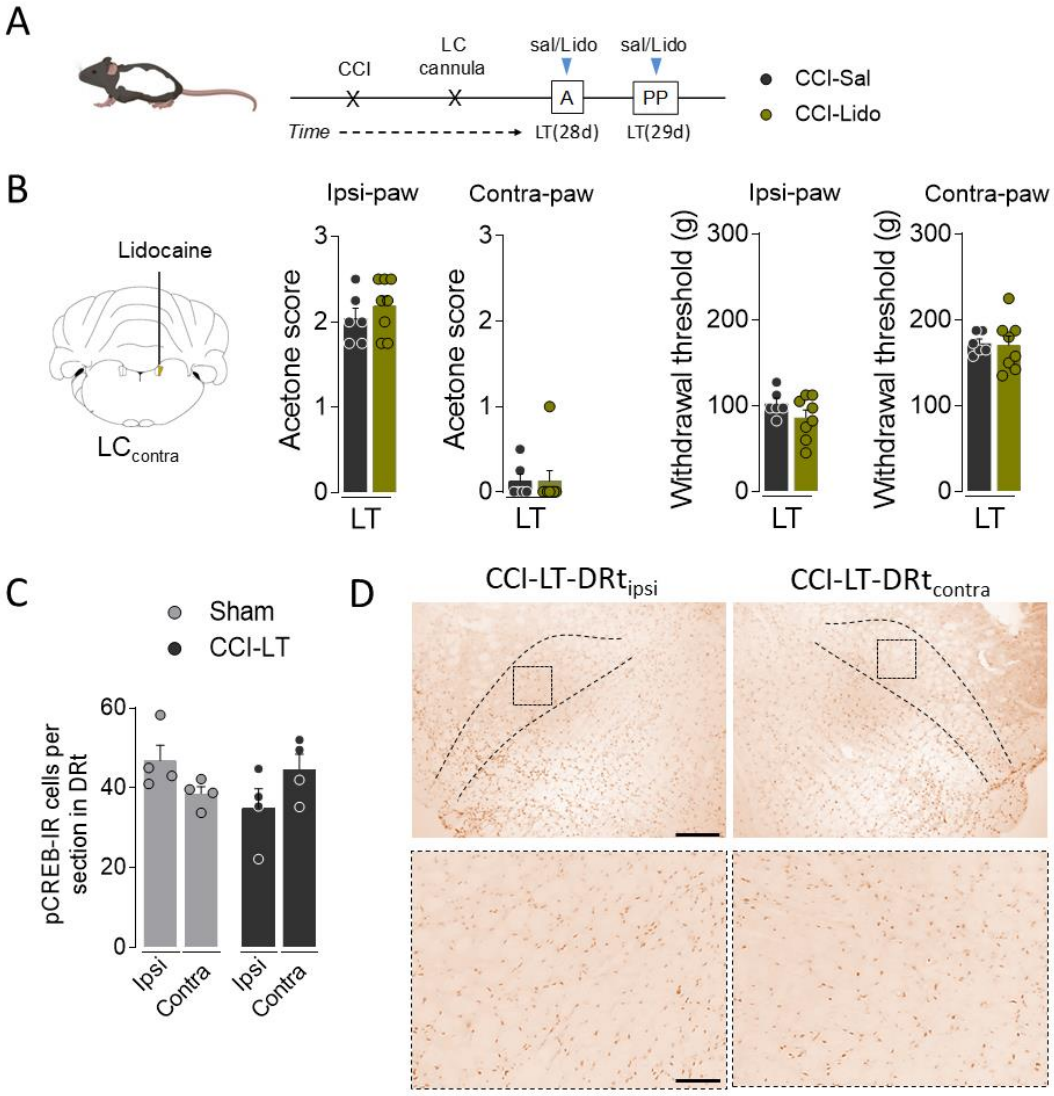

Fig. S3. (**A)** Timeline of contralateral-LC (LC_{contra}) inhibition with a lidocaine (4%) microinjection in Long-Evans rats. (**B)** Representative image of LC_{contra} inhibition by lidocaine (4%) microinjection. The graphs show the withdrawal threshold of the ipsilateral and contralateral paw of CCI-LT rats in acetone and paw pressure test (CCI-Sal n=6, CCI-Lido n=8). (**C)** Quantification of pCREB positive neurons to the ipsilateral DRt (DRt_{ipsi}) and contralateral (DRt_{contra}) of sham and CCI-LT rats of Long-Evans rats (Sham n=4, CCI n=4). (**D)** Representative image of pCREB positive neurons into the DRt_{ipsi} or DRt_{contra} of CCI-LT rats. CCI, Chronic constriction injury; LT, Long-term; LC, locus coeruleus; DRt, dorsal reticular nucleus; IR, immunoreactivity; A, acetone; PP, paw pressure; Sal, Saline; Lido, Lidocaine; Ipsi-paw, ipsilateral paw; Contra-paw, contralateral paw. Some elements of this figure were produced using BioRender (www.BioRender.com).

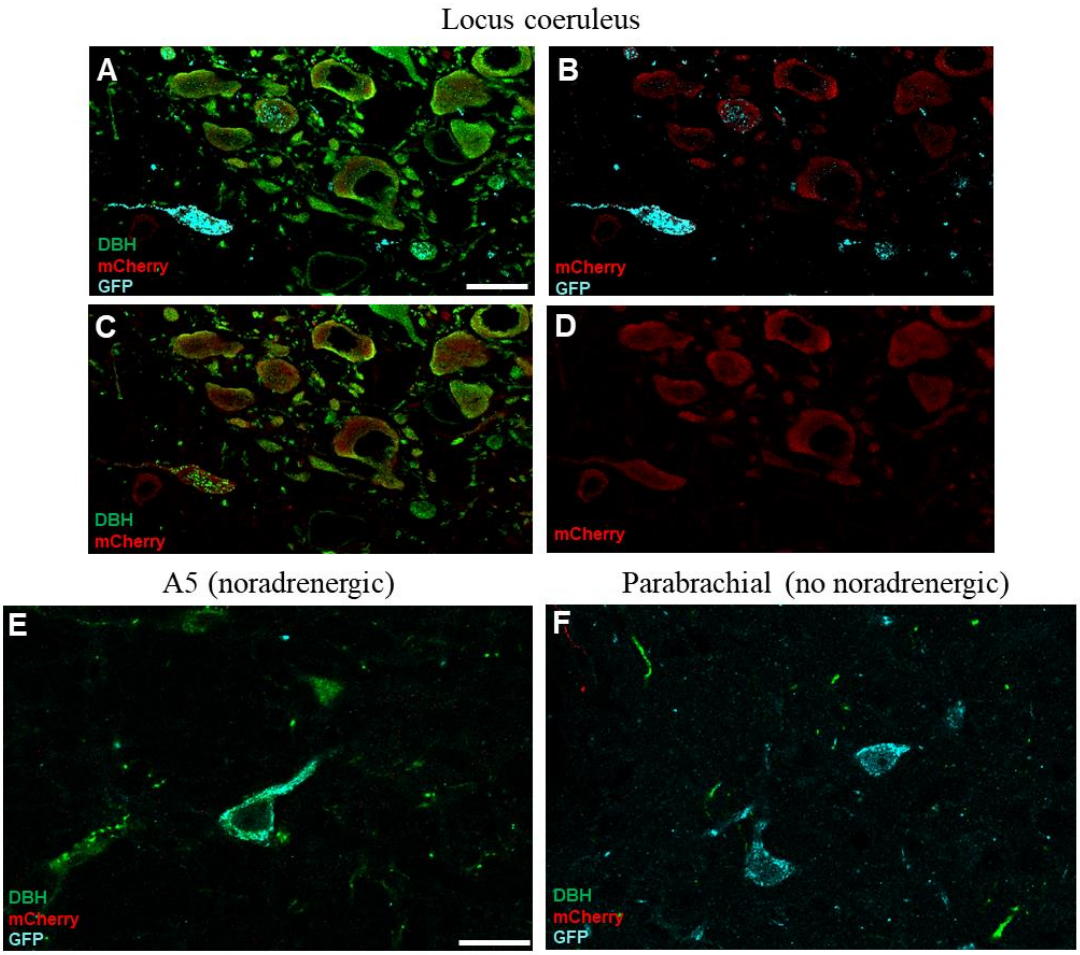

Fig. S4. Representative immunofluorescence of DBH, mCherry and GFP expression in (A-D) locus coeruleus neurons (E) A5 noradrenergic nucleus and (F) parabrachial nucleus (no noradrenergic). Scale bar: 20 μm.

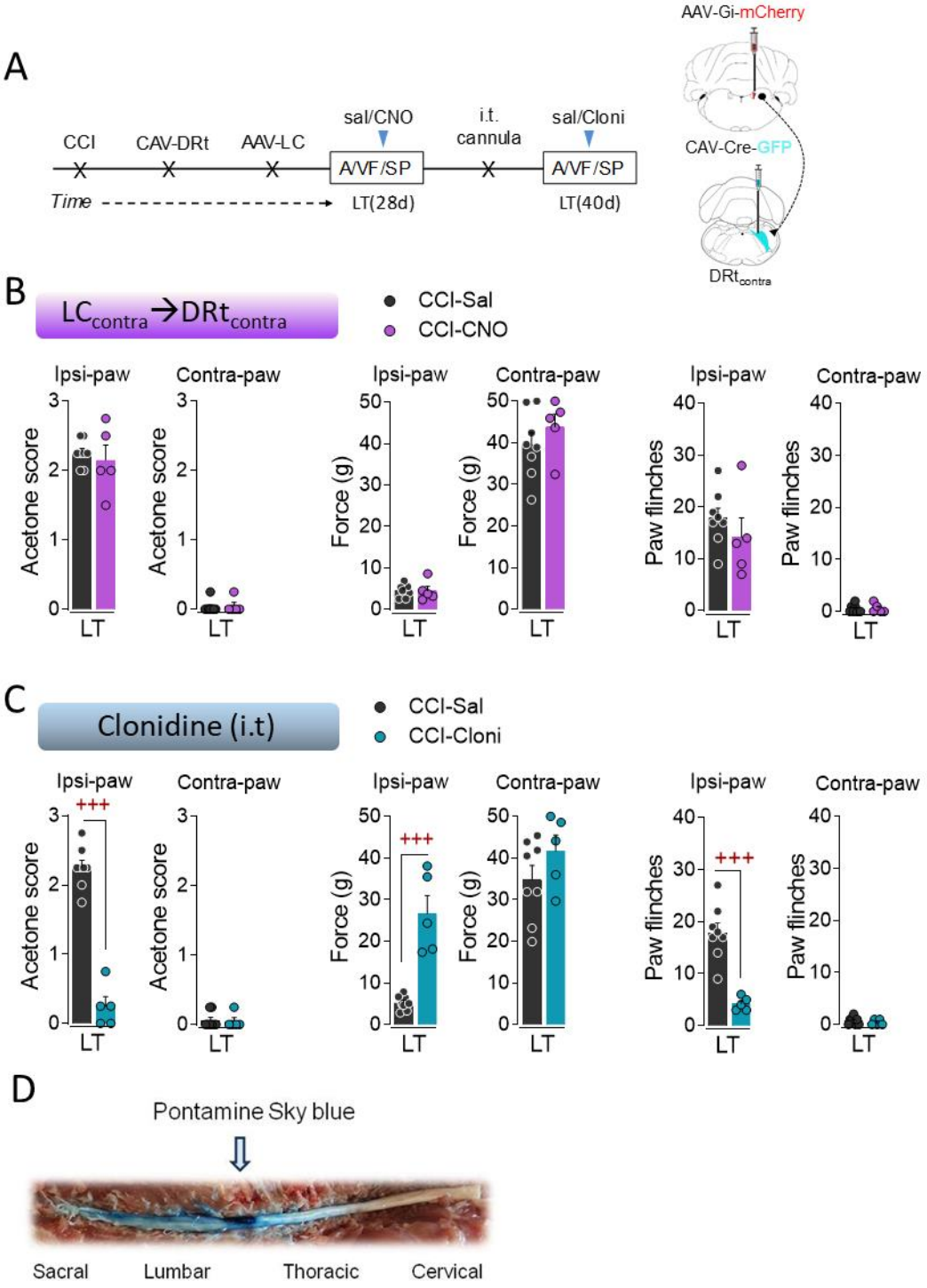

Fig. S5. (A) Timeline and scheme of the retrograde CAV-Cre-GFP injection into the DRt_{contra} and AAV-mCherry (control virus) into LC_{contra} of Sprague-Dawley rats to test that CNO does not provoke changes in the nociceptive tests. **(B)** The graphs show the response of the Ipsilateral and Contralateral paw in the acetone, von Frey and spontaneous pain tests after CNO (1 mg/kg, i.p.) administration to CCI-LT animals (CCI-Sal n=8; CCI-CNO n=5). (**C)** The graphs show the response of the Ipsilateral and Contralateral paw in the acetone, von Frey and spontaneous pain tests after clonidine (20 µg, i.t.) administration (CCI-Sal

n=8; CCI-Cloni n=5): +++p<0.001 vs CCI-Sal. **(D)** Representative image of the intrathecal injection of Pontamine Sky Blue solution. CCI, Chronic constriction injury; LC, locus coeruleus; DRt, dorsal reticular nucleus; LT, Long-term; CNO, clozapine-n-oxide; Sal, Saline; Cloni, clonidine; A, acetone test; VF, von Frey test; SP, spontaneous pain test; i.t., intrathecal; i.p., intraperitoneal; Ipsi-paw, ipsilateral paw; Contra-paw, contralateral paw.

Table 1. Statistical analysis for Fig.1A

- **Shapiro-Wilk normality test:**

Ipsilateral paw	ST (CCI-2d)		MT (CCI-7d)		LT (CCI-28d)	
Acetone test	Sham	CCI	Sham	CCI	Sham	CCI
W	0,921	0,851	0,845	0,776	0,825	0,891
P value	0,396	0,077	0,065	0,011	0,039	0,204
Passed normality test (alpha= 0.05)?	Yes	Yes	Yes	No	No	Yes

Contralateral paw	ST (CCI-2d)		MT (CCI-7d)		LT (CCI-28d)	
Acetone test	Sham	CCI	Sham	CCI	Sham	CCI
W	0,655	0,638	0,909	0,963	0,917	0,795
P value	0,000	0,000	0,308	0,830	0,364	0,018
Passed normality test (alpha= 0.05)?	No	No	Yes	Yes	Yes	No

- **Non-parametric test:**

	ST (CCI-2d)		MT (CCI-7d)		LT (CCI-28d)	
Acetone Test	Ipsilateral paw	Contralateral paw	Ipsilateral paw	Contralateral paw	Ipsilateral paw	Contralateral paw
Mann-Whitney test:						
P value	0,001**	0,090	0,000***	0,833	0,000***	0,525
Mann-Whitney U	6	20,5	0	38	0	32,5

Table 2. Statistical analysis for Fig.1C and Fig. S1B

- **Shapiro-Wilk normality test**

Ipsilateral paw	ST (CCI-2d)				MT (CCI-7d)				LT (CCI-28d)			
Acetone test	Sham-Sal	Sham-Lido	CCI-Sal	CCI-Lido	Sham-Sal	Sham-Lido	CCI-Sal	CCI-Lido	Sham-Sal	Sham-Lido	CCI-Sal	CCI-Lido
W	0,971	0,727	0,901	0,824	0,640	0,853	0,884	0,870	0,601	0,724	0,864	0,951
P value	0,906	0,003	0,257	0,051	0,001	0,167	0,208	0,187	0,000	0,004	0,107	0,697
Passed normality test (alpha= 0.05)?	Yes	No	Yes	Yes	No	Yes	Yes	Yes	No	No	Yes	Yes
Paw Pressure test												
W	0,863	0,920	0,971	1	0,895	0,895	0,993	0,981	0,827	0,920	0,855	0,887
P value	0,272	0,539	0,85	>0,999	0,406	0,406	0,972	0,911	0,161	0,538	0,253	0,369
Passed normality test (alpha= 0.05)?	Yes	Yes	Yes	Yes	Yes	Yes	Yes	Yes	Yes	Yes	Yes	Yes

Contralateral paw	ST (CCI-2d)				MT (CCI-7d)				LT (CCI-28d)			
Acetone test	Sham-Sal	Sham-Lido	CCI-Sal	CCI-Lido	Sham-Sal	Sham-Lido	CCI-Sal	CCI-Lido	Sham-Sal	Sham-Lido	CCI-Sal	CCI-Lido
W	0,889	0,916	0,684	0,827	0,907	0,915	0,801	0,858	0,782	0,693	0,617	0,813
P value	0,194	0,364	0,001	0,055	0,415	0,473	0,030	0,144	0,018	0,002	0,000	0,028
Passed normality test (alpha= 0.05)?	Yes	Yes	No	Yes	Yes	Yes	No	Yes	No	No	No	No
Paw Pressure test												
W	0,863	0,963	0,971	0,964	0,827	0,998	0,971	0,916	0,993	0,827	1	0,939
P value	0,272	0,798	0,85	0,637	0,161	0,995	0,85	0,513	0,972	0,161	>0,999	0,650
Passed normality test (alpha= 0.05)?	Yes	Yes	Yes	Yes	Yes	Yes	Yes	Yes	Yes	Yes	Yes	Yes

➢ **Non-parametric test**

	ST (CCI-2d)		MT (CCI-7d)		LT (CCI-30d)	
Acetone Test	Ipsilateral paw	Contralateral paw	Ipsilateral paw	Contralateral paw	Ipsilateral paw	Contralateral paw
Kruskal-Wallis test:						
P value	<0,000***	0,286	0,000***	0,569	<0,000***	0,566
Kruskal-Wallis statistic	27,27	3,785	19,86	2,015	25,36	2,029
Mann-Whitney test:						
Sham-Sal vs Sham-Lido						
P value	0,075	0,196	0,688	0,794	0,928	0,922
Mann-Whitney U	20	25	14	15	28,5	29
Sham-Sal vs CCI-Sal						
P value	0,002**	0,195	0,000***	0,667	<0,000***	0,413
Mann-Whitney U	6,5	25	0	20	0	27
CCI-Sal vs CCI-Lido						
P value	0,001**	0,767	0,536	>0,999	0,992	0,250
Mann-Whitney U	5,5	33	22,5	28	40	25,5

➢ **Parametric test**

Two-way ANOVA:	ST (CCI-2d)		MT (CCI-7d)		LT (CCI-30d)	
Paw Pressure test	Ipsilateral paw	Contralateral paw	Ipsilateral paw	Contralateral paw	Ipsilateral paw	Contralateral paw
Surgery	F(1,11)=164,159***	F(1,11)=0,173	F(1,12)=107,391***	F(1,12)=0,000	F(1,11)=60,172***	F(1,11)=0,688
Treatment	F(1,11)=10,743**	F(1,11)=0,530	F(1,12)=0,023	F(1,12)=6,000	F(1,11)=0,164	F(1,11)=0,416
Interaction	F(1,11)=4,350	F(1,11)=3,908	F(1,12)=6,519*	F(1,12)=0,050	F(1,11)=0,335	F(1,11)=1,910

Table 3. Statistical analysis for Fig.1D and Fig. S1C

- **Shapiro-Wilk normality test**

Ipsilateral paw	ST (CCI-2d)				MT (CCI-7d)				LT (CCI-30d)			
Acetone test	Sham-Sal	Sham-Lido	CCI-Sal	CCI-Lido	Sham-Sal	Sham-Lido	CCI-Sal	CCI-Lido	Sham-Sal	Sham-Lido	CCI-Sal	CCI-Lido
W	0,736	0,825	0,919	0,939	0,889	0,892	0,838	0,907	0,818	0,947	0,939	0,924
P value	0,006	0,029	0,424	0,541	0,194	0,177	0,042	0,259	0,062	0,663	0,571	0,391
Passed normality test (alpha= 0.05)?	No	No	Yes	Yes	Yes	Yes	No	Yes	Yes	Yes	Yes	Yes
Paw Pressure test												
W	0,856	0,823	0,913	0,968	0,965	0,974	0,895	0,819	0,911	0,945	0,867	0,907
P value	0,11	0,028	0,374	0,873	0,848	0,926	0,194	0,025	0,400	0,637	0,113	0,260
Passed normality test (alpha= 0.05)?	Yes	No	Yes	Yes	Yes	Yes	Yes	No	Yes	Yes	Yes	Yes

Contralateral paw	ST (CCI-2d)				MT (CCI-7d)				LT (CCI-30d)			
Acetone test	Sham-Sal	Sham-Lido	CCI-Sal	CCI-Lido	Sham-Sal	Sham-Lido	CCI-Sal	CCI-Lido	Sham-Sal	Sham-Lido	CCI-Sal	CCI-Lido
W	0,798	0,872	0,877	0,858	0,874	0,879	0,911	0,904	0,820	0,841	0,883	0,769
P value	0,027	0,105	0,178	0,073	0,137	0,127	0,287	0,245	0,064	0,059	0,170	0,006
Passed normality test (alpha= 0.05)?	No	Yes	Yes	Yes	Yes	Yes	Yes	Yes	Yes	Yes	Yes	No
Paw Pressure test												
W	0,968	0,919	0,983	0,929	0,866	0,896	0,961	0,941	0,868	0,920	0,977	0,884
P value	0,882	0,352	0,975	0,437	0,111	0,197	0,793	0,560	0,179	0,396	0,946	0,146
Passed normality test (alpha= 0.05)?	Yes	Yes	Yes	Yes	Yes	Yes	Yes	Yes	Yes	Yes	Yes	Yes

➢ **Non-parametric test**

	ST (CCI-2d)		MT (CCI-7d)		LT (CCI-30d)	
Acetone test	Ipsilateral paw	Contralateral paw	Ipsilateral paw	Contralateral paw	Ipsilateral paw	Contralateral paw
Kruskal-Wallis test:						
P value	0,002**	0,183	<0,000***			0,307
Kruskal-Wallis statistic	14,850	4,847	24,530			3,604
Mann-Whitney test:						
Sham-Sal vs Sham-Lido						
P value	>0,999	0,163	0,609			0,292
Mann-Whitney U	38,5	25	38			21
Sham-Sal vs CCI-Sal						
P value	0,000***	0,076	<0,000***			0,472
Mann-Whitney U	1,5	15,5	0,5			24,5
CCI-Sal vs CCI-Lido						
P value	0,344	0,997	0,002**			0,249
Mann-Whitney U	29	39	10,5			31
Paw pressure test						
Kruskal-Wallis test:						
P value	0,005**		<0,000***			
Kruskal-Wallis statistic	12,87		30,67			
Mann-Whitney test:						
Sham-Sal vs Sham-Lido						
P value	0,113		0,082			
Mann-Whitney U	22		23,5			
Sham-Sal vs CCI-Sal						
P value	0,044*		<0,000***			
Mann-Whitney U	13		0			
CCI-Sal vs CCI-Lido						
P value	0,840		0,031*			
Mann-Whitney U	37,5		22			

➢ **Parametric test**

Two-way ANOVA	ST (CCI-2d)		MT (CCI-7d)		LT (CCI-30d)	
Acetone test	Ipsilateral paw	Contralateral paw	Ipsilateral paw	Contralateral paw	Ipsilateral paw	Contralateral paw
Surgery				F(1,35)=1,537	F(1,31)=22,141***	
Treatment				F(1,35)=0,622	F(1,31)=21,455***	
Interaction				F(1,35)=0,001	F(1,31)=21,962***	
Paw pressure test						
Surgery		F(1,32)=3,564		F(1,35)=2,446	F(1,31)=173,447***	F(1,31)=2,611
Treatment		F(1,32)=2,917		F(1,35)=0,612	F(1,31)=35,392***	F(1,31)=0,012
Interaction		F(1,32)=0,655		F(1,35)=1,184	F(1,31)=21,401***	F(1,31)=1,518

Table 4. Statistical analysis for Fig. S2

➢ **Shapiro-Wilk normality test**

	CCI-sal (15')	CCI-Lido (15')	CCI-sal (120')	CCI-Lido (120')
Acetone test				
W	0,939	0,924	0,968	0,900
P value	0,571	0,392	0,875	0,216
Passed normality test (alpha= 0.05)?	Yes	Yes	Yes	Yes

Parametric test

Acetone test	
One-way ANOVA with repeated measure:	
Treatment	F(1,17)=12,335**
Time	F(1,17)=5,893*
Treatment x Time	F(1,17)=13,637**
Unpaired Student's t-test:	
CCI-Lido vs CCI-Sal (in-LC)	t (17)=5,710***
CCI-Lido vs CCI-Sal (out-LC)	t (10)=0.609

Table 5. Statistical analysis of Fig. S3B

- **Shapiro-Wilk normality test**

	Ipsilateral paw		Contralateral paw	
Acetone test	CCI-Sal	CCI-Lido	CCI-Sal	CCI-Lido
W	0,908	0,843	0,701	0,418
P value	0,421	0,082	0,006	<0,0001
Passed normality test (alpha= 0.05)?	Yes	Yes	No	No
Paw Pressure test				
W	0,916	0,920	0,876	0,934
P value	0,473	0,433	0,252	0,551
Passed normality test (alpha= 0.05)?	Yes	Yes	Yes	Yes

- **Non-parametric test**

Acetone test	Ipsilateral paw	Contralateral paw
Mann-Whitney test:		
P value		0,539
Mann-Whitney U		20

- **Parametric tests**

	Ipsilateral paw	Contralateral paw
Acetone test		
Unpaired Student's t-test:	t(12)=0,874	
Paw pressure test		
Unpaired Student's t-test:	t(12)=1,139	t(12)=0,143

Table 6. Statistical analysis for Fig. 2A

- **Shapiro-Wilk normality test**

	Immobility		Climbing		Swimming	
Forced swimming test	Sham	CCI	Sham	CCI	Sham	CCI
W	0,791	0,866	0,993	0,891	0,801	0,907
P value	0,087	0,210	0,972	0,324	0,103	0,415
Passed normality test (alpha= 0.05)?	Yes	Yes	Yes	Yes	Yes	Yes

- **Parametric test**

Forced swimming test	Immobility	Climbing	Swimming
Unpaired Student's t-test:	t(8)=11***	t(8)=14,06***	t(8)=0,388

Table 7. Statistical analysis for Fig. 2B

- **Shapiro-Wilk normality test**

Ipsilateral LC	Immobility				Climbing				Swimming			
Forced swimming test	Sham-Sal	Sham-Lido	CCI-Sal	CCI-Lido	Sham-Sal	Sham-Lido	CCI-Sal	CCI-Lido	Sham-Sal	Sham-Lido	CCI-Sal	CCI-Lido
W	0,867	0,952	0,979	0,890	0,857	0,928	0,739	0,917	0,822	0,850	0,914	0,914
P value	0,214	0,760	0,928	0,272	0,178	0,566	0,023	0,448	0,091	0,158	0,490	0,421
Passed normality test (alpha= 0.05)?	Yes	Yes	Yes	Yes	Yes	Yes	No	Yes	Yes	Yes	Yes	Yes

Contralateral LC	Immobility				Climbing				Swimming			
Forced swimming test	Sham-Sal	Sham-Lido	CCI-Sal	CCI-Lido	Sham-Sal	Sham-Lido	CCI-Sal	CCI-Lido	Sham-Sal	Sham-Lido	CCI-Sal	CCI-Lido
W	0,933	0,950	0,895	0,963	0,905	0,938	0,843	0,922	0,896	0,591	0,843	0,887
P value	0,479	0,671	0,191	0,820	0,247	0,531	0,048	0,371	0,198	<0,0001	0,048	0,157
Passed normality test (alpha= 0.05)?	Yes	Yes	Yes	Yes	Yes	Yes	No	Yes	Yes	No	No	Yes

- **Non-parametric test**

	Ipsilateral LC			Contralateral LC		
Forced swimming test	Immobility	Climbing	Swimming	Immobility	Climbing	Swimming
Kruskal-Wallis test:						
P value		0,007**			0,001**	0,715
Kruskal-Wallis statistic		12,03			16	1,359
Mann-Whitney test:						
Sham-Sal vs Sham-Lido						
P value		0,429			0,516	0,676
Mann-Whitney U		12,5			41	44
Sham-Sal vs CCI-Sal						
P value		0,004**			0,008**	0,490
Mann-Whitney U		0			16	40,5
CCI-Sal vs CCI-Lido						
P value		0,003**			<0,000***	0,667
Mann-Whitney U		0			0	44

➢ **Parametric test**

Forced swimming test	Ipsilateral LC			Contralateral LC		
Two-way ANOVA:	Immobility	Climbing	Swimming	Immobility	Climbing	Swimming
Surgery	F(1,20)=8,735**		F(1,20)=0,073	F(1,36)=6,191*		
Treatment	F(1,20)=3,627		F(1,20)=0,025	F(1,36)=7,510**		
Surgery x Treatment	F(1,20)=11,865**		F(1,20)=2,540	F(1,36)=10,300**		

Table 8. Statistical analysis for Fig. 2C

➢ **Shapiro-Wilk normality test**

Contralateral LC	Sham-Sal	Sham-Lido	CCI-Sal	CCI-Lido
Spontanous locomotor activity				
W	0,969	0,903	0,912	0,922
P value	0,889	0,309	0,369	0,444
Passed normality test (alpha= 0.05)?	Yes	Yes	Yes	Yes

➢ **Parametric test**

Spontanous locomotor activity	
Two-way ANOVA (repeated measure):	
Surgery	F(1,13)=0,330
Treatment	F(1,13)=0,002
Surgery x Treatment	F(1,13)=0,033
Time	F(7,91)=83,612***
Surgery x Time	F(7,91)=0,647
Treatment x Time	F(7,91)=0,501
Surgery x Treatment x Time	F(7,91)=0,536

Table 9. Statistical analysis for Fig. 3B

- **Shapiro-Wilk normality test**

Distribution FG (%)	Ipsilateral LC	Contralateral LC
W	0,947	0,947
P value	0,554	0,554
Passed normality test (alpha= 0.05)?	Yes	Yes

- **Parametric tests**

Distribution FG (%)	
Unpaired Student's t-test:	t(4)=6,179**

Table 10. Statistical analysis for Fig. 3C

- **Shapiro-Wilk normality test**

	Ipsilateral LC		Contralateral LC	
Distribution FG (%)	Dorsal	Ventral	Dorsal	Ventral
W	0,835	0,835	0,852	0,852
P value	0,202	0,202	0,245	0,245
Passed normality test (alpha= 0.05)?	Yes	Yes	Yes	Yes

- **Parametric tests**

	Ipsilateral LC	Contralateral LC
Distribution FG (%)		
Unpaired Student's t-test:	t(4)=2,568	t(4)=1,795

Table 11. Statistical analysis for Fig. 3D

Shapiro-Wilk normality test

	Ipsilateral paw		contralateral paw	
pCREB expression (DRt)	Sham	CCI	Sham	CCI
W	0,989	0,999	0,775	0,937
P value	0,953	0,953	0,064	0,516
Passed normality test (alpha= 0.05)?	Yes	Yes	Yes	Yes

Parametric test

Two-way ANOVA:	
pCREB expression (DRt)	
Surgery	F(1,10)=4,275
Side (LC)	F(1,10)=5,581*
Surgery x Side (LC)	F(1,10)=15,994**

Table 12. Statistical analysis of Fig. S3C

- **Shapiro-Wilk normality test**

	Ipsilateral paw		contralateral paw	
pCREB expression into DRt	Sham	CCI	Sham	CCI
W	0,989	0,999	0,775	0,937
P value	0,953	0,953	0,064	0,516
Passed normality test (alpha= 0.05)?	Yes	Yes	Yes	Yes

- **Parametric test**

Two-way ANOVA:	
pCREB expression into DRt	
Surgery	F(1,12)=0,588
LC	F(1,12)=0,036
Surgery x LC	F(1,12)=5,799

Table 13. Statistical analysis for Fig. 4B

- **Shapiro-Wilk normality test**

	Ipsilateral paw				Contralateral paw			
Acetone test	Sham-Sal	Sham-CNO	CCI-Sal	CCI-CNO	Sham-Sal	Sham-CNO	CCI-Sal	CCI-CNO
W	0,866	0,833	0,849	0,940	0,496	0,645	0,418	0,509
P value	0,212	0,086	0,093	0,549	<0,000	0,001	<0,000	<0,000
Passed normality test (alpha= 0.05)?	Yes	Yes	Yes	Yes	No	No	No	No
Von Frey test								
W	0,943	0,938	0,938	0,908	0,940	0,829	0,954	0,852
P value	0,685	0,617	0,594	0,271	0,656	0,079	0,746	0,062
Passed normality test (alpha= 0.05)?	Yes	Yes	Yes	Yes	Yes	Yes	Yes	Yes
Spontaneous pain test								
W	0,640	0,664	0,971	0,991	0,496	0,646	0,724	0,641
P value	0,001	0,002	0,908	0,998	<0,000	0,001	0,004	0,000
Passed normality test (alpha= 0.05)?	No	No	Yes	Yes	No	No	No	No

➢ **Non-parametric test**

	Ipsilateral paw	Contralateral paw
Acetone test		
Kruskal-Wallis test:		
P value		0,270
Kruskal-Wallis statistic		3,918
Mann-Whitney test:		
Sham-Sal vs Sham-CNO		
P value		<0.999
Mann-Whitney U		19,000
Sham-Sal vs CCI-Sal		
P value		0,528
Mann-Whitney U		17,500
CCI-Sal vs CCI-CNO		
P value		0,261
Mann-Whitney U		28,000
Spontaneous pain test		
Kruskal-Wallis test:		
P value	<0,000***	0,801
Kruskal-Wallis statistic	26,06	1,001
Mann-Whitney test:		
Sham-Sal vs Sham-CNO		
P value	>0,999	0,853
Mann-Whitney U	19	18,000
Sham-Sal vs CCI-Sal		
P value	0,001***	0,497
Mann-Whitney U	0	18,500
CCI-Sal vs CCI-CNO		
P value	0,000***	>0,999
Mann-Whitney U	4	39,000

➢ **Parametric test**

Two-way ANOVA:	Ipsilateral paw	Contralateral paw
Acetone test		
Surgery	F(1,27)=168,304***	
Treatment	F(1,27)=41,967***	
Surgery x Treatment	F(1,27)=38,424***	
Von Frey test		
Surgery	F(1,27)=91,314***	F(1,27)=0,486
Treatment	F(1,27)=9,220**	F(1,27)=0,701
Surgery x Treatment	F(1,27)=7,249*	F(1,27)=1,182

Table 14. Statistical analysis for Fig. 4C

➢ **Shapiro-Wilk normality test**

	Ipsilateral paw				Contralateral paw			
Acetone test	Sham-Sal	Sham-Cloni	CCI-Sal	CCI-Cloni	Sham-Sal	Sham-Cloni	CCI-Sal	CCI-Cloni
W	0,552	0,496	0,932	0,820	0,552	0,640	0,566	0,650
P value	0,000	<0,000	0,534	0,025	0,000	0,001	<0,000	0,000
Passed normality test (alpha= 0.05)?	No	No	Yes	No	No	No	No	No
Von Frey test								
W	0,983	0,931	0,964	0,909	0,893	0,990	0,899	0,882
P value	0,949	0,587	0,851	0,278	0,375	0,987	0,285	0,136
Passed normality test (alpha= 0.05)?	Yes	Yes	Yes	Yes	Yes	Yes	Yes	Yes
Spontaneous pain test								
W	0,684	0,775	0,971	0,887	0,684	0,640	0,827	0,684
P value	0,006	0,035	0,908	0,184	0,006	0,001	0,055	0,001
Passed normality test (alpha= 0.05)?	No	No	Yes	Yes	No	No	Yes	No

➢ **Non-parametric test**

	Ipsilateral paw	Contralateral paw
Acetone test		
Kruskal-Wallis test:		
P value	<0,000***	0,950
Kruskal-Wallis statistic	22,1	0,351
Mann-Whitney test:		
Sham-Sal vs Sham-Cloni		
P value	>0.999	>0,999
Mann-Whitney U	14,5	13
Sham-Sal vs CCI-Sal		
P value	0,000***	>0,999
Mann-Whitney U	0	19
CCI-Sal vs CCI-CNO		
P value	0,000***	0,843
Mann-Whitney U	0	37
Spontaneous pain test		
Kruskal-Wallis test:		
P value	<0,000****	0,586
Kruskal-Wallis statistic	23,34	1,935
Mann-Whitney test:		
Sham-Sal vs Sham-Cloni		
P value	0,664	0,567
Mann-Whitney U	11,5	11
Sham-Sal vs CCI-Sal		
P value	0,000***	>0,999
Mann-Whitney U	0	18
CCI-Sal vs CCI-Cloni		
P value	0,000***	0,426
Mann-Whitney U	2,5	26,5

- **Parametric test**

Two-way ANOVA:	Ipsilateral paw	Contralateral paw
Von Frey test		
Surgery	F(1,25)=50,891***	F(1,25)=0,073
Treatment	F(1,25)=6,858*	F(1,25)=1,142
Interaction	F(1,25)=3,899	F(1,25)=0,118

Table 15. Statistical analysis for Fig. S5B

- **Shapiro-Wilk normality test**

	Ipsilateral paw		Contralateral paw	
Acetone test	CCI-Sal	CCI-CNO	CCI-Sal	CCI-CNO
W	0,849	0,953	0,418	0,552
P value	0,093	0,758	<0,000	0,000
Passed normality test (alpha= 0.05)?	Yes	Yes	No	No
Von Frey test				
W	0,938	0,850	0,953	0,855
P value	0,594	0,194	0,746	0,211
Passed normality test (alpha= 0.05)?	Yes	Yes	Yes	Yes
Spontaneous pain test				
W	0,971	0,849	0,724	0,771
P value	0,908	0,192	0,004	0,046
Passed normality test (alpha= 0.05)?	Yes	Yes	No	No

- **Non-parametric test**

	Ipsilateral paw	Contralateral paw
Acetone test		
Mann-Whitney test:		
P value		>0.999
Mann-Whitney U		18,5
Spontaneous pain test		
Mann-Whitney test:		
P value		>0,999
Mann-Whitney U		19

- **Parametric tests**

	Ipsilateral paw	Contralateral paw
Acetone test		
Unpaired Student's t-test:	t(11)=0,531	
Von Frey test		
Unpaired Student's t-test:	t(11)=0,154	t(11)=0,992
Spontaneous pain test		
Unpaired Student's t-test:	t(11)=0,989	

Table 16. Statistical analysis for Fig. S5C

- **Shapiro-Wilk normality test**

	Ipsilateral paw		Contralateral paw	
Acetone test	CCI-Sal	CCI-CNO	CCI-Sal	CCI-CNO
W	0,932	0,833	0,566	0,552
P value	0,534	0,146	<0,000	0,000
Passed normality test (alpha= 0.05)?	Yes	Yes	No	No
Von Frey test				
W	0,964	0,864	0,899	0,914
P value	0,851	0,245	0,285	0,493
Passed normality test (alpha= 0.05)?	Yes	Yes	Yes	Yes
Spontaneous pain test				
W	0,971	0,902	0,827	0,684
P value	0,908	0,421	0,055	0,006
Passed normality test (alpha= 0.05)?	Yes	Yes	Yes	No

- **Non-parametric test**

	Ipsilateral paw	Contralateral paw
Acetone test		
Mann-Whitney test:		
P value		>0,999
Mann-Whitney U		19
Spontaneous pain test		
Mann-Whitney test:		
P value		0,499
Mann-Whitney U		14,5

➢ **Parametric tests**

	Ipsilateral paw	Contralateral paw
Acetone test		
Unpaired Student's t-test:	t(11)=11,64***	
Von Frey test		
Unpaired Student's t-test:	t(11)=6,311***	t(11)=1,291
Spontaneous pain test		
Unpaired Student's t-test:	t(11)=5,575***	

Table 17. Statistical analysis for Fig. 5B

- **Shapiro-Wilk normality test**

	Immobility				Climbing				Swimming			
Forced swimming test	Sham-Sal	Sham-CNO	CCI-Sal	CCI-CNO	Sham-Sal	Sham-CNO	CCI-Sal	CCI-CNO	Sham-Sal	Sham-CNO	CCI-Sal	CCI-CNO
W	0,809	0,960	0,897	0,869	0,809	0,960	0,905	0,864	0,366	0,390	0,486	0,392
P value	0,019	0,797	0,172	0,119	0,019	0,797	0,214	0,106	<0.000	<0.000	<0.000	<0.000
Passed normality test (alpha= 0.05)?	No	Yes	Yes	Yes	No	Yes	Yes	Yes	No	No	No	No

- **Non-parametric test**

	Ipsilateral LC		
Forced swimming test	Immobility	Climbing	Swimming
Kruskal-Wallis test:			
P value	0,023*	0,019*	0,816
Kruskal-Wallis statistic	9,494	9,993	0,937
Mann-Whitney test:			
Sham-Sal vs Sham-CNO			
P value	0,007**	0,007**	>0.999
Mann-Whitney U	13	13	44,50
Sham-Sal vs CCI-Sal			
P value	0,002**	0,000***	0,563
Mann-Whitney U	13	10,5	49,50
CCI-Sal vs CCI-CNO			
P value	0,751	0,751	0,864
Mann-Whitney U	45	45	47,50

Table 18. Statistical analysis for Fig. 5C

- **Shapiro-Wilk normality test**

	Sham-Sal	Sham-CNO	CCI-Sal	CCI-CNO
Spontanous motor activity				
W	0,916	0,910	0,906	0,880
P value	0,399	0,352	0,326	0,189
Passed normality test (alpha= 0.05)?	Yes	Yes	Yes	Yes

- **Parametric test**

Spontanous motor activity	
Two-way ANOVA (repeated measure):	
Surgery	F(1,35)=0,163
Treatment	F(1,35)=0,515
Surgery x Treatment	F(1,35)=0,192
Time	F(7,245)=5,098***
Surgery x Time	F(7,245)=0,983
Treatment x Time	F(7,245)=0,769
Surgery x Treatment x Time	F(7.245)=0.568

Table 19. Statistical analysis for Fig. 5D

- **Shapiro-Wilk normality test**

20 min after CNO	Ipsilateral paw				Contralateral paw			
Acetone test	Sham-Sal	Sham-CNO	CCI-Sal	CCI-CNO	Sham-Sal	Sham-CNO	CCI-Sal	CCI-CNO
W	0,859	0,684	0,952	0,952	0,731	0,684	0,655	0,794
P value	0,074	0,001	0,709	0,712	0,002	0,001	0,000	0,017
Passed normality test (alpha= 0.05)?	Yes	No	Yes	Yes	No	No	No	No
Von Frey test								
W	0,925	0,914	0,852	0,944	0,840	0,870	0,934	0,899
P value	0,404	0,346	0,078	0,621	0,044	0,122	0,517	0,247
Passed normality test (alpha= 0.05)?	Yes	Yes	Yes	Yes	No	Yes	Yes	Yes

360 min after CNO	Ipsilateral paw				Contralateral paw			
Acetone test	Sham-Sal	Sham-CNO	CCI-Sal	CCI-CNO	Sham-Sal	Sham-CNO	CCI-Sal	CCI-CNO
W	0,594	0,780	0,910	0,883	0,778	0,825	0,617	0,655
P value	<0.000	0,012	0,314	0,169	0,008	0,039	0,000	0,000
Passed normality test (alpha= 0.05)?	No	No	Yes	Yes	No	No	No	No
Von Frey test								
W	0,984	0,963	0,885	0,784	0,928	0,891	0,945	0,814
P value	0,984	0,826	0,178	0,014	0,428	0,205	0,633	0,030
Passed normality test (alpha= 0.05)?	Yes	Yes	Yes	No	Yes	Yes	Yes	No

➢ **Non-parametric test**

	20 min after CNO		360 min after CNO	
Acetone test	Ipsilateral paw	Contralateral paw	Ipsilateral paw	Contralateral paw
Kruskal-Wallis test:				
P value	<0.000***	0,387	P<0,000***	0,274
Kruskal-Wallis statistic	57,58	7.41	28,37	3,888
Mann-Whitney test:				
Sham-Sal vs Sham-CNO				
P value	0.256	0950	0,550	0,661
Mann-Whitney U	31	42.50	36,5	40
Sham-Sal vs CCI-Sal				
P value	<0.000***	0,565	0,000***	0,106
Mann-Whitney U	0	39	0	25,5
CCI-Sal vs CCI-CNO				
P value	0.001**	0,362	0,413	>0.999
Mann-Whitney U	6	29,5	31	36
Von Frey test				
Kruskal-Wallis test:				
P value		0,850	<0,000***	0,560
Kruskal-Wallis statistic		3,361	26,74	2,062
Mann-Whitney test:				
Sham-Sal vs Sham-CNO				
P value		0,940	0,734	0,870
Mann-Whitney U		44,5	40,5	42,5
Sham-Sal vs CCI-Sal				
P value		0,840	0,000***	0.988
Mann-Whitney U		42	0	44,5
CCI-Sal vs CCI-CNO				
P value		0,781	0,462	0,285
Mann-Whitney U		37	38,5	28

- **Parametric test**

Two-way ANOVA:

Von Frey test 20 min	Ipsilateral paw	Contralateral paw
Surgery	F(1,33)=225,011***	
Treatment	F(1,33)=4,750*	
Interaction	F(1,33)=6.528*	

STUDY II

Title: Pain and depression comorbidity causes asymmetric plasticity in the locus coeruleus neurons.

Authors: Meritxell Llorca-Torralba†, Carmen Camarena-Delgado†, Irene Suárez-Pereira, Lidia Bravo, Patricia Mariscal, Jose Antonio Garcia-Partida, Carolina López-Martín, Hong Wei, Antti Pertovaara, Juan Antonio Mico and Esther Berrocoso.

†These authors contributed equally to this work.

Journal: Brain

DOI: 10.1093/brain/awab239

Publisher: Brain. 2021 Aug 9; awab239. doi: 10.1093/brain/awab239. Online ahead of print.

ISSN: 0006-8950 (online)/ 1460-2156

Journal of Citations Report 2021 2-year Impact Factor: 13.501

Journal of Citations Report 2021 5-year Impact Factor: 14.250

Category	**Rank**	**Quartile**
Neurosciences	10/273	Q1/D1
Clinical Neurology	6/208	Q1/D1

All co-authors, the undersigned, in order to fulfil the requirements issued by Article 23 of the UCA/CG06/2012 regulation, dated 27 June 2012, on the organisation of doctoral studies at the University of Cádiz, hereby declare that:

- The PhD candidate, María del Carmen Camarena Delgado, contributed to performing the stereotactic microsurgery and behavioural experiments. In addition, she collaborated in the experimental design, data analysis and the writing of the first draft of the manuscript.

- They expressly and formally agree for this scholarly publication to be included as a part of the compendium of publications to be submitted by the PhD candidate.

- They expressly and formally renounce to reuse this scholarly publication as a part of another PhD thesis at any other university.

LLORCA TORRALBA MARITSELL - 48964174A

Firmado digitalmente por LLORCA TORRALBA MARITSELL - 48964174A
Nombre de reconocimiento (DN): c=ES, serialNumber=IDCES-48964174A, givenName=MARITSELL, sn=LLORCA TORRALBA, cn=LLORCA TORRALBA MARITSELL - 48964174A
Fecha: 2021.11.25 08:48:44 +01'00'

M. Llorca-Torralba:

SUAREZ PEREIRA IRENE - 28809292K

Firmado digitalmente por SUAREZ PEREIRA IRENE - 28809292K
Fecha: 2021.11.24 20:36:28 +01'00'

I. Suárez-Pereira:

BRAVO GARCIA LIDIA - 53580566L

Firmado digitalmente por BRAVO GARCIA LIDIA - 53580566L
Nombre de reconocimiento (DN): c=ES, serialNumber=IDCES-53580566L, givenName=LIDIA, sn=BRAVO GARCIA, cn=BRAVO GARCIA LIDIA - 53580566L
Fecha: 2021.11.24 11:27:47 +01'00'

L. Bravo:

MARISCAL RAMIREZ PATRICIA - 32068682N

Firmado digitalmente por MARISCAL RAMIREZ PATRICIA - 32068682N
Fecha: 2021.11.24 21:49:33 +01'00'

P. Mariscal:

GARCIA PARTIDA JOSE ANTONIO - 31257827E

Firmado digitalmente por GARCIA PARTIDA JOSE ANTONIO - 31257827E
Fecha: 2021.11.22 11:50:26 +01'00'

J.A. García-Partida:

LOPEZ MARTIN CAROLINA - 49041195C

Firmado digitalmente por LOPEZ MARTIN CAROLINA - 49041195C
Fecha: 2021.11.24 22:43:03 +01'00'

C. López-Martín:

H. Wei:

A. Pertovaara :

BERROCOSO DOMINGUEZ ESTHER MARIA - 52928983A

Firmado digitalmente por BERROCOSO DOMINGUEZ ESTHER MARIA - 52928983A
Nombre de reconocimiento (DN): c=ES, serialNumber=IDCES-52928983A, givenName=ESTHER MARIA, sn=BERROCOSO DOMINGUEZ, cn=BERROCOSO DOMINGUEZ ESTHER MARIA - 52928983A
Fecha: 2021.11.24 15:51:24 +01'00'

E. Berrocoso:

Estudio II

Pain and depression comorbidity causes asymmetric plasticity in the locus coeruleus neurons.

Meritxell Llorca-Torralba†, Carmen Camarena-Delgado†, Irene Suárez-Pereira, Lidia Bravo, Patricia Mariscal, Jose Antonio Garcia-Partida, Carolina López-Martín, Hong Wei, Antti Pertovaara, Juan Antonio Mico and Esther Berrocoso.

†These authors contributed equally to this work.

Brain, 2021

(*Online available*) DOI: 10.1093/brain/awab239

F.I.: 13.501

Existe una fuerte comorbilidad entre el dolor crónico y la depresión, aunque los circuitos neuronales y los mecanismos que subyacen a esta asociación siguen sin estar claros. Combinando la inmunohistoquímica, los estudios de trazadores y western-blotting, con el uso de diferentes DREADDs (Designer Receptor Exclusivamente Activado por Drogas de Diseño) y enfoques conductuales en un modelo de rata de dolor neuropático (lesión por constricción crónica), exploramos cómo surge esta comorbilidad. Para ello, evaluamos la plasticidad dependiente del tiempo de las neuronas noradrenérgicas del locus coeruleus (LC) en relación con el lugar de la lesión: ipsilateral (LC_{ipsi}) o contralateral (LC_{contra}) en tres momentos diferentes: a corto (2 días), a medio (7 días) y a largo plazo (30-35 días desde la lesión del nervio). La lesión nerviosa provocó una hipersensibilidad sensorial desde el inicio de la lesión, mientras que el comportamiento de tipo depresivo sólo fue evidente tras el dolor a largo plazo. El bloqueo quimiogenético global del sistema LC_{ipsi} por sí solo aumentó la sensibilidad al dolor a corto plazo, mientras que el bloqueo del LC_{ipsi} o del LC_{contra} alivió la depresión inducida por el dolor. La contribución asimétrica de los módulos neuronales del LC también fue evidente a medida que se desarrollaba la neuropatía. Por lo tanto, el bloqueo quimiogenético del

LC_{ipsi}→proyección de la SC, aumentó los comportamientos relacionados con el dolor a corto plazo. Sin embargo, este circuito lateralizado no es universal, ya que la quimiogenética bilateral La inactivación quimiogenética de la vía LC-corteza cingulada anterior (ACCr) o el antagonismo intra-ACCr de los adrenoreceptores alfa1 y alfa2 revirtió la depresión inducida por el dolor a largo plazo. Además, la activación quimiogenética del LC a la SC, principalmente a través de LC_{ipsi}, redujo la hipersensibilidad sensorial con independencia del tiempo posterior a la lesión. Nuestros resultados indican que la activación asimétrica de módulos específicos de la LC promueve la analgesia reparadora, así como un comportamiento tardío de tipo depresivo en el dolor crónico y la comorbilidad de la depresión.

Pain and depression comorbidity causes asymmetric plasticity in the locus coeruleus neurons

Meritxell Llorca-Torralba,[1,2,3,†] Carmen Camarena-Delgado,[1,2,†] Irene Suárez-Pereira,[2,3,4] Lidia Bravo,[2,3,4] Patricia Mariscal,[2,4] Jose Antonio Garcia-Partida,[2,4] Carolina López-Martín,[1,2] Hong Wei,[5] Antti Pertovaara,[5] Juan Antonio Mico[2,3,4] and Esther Berrocoso[1,2,3]

[†]**These authors contributed equally to this work.**

Abstract

There is strong comorbidity between chronic pain and depression, although the neural circuits and mechanisms underlying this association remain unclear. By combining immunohistochemistry, tracing studies and western-blotting, with the use of different DREADDs (*Designer Receptor Exclusively Activated by Designer Drugs*) and behavioural approaches in a rat model of neuropathic pain (chronic constriction injury), we explore how this comorbidity arises. To this end, we evaluated the time-dependent plasticity of noradrenergic-locus coeruleus (LC) neurons relative to the site of injury: ipsilateral (LC_{ipsi}) or contralateral (LC_{contra}) at three different time points: short- (2 days), mid- (7 days), and long-term (30-35 days from nerve injury). Nerve injury led to sensorial hypersensitivity from the onset of injury, whereas depressive-like behavior was only evident following long-term pain. Global chemogenetic blockade of the LC_{ipsi} system alone increased short-term pain sensitivity while the blockade of the LC_{ipsi} or LC_{contra} relieved pain-induced depression. The asymmetric contribution of LC-modules was also evident as neuropathy develops. Hence, chemogenetic blockade of the LC_{ipsi}→spinal cord projection, increased pain-related behaviours in the short-term. However, this lateralized circuit is not universal as the bilateral chemogenetic inactivation of the LC-rostral anterior cingulate cortex (rACC) pathway or the intra-rACC antagonism of alpha1- and alpha2-adrenoreceptors reversed long-term pain-induced depression. Furthermore, chemogenetic LC to spinal cord activation, mainly through LC_{ipsi}, reduced sensorial hypersensitivity irrespective of the time post-injury. Our results indicate that asymmetric activation of specific LC modules promotes early restorative-analgesia, as well as late depressive-like behavior in chronic pain and

depression comorbidity.

Author affiliations:

1 Neuropsychopharmacology and Psychobiology Research Group, Department of Psychology, University of Cádiz, Cádiz, Spain

2 Instituto de Investigación e Innovación Biomédica de Cádiz, INiBICA, Hospital Universitario Puerta del Mar, Cádiz, Spain

3 Centro de Investigación Biomédica en Red de Salud Mental (CIBERSAM), Instituto de Salud Carlos III, Madrid, Spain

4 Neuropsychopharmacology and Psychobiology Research Group, Department of Neuroscience, University of Cádiz, Cádiz, Spain

5 Department of Physiology, Faculty of Medicine, University of Helsinki, Helsinki, Finland

Correspondence to: Esther Berrocoso, PhD

Neuropsychopharmacology and Psychobiology Research Group, Psychobiology Area, Department of Psychology, University of Cádiz, 11510 Puerto Real, Cádiz, Spain

E-mail: esther.berrocoso@uca.es

Running tittle: The locus coeruleus in pain and depression

Keywords: locus coeruleus; depression; neuropathic pain; anterior cingulate cortex; spinal cord

Abbreviations: A5 = Noradrenergic cell group; AAV= Adeno-associated virus, BLA= Basolateral amygdala; CCI= chronic constriction injury; CNO= Clozapine-n-oxide; contra= contralateral; DREADDs= Designer Receptor Exclusively Activated by Designer Drugs; FG= Fluoro-Gold; FST= forced swimming test; ipsi; ipsilateral; LC= locus coeruleus; LT= long-term; MT= mid-term, PFC= Prefrontal Cortex; rACC= rostral Anterior Cingulate Cortex; Sal= saline; SC= spinal cord; ST= short-term.

Introduction

Pain and depression represent two highly prevalent and deleterious disorders with high comorbidity rates (from 18 to 85%). Hence, pain is a major risk factor for depression, and depression can exacerbate chronic pain and obstruct effective therapies [1, 2] but the mechanisms underlying the overlap between these conditions remain unclear.

When pain induces depression, we speculate that the balance between the recruitment of restorative analgesia and harmful pro-nociceptive mechanisms determines whether pain following injury resolves or if it persists and becomes chronic, with the ensuing appearance of comorbid anxiodepressive symptoms. The noradrenergic locus coeruleus (LC) in the pontine brainstem is one of the brain regions that may mediate this neuroplasticity. Indeed, while descending inhibition of acute pain by the LC has been well established [3, 4], in the last decade there have been several reports of its role in facilitating or inhibiting chronic pain [5-7]. Furthermore, the role of the LC circuits in depression is still elusive, despite the many changes in the LC reported in animal models [8-10], depressed patients [11, 12] and its key role in the action of antidepressants [13, 14]. Therefore, here we will address how depression arises after the induction of pain to understand the mechanisms involved in pain-depression comorbidity. Specifically, we will focus on the pain caused by nerve injury (neuropathic pain), not least because neuropathic pain is a debilitating condition affecting around 7%–10% of the general population and it is notoriously resistant to currently available analgesic treatments [15, 16].

Here, we explored the time-dependent LC neural network reconfiguration in a rat model of neuropathic pain induced by chronic constriction injury (CCI), assessing the changes in the ipsilateral (LC_{ipsi}) or contralateral (LC_{contra}) pathways at three time points after nerve injury induction: short- (CCI-ST, 2 days), mid- (CCI-MT, 7 days), and long-term (CCI-LT, 30-35 days 4-5 weeks). Furthermore, as the LC is apparently composed of modules that might produce targeted neuromodulation [17, 18], we assessed the effects induced by the LC as a whole, as well as its specific efferent pathways to areas critical for sensory and unpleasant emotional experiences: the spinal cord (SC) and rostral anterior cingulate cortex (rACC) [6, 19].

Materials and methods

A detailed description of the experimental procedure is provided in Supplementary material.

Animals and pain model

Male transgenic Long-Evans tyrosine hydroxylase:Cre (TH:Cre) and wild-type Long-Evans rats (350-450g) were produced and maintained under standard laboratory conditions. CCI was used as a model of neuropathic pain [20, 21].

Virus and tracer injection

Rats were injected with a *Designer Receptor Exclusively Activated by Designer Drugs* (DREADD) virus (hM4D(Gi)- DREADD, rM3D(Gs)-DREADD or control-DREADD) into the LC (AP: -3.2 mm, ML: ±1.3 mm, DV: 6.2 mm) [22] and Fluoro-Gold (FG) tracer into rACC (AP: +3.0 mm, ML: ±1.0 mm and DV: 1.2 mm) [23] or SC (L4-L6 segments) [24]. See methodological validation of DREADD approach in [22] and Supplementary Figures (Supplementary Figs. 1, 2 and 11).

Behavioral assessment

Acetone test: Cold hypersensitivity was evaluated using the acetone test. Animals were placed individually into Plexiglas chambers on a metal grid, and a drop of acetone (100 µl) was applied to the center of the ipsilateral and contralateral hind paw with a pipette. The acetone was applied 4 times to each hind paw alternately at 5 minute intervals and the responses were recorded over 1 min according to the following scale: 0, no response; 1, quick withdrawal, flick or stamping of the paw; 2, prolonged withdrawal or repeated flicking of the paw; 3, repeated flicking of the paw with persistent licking directed at the ventral side of the paw. The cumulative score for each rat was obtained by summing the score and dividing it by the number of assays [25].

Von Frey test: Mechanical hypersensitivity was measured with the von Frey test (Dynamic Plantar Aesthesiometer, Ugo Basile, Italy), applying a vertical force to the ipsilateral or contralateral hind paw that was increased from 0 to 50 g over a period of 20 s. Mechanical hypersensitivity was indicated by a reduction in the force that provokes paw withdrawal [26].

Cold plate test: Cold hypersensitivity was measured using the cold plate test. Animals were placed on a cold metal plate maintained at 4 ± 1 ºC (Panlab S.L., Spain) and the number of times the animal briskly lifted its ipsilateral hind paw was measured over a period of 2 min [21].

Forced Swimming Test (FST): Depressive-like behavior was evaluated in the FST over two different sessions, a 15 min pre-test was followed by a 5 min test performed 24 hours later. The predominant behaviors were recorded (climbing -CL, swimming -SW, or immobility -IM), and scored in each 5 s period of the 300 s test session [27, 28].

Locomotor spontaneous activity test: The total distance travelled (arbitrary units, A.U., %) was measured as an indicator of locomotor activity [22].

Immunohistochemistry and histology

Immunohistochemistry was performed to evaluate the expression of DREADDs-mCherry, FG-tracer and c-fos in the LC, as well as DBH in the SC. The cannula placement in the rACC and SC was also verified [22, 29].

Western blotting

Western blotting was performed to evaluate the expression of pCREB and TH proteins in the LC, which it was normalized to the level of β-actin [22].

Statistical Analysis

Results are presented as the means ± SEM. An unpaired Student's T test was used to compare the values between the two groups. One- or two-way or repeated measures ANOVA followed by Newman-Keuls test were used to compare between more than two groups. $p<0.05$ was considered significant.

Data availability

Data are available upon request to the corresponding author.

Results

Analgesia is driven by the activation of noradrenergic-LC_{ipsi} neurons

Sensorial hypersensitivity was evaluated through the acetone test and as expected, it appears immediately in the ipsilateral hindpaw after nerve damage and it remained constant over time (ST, MT and LT: $p<0.001$ vs sham, Fig. 1). By contrast, depressive-like behavior was only observed in CCI-LT animals (immobility and climbing: $p<0.01$ and $p<0.05$ vs sham, Fig. 1). This finding indicates that pain-induced depression evolves after pain has lasted at least 4-5 weeks [1, 22, 25, 27, 30, 31]. To assess the pontine mechanisms underlying the time-dependence of this phenotype further, we selectively expressed hM4D(Gi)- or rM3D(Gs)-DREADD in the LC_{ipsi} or LC_{contra} to selectively manipulate LC activity at different time points from nerve injury. In agreement with our recent work [22], selective expression of hM4D(Gi)- or rM3D(Gs)-DREADD was achieved in noradrenergic LC neurons (Fig. 2A and Supplementary Fig. 1A-H). Thus, we assessed how hM4D(Gi)-DREADD-mediated LC inhibition affected sensorial hypersensitivity after systemic clozapine N-oxide (CNO) administration. LC_{ipsi} blockade only significantly enhanced hypersensitivity in the ipsilateral hindpaw in the CCI-ST animals (Acetone test: $p<0.001$ vs the CCI-ST-Sal: Fig. 2B and Supplementary Fig. 2). Furthermore, this effect of CNO was also evident when exploring the number of lifts of the ipsilateral hindpaw in a different pain test (cold plate test: $p<0.001$, Fig. 1C). Enhancement of the cold plate response disappeared completely after 360 minutes (Fig. 1C), in line with the duration of the inactivation produced by CNO previously [32]. Surprisingly, no significant effect on acetone test was seen at any time point post-injury when the LC_{contra} was chemogenetically blocked (Fig. 1D).

As previous studies have shown that the pain threshold increases following acute electrical or chemogenetic stimulation of the LC [5, 33], we explored the effect of global noradrenergic LC activation using rM3D(Gs)-DREADDs at various phases of the development of neuropathy (Fig. 1E-F and Supplementary Fig. 1E-H). CNO activation of the LC_{ipsi} significantly reduced CCI evoked thermal and mechanical hypersensitivity in the ST, MT and LT animals relative to their respective CCI-Sal controls (acetone test ST, MD and LT $p<0.001$; von Frey test ST $p<0.01$; MT $p<0.05$; and LT $p<0.01$: Fig. 2E). By contrast, CNO-mediated activation of LC_{contra} neurons did not significantly

modify CCI-induced pain at any time point (Fig. 2F). Furthermore, chemogenetic $LC_{ipsi/contra}$ inhibition/activation did not significantly modify the sensorial responses in the sham group or in the contralateral hindpaws of the CCI group (Fig. 2B-F and Supplementary Fig. 3A-D).

Chemogenetic blockade of either the LC_{ipsi} or LC_{contra} neurons relieves pain-induced depression

As long-term pain induces depressive-like behavior (Fig. 1), we used the same chemogenetic approaches to explore the effect of silencing or activating the LC_{ipsi} or LC_{contra} in depressive CCI-LT rats. Unlike the sensory tests, chemogenetic silencing the LC_{ipsi} or LC_{contra} had a marked effect on emotional behavior, reflected by the significant decrease in immobility (LC_{ipsi} and LC_{contra} $p<0.001$) and the increased climbing (LC_{ipsi} $p<0.01$ and LC_{contra} $p<0.001$) behavior of these animals (Fig. 3A-B). Alternatively, blocking either LC_{ipsi} or LC_{contra} had no effect on sham-animals (Fig. 3A-B), although significant depressive behavior was triggered in sham animals by rM3D(Gs)-DREADD LC activation (LC_{ipsi} $p<0.01$ and LC_{contra} $p<0.001$ vs Sham-Sal: Fig. 3C). Furthermore, LC activation in CCI-LT rats did not further augment the already elevated immobility time in the FST (Fig. 3C). None of the behaviors evaluated were affected by any locomotor dysfunction (Supplementary Fig. 4A-B). In addition, a bilateral activation of the LC was evident through the increase in the rate-limiting enzyme in noradrenaline biosynthesis, tyrosine hydroxylase (TH, LC_{ipsi} and LC_{contra} $p<0.05$ vs sham), and that of phosphorylated CREB (LC_{ipsi} $p=0.07$ and LC_{contra} $p<0.01$ vs sham: Supplementary Fig. 5).

Activation of the noradrenergic-LC_{ipsi}→SC pathway relieves pain

To study the specific afferent pathways that modulate the evolution of neuropathy, we explored how the descending noradrenergic-LC pathway to the SC influences the pain-related phenotype. Unilateral administration of the retrograde fluorescent tracer FG into the superficial dorsal horn of the ipsilateral SC labeled a similar number of neurons in the LC_{ipsi} and LC_{contra} along the rostro-caudal axis, these neurons predominantly located in the central LC (Fig. 4A-B and Supplementary Fig. 6A). Hence, the LC appears to

project bilaterally to the SC and most of the spinally projecting neurons (around 80%) are situated in the ventral aspect of the nucleus (Fig. 4C).

In other experiment set, FG was injected unilaterally into the ipsilateral SC of CCI-ST and CCI-LT rats, and the expression of c-Fos in the LC was assessed (Fig. 4D-G). Nerve injury significantly increased the number of c-Fos labeled neurons in LC of CCI-ST rats bilaterally relative to the sham-ST rats (LC_{ipsi}: $p<0.001$ and LC_{contra}: $p<0.001$: Fig. 4E). Importantly, LC_{ipsi} c-Fos expression was significantly higher than that in the LC_{contra} of CCI-ST animals ($p<0.01$, Fig. 4E). This lateralized LC c-Fos expression was also evident in sham animals ($p<0.05$, Fig. 4E), suggesting an acute LC activation related to skin and muscle injury in sham animals. Furthermore, these c-Fos labeled neurons were preferentially located in the dorsal pole of the LC (around 90%, Fig. 4E). When exploring which c-Fos neurons also expressed FG, we found that there was only a small population in the dorsal LC_{ipsi} pole of the CCI-ST rats ($p<0.05$ vs sham: Fig. 4F). However, c-Fos/FG co-labeling was not found in either sham-LC_{ipsi}/LC_{contra} or CCI-ST LC_{contra} (Fig. 4F). Regarding LT pain, significantly stronger c-Fos expression was evident in the dorsal LC_{ipsi} and LC_{contra} of CCI-LT animals relative to the respective LC area in the sham rats (LC_{ipsi} $p<0.001$ and LC_{contra} $p<0.001$), although there was no difference between sides (Fig. 4G). Moreover, no c-Fos/FG co-labelled LC neurons projected to the SC in CCI-LT rats. In CCI-ST and -LT rats, the expression of the noradrenaline synthesizing enzyme dopamine beta-hydroxylase (DBH) was also studied in the superficial dorsal horn of LC projecting segments (Supplementary Fig. 7). A bilateral increase in the expression of DBH fibres was evident in CCI animals just after nerve injury that was significant in the L5 and L6 lumbar dorsal horn sections (ST, $p<0.05$ vs sham: Supplementary Fig. 7A-B). By contrast, there was a loss of noradrenergic fibres after CCI-LT in the L6 segment (LT, $p<0.05$ vs sham animals: Supplementary Fig. 7A). These data demonstrate lateralized changes in the activation of the LC→SC pathway along neuropathy development.

DREADD-mediated inactivation of the noradrenergic LC_{ipsi} or $LC_{contral}$→SC pathway was explored behaviorally and like the global LC blockade (Fig. 2B and 2D), intrathecal CNO administration following hM4D(Gi)-DREADD administration to the LC_{ipsi} enhanced thermal and mechanical hypersensitivity in the ipsilateral hindpaw of CCI-ST rats, yet not at later times (Fig. 5A). This was shown by the significant increase in the acetone score ($p<0.001$), a decrease in the mechanical withdrawal threshold ($p<0.05$)

and an increase in the number of ipsilateral paw lifts in the cold plate test of CCI-ST-CNO as opposed to CCI-ST-Sal animals ($p<0.001$). When exploring the outcome of blocking the LC_{contra}→SC pathway, no significant changes in evoked pain responses were observed (Fig. 5B). Like after global LC_{ipsi} or LC_{contra} inhibition, no significant effect was found in sham animals or in the response of the contralateral hindpaw of CCI animals after blocking the LC_{ipsi} or LC_{contra}→SC pathway (Fig. 5A-B and Supplementary Fig. 8A-B).

The rM3D(Gs)-DREADD activation of the noradrenergic LC_{ipsi} or LC_{contra}→SC pathway was also explored. Like global LC activation (Fig. 2E-F), DREADD-mediated activation of noradrenergic LC_{ipsi} neurons projecting to the SC reduced peripheral stimulus-evoked hypersensitivity in CCI-ST, -MT and -LT rats, as shown by the significant analgesic effects in the acetone, von Frey and cold plate tests (Fig. 6A). However, no change in thermal or mechanical allodynia was evident at any time point when the LC_{contra} to SC pathway was activated (Fig. 6B). To verify that the local activation of α2-adrenoreceptors is still able to produce analgesia in these animals, the α2-adrenoreceptor agonist clonidine was intrathecally administered producing a clear analgesic effect in CCI-LT rats (acetone test $p<0.001$, von Frey test $p<0.05$ vs CCI-LT-Sal: Fig. 6B). Finally, and like after global LC_{ipsi} or LC_{contra} activation, no change was found in sham animals or in the contralateral hindpaws of CCI animals (Fig. 6A-B and Supplementary Fig. 9A-C).

Bilateral chemogenetic inhibition of the LC→rACC pathway relieves pain-induced depression

One of the main LC targets involved in mood and pain-related emotions is the rostral anterior cingulate cortex (rACC) [19]. Administration of FG into the ipsilateral rACC produced abundant labeling of neurons in the LC_{ipsi} (≈ 80%), suggesting that the projection of the LC to the rACC is lateralized. Most marked neurons were located in the central LC along the rostro-caudal axis (Fig. 7A-B and Supplementary Fig. 6B). Bilateral administration of FG to the rACC was also performed and as expected, there was a similar distribution of FG positive neurons bilaterally in the LC and preferentially in the dorsal pole (Fig. 7C-E and Supplementary Fig. 6C). The expression of c-Fos in the LC neurons of LT animals was also explored (Fig. 7F-H). As found previously (Fig.

4G), there was a similar bilateral increase in neurons expressing c-Fos in the dorsal LC pole of CCI-LT rats (LC_{ipsi} and LC_{contra} $p<0.001$ vs sham: Fig. 7G). Following bilateral administration of the FG tracer to the rACC, more than 20% of c-Fos positive neurons projected specifically to the rACC and these projection neurons were located in the dorsal pole of the LC (Fig. 7H). No differences were found between the sides of the LC, demonstrating a bilateral over-activation of this pathway in CCI-LT animals in agreement with western blotting experiments about TH and phosphorylated CREB (Supplementary Fig. 5). Bilateral blockade of the LC-rACC pathway using hM4D(Gi)-DREADD had no significant effect on the evoked pain (acetone, von Frey and cold plate tests: Fig. 8A and Supplementary Fig. 10A-B). However, a reversion of the depressive phenotype was observed in CCI-LT rats (immobility and climbing $p<0.01$ vs CCI-Sal: Fig. 8A). No impairment of spontaneous locomotion was found (Supplementary Fig. 10C).

In addition, reduced c-Fos expression (LC_{ipsi} and LC_{contra} $p<0.001$ vs CCI-Sal: Supplementary Fig. 11A-C) and reduced c-Fos/FG co-labeling (LC_{ipsi} $p<0.01$ and LC_{contra} $p<0.05$ vs CCI-Sal: Supplementary Fig. 11D) was observed in the LC after chemogenetic inhibition of the LC→rACC pathway in CCI-LT rats.

Blockade of α-adrenoreceptors in the rACC relieves pain-induced depression

To test whether blocking adrenoreceptor activity in the rACC might reverse pain-induced depression, we administered the α1-adrenoreceptor antagonist prazosin (5 µg/0.5 µl), the α2-adrenoreceptor antagonist idazoxan (9 µg/0.5 µl) or the β-adrenoreceptor antagonist propranolol (1 µg/0.5 µl) intra-rACC. Prazosin and idazoxan administration reversed depressive-like behavior (prazosin: immobility and climbing $p<0.01$, idazoxan: immobility and climbing $p<0.001$ vs CCI-Sal), although they did not change pain behaviors (acetone, von Frey and cold plate tests: Fig. 8B-C and Supplementary Fig. 12A-F). However, propranolol failed to modify pain- or depression-related behaviors in CCI-LT rats although it significantly increased depressive-like behavior in Sham (immobility and climbing $p<0.01$ vs Sham-Sal: Fig. 8D and Supplementary Fig. 12G-I). Locomotor activity was not modified in any of the groups of rats evaluated (Supplementary Fig. 12B,E,H). These data suggest an involvement of α-adrenoreceptors in pain-induced depression at the rACC level.

Discussion

We demonstrate that there are time-dependent plastic changes in the noradrenergic-LC system as pain develops from acute to chronic, and that these changes are associated with behavioral despair.

Sensorial hypersensitivity appears immediately after nerve injury, whereas anxiodepressive and cognitive symptoms arise after several weeks (4-6 weeks) [1, 22, 25, 27, 30, 31]. To assess noradrenergic-LC changes when nociceptive signaling persists, LC activity in both hemispheres was explored at various times after unilateral nerve injury (from CCI-ST to CCI-LT). Immunohistochemistry revealed that there is increased c-Fos expression after nerve injury, both in the short-term and long-term. However, the expression of c-Fos is higher in the ipsilateral side of the LC than on the contralateral side at short-term, while the increase is of equal magnitude bilaterally in the LC of CCI-LT animals. These results show that the nerve injury-induced LC changes vary on either side of the body, as well as with the duration of the injury. Chemogenetic suppression of the LC activity shows that activity of LC_{ipsi} neurons contributes to a milder pain phenotype, yet only in the early phase of nerve injury. However, LC_{contra} blockade did not modify pain perception at any time point. Contrary to sensorial sensitivity, the blockade of either the LC_{ipsi} or the LC_{contra} completely reversed the depressive phenotype developed at CCI-LT. Furthermore, bilateral stronger expression of TH, pCREB and c-Fos of the LC was found at long-term, in agreement with previous data in major depression disorder patients (TH: [12]) and in CCI-LT animals were both LCs were evaluated as a pool [22, 27, 30]. Overall the results suggest an early lateralized activation of the LC that reduces the pain phenotype but a later bilateral activation that leads to behavioral despair in nerve-injured animals. Interestingly, hM4D(Gi)-DREADD–mediated inhibition of the LC did not affect sensorial exploration or depressive-like phenotype in sham animals, suggesting a weak tonic drive of LC activity in the uninjured state [4]. We also explored the consequences of activating the LC globally. In sham animals, global LC activation had no effect on the sensory threshold, although significant depressive behavior was triggered when the LC_{ipsi} or LC_{contra} was activated chemogenetically, consistent with previous findings showing that the optogenetic/chemogenetic activation of LC neurons is itself anxiogenic [34, 35]. In terms of

neuropathic pain, rM3D(Gs)-DREADD activation of LC neurons relieved pain at any time point, albeit with different contributions of the LC_{ipsi} and LC_{contra}. Indeed, global chemogenetic activation of the LC_{ipsi} produced a clear anti-neuropathic effect at all time points after nerve injury. However, global activation of LC_{contra} did not combat thermal and mechanical hypersensitivity at any time point. Furthermore, as depressive-like behavior is associated with long-term pain, the effect of LC activation was explored in the FST. Chemogenetic LC activation did not modify the pain-induced depression-like state, perhaps reflecting that maximal activation had already been achieved by long-term nerve injury.

In the light of these findings, we explored the role of LC→SC pathway along pain development. As occurred with global LC activity, hM4D(Gi)-DREADD blockade of the LC_{ipsi}→SC projection rather than the LC_{contra} projection reduced pain in the short-term. This was consistent with the c-Fos activation of the LC_{ipsi}-neurons projecting to the SC in the short-term and not at long-term (Fig. 2F). Accordingly, there are more DBH in the fibres of the SC in the CCI-ST, and fewer in the CCI-LT. Alterations in spinal DBH at different time points from nerve injury have been shown before in several rodent models [36-38]. We extend these previous findings evaluating changes in spinal DBH along with spontaneous activity of LC→SC projecting neurons (c-Fos) and the behavioral effect of the chemogenetic LC blockade at two different time points from nerve injury. Overall, these changes would suggest an activation of the noradrenergic descending LC pathway to the SC at short-term, reducing the pain phenotype soon after injury but later failing when the insult persists. Furthermore, chemogenetic activation of both LC to SC neurons produces analgesia when neuropathy is well established (from 4 weeks after nerve injury) [5], and we now show that this effect is mainly contributed by the LC_{ipsi} and can be triggered at any time point from injury. Our global evaluation of the LC and of the specific projection to the SC seems to refute the idea that the LC serves to generate pain under conditions of chronic pain (review in [7]). Indeed, intracerebroventricular (i.c.v.) administration of the neurotoxin anti-dopamine-β-hydroxylase saporin (anti-DβH-saporin) or intra-LC administration of lidocaine dampened the evoked pain in conditions of long-term nerve-injury [39]. However, i.c.v. injection of anti-DβH-saporin disrupts all noradrenergic nuclei (A1-A7), some of which contribute to sensorial hypersensitivity (A5: [40, 41], although our experiments focused only on the LC. On the other hand, lidocaine administered at the level of the LC will

block the activity of noradrenergic and non-noradrenergic cells [42], and our approach is to target only noradrenergic LC cells. Another important issue is the modular composition of the LC, whereby different projections may have opposing actions in a time-dependent manner. In this sense, the pain-inhibitory actions of noradrenaline in the spinal cord may be countered or even superseded by the activation of supraspinal facilitating pathways to the dorsal reticular nucleus (contributing to evoked pain: [41]), to the trigeminal spinal nucleus caudalis (evoked pain: [43]), or to the prefrontal cortex (PFC, spontaneous pain: [5]). Thus, further studies will be necessary to untangle the actions of the LC globally and in a modular fashion, also bearing in mind the strain differences that have been described in the noradrenergic pathways (see review in [6]).

One of the LC-related networks involved in affective dimensions and manifestations of pain-related expression of emotions is the rACC [19, 44]. Accordingly, hyperactivity in the ACC is seen in depressed patients [45] and it has chronic neuropathic pain-induced anxiodepressive-like consequences [46]. In this line, a bilateral increase of noradrenaline in the prefrontal cortex has been associated with long-term neuropathic pain (6 weeks after nerve injury) [47], suggesting an overactivation of the noradrenergic system in long-term pain. Furthermore, optogenetic activation of the LC-ACC projection enhances excitatory neurotransmission in vitro [48]. As such, the FG and c-Fos co-labeling here reveals a significant bilateral increase in c-Fos expressing neurons that specifically project to the rACC in CCI-LT. The blockade of the LC_{ipsi} and LC_{contra} neurons projecting to the rACC completely reverses the depressive-like behavior, yet it did not modify stimulus-evoked pain responses. Furthermore, site-specific pharmacological blockade indicates that α1- and α2-adrenoreceptors within the rACC are necessary for this behavior. Mechanistically, electrophysiological studies in the medial PFC indicated that noradrenaline-persistent responses are mainly mediated by synergy between presynaptic α1-adrenoreceptor-mediated enhancement of glutamate release and postsynaptic α2-adrenoreceptor-mediated inhibition of hyperpolarization-activated cyclic nucleotide-gated cation channels [49]. Thus, long-term pain overactivates the LC-ACC pathway (α-adrenoreceptors), leading to behavioral despair, and overactivation of the LC-basolateral amygdala pathway (BLA) (β-adrenergic receptors) mediates anxiety and enhanced aversive learning [22]. A similar phenomenon has been described when evaluating bilateral chemogenetic activation of the LC using resting-state functional MRI, which rapidly interrupts ongoing behavior, dampens exploratory activity and

augments anxiety, in conjunction with synchronized hyperconnectivity in the salient (that includes the ACC) and the amygdala networks [50]. Zerbi´s finding together with other previous showing that chemogenetic activation of the LC→PFC pathway in neuropathic pain animals (without anxiety) increases anxiogenic-like behavior as well as spontaneous pain [5] raise important questions about the involvement of the LC→ACC pathway in anxiety and that of non-evoked pain in long-term neuropathic pain. Thus, experiments will be needed to determine if anxiety is triggered by different LC projections (LC→BLA and LC→ACC). Indeed, from a translational point of view it will be particularly relevant to determine if the blockade of β-adrenergic receptors, which has been shown to have an anxiolytic effect at BLA level [29] also has a similar beneficial effect at the ACC level.

Pain induces plasticity in the brain and it potentiates communication between brain nuclei by enhancing specific pathways, at the same time silencing other nuclei and pathways [51]. Our study shows short-term asymmetrical endogenous LC activation after nerve injury, as witnessed by the c-Fos activity, and by the fact that global LC and LC-SC pathway blockade attenuates injury-induced neuropathic pain ipsilaterally during the early post-injury period. However, this restorative LC analgesia fails over time, with the harmful bilateral activation of the LC and their projections to the rACC. These projections contribute to depression in the long-term through α1- and α2-adrenoceptor activity. These data suggest that pain-induced depression is not a direct consequence of the failure of the descending pain inhibition at LC level (LC→SC pathway). On the other hand, therapeutic approaches should focus on increasing noradrenaline exclusively at the SC level to avoid any deleterious effects at supraspinal sites [5]. These findings explain why drugs that systemically increase noradrenaline availability are rarely used (e.g., reboxetine, desipramine), while drugs with complementary serotoninergic or opioidergic actions (antidepressants (serotonin-noradrenaline reuptake inhibitors), tramadol, tapentadol) are more commonly chosen to treat pain or pain-depression comorbidity [52-54].

Acknowledgements

We are very grateful to Mr Santiago Muñoz, Ms Paula Reyes Perez and Ms Elena Marín Álvarez for their excellent technical assistance. The Central Services of Scientific

and Technological Research, Health Sciences, and Animal Research from the University of Cadiz.

Funding

This study was supported by grants co-financed by the "Fondo Europeo de Desarrollo Regional" (FEDER)-UE "A way to build Europe" from the "Ministerio de Economía y Competitividad" (MINECO: RTI2018-099778-B-I00) and by the "Ministerio de Salud-Instituto de Salud Carlos III (PI18/01691); the "Consejería de Salud de la Junta de Andalucía" (PI-0134-2018); the "Programa Operativo de Andalucía FEDER, Iniciativa Territorial Integrada ITI 2014-2020 Consejería Salud, Junta de Andalucía" (PI-0080-2017); Instituto de Investigación e Innovación en Ciencias Biomédicas de Cádiz (INiBICA LI19/06IN- CO22); the "Consejería de Economía, Innovación, Ciencia y Empleo de la Junta de Andalucía" (CTS-510); and the "Centro de Investigación Biomédica en Red de Salud Mental-CIBERSAM" (CB/07/09/0033); and the Academy of Finland (315043).

All authors report no biomedical financial interests or potential conflicts of interest.

Competing interests

The authors report no competing interests

Supplementary material

Supplementary material is available at *Brain* online.

References

1. Bravo L, Llorca-Torralba M, Suarez-Pereira I, Berrocoso E. Pain in neuropsychiatry: Insights from animal models. *Neurosci Biobehav Rev* 2020; 115: 96-115.

2. Doan L, Manders T, Wang J. Neuroplasticity underlying the comorbidity of pain and depression. *Neural Plast* 2015; 2015: 504691.

3. Millan MJ. Descending control of pain. *Prog Neurobiol* 2002; 66(6): 355-474.

4. Pertovaara A. Noradrenergic pain modulation. *Prog Neurobiol* 2006; 80(2): 53-83.

5. Hirschberg S, Li Y, Randall A, Kremer EJ, Pickering AE. Functional dichotomy in spinal- vs prefrontal-projecting locus coeruleus modules splits descending noradrenergic analgesia from ascending aversion and anxiety in rats. *Elife* 2017; 6.

6. Llorca-Torralba M, Borges G, Neto F, Mico JA, Berrocoso E. Noradrenergic Locus Coeruleus pathways in pain modulation. *Neuroscience* 2016; 338: 93-113.

7. Taylor BK, Westlund KN. The noradrenergic locus coeruleus as a chronic pain generator. *J Neurosci Res* 2017; 95(6): 1336-1346.

8. Bangasser DA, Valentino RJ. Sex differences in stress-related psychiatric disorders: neurobiological perspectives. *Front Neuroendocrinol* 2014; 35(3): 303-319.

9. Isingrini E, Perret L, Rainer Q, Amilhon B, Guma E, Tanti A *et al.* Resilience to chronic stress is mediated by noradrenergic regulation of dopamine neurons. *Nature neuroscience* 2016; 19(4): 560-563.

10. Zhang H, Chaudhury D, Nectow AR, Friedman AK, Zhang S, Juarez B *et al.* alpha1- and beta3-Adrenergic Receptor-Mediated Mesolimbic Homeostatic Plasticity Confers Resilience to Social Stress in Susceptible Mice. *Biological psychiatry* 2019; 85(3): 226-236.

11. Bernard R, Kerman IA, Thompson RC, Jones EG, Bunney WE, Barchas JD *et al.* Altered expression of glutamate signaling, growth factor, and glia genes in the locus coeruleus of patients with major depression. *Mol Psychiatry* 2011; 16(6): 634-646.

12. Ordway GA, Smith KS, Haycock JW. Elevated tyrosine hydroxylase in the locus coeruleus of suicide victims. *J Neurochem* 1994; 62(2): 680-685.

13. Belmaker RH, Agam G. Major depressive disorder. *N Engl J Med* 2008; 358(1): 55-68.

14. Perez-Caballero L, Torres-Sanchez S, Romero-Lopez-Alberca C, Gonzalez-Saiz F, Mico JA, Berrocoso E. Monoaminergic system and depression. *Cell Tissue Res* 2019; 377(1): 107-113.

15. Bouhassira D, Lanteri-Minet M, Attal N, Laurent B, Touboul C. Prevalence of chronic pain with neuropathic characteristics in the general population. *Pain* 2008; 136(3): 380-387.

16. Finnerup NB, Attal N, Haroutounian S, McNicol E, Baron R, Dworkin RH *et al.* Pharmacotherapy for neuropathic pain in adults: a systematic review and meta-analysis. *Lancet Neurol* 2015; 14(2): 162-173.

17. Chandler DJ, Jensen P, McCall JG, Pickering AE, Schwarz LA, Totah NK. Redefining Noradrenergic Neuromodulation of Behavior: Impacts of a Modular Locus Coeruleus Architecture. *The Journal of neuroscience : the official journal of the Society for Neuroscience* 2019; 39(42): 8239-8249.

18. Uematsu A, Tan BZ, Ycu EA, Cuevas JS, Koivumaa J, Junyent F *et al.* Modular organization of the brainstem noradrenaline system coordinates opposing learning states. *Nature neuroscience* 2017; 20(11): 1602-1611.

19. Barthas F, Sellmeijer J, Hugel S, Waltisperger E, Barrot M, Yalcin I. The anterior cingulate cortex is a critical hub for pain-induced depression. *Biological psychiatry* 2015; 77(3): 236-245.

20. Bennett GJ, Xie YK. A peripheral mononeuropathy in rat that produces disorders of pain sensation like those seen in man. *Pain* 1988; 33(1): 87-107.

21. Berrocoso E, De Benito MD, Mico JA. Role of serotonin 5-HT1A and opioid receptors in the antiallodynic effect of tramadol in the chronic constriction injury model of neuropathic pain in rats. *Psychopharmacology (Berl)* 2007; 193(1): 97-105.

22. Llorca-Torralba M, Pilar-Cuellar F, Bravo L, Bruzos-Cidon C, Torrecilla M, Mico JA *et al.* Opioid Activity in the Locus Coeruleus Is Modulated by Chronic Neuropathic Pain. *Mol Neurobiol* 2019; 56(6): 4135-4150.

23. Johansen JP, Fields HL, Manning BH. The affective component of pain in rodents: direct evidence for a contribution of the anterior cingulate cortex. *Proc Natl Acad Sci U S A* 2001; 98(14): 8077-8082.

24. David-Pereira A, Sagalajev B, Wei H, Almeida A, Pertovaara A, Pinto-Ribeiro F. The medullary dorsal reticular nucleus as a relay for descending pronociception induced by the mGluR5 in the rat infralimbic cortex. *Neuroscience* 2017; 349: 341-354.

25. Bravo L, Mico JA, Rey-Brea R, Perez-Nievas B, Leza JC, Berrocoso E. Depressive-like states heighten the aversion to painful stimuli in a rat model of comorbid chronic pain and depression. *Anesthesiology* 2012; 117(3): 613-625.

26. Berrocoso E, Mico JA, Vitton O, Ladure P, Newman-Tancredi A, Depoortere R *et al.* Evaluation of milnacipran, in comparison with amitriptyline, on cold and mechanical allodynia in a rat model of neuropathic pain. *Eur J Pharmacol* 2011; 655(1-3): 46-51.

27. Alba-Delgado C, Llorca-Torralba M, Horrillo I, Ortega JE, Mico JA, Sanchez-Blazquez P *et al.* Chronic pain leads to concomitant noradrenergic impairment and mood disorders. *Biological psychiatry* 2013; 73(1): 54-62.

28. Detke MJ, Rickels M, Lucki I. Active behaviors in the rat forced swimming test differentially produced by serotonergic and noradrenergic antidepressants. *Psychopharmacology (Berl)* 1995; 121(1): 66-72.

29. Llorca-Torralba M, Suarez-Pereira I, Bravo L, Camarena-Delgado C, Garcia-Partida JA, Mico JA *et al.* Chemogenetic Silencing of the Locus Coeruleus-Basolateral Amygdala Pathway Abolishes Pain-Induced Anxiety and Enhanced Aversive Learning in Rats. *Biological psychiatry* 2019; 85(12): 1021-1035.

30. Alba-Delgado C, Llorca-Torralba M, Mico JA, Berrocoso E. The onset of treatment with the antidepressant desipramine is critical for the emotional consequences of neuropathic pain. *Pain* 2018; 159(12): 2606-2619.

31. Bravo L, Torres-Sanchez S, Alba-Delgado C, Mico JA, Berrocoso E. Pain exacerbates chronic mild stress-induced changes in noradrenergic transmission in rats. *European neuropsychopharmacology : the journal of the European College of Neuropsychopharmacology* 2014; 24(6): 996-1003.

32. Tervo DGR, Proskurin M, Manakov M, Kabra M, Vollmer A, Branson K *et al.* Behavioral variability through stochastic choice and its gating by anterior cingulate cortex. *Cell* 2014; 159(1): 21-32.

33. Viisanen H, Pertovaara A. Influence of peripheral nerve injury on response properties of locus coeruleus neurons and coeruleospinal antinociception in the rat. *Neuroscience* 2007; 146(4): 1785-1794.

34. McCall JG, Al-Hasani R, Siuda ER, Hong DY, Norris AJ, Ford CP *et al.* CRH Engagement of the Locus Coeruleus Noradrenergic System Mediates Stress-Induced Anxiety. *Neuron* 2015; 87(3): 605-620.

35. Sciolino NR, Plummer NW, Chen YW, Alexander GM, Robertson SD, Dudek SM *et al.* Recombinase-Dependent Mouse Lines for Chemogenetic Activation of Genetically Defined Cell Types. *Cell Rep* 2016; 15(11): 2563-2573.

36. Hayashida K, Clayton BA, Johnson JE, Eisenach JC. Brain derived nerve growth factor induces spinal noradrenergic fiber sprouting and enhances clonidine analgesia following nerve injury in rats. *Pain* 2008; 136(3): 348-355.

37. Hughes SW, Hickey L, Hulse RP, Lumb BM, Pickering AE. Endogenous analgesic action of the pontospinal noradrenergic system spatially restricts and temporally delays the progression of neuropathic pain following tibial nerve injury. *Pain* 2013; 154(9): 1680-1690.

38. Ma W, Eisenach JC. Chronic constriction injury of sciatic nerve induces the up-regulation of descending inhibitory noradrenergic innervation to the lumbar dorsal horn of mice. *Brain Res* 2003; 970(1-2): 110-118.

39. Brightwell JJ, Taylor BK. Noradrenergic neurons in the locus coeruleus contribute to neuropathic pain. *Neuroscience* 2009; 160(1): 174-185.

40. Marques-Lopes J, Pinho D, Albino-Teixeira A, Tavares I. The hyperalgesic effects induced by the injection of angiotensin II into the caudal ventrolateral medulla are mediated by the pontine A5 noradrenergic cell group. *Brain research* 2010; 1325: 41-52.

41. Martins I, Carvalho P, de Vries MG, Teixeira-Pinto A, Wilson SP, Westerink BH *et al.* Increased noradrenergic neurotransmission to a pain facilitatory area of the brain is implicated in facilitation of chronic pain. *Anesthesiology* 2015; 123(3): 642-653.

42. Martin JH. Autoradiographic estimation of the extent of reversible inactivation produced by microinjection of lidocaine and muscimol in the rat. *Neuroscience letters* 1991; 127(2): 160-164.

43. Kaushal R, Taylor BK, Jamal AB, Zhang L, Ma F, Donahue R *et al.* GABA-A receptor activity in the noradrenergic locus coeruleus drives trigeminal neuropathic pain in the rat; contribution of NAalpha1 receptors in the medial prefrontal cortex. *Neuroscience* 2016; 334: 148-159.

44. Shackman AJ, Salomons TV, Slagter HA, Fox AS, Winter JJ, Davidson RJ. The integration of negative affect, pain and cognitive control in the cingulate cortex. *Nature reviews Neuroscience* 2011; 12(3): 154-167.

45. Mayberg HS, Liotti M, Brannan SK, McGinnis S, Mahurin RK, Jerabek PA *et al.* Reciprocal limbic-cortical function and negative mood: converging PET findings in depression and normal sadness. *Am J Psychiatry* 1999; 156(5): 675-682.

46. Sellmeijer J, Mathis V, Hugel S, Li XH, Song Q, Chen QY *et al.* Hyperactivity of Anterior Cingulate Cortex Areas 24a/24b Drives Chronic Pain-Induced Anxiodepressive-like Consequences. *The Journal of neuroscience : the official journal of the Society for Neuroscience* 2018; 38(12): 3102-3115.

47. Suto T, Eisenach JC, Hayashida K. Peripheral nerve injury and gabapentin, but not their combination, impair attentional behavior via direct effects on noradrenergic signaling in the brain. *Pain* 2014; 155(10): 1935-1942.

48. Koga K, Yamada A, Song Q, Li XH, Chen QY, Liu RH *et al.* Ascending noradrenergic excitation from the locus coeruleus to the anterior cingulate cortex. *Mol Brain* 2020; 13(1): 49.

49. Zhang Z, Cordeiro Matos S, Jego S, Adamantidis A, Seguela P. Norepinephrine drives persistent activity in prefrontal cortex via synergistic alpha1 and alpha2 adrenoceptors. *PLoS One* 2013; 8(6): e66122.

50. Zerbi V, Floriou-Servou A, Markicevic M, Vermeiren Y, Sturman O, Privitera M *et al.* Rapid Reconfiguration of the Functional Connectome after Chemogenetic Locus Coeruleus Activation. *Neuron* 2019; 103(4): 702-718 e705.

51. Apkarian AV, Hashmi JA, Baliki MN. Pain and the brain: specificity and plasticity of the brain in clinical chronic pain. *Pain* 2011; 152(3 Suppl): S49-64.

52. Bravo L, Llorca-Torralba M, Berrocoso E, Mico JA. Monoamines as Drug Targets in Chronic Pain: Focusing on Neuropathic Pain. *Front Neurosci* 2019; 13: 1268.

53. Hughes S, Hickey L, Donaldson LF, Lumb BM, Pickering AE. Intrathecal reboxetine suppresses evoked and ongoing neuropathic pain behaviours by restoring spinal noradrenergic inhibitory tone. *Pain* 2015; 156(2): 328-334.

54. Mico JA, Ardid D, Berrocoso E, Eschalier A. Antidepressants and pain. *Trends Pharmacol Sci* 2006; 27(7): 348-354.

Figure legends

Figure 1. Sensory and affective characterization of the development of neuropathic pain. (**A**) Scheme of the chronic constriction injury (CCI) model, timeline and graphs showing the response of the ipsilateral and contralateral paw in the acetone test and the predominant behavior (immobility, IM; climbing, CL; swimming, SW) in the forced swimming test (FST) in the short-term (ST), mid-term (MT) and long-term (LT) after CCI in wild-type rats (n=10 animals/group): *p<0.05, **p<0.01, ***p<0.001 vs Sham, Student´s t-test for each time point (ST, MT and LT). d, days.

Figure 2. Effect of chemogenetic inhibition and activation of ipsilateral and contralateral LC on nociceptive behavior after nerve-injury. (**A**) Scheme of noradrenergic LC inhibition or activation using the DREADD strategy in TH:Cre rats and representative immunohistofluorescence image (scale bar = 10 μm) of mCherry expression in noradrenergic LC neurons (red = mCherry, green = DBH). (**B**) Response of the ipsilateral paw of CCI-ST, -MT and -LT rats in the acetone test after ipsilateral LC (LC_{ipsi}) noradrenergic inhibition by CNO (1 mg/kg, i.p.) (n = 8-10 animals/group: ***p<0.001 vs Sham-Sal; +++p<0.01 vs CCI-Sal). (**C**) Response of the ipsilateral paw to thermal stimulus 20 and 360 min after LC_{ipsi} inhibition by CNO (1 mg/kg, i.p.) (n = 9 animals/group: +++p<0.001 vs CCI-Sal). (**D**) Response of the ipsilateral paw of CCI-ST, -MT and -LT rats in the acetone test after noradrenergic contralateral LC (LC_{contra}) inhibition by CNO (1 mg/kg, i.p.) (n = 9-10 animals/group: ***p<0.001 vs Sham-Sal). (**E**) Response of the ipsilateral paw of CCI-ST, -MT and -LT rats in the acetone and von Frey tests after noradrenergic LC_{ipsi} activation by CNO (1 mg/kg, i.p.) (n = 9-10 animals/group: ***p<0.001 vs Sham-Sal; +p<0.05, ++p<0.01, +++p<0.001 vs CCI-Sal). (**F**) Response of the ipsilateral paw of CCI-ST, -MT and -LT rats in the acetone and von Frey tests after noradrenergic LC_{contra} activation by CNO (1 mg/kg, i.p.) (n = 10 animals/group: ***p<0.001 vs Sham-Sal). One-way or two-way ANOVA with repeated measures, Newman-Keuls post-hoc test. CCI, chronic constriction injury; ST, short-term, MT, mid-term; LT, long-term; Sal, saline; CNO, Clozapine-n-oxide; LC, locus coeruleus; i.p., intraperitoneal; Ac, acetone test; CP, Cold Plate test; VF, von Frey test; d, days; DBH, dopamine beta-hydroxylase.

Figure 3. Effect of chemogenetic inhibition and activation of ipsilateral and contralateral LC on depressive-like behavior after long-term neuropathy. (**A**) Timeline of noradrenergic LC inhibition or activation using the DREADD strategy in TH:Cre rats. (**B**) Representative image of noradrenergic LC_{ipsi} or LC_{contra} inhibition and predominant behavior in the FST after CNO (1 mg/kg, i.p.) (n = 8-10 animals/group: **p<0.001 vs Sham-Sal; ++p<0.01, +++p<0.001 vs CCI-Sal). (**C**) Representative image of noradrenergic LC_{ipsi} or LC_{contra} activation and predominant behavior in the FST after CNO (1 mg/kg, i.p.) (n = 8-10 animals/group: **p<0.001, ***p<0.001 vs Sham-Sal). Two-way ANOVA, Newman-Keuls post-hoc test. CCI, chronic constriction injury; FST, forced swimming test; IM, immobility; CL, climbing; SW, swimming; Sal, saline; CNO, Clozapine-n-oxide; LC, locus coeruleus; i.p., intraperitoneal; d, days.

Figure 4. Study of the LC projections to the SC. (**A-B**) Retrograde FG tracer strategy and representative image (scale bar = 500 μm) to target LC neurons that project to the ipsilateral SC in wild-type rats. Ipsilateral and contralateral distribution of FG labeled LC neurons and FG positive neurons along the rostral-caudal axis of the ipsilateral (LCipsi) and contralateral (LCcontra) LC (mean + SEM of the number of neurons per slice, n = 4 animals: Student´s t-test and one-way ANOVA, Newman-Keuls post-hoc test). (**C**) Representative immunofluorescence of the central LCipsi and LCcontra showing the dorso-ventral aspect (half height relative to DBH expression) (scale bar = 200 μm). The graphs show the dorso-ventral distribution of the central LCipsi and LCcontra projections to the SCipsi (n = 4 animals: ***p<0.001 vs Ventral LC, Student´s t-test). (**D**) Representative immunofluorescence of the central LC showing the DBH, c-Fos, FG expression and merged image. The inset shows an example of c-Fos+FG positive neurons (scale, bar = 100 μm). (**E-F**) Numbers of c-Fos and c-Fos+FG positive neurons of central LCipsi and LCcontra, as well as the dorso-ventral distribution in Sham and CCI-ST rats (mean + SEM of the number of neurons per slice, n = 6 animals/group: *p<0.05, ***p<0.001 vs Sham; #p<0.05, ##p<0.01 vs LCipsi, two-way ANOVA, Newman-Keuls post-hoc test; and ***p<0.001 vs Ventral LC, Student´s t-test). (**G**) Numbers of c-Fos positive neurons of central LCipsi and LCcontra, as well as the dorso-ventral distribution in Sham and CCI-LT rats (mean + SEM neurons per slice, n = 4 animals/group: ***p<0.001 vs Sham, two-way ANOVA, Newman-Keuls post-hoc test; and ***p<0.001 vs Ventral LC, Student´s t-test). CCI, chronic constriction injury;

LC, locus coeruleus; SC, spinal cord; FG, Fluoro-Gold (yellow); DBH, dopamine beta-hydroxylase (green); c-Fos (red).

Figure 5. Effect of chemogenetic inhibition of the $LC_{ipsi/contra}$→SC pathway on the time-course of nociceptive behavior after nerve-injury. (**A-B**) Timeline and representative image of noradrenergic LC_{ipsi}→SC or LC_{contra}→SC pathway inhibition using the AAV-Gi-mCherry strategy in TH:Cre rats. Response of the ipsilateral paw in the acetone, von Frey and cold plate tests after CNO (3 μM, i.t) administration to rats in the short-term (ST), mid-term (MT) and long-term (LT) after CCI (n = 4 animals/group: **p<0.01, ***p<0.001 vs Sham-Sal; +p<0.05, +++p<0.001 vs CCI-Sal, two-way ANOVA with repeated measures, Newman-Keuls post-hoc test). CCI, chronic constriction injury; LC, locus coeruleus; SC, spinal cord; Sal, saline; CNO, clozapine-n-oxide; i.t., intrathecal; Ac, acetone test; VF, von Frey test; CP, cold plate test; d, days.

Figure 6. Effect of chemogenetic activation of the $LC_{ipsi/contra}$→SC pathway on the time-course of nociceptive behavior after nerve-injury. (**A-B**) Timeline and representative image of noradrenergic LC_{ipsi}→SC or LC_{contra}→SC pathway activation using the AAV-Gs-mCherry strategy in LE-TH:Cre rats. (**A**) Response of the ipsilateral paw in the acetone, von Frey and cold plate tests after CNO (3 μM, i.t) administration to ras in the short-term (ST), mid-term (MT) and long-term (LT) after CCI (n= 6-8 animals/group: ***p<0.001 vs Sham-Sal; +p<0.05, ++p<0.01, +++p<0.001 vs CCI-Sal). (**B**) Response of the ipsilateral paw of CCI-ST, -MT and -LT rats in the acetone and von Frey tests after CNO (3 μM, i.t) administration (n= 6 animals/group: ***p<0.001 vs Sham-Sal). In addition, the response of the ipsilateral paw of CCI-LT rats was evaluated in the acetone and von Frey tests after clonidine (20 μg, i.t) administration (n= 5-6 animals/group: ***p<0.001 vs Sham-Sal; +p<0.05, +++p<0.001 vs CCI-Sal). Two-way ANOVA with or without repeated measures, Newman-Keuls post-hoc test). CCI, chronic constriction injury; LC, locus coeruleus; SC, spinal cord; Sal, saline; CNO, clozapine-n-oxide; Cloni, clonidine; i.t., intrathecal; Ac, acetone test; VF, von Frey test; CP, cold plate test; d, days.

Figure 7. Neuroanatomical study of the LC projections to the rACC. (**A-B**) Retrograde FG tracer strategy to target LC neurons that project to the ipsilateral rACC in wild-type rats and a representative image (scale bar = 500 μm). The ipsilateral and contralateral distribution of FG labeled LC neurons, and of FG positive neurons along the rostral-caudal axis of ipsilateral (LC_{ipsi}) and contralateral (LC_{contra}) LC (mean + SEM of the number of neurons per slice, n = 4 animals: ***p<0.001 vs Ipsi, Student´s t-test; one-way ANOVA, Newman-Keuls post-hoc test). (**C-D**) Retrograde FG tracer strategy to target LC neurons that project to the bilaterally rACC and representative image (scale bar = 500 μm). Ipsilateral and contralateral distribution of FG labeled LC neurons and FG positive neurons along the rostral-caudal axis of LC_{ipsi} and LC_{contra} (mean + SEM of the number of neurons per slice, n = 4 animals: Student´s t-test and one-way ANOVA, Newman-Keuls post-hoc test). (**E**) Representative immunofluorescence images of central LC_{ipsi} and LC_{contra} (-9.84 from Bregma: Paxinos and Watson, 2007) showing the dorso-ventral aspect (half height relative to DBH expression) (scale bar = 100 μm). The graphs show the dorso-ventral distribution of the central LC_{ipsi} and LC_{contra} projection to the rACC (n = 4 animals: ***p<0.001 vs Ventral LC, Student´s t-test). (**F**) Representative immunofluorescence of the central LC showing the DBH, c-Fos, FG expression and merged image (c-Fos+FG). The inset shows an example of c-Fos+FG positive neurons (scale, bar = 100 μm). (**G-H**) Numbers of c-Fos and c-Fos+FG positive neurons of central LCipsi and LCcontra as well as the dorso-ventral distribution in Sham and CCI-LT rats (mean + SEM neurons per slice, n = 4 animals/group: ***p<0.001 vs Sham, two-way ANOVA, Newman-Keuls post-hoc test; and ***p<0.001 vs Ventral LC, Student´s t-test. CCI, chronic constriction injury; LT, Long-term; LC, locus coeruleus; rACC, rostral Anterior Cingulate Cortex; FG, Fluoro-Gold (yellow); DBH, dopamine beta-hydroxylase (green); c-Fos (red).

Figure 8. Effect of the chemogenetic inhibition of the LC-rACC pathway and the pharmacological blockade of adrenoreceptor activity in the rACC after long-term neuropathy. (**A**) Timeline and cartoon of the bilateral AAV-Gi-mCherry injection into the LC, and intra-rACC CNO (3 μM) administration to inhibit the noradrenergic LC→rACC pathway of TH:Cre rats. Response of the ipsilateral hindpaw of CCI-LT rats in the acetone, von Frey and cold plate tests. The predominant behavior in the forced swimming test (FST: immobility, IM; climbing, CL; swimming, SW) was evaluated (n=

8-10 animals/group: **p<0.01, ***p<0.001 vs Sham-Sal; ++p<0.01 vs CCI-Sal, two-way ANOVA, Newman-Keuls post-hoc test). (**B-D**) Timeline and cartoon of the pharmacological inhibition of α1-adrenoceptors (prazosin, 5 μg; n = 8-10 animals/group), α2-adrenoceptors (idazoxan, 9 μg; n = 6-10 animals/group) or β-adrenoceptors (propranolol, 1 μg; n = 7-10 animals/group) in the rACC of CCI-LT wild-type rats: **p<0.01, ***p<0.001 vs Sham-Sal; ++p<0.01, +++p<0.001 vs CCI-Sal, two-way ANOVA, Newman-Keuls post-hoc test. CCI, chronic constriction injury; LC, locus coeruleus; rACC, rostral anterior cingulate cortex; Sal, saline; CNO, Clozapine-N-oxide; Praz, prazosin; Idx, Idazoxan; Prop, propranolol; Ac, acetone test; VF, von Frey test; CP, cold plate test; LT, Long-term; d, days.

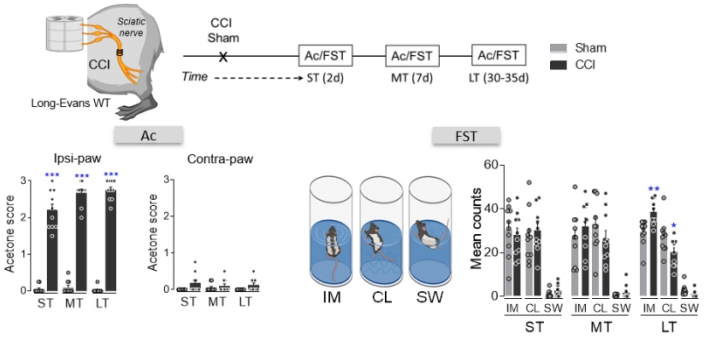

Figure 1

222x90mm (150 x 150 DPI)

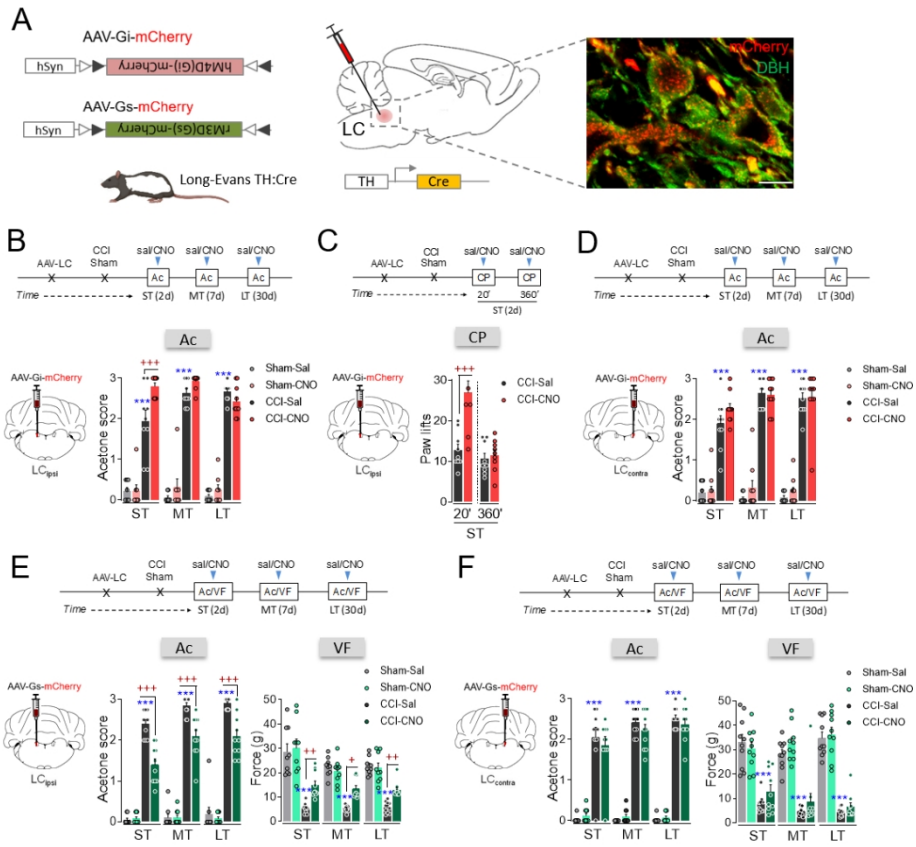

Figure 2

204x200mm (150 x 150 DPI)

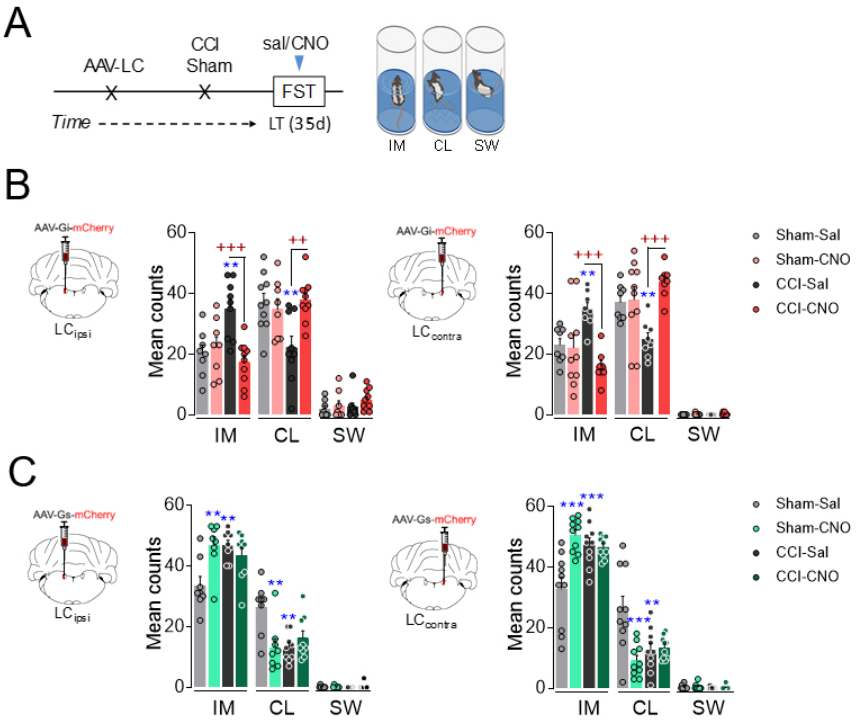

Figure 3

150x122mm (150 x 150 DPI)

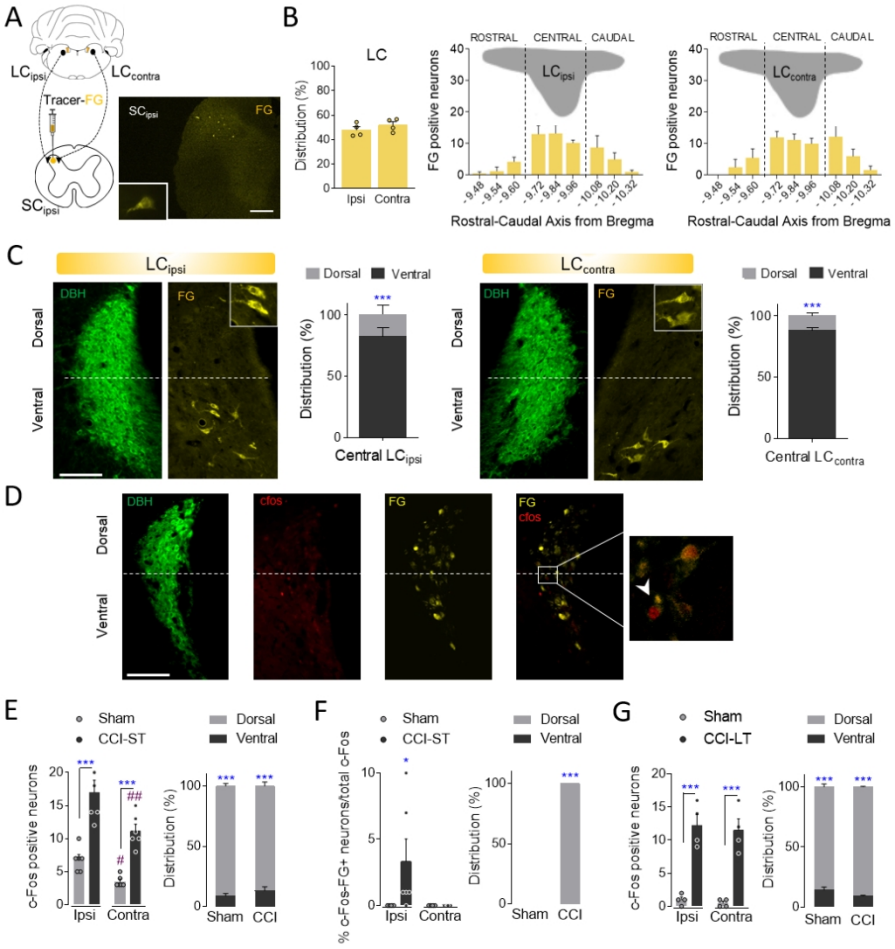

Figure 4

195x203mm (150 x 150 DPI)

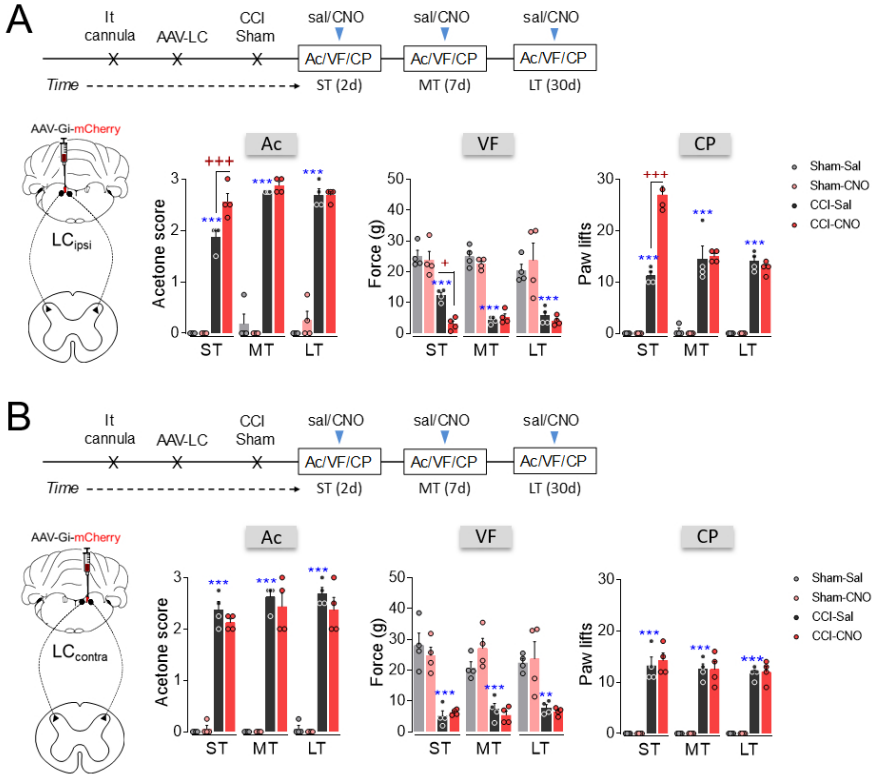

Figure 5

177x162mm (150 x 150 DPI)

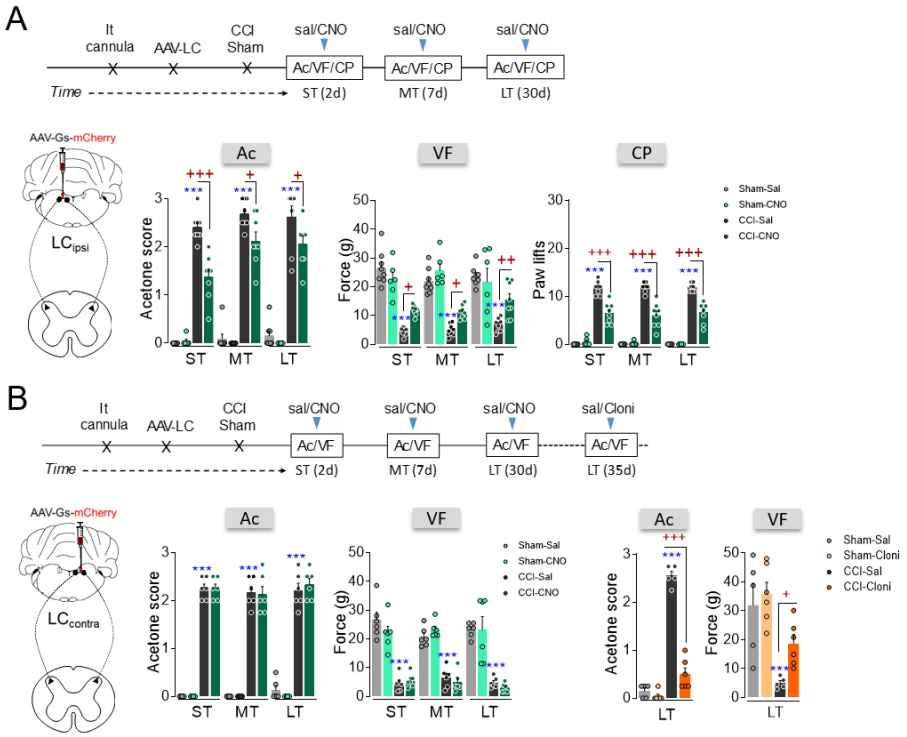

Figure 6

190x160mm (150 x 150 DPI)

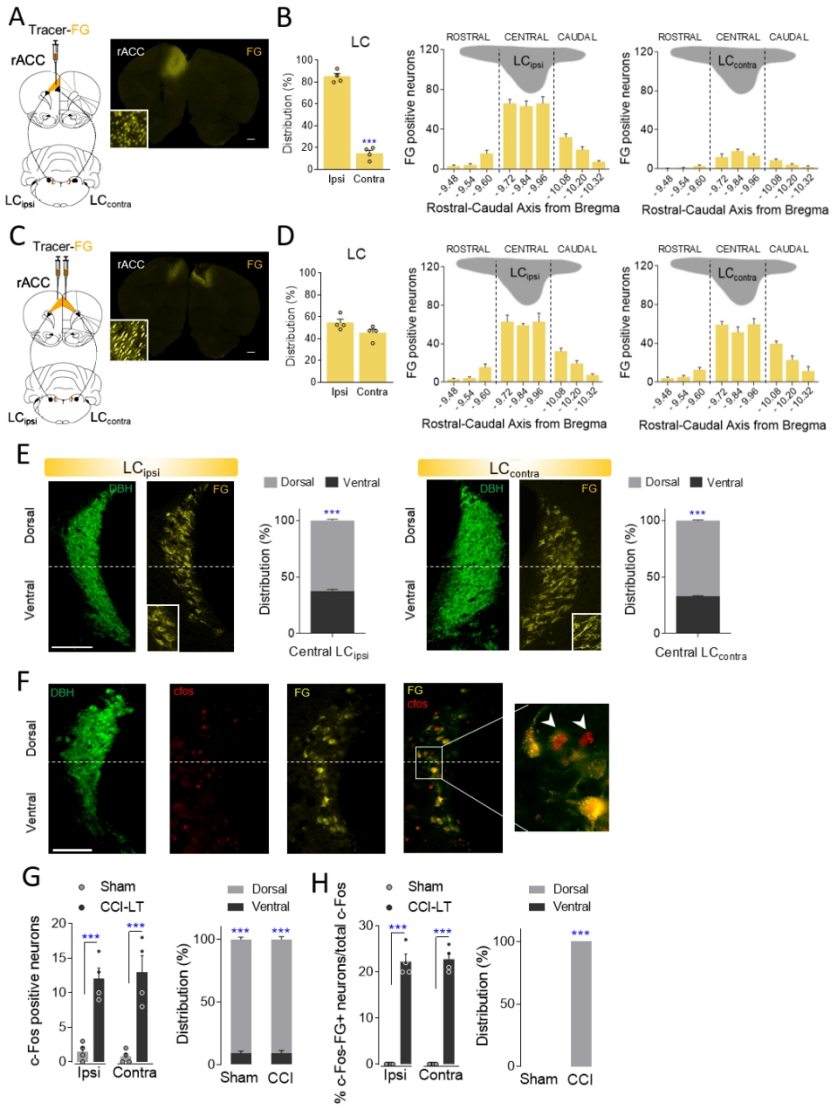

Figure 7

190x256mm (150 x 150 DPI)

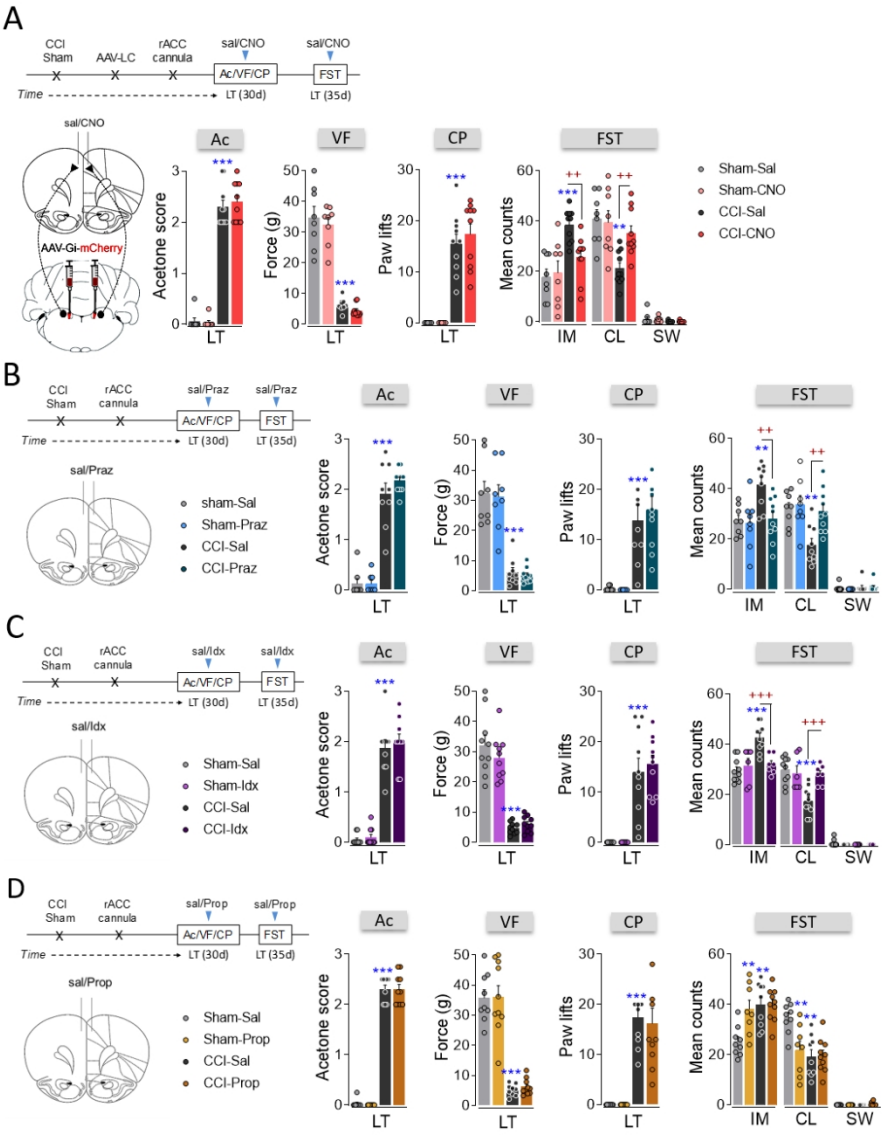

Figure 8

185x238mm (150 x 150 DPI)

Supplementary Information

Materials and methods

Animals

Experiments were carried out on male transgenic Long-Evans tyrosine hydroxylase:Cre (TH:Cre) and wild-type Long-Evans rats, all with a body weight of 350-450 g and maintained under standard laboratory conditions (22 ºC, 12 h light/dark cycle, lights on at 08:00 AM, food and water *ad libitum*). The TH:Cre founders were provided by the Rat Resource and Research Center (RRCC, USA: donated by K. Deisseroth). All animal handling and procedures were carried out in accordance with the European Commission guidelines (2010/63/EC) and Spanish Law (RD 53/2013) regulating animal research. Furthermore, all experimental protocols were approved by the Committee for Animal Experimentation at the University of Cadiz (Spain).

Neuropathic pain model

Chronic constriction injury (CCI) of the sciatic nerve was used here as a model of neuropathic pain (Bennett and Xie, 1988; Berrocoso *et al.*, 2007). The rats were anesthetized with isoflurane (induction with 3-4% and maintenance with 1.5-2.5%), and the left sciatic nerve was then exposed at the mid-thigh level, proximal to the sciatic trifurcation. Four chrome gut (4–0) ligatures were tied loosely around the nerve, separated by 1.0–1.5 mm so as not to compromise the vascular supply. The overlying layers of muscle were then closed with 4–0 non-absorbable silk thread and the skin was sutured with 2–0 silk thread. Sham operations were performed in the same manner but without nerve ligation. The experimental procedures were then carried out 2 days (short-term, ST), 7 days (mid-term, MT) and 30-35 days (long-term, LT) days after CCI.

Drugs

The following drugs were administered to awake animals that were well-habituated to handling: Clozapine-n-oxide (CNO, 1 mg/kg intraperitoneal -i.p.-, 3 µM/20 µl intrathecal -i.t.- and 3 µM/0.5 µl intra-rACC, administered 20 min before the behavioral tests: Carbosynth, UK); clonidine hydrochloride (20 µg/10 µl i.t., administered 30 min before testing: Sigma-Aldrich, Spain); prazosin hydrochloride (5 µg/0.5 µl intra-rACC, administered 30 min before nociceptive tests, or 24, 5 and 1h before the forced swimming test (FST): Sigma-Aldrich, Spain); idazoxan hydrochloride (9 µg/0.5 µl intra-rACC, administered 20 min before testing or 24, 5 and 1h before the FST: Sigma-Aldrich, Spain); and propranolol hydrochloride (1 µg/0.5 µl intra-rACC, administered 20 min before nociceptive tests, or 24, 5 and 1h before the FST: Sigma-Aldrich, Spain). In the locomotor spontaneous activity test, drugs were administered at the beginning of the test.

Forced Swimming test (FST)

Depressive-like behavior was evaluated in the FST over two different sessions, a 15 min pre-test was followed by a 5 min test performed 24 hours later. Rats were placed individually into a Plexiglas cylinder (height 40 cm, diameter 18 cm) filled to a depth of 30 cm with water at 25 ± 1 °C. Using a time-sampling technique, the predominant behaviors were recorded (climbing -CL, swimming -SW, or immobility -IM), and scored in each 5 s period of the 300 s test session using customized software (Red-Mice, Spain), providing a total of 60 scores. Immobility behavior was determined when no activity was observed other than the movements necessary to keep the animals head above water. Climbing behavior was measured when the rats made vigorous upward movements with their forepaws in and out of the water. Swimming was considered the predominant behavior when the rats moved around the cylinder. Depressive-like behavior was defined as an increase in the mean immobility behavior.

Locomotor spontaneous activity test

Free exploratory ambulation was recorded individually over 40 min in a light-attenuated room (13-14 lux), and in a transparent box (40 x 40 x 40 cm), using a Spontaneous Motor Activity Recording and Tracking (SMART) video system (v3.0, Panlab S.L., Spain). The total distance travelled (arbitrary units, A.U., %) was measured as an indicator of locomotor activity (Llorca-Torralba *et al.*, 2019). In addition, the arena was divided into peripheral and central regions in order to perform an initial screen for anxiety-related behaviours during the first 10 min of the test, based on our earlier demonstration that CCI-LT male Sprague Dawley rats display an anxiogenic-like phenotype in this test (Alba-Delgado *et al.*, 2016). However, we did not detect significant differences between sham (25.41±4.99%) and CCI-LT animals (17.50±0.77%, $p>0.05$ by Student T' test) in terms of the relative time spent in the central zone during this period. The discrepancy between these studies could be explained by the much lower illumination (1.79 lux) used in our previous study (Alba-Delgado *et al.*, 2016) and the different rat strains analysed (Sprague-Dawley and Long Evans rats).

Designer Receptor Exclusively Activated by Designer Drugs (DREADDs) approaches

DREADDs approaches were performed as in our previous publication were a high level of colocalization between mCherry and noradrenergic neurons were found in the LC of TH:CRE rats (Llorca-Torralba *et al.*, 2019):

Stereotaxic surgery

The following vectors were used in these studies: DREADDs (from Virus Vector Core, Gene Therapy Center Vector Core at the University of North Carolina, USA); AAV2/hSyn-DIO-hM4D(Gi)-mCherry (hM4D(Gi)-DREADD, inhibitor virus, titer 3 x 10^12 vg/ml, 1.4 µl/ LC); AAV2/hSyn-DIO-rM3D(Gs)-mCherry (rM3D(Gs)-DREADD, activator virus, titer 3 x 10^12 vg/ml, 1.4 µl/LC); and AAV2/hSyn-DIO-mCherry (control-DREADD; titer 5.6 x 10^12 vg/ml, 1.4 µl/LC). The control vector contained a mCherry reporter protein without the DREADD reporter.

For DREADDs vectors injections into the LC, TH:CRE rats were anesthetized with an i.p. injection of ketamine (100 mg/kg: Richter Pharma, Spain) and xylazine (20 mg/kg: Calier laboratory, S.A, Spain), and placed into a stereotaxic frame with the skull level along both the antero-posterior (AP) and medio-lateral (ML) axis for precise targeting. Cranial windows were opened above the LC coordinates: AP: -3.2 mm, ML: ±1.3 mm, dorso-ventral (DV): 6.2 mm, with the head oriented at a 15º angle to the horizontal plane. After injection, the wound was cleaned with 0.9% saline, disinfected with iodine polyvidone and the skin was sutured with 4–0 non-absorbable silk thread. To enhance vector expression, the behavioral studies were carried out 3 weeks after the injections.

Virus expression

Animals were perfused with paraformaldehyde (4%) at the end of the experiments (Bravo *et al.*, 2013; Llorca-Torralba *et al.*, 2019), to verify the expression of mCherry into the LC. Additionally, the percentage of expression of mCherry in DBH positive neurons in the LC was quantified. All LC sections (30 µm) were incubated for 48 hours at 4 ºC with an antibody against red fluorescent protein [5F8] (RFP, 1:500, Chromotek, Germany) and mouse anti-dopamine beta hydroxylase antibody (DBH, 1:1000, Merck Chemicals & Life Science S.A., Spain). Subsequently, the antibodies were detected with a biotinylated donkey anti-rat antibody (1:200, Jackson ImmunoResearch Europe, UK), which was visualized with Alexa Fluor 568 streptavidin or a donkey anti-mouse Alexa Fluor 488 (1:1000, Invitrogen™, USA). The sections were then washed and coverslipped in fluoro-gel aqueous mounting medium and the images were acquired on a Zeiss LSM 880 Confocal microscope with FAST Airyscan (Carl Zeiss Microscopy GmbH, Germany). The selective expression of DREADD was also assessed in the A5 noradrenergic nucleus and ventral tegmental area (VTA), the latter incubated with a rabbit TH primary antibody diluted 1:1,000 and visualized with a donkey anti-rabbit Alexa Fluor 488 (Invitrogen™, USA).

Tracer approach

Fluoro-Gold (FG) was used as retrograde tracer (4%/0.2 µl for the rACC- or 4%/0.4 µl for the SC: Fluorochrome, USA). For FG injections at the lumbar level of the SC, rats were anesthetized with sodium pentobarbital (50 mg/kg, i.p.: Vetoquinol S.A, Spain) and local analgesia was administered subcutaneously: karprophen (10 mg/kg: Zoetis, Spain); bupivacaine (2 mg/kg: B. Braun Medical S.A., Spain). Additional doses of pentobarbital were administered as required. Rats were placed in a stereotaxic frame and a laminectomy was performed at the level of the T12–L2 vertebrae to expose the L4-L6 segments of the SC. The dura was then removed and FG was administered at four sites along the ipsilateral L4-L6 dorsal horn of the SC (SC_{ipsi}). After FG injection, the skin was closed with staples, and the wound was cleaned with 0.9% saline and disinfected with iodine polyvidone. In another experimental set, the FG was microinjected unilateral- or bilaterally into the rACC according to the same stereotaxic surgery performed in DREADD approach (see above). The target coordinates for rACC were AP: +3.0 mm, ML: ±1.0 mm and DV: 1.2 mm, with the head oriented at a 0º angle to the horizontal plane.

To enhance tracer expression, the neuroanatomical studies were carried out 4 days after the injections.

The location of the FG injection site was verified to be within the SC and rACC in all the animals studied. Sequential SC and rACC (40 µm) sections were visualized directly on an Olympus BX40 fluorescent microscope equipped with an Olympus DP73 camera (Spain).

rACC cannula implantation

Rats were anesthetized with an i.p. injection of ketamine (100 mg/kg) and xylazine (20 mg/kg), and placed in a stereotaxic frame. A cannula was implanted bilaterally into the rACC (AP +3.0 mm, ML ±1.0 mm and DV 1.2 mm) with the head oriented at a 0º angle to the horizontal plane, and fixed in place with dental cement and four anchor screws. The cannulae were maintained closed until the test session by inserting a stainless-steel wire.

Cannula placement into the intra-rACC was verified by injection of 0.5 µl Pontamine Sky Blue at the injection site just before the animals were perfused. Sequential rACC (40 µm) sections were stained with neutral red, and the images were acquired on an Olympus BX40 microscope equipped with an Olympus DP73 camera (Spain).

The animals whose cannulas were not appropriately located in the target area were not included in the results.

Intrathecal catheter installation

For i.t. drug injection, a catheter (PE-10) was implanted into the lumbar SC under isoflurane anesthesia (see above for CCI) (Wei *et al.*, 2016). An incision was made in the skin and a cannula (20 ga, 0.9 x 40 mm) was introduced in a slightly medial cranial direction along the

surface of L6 up to L5. Correct placement of the cannula was confirmed by a tail flick, a retraction of the leg or the reflux of cerebrospinal fluid. A polyethylene catheter (0.68 mm diameter) was introduced from the end of the cannula until it reached the caudal rib level and the cannula was removed. The catheter was first fixed onto the surface of the lumbar musculature and the rest was passed subcutaneously along the spine, appearing through the skin in the occipital region. Lidocaine (4%/15 µl, i.t.) was administered to verify the correct placement of the intraspinal cannula over time (CCI-ST, -MT and -LT), observing immediate motor paralysis of the posterior third of the animal that lasted for about 10-20 min. Those animals that not lost motor paralysis were excluded from the analysis.

Cannula placement into the intrathecal was verified by injection of 0.5 µl Pontamine Sky Blue at the injection site just before the animals were perfused. The images were acquired with Leica camera.

Immunohistochemistry

FG expression in LC

FG expression of the ipsilateral and contralateral projections from the LC was evaluated in sequential LC sections (9 representative sections of 30 µm per animals along the rostra-caudal axis), incubating them for 48 hours at 4 ºC with a rabbit anti-FG antibody (1:1,000, Merck Chemicals & Life Science S.A., Spain) and a mouse anti-DBH antibody (1:1,000, Merck Chemicals & Life Science S.A., Spain). The antibodies were visualized with a biotinylated donkey anti-rabbit IgG (1:200, Jackson ImmunoResearch Europe, UK) followed by Alexa Fluor 488 streptavidin (1:1,000, Invitrogen™, USA) or a donkey anti-mouse Alexa Fluor 568 (1:1,000, Invitrogen™, USA). After washing and coverslipping in fluoro-gel aqueous mounting medium, images were acquired on a fluorescent Olympus BX40 microscope equipped with an Olympus DP73 camera (Spain). Ipsilateral and contralateral distribution of FG labeled LC neurons and the number of FG-positive neurons along the rostro-caudal axis in both the ipsilateral and contralateral LC were counted manually, and represented as the mean + SEM per representative slice. Additionally, the number of FG positive cells per LC area in each slice was quantified. The LC area per slice was measured using the Fiji Image software (USA).

In addition, we studied the dorsoventral distribution of FG labelled neurons in the central ipsilateral and contralateral LC (-9.72 to -9.96 mm from Bregma, 3 slices per animal). The half height with respect to DBH expression was established as the dorso-ventral criteria and it was represented as the proportion relative to the total number of FG-labelled neurons.

c-Fos expression in LC

The activation of ipsilateral and contralateral LC along of neuropathy (ST and LT) was evaluated by c-Fos expression. Additionally, the colocalization of c-Fos and FG expression was assessed in ipsilateral and contralateral LC projections to the SC or rACC. On the other hand, AAV-Gi-mCherry-mediated inhibition of LC neurons projecting to rACC was also evaluated. The rats were perfused and ipsilateral and contralateral sequential central LC sections (-9.72 to -9.96 from Bregma, 3 slices of 30 µm per animal) were incubated for 48 hours at 4 ºC with a rabbit anti-c-fos antiserum (1:1,000, Synaptic System, Germany) and a mouse anti-DBH antibody (1:1,000, Merck Chemicals & Life Science S.A., Spain). The antibodies were then visualized with a biotinylated donkey anti-rabbit IgG (1:200, Jackson ImmunoResearch Europe, UK) followed by Alexa Fluor 488 streptavidin (1:1,000, Invitrogen™, USA) or a donkey anti-mouse Alexa Fluor 568 (1:1,000, Invitrogen™, USA). After washing and mounting in fluoro-gel aqueous medium, images were acquired on a fluorescent Olympus BX40 microscope equipped with an Olympus DP73 camera (Spain). The number of c-Fos labelled neurons in the ipsilateral and contralateral central LC were counted manually, and represented as the mean + SEM per LC slice. The number of c-Fos and FG labelled neurons in the ipsilateral and contralateral central LC were also counted manually by overlapping c-Fos and FG expression using Fiji Image software (USA), represented as the proportion of the total number of c-Fos labelled neurons. In both quantifications, the dorso-ventral distribution was also studied in the central LC (-9.72 to -9.96 from Bregma, 3 slices per animal) of the ipsilateral and contralateral LC. The half height relative to the DBH expression was established as a dorso-ventral criteria and represented as the proportion relative to the total number of c-Fos labelled neurons or c-Fos/FG-labelled neurons, respectively.

DBH expression in the SC

To evaluate the DBH fibres in the SC dorsal horn (L4-L6), sections (3-4 animals per group) were incubated for 2 nights at 4 ºC with a mouse anti-DBH antibody (1:1000, Merck Chemicals & Life Science S.A., Spain). Subsequently, the sections were incubated with biotinylated donkey anti-mouse antibody (1:200, Jackson ImmunoResearch Europe, UK), which were visualized with an ultra-sensitive ABC peroxidase staining kit (1:1,000, Thermo Scientific, Spain) and 3,3'-diaminobenzidine tetrahydrochloride (DAB) (Llorca-Torralba *et al.*, 2019). The sections were mounted on slides, cleared in xylene and coverslipped with DPX, and the images were acquired at the same exposure and illumination settings on an Olympus BX40 microscope equipped with an Olympus DP73 camera. The optical density of DBH expression was calculated in the grey matter of the SC dorsal horn with the Fiji Image software (USA), defining 5 regions of interest of the same size per section and applying the mean intensity, subtracting the background noise from each section (3 sequential sections of 40 µm from each ipsilateral and contralateral side from L4-L6).

Western blotting

Sham and CCI-LT animal were killed by decapitation and the ipsilateral and contralateral LC was removed (Llorca-Torralba *et al.*, 2019). Equal amounts of protein from tissue homogenates were separated by SDS-PAGE (sodium dodecyl sulfate-polyacrylamide gel electrophoresis) and transferred to polyvinylidene difluoride membranes (PVDF). The membranes were probed overnight at 4 °C with primary antibodies against pCREB (1:1000; Millipore, Spain), CREB (1:500; #9197, Cell Signaling, USA), tyrosine hydroxylase (TH, 1:5000; Abcam plc, UK). The primary antibodies were detected using the corresponding secondary antibody (1:10,000, Bonsai Advanced Technologies, Spain): IRDye 800CW goat anti-rabbit (green), IRDye 680LT goat anti-mouse (red). The protein signals were detected using a LI-COR Odyssey® two-channel quantitative fluorescence imaging system (Bonsai Advanced Technologies, Spain). Digital images of Western blots were analyzed by densitometry using the ImageJ free access software (National Institutes of Health, USA), and the protein levels were normalized to the level of β-actin.

Experimental designs

For the chemogenetic modulation of global noradrenergic LC neuron activity, DREADDs, AAV-Gi-mCherry, AAV-Gs-mCherry or AAV-mCherry (control virus) were injected into the LC_{ipsi} or LC_{contra} of TH-Cre rats 21 days before inducing CCI. The behavioral tests were performed on the same experimental groups of CCI-ST, -MT and -LT rats, administering CNO (i.p.) 20 min before performing the behavioral tests. FST test was performed only in the CCI-LT group.

For the chemogenetic modulation of noradrenergic LC projections to the SC (LC→SC pathway), a catheter was inserted (i.t.) 28 days before inducing the CCI. After 7 days of catheter insertion, AAV-Gi-mCherry or AAV-Gs-mCherry was injected into the LC_{ipsi} or LC_{contra} of TH-Cre rats and the behavioral tests were performed on the same experimental CCI-ST, -MT and -LT rats. CNO was administered (i.t.) 20 min before performing the behavioral tests and 7 days after CNO administration, clonidine (i.t.) was administered 30 min before performing the behavioral tests.

For the chemogenetic modulation of noradrenergic LC projections to the rACC (LC→rACC pathway), AAV-Gi-mCherry was injected into the LC of TH:Cre rats 14 days after inducing CCI. After a further 14 days, 28 days after CCI induction, a cannula was implanted bilaterally into the rACC and the behavioral tests were performed on the CCI-LT rats. CNO was administered (i.p.) 20 min before performing the behavioral tests.

For the pharmacological blockade of adrenoreceptors in the rACC, a cannula was implanted bilaterally into the rACC of LE rats 28 days after CCI induction. The behavioral tests were performed on CCI-LT rats, and prazosin, idazoxan or propranolol were administered 30 or 20 min before performing the behavioral tests (see above drug section) or 24, 5 and 1h before the mFST.

Statistical Analysis

All the data are presented as the means ± SEM and the results were all analyzed using STATISTICA 10.0 (StatSoft, USA) or GraphPad Prism 5 software (GraphPad Software, USA). An unpaired Student's T test was used to compare the values between the two groups. Two-way analyses of variance (with/without repeated measures) were followed by Newman-Keuls post hoc tests. In all cases, $p<0.05$ was considered significant.

References

Alba-Delgado C, Cebada-Aleu A, Mico JA, Berrocoso E. Comorbid anxiety-like behavior and locus coeruleus impairment in diabetic peripheral neuropathy: A comparative study with the chronic constriction injury model. Progress in neuro-psychopharmacology & biological psychiatry 2016; 71: 45-56.

Bennett GJ, Xie YK. A peripheral mononeuropathy in rat that produces disorders of pain sensation like those seen in man. Pain 1988; 33(1): 87-107.

Berrocoso E, De Benito MD, Mico JA. Role of serotonin 5-HT1A and opioid receptors in the antiallodynic effect of tramadol in the chronic constriction injury model of neuropathic pain in rats. Psychopharmacology (Berl) 2007; 193(1): 97-105.

Bravo L, Alba-Delgado C, Torres-Sanchez S, Mico JA, Neto FL, Berrocoso E. Social stress exacerbates the aversion to painful experiences in rats exposed to chronic pain: the role of the locus coeruleus. Pain 2013; 154(10): 2014-23.

Llorca-Torralba M, Suarez-Pereira I, Bravo L, Camarena-Delgado C, Garcia-Partida JA, Mico JA*, et al.* Chemogenetic Silencing of the Locus Coeruleus-Basolateral Amygdala Pathway Abolishes Pain-Induced Anxiety and Enhanced Aversive Learning in Rats. Biol Psychiatry 2019; 85(12): 1021-35.

Wei H, Viisanen H, You HJ, Pertovaara A. Spinal histamine in attenuation of mechanical hypersensitivity in the spinal nerve ligation-induced model of experimental neuropathy. Eur J Pharmacol 2016; 772: 1-10.

Supplementary Figures

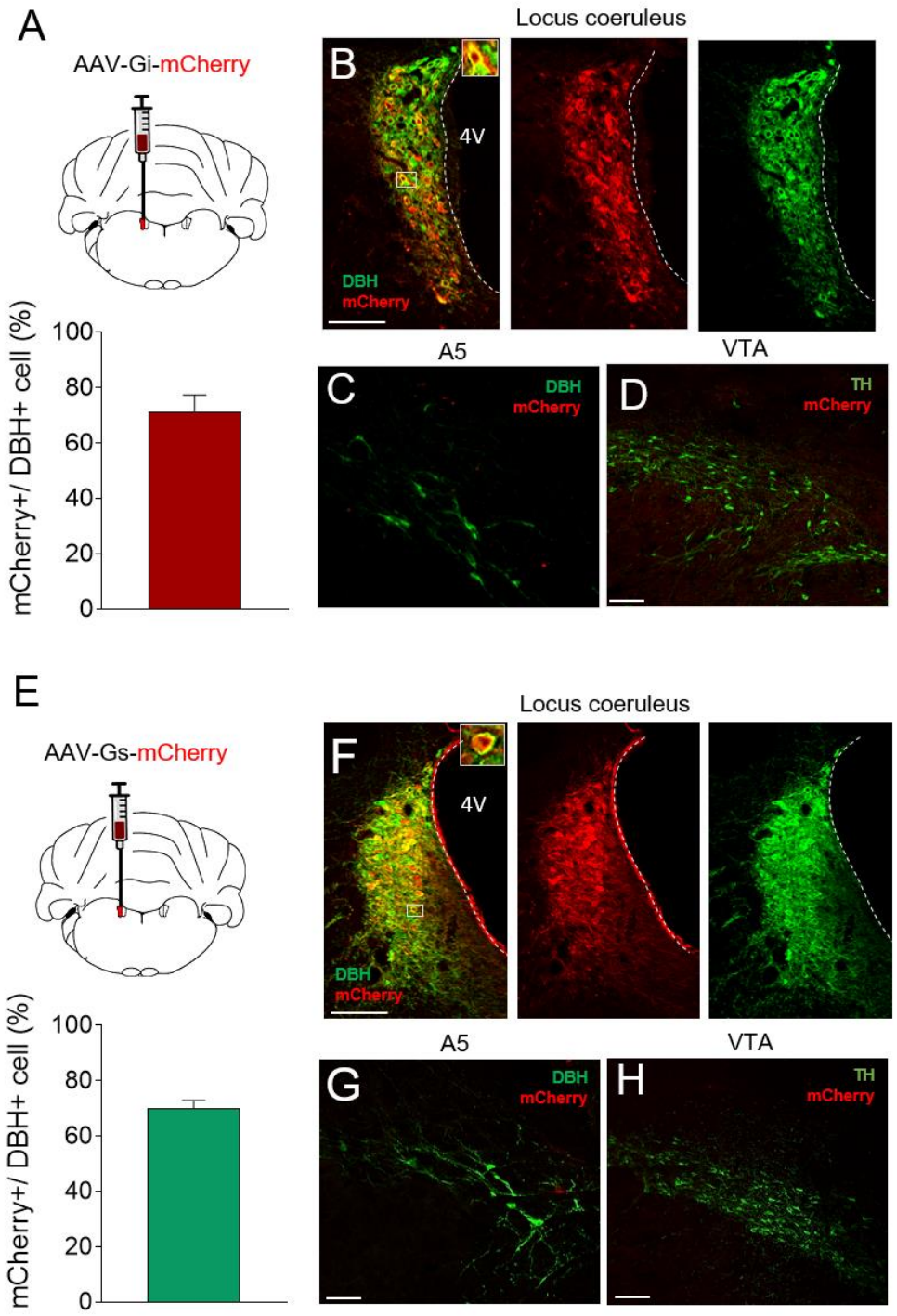

Supplementary Fig. 1. (A) Cartoon of the intra-LC AAV-Gi-mCherry unilateral injection and quantification of mCherry expression in LC-DBH neurons of TH:Cre rats. (B) Representative immunohistochemistry to show the strong mCherry expression in LC-DBH neurons. The magnified image shows an example of merged DBH+mCherry positive neuron (red = mCherry, green = DBH: scale bar =

100 µm). (C) No expression of mCherry was observed in A5 noradrenergic neurons and (D) VTA dopamine neurons (red = mCherry, green = TH: scale bars = 100 µm). (E) Cartoon of the intra-LC AAV-Gs-mCherry unilateral injection and quantification of mCherry expression in LC-DBH neurons. (F) Representative immunohistochemistry shows strong mCherry expression in LC-DBH neurons. The magnified image shows an example of a merged DBH+mCherry positive neuron (red = mCherry, green = DBH: scale bar = 100 µm). (G) No expression of mCherry was observed in A5 noradrenergic neurons or (H) VTA dopamine neurons (red = mCherry, green = TH: scale bars = 100 µm). DBH, dopamine beta-hydroxylase; TH, tyrosine hydroxylase; 4V, fourth ventricle; VTA, ventral tegmental area.

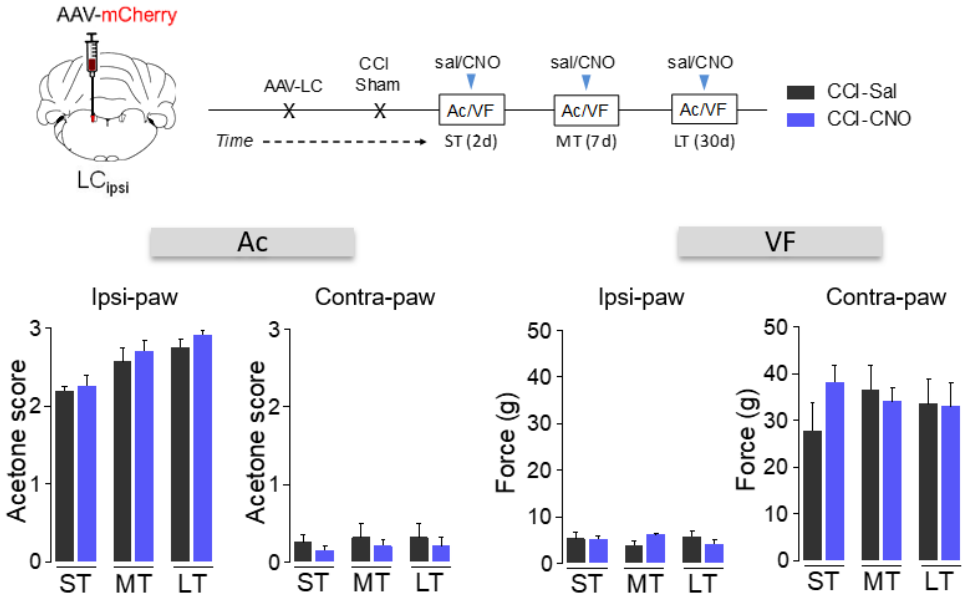

Supplementary Fig. 2. Timeline and scheme of AAV-mCherry (control-DREADD) injection into the ipsilateral LC (LC_{ipsi}) to test that CNO does not elicit changes in the nociceptive tests on TH:Cre rats. Response of the ipsilateral (Ipsi-paw) and contralateral (Contra-paw) hind paw in the acetone and von Frey tests after CNO (1 mg/kg, i.p.) administration to short- (ST), mid- (MT) or long-term (LT) chronic constriction injury (CCI) rats (n= 4-5 animals/group: one-way ANOVA with repeated measures, Newman-Keuls post-hoc test). LC, locus coeruleus; Sal, saline; CNO, clozapine-n-oxide; Ac, acetone test; VF, von Frey test; i.p., intraperitoneal.

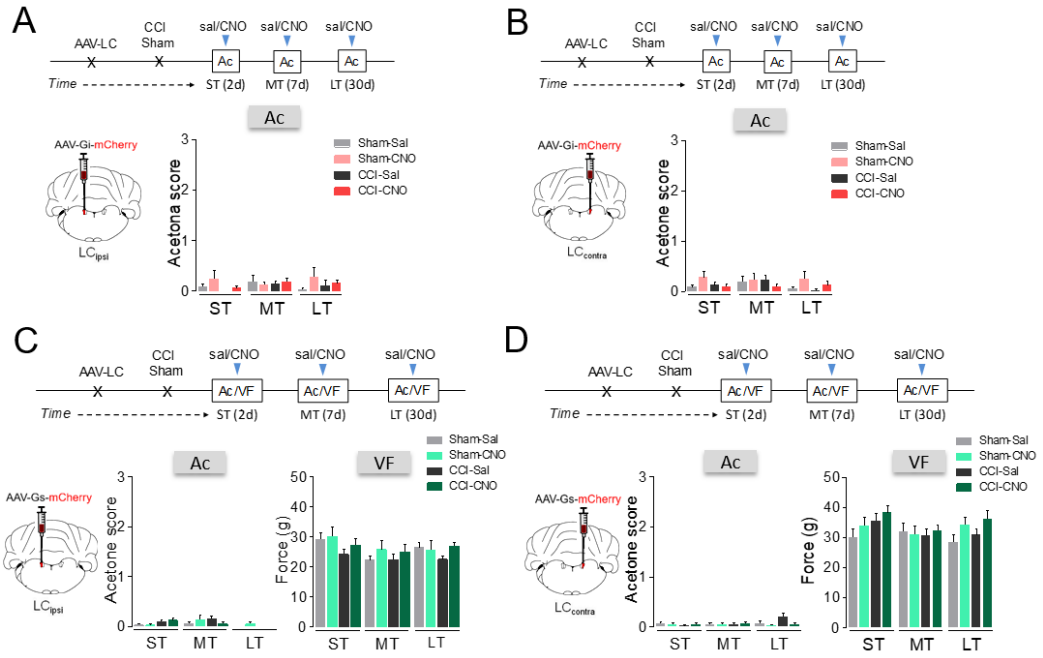

Supplementary Fig. 3. (A) Response of the contralateral paw of CCI-ST, -MT and -LT rats in the acetone test after noradrenergic ipsilateral LC (LCipsi) inhibition with CNO (1 mg/kg, i.p.) administered to TH:Cre rats (n = 8-10 animals/group) (B) Response of the contralateral paw of CCI-ST, -MT and -LT rats in the acetone test after noradrenergic contralateral LC (LCcontra) inhibition by CNO (1 mg/kg, i.p.) (n = 9-10 animals/group). (C) Response of the contralateral paw of CCI-ST, -MT and -LT rats in the acetone and von Frey tests after noradrenergic LCipsi activation by CNO (1 mg/kg, i.p.) (n = 9-10 animals/group). (D) Response of the contralateral paw of CCI-ST, -MT and -LT rats in the acetone and von Frey tests after noradrenergic LCcontra activation by CNO (1 mg/kg, i.p.) (n = 10 animals/group). Two-way ANOVA with repeated measures, Neuman-Keuls post-hoc test. Sal, saline; CNO, Clozapine-n-oxide; LC, locus coeruleus; i.p., intraperitoneal; Ac, acetone test; VF, von Frey test.

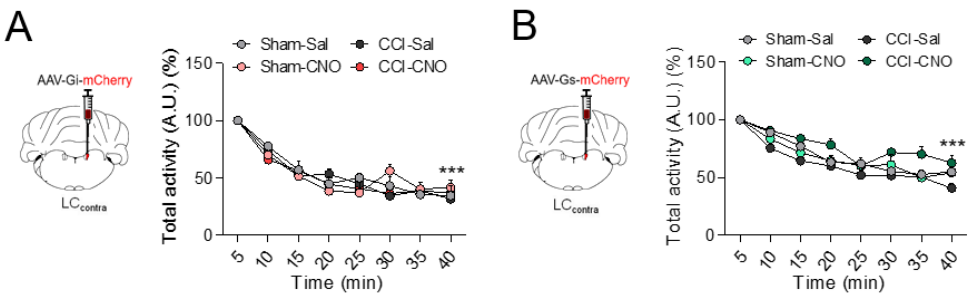

Supplementary Fig. 4. (A) Locomotor activity (arbitrary units, A.U. (%)) after noradrenergic contralateral LC (LCcontra) inhibition with CNO (1 mg/kg, i.p.) in TH:Cre rats (n=4-6 animals/group): *** p<0.001 vs min 5). (B) Locomotor activity (arbitrary units, A.U. (%)) after noradrenergic contralateral LC (LCcontra) activation by CNO (1 mg/kg, i.p.) in TH:Cre rats (n=5-6 animals/group: *** p<0.001 vs min 5). Two-way ANOVA with repeated measures, Newman-Keuls post-hoc test. Sal, saline; CNO, Clozapine-n-oxide; LC, locus coeruleus; i.p., intraperitoneal.

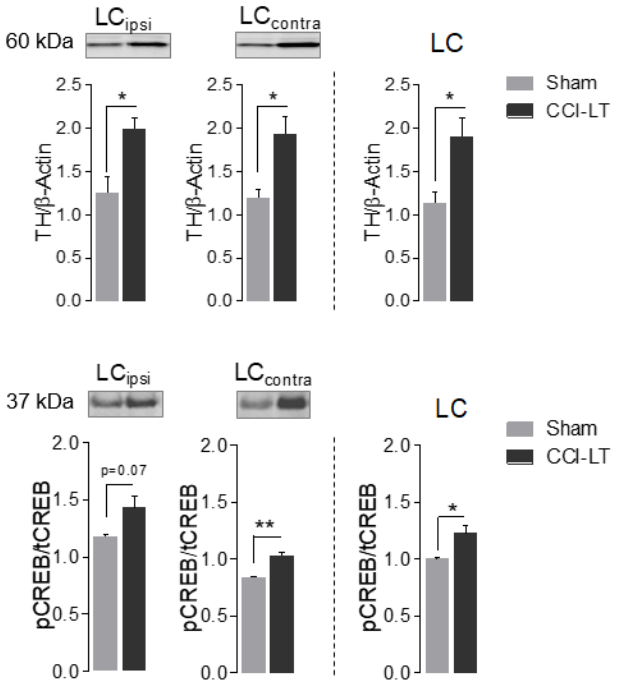

Supplementary Fig. 5. Representative blot and quantification of tyrosine hydroxylase (TH) and pCREB/tCREB in the ipsilateral (LC_{ipsi}) or contralateral (LC_{contra}) locus coeruleus (LC), and of the average of both in sham and long-term chronic constriction injury (CCI-LT) wild-type rats (n= 3 animals/group: *p<0.05, **p<0.01 vs Sham, Student´s t-test).

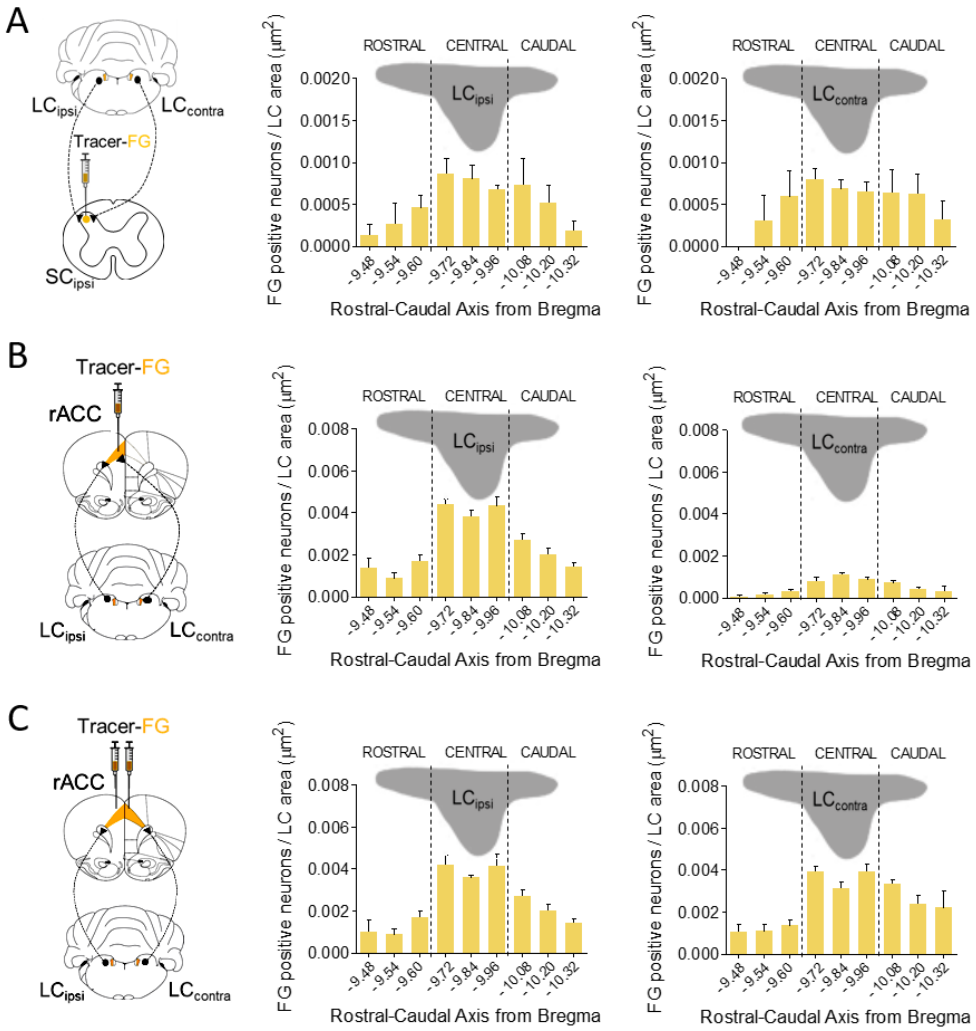

Supplementary Fig. 6. (A-C) Retrograde FG tracer strategy and representative image to target LC neurons that project to the ipsilateral SC, ipsilateral rACC or bilateral rACC in wild-type rats. Ipsilateral and contralateral distribution of FG labeled LC neurons and FG positive neurons along the rostral-caudal axis of the ipsilateral (LCipsi) and contralateral (LCcontra) LC relative to the total LC area (mean + SEM of the number of neurons per slice per LC area, n = 4 animals: Student´s t-test and one-way ANOVA, Newman-Keuls post-hoc test).

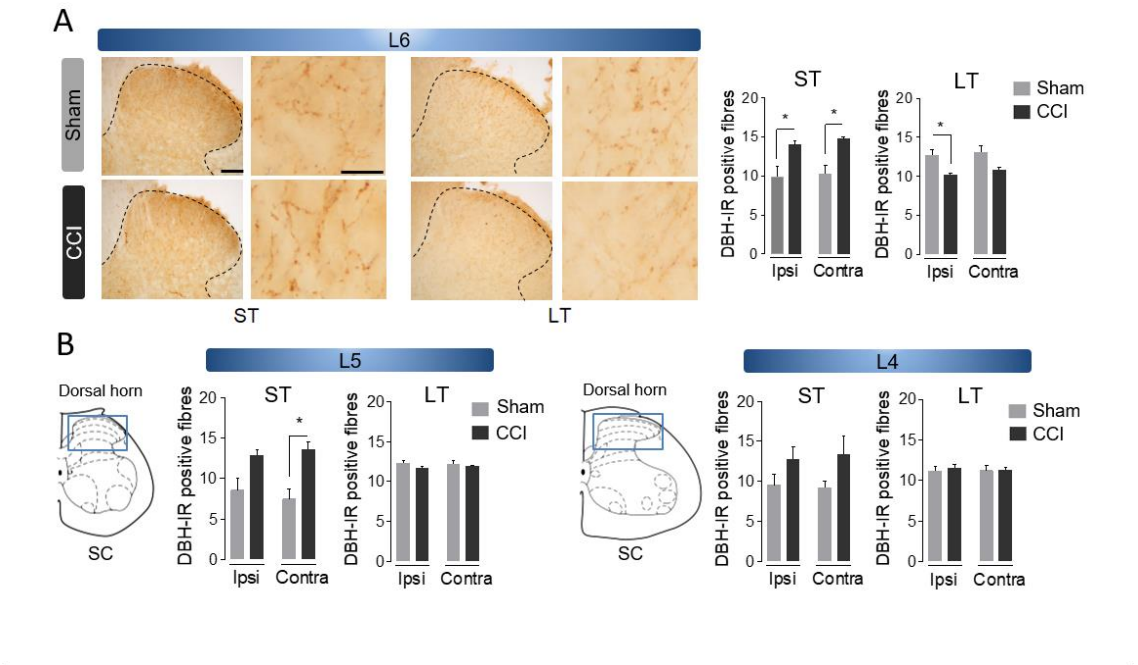

Supplementary Fig. 7. (A) Representative immunohistochemistry of DBH positive fibres in the ipsilateral dorsal horn (L6) of Sham-ST, Sham-LT, CCI-ST and CCI-LT wild-type rats (scale bar = 100 µm). DBH labeled fibers are shown in the inset for each group (scale bar = 25 µm). Quantification of the DBH positive fibers of the ipsilateral (Ipsi) and contralateral (Contra) L6 of Sham-ST, Sham-LT, CCI-ST and CCI-LT rats (n = 3-4 animals/group): *p<0.05 vs Sham, Student´s t-test. (B) Cartoon of the spinal cord (SC) at the L5 and L4 dorsal horn level (Paxinos and Watson, 1997). Quantification of the DBH positive fibers of the ipsilateral and contralateral L5 and L4 of ST- and LT-Sham and ST- and LT-CCI wild-type rats (n= 3-4 animals/group: *p<0.05 vs Sham, Student´s t-test). CCI, chronic constriction injury; ST, Short-term; LT, Log-term; DBH, dopamine beta-hydroxylase; IR, immunoreactivity.

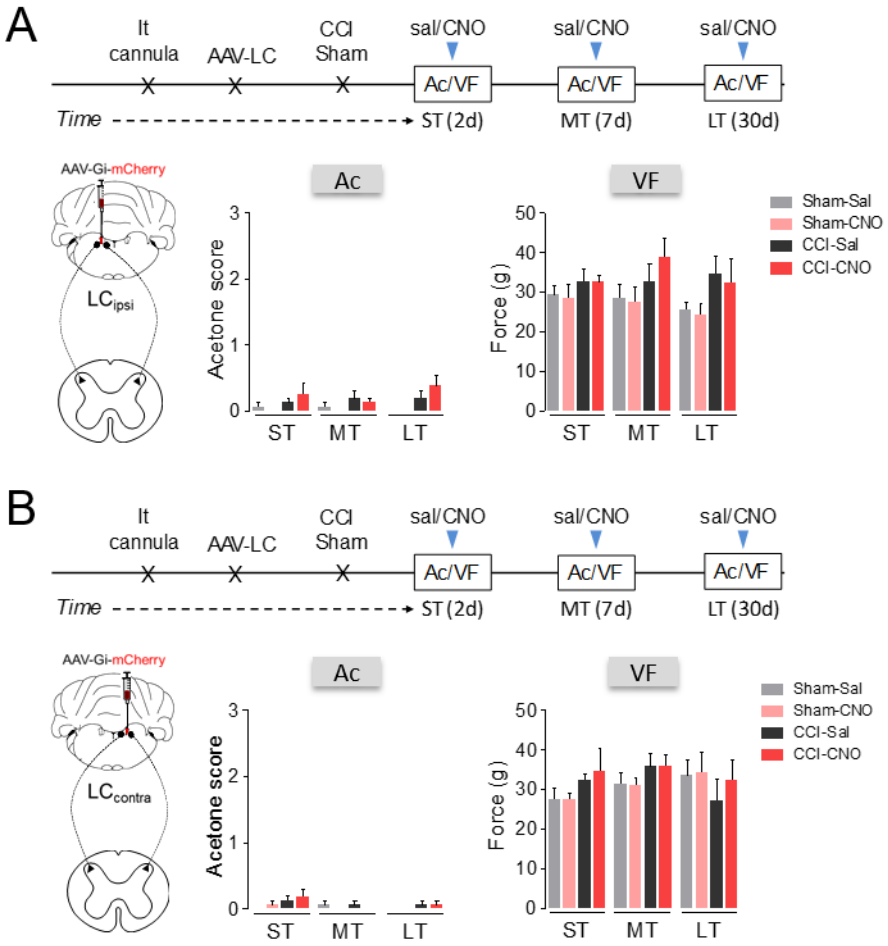

Supplementary Fig. 8. (A-B) Timeline and cartoon of noradrenergic LCipsi→SC or LCcontra→SC pathway inhibition via the AAV-Gi-mCherry strategy in TH:Cre rats. Response of the contralateral paw in the acetone and von Frey tests after CNO (3 µM, i.t) administration to rats short-term (ST), mid-term (MT) and long-term (LT) after CCI (n = 4 animals/group: two-way ANOVA with repeated measures, Newman-Keuls post-hoc test). CCI, chronic constriction injury; LC, locus coeruleus; SC, spinal cord; Sal, saline; CNO, clozapine-n-oxide; i.t., intrathecal; Ac, acetone test; VF, von Frey test.

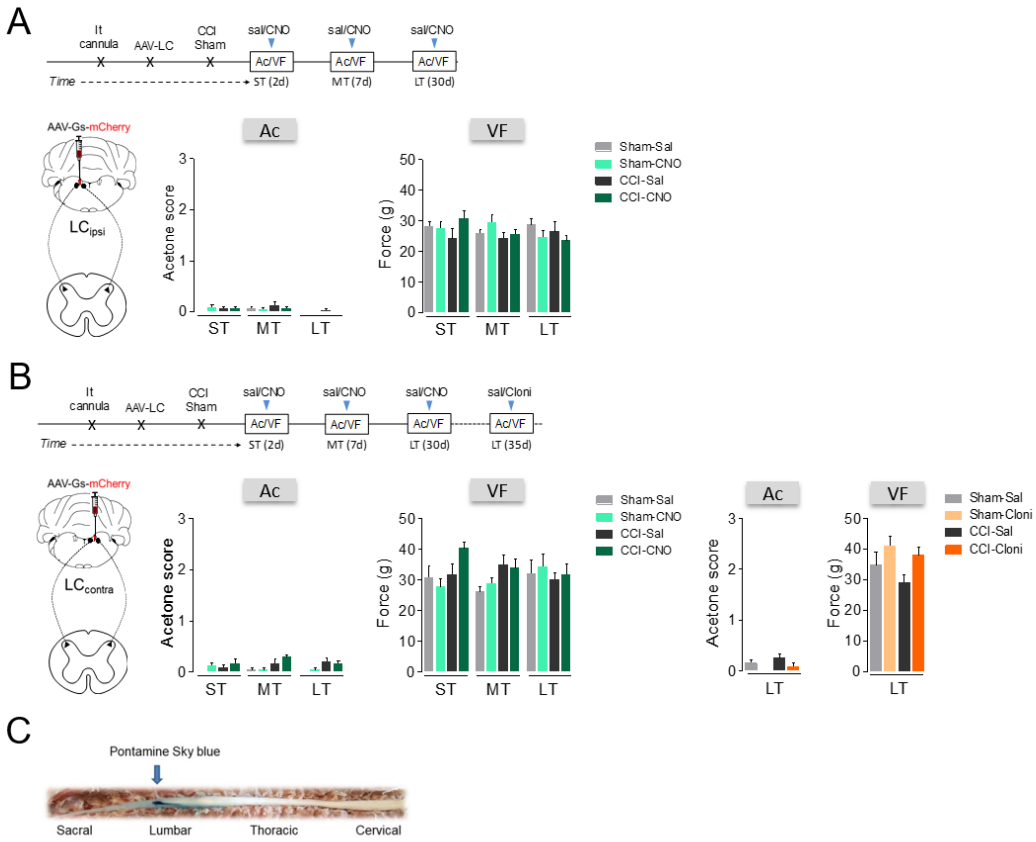

Supplementary Fig. 9. (A-B) Timeline and representative image of the noradrenergic LCipsi→SC or LCcontra→SC pathway activation employing the AAV-Gs-mCherry strategy in TH:Cre rats. (A) Response of the contralateral paw in the acetone and von Frey tests after CNO (3 μM, i.t) administration to short-term (ST), mid-term (MT) and long-term (LT) after CCI rats (n= 6-8 animals/group). (B) Response of the contralateral paw of CCI-ST, -MT and -LT rats in the acetone and von Frey tests after CNO (3 μM, i.t) administration (n= 6 animals/group). In addition, the response of the contralateral paw of CCI-LT rats was evaluated in the acetone and von Frey tests after clonidine (20 μg, i.t) administration (n= 5-6 animals/group: two-way ANOVA with or without repeated measures, Newman-Keuls post-hoc test). (C) Representative image of the intrathecal injection of Pontamine Sky Blue solution. CCI, chronic constriction injury; LC, locus coeruleus; SC, spinal cord; Sal, saline; CNO, clozapine-n-oxide; Cloni, clonidine; i.t., intrathecal; Ac, acetone test; VF, von Frey test; Ipsi, ipsilateral; contra, contralateral.

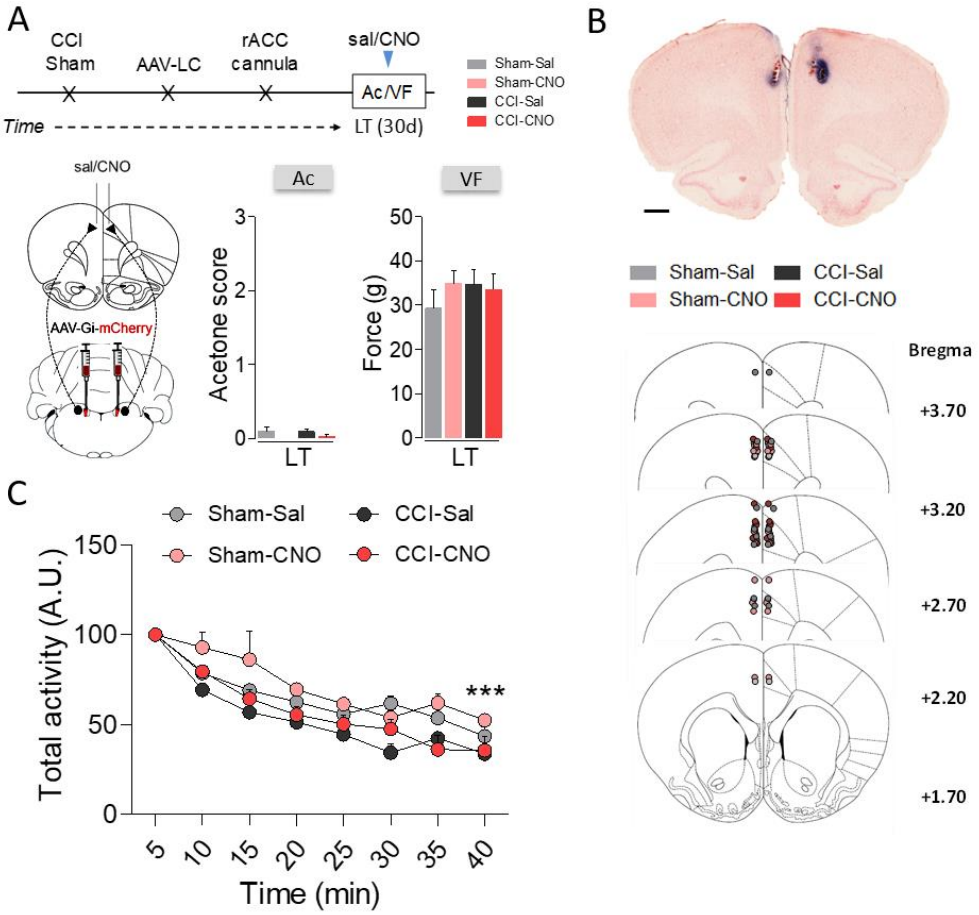

Supplementary Fig. 10. (A) Timeline and cartoon of bilateral AAV-Gi-mCherry injection into the LC and intra-rACC CNO (3 μM) administration to inhibit the noradrenergic LC→rACC pathway of TH:Cre rats. Response of the contralateral hindpaw of CCI-LT rats in the acetone and von Frey tests (n= 8-10 animals/group: Two-way ANOVA, Newman-Keuls post-hoc test). (B) Photomicrograph of a coronal section (neutral red stain) from a TH:Cre rat brainstem showing the spread of Pontamine Sky Blue solution after its administration into the rACC (scale bar = 1 mm). Diagrams adapted from the Paxinos and Watson atlas (Paxinos and Watson, 2007) showing the sites of CNO microinjection in the rACC. (C) Effect of CNO administration on locomotor activity (arbitrary units, A.U. (%), n=3-6 animals/group: ***p<0.001 vs min 5, two-way ANOVA with repeated measures, Newman-Keuls post-hoc test). CCI, chronic constriction injury; LC, locus coeruleus; rACC, rostral anterior cingulate cortex; CNO, clozapine N-oxide; LT, Long-term; Ac, acetone; VF, von frey.

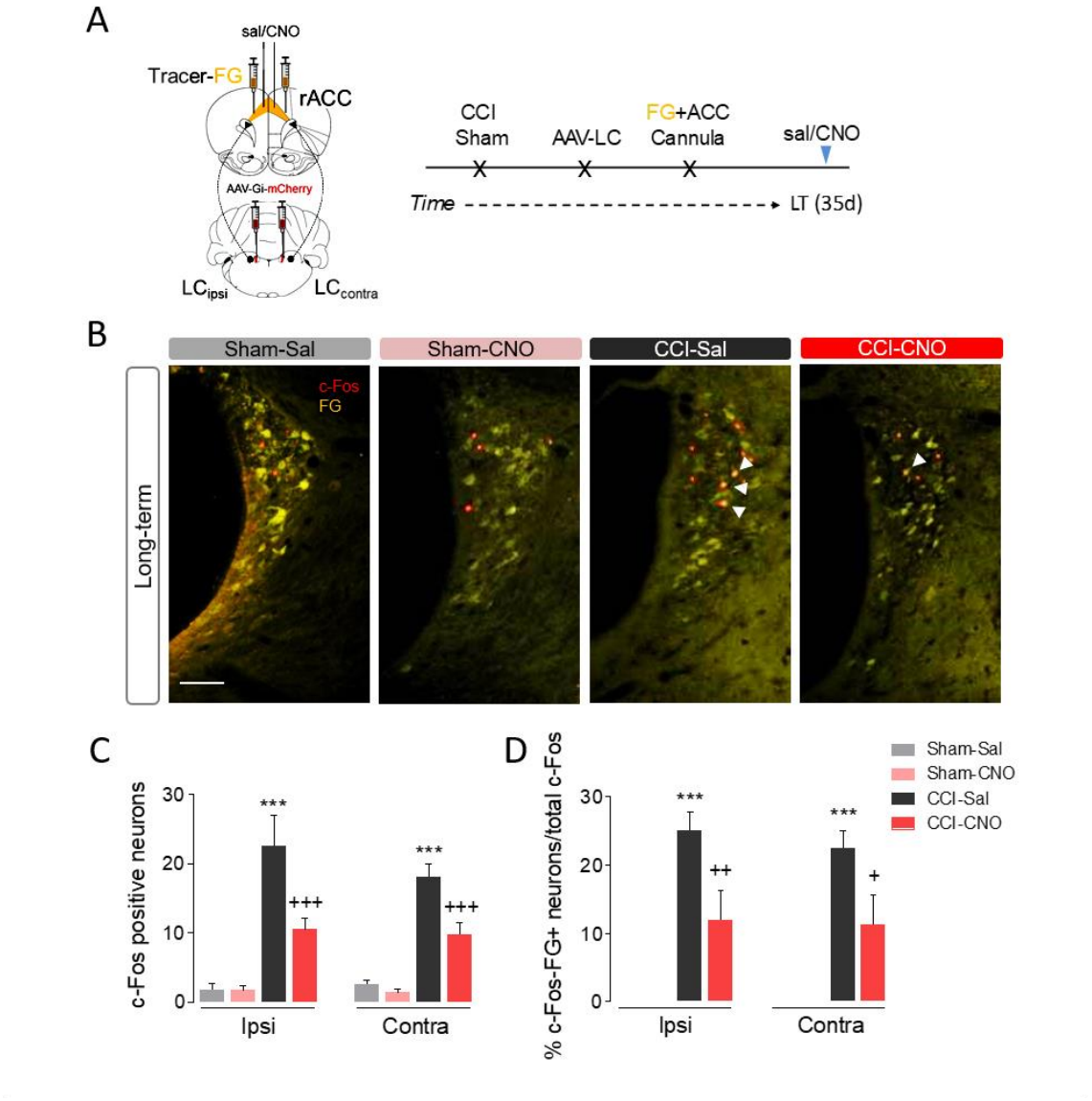

Supplementary Fig. 11. (A) Timeline and cartoon of retrograde FG tracer and AAV-Gi-mCherry bilateral injection to target LC neurons that project to the rACC and intra-rACC CNO administration (3 μM) to inhibit the noradrenergic LC→rACC pathway of TH:Cre rats. (B) Representative immunofluorescence in the central LC showing c-Fos and FG expression (red, c-Fos; yellow, FG) (scale bar: 100 μm). (C) Quantification of c-Fos positive neurons in the central LC_{ipsi} and LC_{contra} of sham and LT-CCI rats after intra-rACC saline or CNO administration. The data are represented as the mean + SEM neurons per slice (n= 2-5 animals/group: ***p<0.001 vs Sham-Sal; +++p<0.001 vs CCI-Sal, two-way ANOVA, Neuman-Keuls post-hoc test). (D) Quantification of c-Fos and FG positive neurons in the central LC_{ipsi} and LC_{contra} of sham and LT-CCI rats after intra-rACC saline or CNO administration. The data represented the % respect to the total c-Fos positive neurons + SEM neurons per slice (n= 2-5 animals/group: ***p<0.001 vs Sham-Sal; +p<0.05, ++p<0.01 vs CCI-Sal, two-way ANOVA, Neuman-Keuls post-hoc test). LC,

locus coeruleus; rACC, rostral anterior cingulate cortex; Sal, saline; CNO, clozapine-n-oxide; Ipsi, ipsilateral; Contra, contralateral; CCI, chronic constriction injury; LT, Long-term.

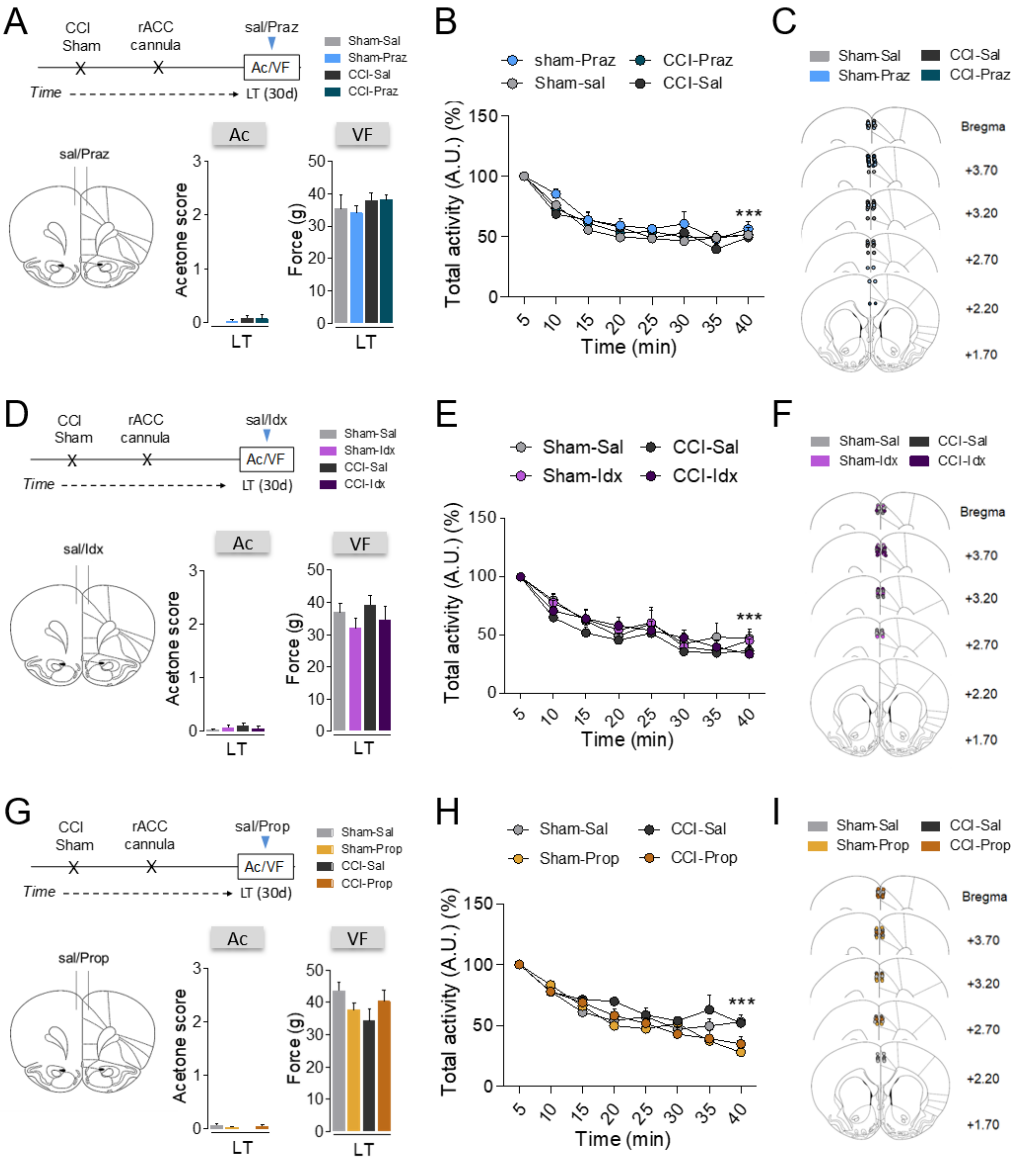

Supplementary Fig. 12. (A) Timeline and cartoon of the pharmacological inhibition of α1-adrenoceptors (prazosin, 5 µg) in the rostral anterior cingulate cortex (rACC) of long-term chronic constriction injury (CCI-LT) wild-type rats. Response of the contralateral paw in the acetone and von Frey tests (n= 8-10 animals/group: two-way ANOVA, Newman-Keuls post-hoc test). (B) Effect of prazosin administration on locomotor activity (arbitrary units, A.U. (%)) (n=3-6 animals/group: ***p<0.001 vs min 5, two-way ANOVA with repeated measures, Newman-Keuls post-hoc test). (C) Diagrams adapted from the Paxinos and Watson atlas (Paxinos and Watson,

2007) showing the sites of prazosin microinjection into the rACC. (D) Timeline and representative image of the pharmacological inhibition of α2-adrenoceptors (idazoxan, 9 μg) in the rACC of LT-CCI wild-type rats. Response of the contralateral paw in the acetone and von Frey tests (n = 6-10 animals/group: two-way ANOVA, Newman-Keuls post-hoc test). (E) Effect of idazoxan administration on locomotor activity (arbitrary units, A.U. (%)) (n=4-6 animals/group: ***p<0.001 vs min 5, two-way ANOVA with repeated measures, Newman-Keuls post-hoc test). (F) Diagrams adapted from the Paxinos and Watson atlas showing the sites of idazoxan microinjection into the rACC. (G) Timeline and representative image of the pharmacological inhibition of β-adrenoceptors (propranolol, 1 μg) in the rACC of CCI-LT wild-type rats. Response of the contralateral paw in the acetone and von Frey tests (n = 7-10 animals/group: two-way ANOVA, Newman-Keuls post-hoc test). (H) Effect of propranolol administration on locomotor activity (arbitrary units, A.U. (%)) (n=7-9 animals/group: ***p<0.001 vs min 5, two-way ANOVA with repeated measures, Newman-Keuls post-hoc test). (I) Diagrams adapted from the Paxinos and Watson atlas showing the sites of propranolol microinjection in the rACC. LC, locus coeruleus; rACC, rostral anterior cingulate cortex; Sal, saline; CNO, Clozapine-N-oxide; Praz, prazosin; Idx, Idazoxan; Prop, propranolol; Ac, acetone test; VF, von Frey test; min, minutes; LT, Long-term.

7. DISCUSION GENERAL

El dolor es un proceso fisiológico al que todos nos hemos enfrentado en alguna ocasión, sin embargo, cuando el dolor se cronifica y se torna patológico empieza a ser un problema de salud grave. Actualmente se conoce que el dolor crónico de tipo neuropático afecta entre el 7-10% de la población general. Es una condición discapacitante y también resulta un problema a la hora de establecer un tratamiento analgésico óptimo (Bouhassira y cols., 2008; Finnerup y cols., 2015). A menudo, el dolor crónico actúa como agente precipitante para padecer patologías mentales como la ansiedad y/o depresión (McWilliams y cols., 2003), ya que existen correlatos neurofisológicos comunes para estas patologías (Chopra y Arora, 2014; Sheng y cols., 2017; Humo y cols., 2019; Chandler y cols., 2019). La coexistencia de ambos trastornos en un mismo paciente provoca una dificultad en la prevención y tratamiento. Esto, a su vez, implica que sea de vital importancia estudiar los mecanismos neurobiológicos subyacentes a ambas patologías.

Actualmente, existen modelos animales de dolor crónico fiables y válidos, ya que mimetizan la sintomatología observada en clínica, que nos dotan de una herramienta para estudiar esta comorbilidad desde una perspectiva básica a nivel conductual y molecular (Bravo y cols., 2020; Leite-Almeida y cols., 2015) y utilizando técnicas cada vez más avanzadas y potentes. Estudios previos realizados en nuestro laboratorio han demostrado que el modelo de dolor de tipo neuropático (constricción crónica del nervio ciático, CCI) utilizado en los estudios que componen esta tesis doctoral, muestra una conducta dolorosa evidente a los 2 días después del CCI y permanece estable al menos 28 días después de la cirugía. Además, se demostrado que la conducta ansiosa y depresiva inducida por el dolor crónico aparece de manera dependiente del tiempo de la neuropatía. Existe un aumento de la conducta de inmovilidad en el test de natación forzada (FST), una disminución de tiempo de permanencia en el área abierta con estimulación nociceptiva en la pata dañada en el test de evitación de lugar/escape y una disminución de % de tiempo en el área abierta en test del laberinto elevado circular (EZM) en animales CCI-28 respecto a los otros puntos temporales (CCI-7d y CCI-14d) (Alba-Delgado y cols., 2013). Numerosos estudios preclínicos señalan al LC como una de las estructuras cerebrales claves en la modulación del dolor, así como en la aparición de los trastornos ansio-depresivos asociados (Alba-Delgado y cols., 2013; Bravo y cols., 2016; Hirschberg y cols., 2017; Taylor y Westlund, 2017; Llorca- Torralba y cols., 2019).

El objetivo principal de esta tesis doctoral ha sido estudiar la implicación de diferentes vías noradrenérgicas del LC en la sintomatología sensorial y/o afectiva en el modelo de dolor neuropático de CCI a lo largo del tiempo. Para abordar los diferentes objetivos específicos

planteados se han utilizado técnicas farmacológicas y farmacogenéticas, que han permitido modular la actividad del LC y sus proyecciones, así como evaluar la implicación de receptores adrenérgicos en dicho modelo de dolor.

En primer lugar, hemos evaluado la participación del LC_{ipsi} y LC_{contra} en los aspectos sensoriales a lo largo de la neuropatía. Los resultados obtenidos indican que la inactivación global del LC_{ipsi} después de administrar lidocaína o mediante el uso de quimiogenética produce un aumento de la sensibilidad al dolor de la pata ipsilateral 2 días después de la lesión, pero no más tarde (7d o 30d después de la lesión). Estos resultados están de acuerdo con lo previamente demostrado. Ya que la microinyección de lidocaína en el LC_{ipsi} 3 semanas después de la inducción de la lesión nerviosa no afecta a la hipersensibilidad en la pata lesionada de ratas con lesión nerviosa (Song y cols., 2013). Sin embargo, el bloqueo farmacológico de la actividad del LC_{contra} produjo un efecto analgésico en los días 7 y 28 días después de la inducción de la neuropatía en ratas Sprague-Dawley que, por el contrario, no se observó mediante la inhibición quimiogenética en la cepa Long-Evans TH-Cre.

Estos resultados muestran una diferencia entre cepas que pueden ser debidas a las diferencias en la especificidad de las técnicas utilizadas. En este sentido, la administración de lidocaína en el LC bloquea los canales de sodio produciendo la inactivación de neuronas noradrenérgicas y no noradrenérgicas. Sin embargo, mediante la tecnología DREADD se inhiben de manera específica solo las neuronas noradrenérgicas del LC. Por este motivo, se bloqueó la actividad del LC_{contra} mediante la administración de lidocaína en ambas cepas, y se demostró que en el caso de las ratas Long-Evans TH-Cre no se produce la analgesia observada en la cepa Sprague-Dawley (LC_{contra}, 7d o 30d después de la lesión). Por tanto, de estos resultados se puede extraer de manera general que el LC_{ipsi} está implicado en la analgesia solo a corto plazo y el LC_{contra} tiene una función "pro-dolor" a largo plazo que es dependiente de la cepa.

En estudios previos se ha demostrado el papel clave de la vía descendente noradrenergica hacia la SC en la modulación del dolor (Pertovaara, 2006; Hughes y cols., 2015). Así, en la presente tesis doctoral hemos evaluado específicamente, mediante la técnica DREADD, el papel de la vía noradrenérgica LC-SC en la conducta sensorial durante los diferentes puntos temporales de la neuropatía en ratas Long Evans TH-Cre. Los resultaros mostraron que la inhibición

quimiogenética de la vía LC_{ipsi}-SC produjo un aumento en la conducta nociceptiva en animales con CCI a corto plazo (2 días), tal y como observamos en el estudio de la inhibición global del LC. Sin embargo, no se encontraron cambios en la respuesta al dolor en los puntos temporales de medio o largo plazo de la neuropatía, demostrando el agotamiento funcional de la vía descendente LC_{ipsi}-SC. Estos resultados fueron apoyados por estudios de inmunohistoquímica en el que se mostraba un aumento de los niveles de c-Fos en las neuronas del LC_{ipsi} que proyectan hacía SC en ratas CCI a corto plazo. Además, a nivel anatómico se reportó una expresión de fibras DBH mayor en animales CCI a corto plazo (2 días) que en animales CCI a largo plazo (30 días). Estos hallazgos se han observado en trabajos previos en diferentes modelos de dolor y diferentes cepas de roedores. Uno de estos trabajos indica que existe un aumento de los niveles de DBH en la SC 10 días después de realizar una ligadura del nervio espinal en ratas Sprague-Dawley (Hayashida y cols., 2008). A su vez, en un estudio llevado a cabo por Hughes muestra la existencia de un decremento de los niveles de DBH en fibras de SC, 19-21 días después de la transección del nervio tibial en ratas wistar (Hughes y cols., 2013). En cuanto a la inhibición de la vía LC_{contra}-SC en ratas Long Evans TH-Cre, nuestros resultados no mostraron cambios en el umbral sensorial indicando que esta vía no interviene en la modulación del dolor en este punto temporal.

Teniendo en cuenta que estudios previos han mostrado un efecto analgésico después de la estimulación optogenética o quimiogenética del LC (Hirschberg y cols., 2017; Sciolino y cols., 2016), hemos evaluado el efecto de la activación global de las neuronas noradrenérgicas del LC_{ipsi} y LC_{contra} sobre el umbral sensorial en las diferentes fases del dolor neuropático. La activación del LC_{ipsi} provocó un efecto de la neuropatía evaluados. En cambio, la activación del LC_{contra} analgésico en todos los puntos temporales no provocó ningún cambio a nivel sensorial. Después, de manera específica, se procedió a la activación con DREADDs de la vía LC_{ipsi}-SC. De esta manera, se demostró su implicación en el efecto analgésico del dolor, puesto que el efecto analgésico evidenció en todos los puntos temporales de la neuropatía. Además, mediante la administración intratecal de clonidina se obtuvo el mismo resultado analgésico. Por el contrario, la activación de la vía LC_{contra}-SC no modificó la conducta sensorial, pero al administrar clonidina intratecal si se obtuvo efecto analgésico. Estos resultados son de gran relevancia ya que indican que el agotamiento de la vía LC_{ipsi}-SC observado a lo largo de la

neuropatía se recupera mediante la activación exógena y por lo tanto podría ser una posible diana de tratamiento. De acuerdo con estos resultados, existen estudios previos que demuestran que la administración de antagonistas de receptores adrenérgicos α2 a nivel lumbar suprime el desarrollo de la sensibilización de la pata trasera con lesión nerviosa, aunque solo al comienzo de la lesión y no después (Hughes y cols., 2013). Otros trabajos demuestran que la activación de las neuronas de ambos LC que proyectan hacia SC produce analgesia en el modelo de evitación de lesión del nervio sural a largo plazo (desde 4 semanas después de la lesión nerviosa) (Hirschberg y cols., 2017). Los datos descritos hasta el momento demuestran que la vía LC_{ipsi}-SC se activa inmediatamente ante una lesión en el nervio ciático, que provoca el aumento de la liberación de NA en la SC proporcionando analgesia endógena a través de la activación de los receptores adrenergicos α2 espinales. Sin embargo, este efecto parece perderse poco después de la lesión nerviosa, lo que sugiere el agotamiento de este sistema analgésico endógeno debido a que las neuronas del LC ipsi pierden su capacidad para activarse cuando la lesión persiste.

Atendiendo a lo obtenido en esta tesis doctoral y en otros estudios, la analgesia mediada por la SC se puede lograr de forma exógena incluso después de un dolor prolongado utilizando quimiogenética (Hirschberg y cols., 2017). Sin embargo, en nuestro modelo de neuropatía unilateral (CCI) se ha demostrado que este efecto analgésico es específico de la vía LC_{ipsi}-SC y no de la vía LC_{contra}-SC, en la que la activación de esta no provoca ningún cambio en el modelo CCI de DNP. En este caso, debemos tener en cuenta la composición modular del LC, por lo que diferentes proyecciones pueden tener acciones opuestas de forma dependiente del tiempo. Probablemente las acciones inhibidoras del dolor de la NA en la SC puedan ser contrarrestadas e incluso sustituidas por la activación de vías facilitadoras supraespinales hacia el núcleo reticular dorsal (que contribuye al dolor evocado: Martins y cols., 2015), hacia el núcleo espinal trigeminal caudalis (dolor evocado: Kaushal y cols., 2016), o hacia la corteza prefrontal (dolor espontáneo: Hirschberg y cols., 2017). Por este motivo, estudios más específicos podrán dilucidar las acciones del LC de manera global y modular, teniendo en cuenta que se han descrito diferencias en las vías descendentes noradrenérgicas entre cepas (Clark y cols., 1991; Sluka y Westlund, 1992; Bruinstroop y cols., 2012).

Uno de los núcleos que recibe proyecciones del LC es el DRt el cual tiene un rol en la facilitación de la transmisión del dolor (Lima y Almeida 2002, Martins y Tavares 2017). De hecho, se ha demostrado que la estimulación nociceptiva 2 o 3 semanas después de inducir el modelo de dolor SNI, aumenta la liberación de NA en el DRt sugiriendo que la activación del LC participa en la facilitación descendente del dolor neuropático (Martins y cols., 2015; Martins

y cols., 2010). En este sentido e hipotetizando que esta área podría estar contribuyendo en el mantenimiento del dolor en los animales con DNP, nos focalizamos en su estudio desde diferentes perspectivas. En primer lugar, se evaluó el nivel de activación del DRt en las diferentes cepas (Sprague-Dawley y Long Evans) con dolor neuropático. En el caso de los animales Sprague-Dawley se observaron diferencias entre animales sham y CCI a largo plazo en la expresión de pCREB, y en concreto entre el DRt_{ipsi} y DRt_{contra} a la lesión. Los resultados mostraron una mayor expresión de pCREB en el DRt_{contra} en animales CCI a largo plazo sugiriendo una hiperactivación del DRt_{contra} en la cepa Sprague-Dawley. Sorprendentemente, no se observaron estas diferencias en la cepa Long-Evans TH-Cre. Estas diferencias sugerirían diferentes niveles de activación del núcleo DRt entre las cepas Sprague-Dawley y Long Evans y podrían ser debidas al nivel de activación del LC_{contra} de cada cepa. Estos datos son concordantes con los obtenidos a nivel conductual, en los cuales observamos que la inhibición específica de la vía LC_{contra}-SC no produce ningún cambio significativo en el umbral sensorial a largo plazo de la neuropatía. A nivel funcional se demostraron diferencias en la actividad del LC_{contra} entre cepas en la conducta sensorial. Previamente se ha demostrado un aumento de los niveles de pCREB en LC y un aumento en los niveles de NA en DRt en animales con DNP a largo plazo (Martins y cols., 2015). Estos datos sugieren que las proyecciones del LC hacia el DRt podrían esta hiperactivadas en el dolor crónico. Por tanto, en esta tesis doctoral se hipotetiza que esta vía podría estar involucrada en la modulación de la hipersensibilidad producida por el dolor neuropático a largo plazo. Los resultados previos mostraron una activación y un aumento de los niveles de pCREB del LC_{contra} en ratas neuropáticas Sprague-Dawley. Por lo tanto, resultó interesante estudiar la implicación de la vía contralateral LC-DRt en los aspectos sensoriales del dolor en animales con dolor neuropático a largo plazo. Utilizando la tecnología DREADD, se inhibió la vía LC_{contra}-DRt_{contra} y esta inactivación provocó un efecto analgésico robusto en el dolor evocado y en el dolor espontáneo. De esta manera, se evidencia una vía noradrenérgica de facilitación descendente hacia el DRt y la activación de esta podría contribuir a la sensibilización espinal durante el dolor neuropático siendo, además, dependiente de la cepa (Sotgiu y cols., 2008). Adicionalmente, se administró clonidina intratecal y se observó un efecto analgésico similar al que se produjo con la inhibición quimiogenética de la vía LC-DRt. Los efectos noradrenérgicos del LC hacía el DRt parecen mediados por los receptores α1 del DRt, ya que como se ha demostrado con anterioridad que la

administración de prazosin intra-DRt produce un decremento de la hiperalgesia en animales con dolor inflamatorio y en DNP (Martins y cols., 2013, 2015).

La inhibición de la vía LC_{contra}-DRt_{contra} no afectó al umbral sensorial de los animales sham como ocurrió en otros estudios previos (Safari y cols., 2009; Smith y cols., 2002; Llorca-Torralba y cols., 2019). Además, no se observaron cambios en el umbral sensorial de la pata contralateral de los animales con CCI (Brightwell y cols., 2009; Llorca-Torralba y cols., 2019). En otros estudios se ha observado hiperalgesia y alodinia en la pata contralateral de animales con DNP después de administrar yohimbina (Hughes y cols., 2013), pero en comparación con lo obtenido en los estudios de esta tesis, podría estar provocado por la activación de otros núcleos noradrenérgicos (A5 y A7) (Howorth y cols., 2009a). Es importante tener en cuenta que los diferentes modelos animales de DNP producen activaciones en las vías descendentes de manera heterogénea y la utilización de cepas distintas podría explicar también la falta de sensibilización neuropática de la pata contralateral (De Felice y cols., 2011; Bruinstroop y cols., 2012; Clark y cols., 1991; Llorca-Torralba y cols., 2019a; Sluka y Westlund 1992).

Otro de los objetivos de la presente tesis doctoral ha sido evaluar el papel del LC y sus proyecciones en los aspectos ansioso-depresivos del dolor neuropático. Como ya se ha mencionado anteriormente, el dolor crónico se considera un factor de riesgo para sufrir trastornos psiquiátricos, entre ellos destaca la depresión y la ansiedad. En estudios anteriores con modelos animales de dolor crónico se ha demostrado que el dolor a largo plazo induce cambios en el LC como un aumento de la expresión de c-Fos, pCREB, TH y transportador de NA en el LC, además de una mayor expresión y sensibilidad de los receptores adrenérgicos α2, que coincide temporalmente con el inicio del comportamiento ansiodepresivo (Alba-delgado y cols., 2013; Alba-Delgado y cols., 2018; Llorca-Torralba y cols., 2019; Llorca-Torralba y cols., 2019). Sin embargo, aún se desconoce el papel del LC en la conducta depresiva inducida por dolor crónico. Para ello, se evaluó el efecto de la modulación del LC de manera global mediante el uso de farmacología convencional y mediante el uso de quimiogenética sobre la conducta pro-depresiva en animales con dolor neuropático a largo plazo. En primer lugar, observamos que la inhibición del LC_{ipsi} y LC_{contra} mediante la administración de lidocaína revirtió el fenotipo prodepresivo en animales Sprague-Dawley CCI. Estos mismos resultados fueron observados mediante la inhibición quimiogenética en ratas Long-Evans TH:Cre demostrando que el LC se encuentra hiperactivado en animales CCI a largo plazo y es responsable del fenotipo pro-depresivo. Es relevante mencionar que existen diferencias entre cepas con respecto a la aparición de la conducta depresiva, ya que las ratas Sprague-Dawley muestran este fenotipo

depresivo a los 28-30 días, mientras que las ratas Long-Evans lo hacen a los 35 días. Además, estas diferencias entre cepas también coinciden con las diferencias observadas a nivel de expresión de TH y pCREB en los mismos puntos temporales de la neuropatía.

Por otro lado, evaluamos si la activación quimiogenética del LC_{ipsi} y LC_{contra} provocaba cambios en la conducta pro-depresiva. Los resultados mostraron que la activación unilateral de ambos LC provocó un aumento de la conducta pro-depresiva en animales sham pero ningún cambio en los animales CCI. Este hecho, posiblemente sería debido a que la lesión nerviosa a largo plazo produce una activación que no puede verse aumentada por una exposición a estrés agudo durante el test de natación forzada. En otros estudios, han demostrado que la activación optogenética o quimiogenética de las neuronas del LC es ansiogénica en animales sanos (McCall y cols., 2015; Sciolino y cols., 2016).

En base a todos estos resultados, es de gran interés conocer cuáles son las áreas de las proyecciones noradrenérgicas del LC que podrían estar participando en el desarrollo de la sintomatología ansiodepresiva asociada al dolor crónico.

Estudios previos de nuestro laboratorio han demostrado que el dolor neuropático a largo plazo produce una hiperactivación de las proyecciones del LC dirigidas hacia la BLA que son responsables del fenotipo de ansiedad y de provocar respuestas de aprendizaje ante situaciones aversivas en pruebas de evitación pasiva y de condicionamiento al miedo (Llorca-Torralba y cols., 2019). En estos estudios se observó que la inhibición quimiogenética de la vía LC-BLA suprimió la ansiedad inducida por dolor neuropático y mejoró también el aprendizaje aversivo y este efecto está mediado por los receptores β (1 y 2) adrenérgicos. En cambio, la activación de esta misma vía provocó en animales sham una conducta ansiosa y mejoró el aprendizaje aversivo y de memoria. Sin embargo, afectó poco a los animales con neuropatía a corto y largo plazo. Por otro lado, está vía no parece estar involucrada en los aspectos sensoriales del dolor ni en la memoria episódica (Llorca-Torralba y cols., 2019). Nuestros resultados son complementarios y en la misma línea que estudios anteriores donde demuestran que la estimulación optogenética de la vía noradrenérgica LC-BLA provoca un aumento de la liberación de NE en BLA. En consecuencia, la activación de esta vía, provoca un aumento de la conducta pro-ansiosa y de aversión a través de los receptores β-adrenérgicos de la BLA (McCall y cols., 2017).

En la presente tesis doctoral hemos planteado estudiar otras vías noradrenérgicas que podrían estar involucradas en la conducta afectiva inducida por dolor crónico. En base a los resultados

previamente descritos resulta interesante explorar el papel de la vía LC_{contra}-DRt_{contra} en la conducta pro-depresiva inducida por dolor crónico. Para ello, se inhibió de manera selectiva la vía LC_{contra}- DRt_{contra} en animales Sprague-Dawley mediante el uso de DREADDs y se evaluó el fenotipo depresivo. Los resultados mostraron una conducta pro-depresiva solo en animales sham sugiriendo que la actividad de esta vía es relevante ante el afrontamiento de situaciones de estrés agudo y más concretamente para desencadenar reacciones de alerta que generan una reacción protectora/defensiva al estrés (Barik y cols., 2018). No obstante, la conducta depresiva observada en los animales CCI no se vio modificada sugiriendo que la vía LC_{contra}-DRt_{contra} solo tiene un papel relevante a nivel sensorial en animales con dolor crónico.

Otras de las áreas de proyección noradrenérgica con gran relevancia en las dimensiones afectivas y emocionales relacionadas con el dolor es la CCA (Shackman y cols., 2011; Sellmeijer y cols., 2018). Animales con conducta pro-depresiva inducida por dolor crónico, mostraron un aumento de los niveles de c-Fos en CCA. Lo que indicaría una hiperactividad de esta área durante la cronificación del dolor y la aparición de sintomatología afectiva asociada (Barthas y cols., 2017). Por lo tanto, en esta tesis doctoral se han estudiado el papel de las proyecciones noradrenérgicas del LC hacía la CCAr en la conducta pro-depresiva inducida por dolor crónico. En primer lugar, se observó un aumento de los niveles de c-Fos en ambos LC de las neuronas que proyectan hacia la CCAr (bilateral) en animales con DNP a largo plazo sugiriendo una hiperactivación. Para demostrar esa hipótesis, se inhibió la vía LC-CCAr mediante tecnología DREADD y provocó una reducción de la conducta pro-depresiva. Sin embargo, esta vía no está involucrada en los aspectos sensoriales del dolor (dolor evocado). Estos resultados demuestran que el dolor neuropático a largo plazo produce una sobreactivación de la vía LC-CCAr involucrada en el fenotipo depresivo asociado al dolor crónico. Estos resultados son apoyados por otro estudio que demuestra que la CCAr está hiperactiva en animales con DNP a largo plazo y es la responsable de las conductas ansio-depresivas inducidas por dolor crónico (Barthas y cols., 2015).

En base a estos resultados, fue interesante evaluar la implicación de los receptores adrenérgicos de la CCAr en la conducta sensorial y afectiva del dolor mediante el uso de agonistas y antagonistas de los receptores α1 y 2 y β1 y 2. La administración intra-CCAr de prazosin (agonista de los receptores α1 adrenérgicos) o de idazoxan (antagonista de los receptores α2 adrenérgicos) no produjeron cambios en la respuesta al dolor evocado, pero si revirtieron el fenotipo depresivo en animales CCI a largo plazo. En cambio, la administración de propranolol

intra CCAr (antagonista de los receptores β1 y 2) no produjo ningún cambio en la conducta nociceptiva o fenotipo depresivo. Por tanto, demostramos que la neuropatía a largo plazo provoca una hiperactivación de la CCAr a través de señales noradrenérgicas y al parecer está mediada por receptores α1 y 2 noradernérgicos de la CCAr. Es importante destacar los resultados observados en la conducta depresiva con los antagonistas α1 y α2 ya que ambos revierten el fenotipo depresivo en animales con dolor neuropático. Estudios electrofisiológicos llevados a cabo en la corteza prefrontal medial indicaron que las respuestas persistentes a la NA están mediadas principalmente por la sinergia entre la facilitación de la liberación de glutamato a través de los receptores adrenérgicos α1 presinápticos y la inhibición mediada por los receptores adrenérgicos α2 postsinápticos de canales catiónicos que se despolarizan a través de la unión de nucleótidos (Zhang y cols., 2013). Estos datos podrían dar explicación a los resultados obtenidos sugiriendo que el bloqueo farmacológico específico de los adrenorreceptores α1 y α2 de la CCAr podrían ser necesarios para controlar este comportamiento depresivo. Por otro lado, sería particularmente interesante determinar si el bloqueo de los receptores β-adrenérgicos, que ha demostrado tener un efecto ansiolítico en BLA (Llorca-Torralba y cols., 2019), también tiene un efecto beneficioso similar en ACC. Estudios anteriores han demostrado en ratas Sprague-Dawley que la CCAr modula la sintomatología depresiva pero no la ansiosa (Bissiere y cols., 2006). Estudios más recientes han demostrado que la activación quimiogenética de la LC-PFC en animales con dolor neuropático (sin ansiedad) aumenta el comportamiento ansiogénico (Zerbi y cols., 2019). Sin embargo, se desconoce el mecanismo fisiológico por el que se produce y en este sentido, sería interesante evaluar la implicación en esta área de los receptores β-adrenérgicos en tareas ansiogénicas.

De manera general, en los estudios que forman esta tesis doctoral se demuestra que el dolor provoca plasticidad cerebral y además potencia la comunicación entre áreas cerebrales, provocando la activación de circuitos específicos, al mismo tiempo que se silencian otras vías y núcleos. Entre estas áreas, se destaca el LC debido a su situación estratégica entre la SC y áreas supraespinales. En este sentido, la activación endógena del LC es asimétrica después de una lesión y dependiente del tiempo en el desarrollo y mantenimiento de la neuropatía. Específicamente, la lesión nerviosa induce activación endógena de las neuronas noradrenérgicas del LC_{ipsi}, esto amortigua el fenotipo de dolor neuropático durante un periodo breve de tiempo después de la lesión. Por el contrario, el LC_{contra} desencadena de manera contundente hipersensibilidad sensorial en animales con DNP a largo plazo y en la que parece estar involucrada la vía contralateral LC-DRt en ratas Sprague-Dawley. Sin embargo, la activación mediante DREADDs de la proyección ipsilateral del LC hacia la SC produce un alivio del

dolor. Produciendo un efecto similar al que se consigue con el agonismo de los receptores α2 de la SC mediante la administración intratecal de clonidina. Más tarde, cuando se cronifica el dolor se produce una hiperactivación de ambos LC (Ipsi y contra) que tiene como consecuencia la aparición de sintomatología depresiva, ansiosa y cognitiva inducida por el dolor crónico. En las que toman importancia las vías noradrenérgicas; LC-CCAr, como vía implicada en la aparición de la sintomatología depresiva y la vía LC-BLA, vía que provoca la sintomatología ansiosa y cognitiva.

Apuntando a que el LC es una fuente de inhibición del dolor, pero a su vez, y de manera contraproducente también contribuye al mantenimiento del dolor. Además, provoca su cronificación y como consecuencia provoca la aparición de trastornos afectivos y deterioro cognitivo. Además, apoya la eficacia limitada de los fármacos sistémicos que aumentan la disponibilidad global de NA, como podría darse ante la administración de antidepresivos y los antidepresivos noradrenérgicos más potentes (reboxetina y desipramina) (Attal 2019; Bravo y cols., 2019; Kremer y cols., 2016). Es por este motivo, que un enfoque más específico pueda aumentar la disponibilidad de NA intratecal (en la SC) y podría proporcionar una analgesia más robusta, evitando así la activación colateral de otras áreas que provocarían un aumento de la hipersensibilidad sensorial además de inducir un fenotipo ansiodepresivo. Entre estas áreas hemos demostrado que se encuentran DRt, la corteza prefrontal y la amígdala basolateral. Así mismo, se ha demostrado que la esfera sensorial y emocional del dolor están regulados de manera independiente. Por lo tanto, es probable que los mecanismos subyacentes a la comorbilidad del dolor crónico y los trastornos del estado de ánimo estén relacionados con alteraciones complejas en las redes cerebrales más que con cambios que ocurren en una única estructura cerebral. En este sentido haría falta un estudio más específico y complejo que permita estudiar vías específicas y de vías en conjunto.

8. CONCLUSIONES

1. La activación del LC ipsilateral en la fase temprana del DNP juega un papel analgésico que fracasa en la fase tardía del dolor.

2. El LC contralateral toma un papel relevante contribuyendo al mantenimiento del DNP a lo largo del tiempo mediante la activación noradrenérgica del DRt. Además, esta modulación es dependiente de la cepa.

3. La activación del LC ipsilateral y contralateral contribuye al desarrollo del comportamiento depresivo, sugiriendo que el DNP a largo plazo modifica la actividad del LC de manera bilateral en ambas cepas. Provocando, a su vez, la activación de la vía noradrenérgica del LC-CCAr que está implicada en el desarrollo del fenotipo depresivo inducido por dolor crónico.

4. El fenotipo depresivo inducido por dolor crónico está mediado por los receptores adrenérgicos α1 y α2 de la CCAr.

CONCLUSIONS

1. Ipsilateral LC activation in the early phase of neuropathic pain plays an analgesic role that fails in the late phase of pain.

2. Contralateral LC takes a relevant role contributing to the maintenance of DNP over time through noradrenergic activation of the DRt. Moreover, this modulation is strain-dependent.

3. Both, ipsilateral and contralateral LC activation contributes to the development of depressive behaviour, suggesting that long-term DNP modifies LC activity bilaterally in both strains. In the same way, this LC activation induces an activation of rACC. Therefore, the LC-rACC noradrenergic pathway activation is involved in the development of the chronic pain-induced depressive-like behavior.

4. The chronic pain-induced depressive phenotype is mediated by α1- and α2-adrenergic receptors of CCAr.

9. BIBLIOGRAFIA

A

Abercrombie ED, Jacobs BL (1987a). Microinjected clonidine inhibits noradrenergic neurons of the locus coeruleus in freely moving cats. *Neuroscience letters* 76(2): 203-208.

Abercrombie ED, Jacobs BL (1987b). Single-unit response of noradrenergic neurons in the locus coeruleus of freely moving cats. II. Adaptation to chronically presented stressful stimuli. *The Journal of neuroscience : the official journal of the Society for Neuroscience* 7(9): 2844-2848.

Agster KL, Mejias-Aponte CA, Clark BD, Waterhouse BD (2013). Evidence for a regional specificity in the density and distribution of noradrenergic varicosities in rat cortex. *The Journal of comparative neurology* 521(10): 2195-2207.

Alba-Delgado C, Borges G, Sanchez-Blazquez P, Ortega JE, Horrillo I, Mico JA*, et al.* (2012a). The function of alpha-2-adrenoceptors in the rat locus coeruleus is preserved in the chronic constriction injury model of neuropathic pain. *Psychopharmacology* 221(1): 53-65.

Alba-Delgado C, Llorca-Torralba M, Horrillo I, Ortega JE, Mico JA, Sanchez-Blazquez P*, et al.* (2013). Chronic pain leads to concomitant noradrenergic impairment and mood disorders. *Biological psychiatry* 73(1): 54-62.

Alba-Delgado C, Llorca-Torralba M, Mico JA, Berrocoso E (2018). The onset of treatment with the antidepressant desipramine is critical for the emotional consequences of neuropathic pain. *Pain* 159(12): 2606-2619.

Alba-Delgado C, Mico JA, Sanchez-Blazquez P, Berrocoso E (2012b). Analgesic antidepressants promote the responsiveness of locus coeruleus neurons to noxious stimulation: implications for neuropathic pain. *Pain* 153(7): 1438-1449.

Agster, K. L., Mejias-Aponte, C. A., Clark, B. D., & Waterhouse, B. D. (2013). Evidence for a regional specificity in the density and distribution of noradrenergic varicosities in rat cortex. *Journal of Comparative Neurology*, *521*(10), 2195-2207.

Aldrin-Kirk P, Heuer A, Wang G, Mattsson B, Lundblad M, Parmar M*, et al.* (2016). DREADD Modulation of Transplanted DA Neurons Reveals a Novel Parkinsonian Dyskinesia Mechanism Mediated by the Serotonin 5-HT6 Receptor. *Neuron* 90(5): 955-968.

Almeida A, Cobos A, Tavares I, Lima D (2002). Brain afferents to the medullary dorsal reticular nucleus: a retrograde and anterograde tracing study in the rat. *The European journal of neuroscience* 16(1): 81-95.

Almeida A, Storkson R, Lima D, Hole K, Tjolsen A (1999). The medullary dorsal reticular nucleus facilitates pain behaviour induced by formalin in the rat. *The European journal of neuroscience* 11(1): 110-122.

Almeida A, Tavares I, Lima D (2000). Reciprocal connections between the medullary dorsal reticular nucleus and the spinal dorsal horn in the rat. *European journal of pain* 4(4): 373-387.

Almeida A, Tavares I, Lima D, Coimbra A (1993). Descending projections from the medullary dorsal reticular nucleus make synaptic contacts with spinal cord lamina I cells projecting to that nucleus: an electron microscopic tracer study in the rat. *Neuroscience* 55(4): 1093-1106.

Almeida A, Tjolsen A, Lima D, Coimbra A, Hole K (1996). The medullary dorsal reticular nucleus facilitates acute nociception in the rat. *Brain research bulletin* 39(1): 7-15.

Aoki C, Go CG, Venkatesan C, Kurose H (1994). Perikaryal and synaptic localization of alpha 2A-adrenergic receptor-like immunoreactivity. *Brain research* 650(2): 181-204.

Aoki C, Venkatesan C, Go CG, Forman R, Kurose H (1998). Cellular and subcellular sites for noradrenergic action in the monkey dorsolateral prefrontal cortex as revealed by the immunocytochemical localization of noradrenergic receptors and axons. *Cerebral cortex* 8(3): 269-277.

Apkarian AV, Baliki MN, Geha PY (2009). Towards a theory of chronic pain. *Progress in neurobiology* 87(2): 81-97.

Apkarian AV, Bushnell MC, Treede RD, Zubieta JK (2005). Human brain mechanisms of pain perception and regulation in health and disease. *European journal of pain* 9(4): 463-484.

Apkarian VA, Hashmi JA, Baliki MN (2011). Pain and the brain: specificity and plasticity of the brain in clinical chronic pain. *Pain* 152(3 Suppl): S49-S64.

Armbruster BN, Li X, Pausch MH, Herlitze S, Roth BL (2007). Evolving the lock to fit the key to create a family of G protein-coupled receptors potently activated by an inert ligand. *Proceedings of the National Academy of Sciences of the United States of America* 104(12): 5163-5168.

Arnsten AF (2009). Stress signalling pathways that impair prefrontal cortex structure and function. *Nature reviews. Neuroscience* 10(6): 410-422.

Aston-Jones G, Cohen JD (2005a). Adaptive gain and the role of the locus coeruleus-norepinephrine system in optimal performance. *The Journal of comparative neurology* 493(1): 99-110.

Aston-Jones G, Cohen JD (2005b). An integrative theory of locus coeruleus-norepinephrine function: adaptive gain and optimal performance. *Annual review of neuroscience* 28: 403-450.

ASTON-JONES, G. A. R. Y., Foote, S. L., & Bloom, F. E. (1984). Anatomy and physiology of locus coeruleus neurons: functional implications. *Frontiers of clinical neuroscience*, *2*, 92-116.

Aston-Jones G, Rajkowski J, Cohen J (1999). Role of locus coeruleus in attention and behavioral flexibility. *Biological psychiatry* 46(9): 1309-1320.

Attal N (2019). Pharmacological treatments of neuropathic pain: The latest recommendations. *Revue neurologique* 175(1-2): 46-50.

Attal N, Cruccu G, Baron R, Haanpaa M, Hansson P, Jensen TS*, et al.* (2010). EFNS guidelines on the pharmacological treatment of neuropathic pain: 2010 revision. *European journal of neurology* 17(9): 1113-e1188.

B

Baba H, Shimoji K, Yoshimura M (2000). Norepinephrine facilitates inhibitory transmission in substantia gelatinosa of adult rat spinal cord (part 1): effects on axon terminals of GABAergic and glycinergic neurons. *Anesthesiology* 92(2): 473-484.

Bair MJ, Robinson RL, Katon W, Kroenke K (2003). Depression and pain comorbidity: a literature review. *Archives of internal medicine* 163(20): 2433-2445.

Baliki MN, Geha PY, Fields HL, Apkarian AV (2010). Predicting value of pain and analgesia: nucleus accumbens response to noxious stimuli changes in the presence of chronic pain. *Neuron* 66(1): 149-160.

Bangasser DA, Eck SR, Ordones Sanchez E (2019). Sex differences in stress reactivity in arousal and attention systems. *Neuropsychopharmacology : official publication of the American College of Neuropsychopharmacology* 44(1): 129-139.

Bantel C, Eisenach JC, Duflo F, Tobin JR, Childers SR (2005). Spinal nerve ligation increases alpha2-adrenergic receptor G-protein coupling in the spinal cord. *Brain research* 1038(1): 76-82.

Barik A, Thompson JH, Seltzer M, Ghitani N, Chesler AT (2018). A Brainstem-Spinal Circuit Controlling Nocifensive Behavior. *Neuron* 100(6): 1491-1503 e1493.

Baron R (2006). Mechanisms of disease: neuropathic pain--a clinical perspective. *Nature clinical practice. Neurology* 2(2): 95-106.

Barthas F, Humo M, Gilsbach R, Waltisperger E, Karatas M, Leman S*, et al.* (2017). Cingulate Overexpression of Mitogen-Activated Protein Kinase Phosphatase-1 as a Key Factor for Depression. *Biological psychiatry* 82(5): 370-379.

Barthas F, Sellmeijer J, Hugel S, Waltisperger E, Barrot M, Yalcin I (2015). The anterior cingulate cortex is a critical hub for pain-induced depression. *Biological psychiatry* 77(3): 236-245.

Basbaum AI, Bautista DM, Scherrer G, Julius D (2009). Cellular and molecular mechanisms of pain. *Cell* 139(2): 267-284.

Becerra L, Breiter HC, Wise R, Gonzalez RG, Borsook D (2001). Reward circuitry activation by noxious thermal stimuli. *Neuron* 32(5): 927-946.

Bennett GJ, Xie YK (1988). A peripheral mononeuropathy in rat that produces disorders of pain sensation like those seen in man. *Pain* 33(1): 87-107.

Bernard JF, Bester H, Besson JM (1996). Involvement of the spino-parabrachio -amygdaloid and -hypothalamic pathways in the autonomic and affective emotional aspects of pain. *Progress in brain research* 107: 243-255.

Berridge CW, Waterhouse BD (2003). The locus coeruleus-noradrenergic system: modulation of behavioral state and state-dependent cognitive processes. *Brain research. Brain research reviews* 42(1): 33-84.

Berrocoso E, De Benito MD, Mico JA (2007). Role of serotonin 5-HT1A and opioid receptors in the antiallodynic effect of tramadol in the chronic constriction injury model of neuropathic pain in rats. *Psychopharmacology* 193(1): 97-105.

Berrocoso E, Mico JA, Vitton O, Ladure P, Newman-Tancredi A, Depoortere R*, et al.* (2011). Evaluation of milnacipran, in comparison with amitriptyline, on cold and mechanical allodynia in a rat model of neuropathic pain. *European journal of pharmacology* 655(1-3): 46-51.

Birket-Smith M (2001). Somatization and chronic pain. *Acta anaesthesiologica Scandinavica* 45(9): 1114-1120.

Birnbaum SG, Yuan PX, Wang M, Vijayraghavan S, Bloom AK, Davis DJ*, et al.* (2004). Protein kinase C overactivity impairs prefrontal cortical regulation of working memory. *Science* 306(5697): 882-884.

Bissiere S, McAllister KH, Olpe HR, Cryan JF (2006). The rostral anterior cingulate cortex modulates depression but not anxiety-related behaviour in the rat. *Behavioural brain research* 175(1): 195-199.

Blackburn-Munro G, Blackburn-Munro RE (2001). Chronic pain, chronic stress and depression: coincidence or consequence? *Journal of neuroendocrinology* 13(12): 1009-1023.

Blom SM, Pfister JP, Santello M, Senn W, Nevian T (2014). Nerve injury-induced neuropathic pain causes disinhibition of the anterior cingulate cortex. *The Journal of neuroscience : the official journal of the Society for Neuroscience* 34(17): 5754-5764.

Bouhassira D, Lanteri-Minet M, Attal N, Laurent B, Touboul C (2008). Prevalence of chronic pain with neuropathic characteristics in the general population. *Pain* 136(3): 380-387.

Boyle LM (2013). A neuroplasticity hypothesis of chronic stress in the basolateral amygdala. *The Yale journal of biology and medicine* 86(2): 117-125.

Bravo L, Alba-Delgado C, Torres-Sanchez S, Mico JA, Neto FL, Berrocoso E (2013). Social stress exacerbates the aversion to painful experiences in rats exposed to chronic pain: the role of the locus coeruleus. *Pain* 154(10): 2014-2023.

Bravo L, Llorca-Torralba M, Berrocoso E, Mico JA (2019). Monoamines as Drug Targets in Chronic Pain: Focusing on Neuropathic Pain. *Frontiers in neuroscience* 13: 1268.

Bravo L, Llorca-Torralba M, Suarez-Pereira I, Berrocoso E (2020). Pain in neuropsychiatry: Insights from animal models. *Neuroscience and biobehavioral reviews* 115: 96-115.

Bravo L, Mico JA, Rey-Brea R, Camarena-Delgado C, Berrocoso E (2016). Effect of DSP4 and desipramine in the sensorial and affective component of neuropathic pain in rats. *Progress in neuro-psychopharmacology & biological psychiatry* 70: 57-67.

Bravo L, Mico JA, Rey-Brea R, Perez-Nievas B, Leza JC, Berrocoso E (2012). Depressive-like states heighten the aversion to painful stimuli in a rat model of comorbid chronic pain and depression. *Anesthesiology* 117(3): 613-625.

Brecht S, Courtecuisse C, Debieuvre C, Croenlein J, Desaiah D, Raskin J*, et al.* (2007). Efficacy and safety of duloxetine 60 mg once daily in the treatment of pain in patients with major depressive disorder and at least moderate pain of unknown etiology: a randomized controlled trial. *The Journal of clinical psychiatry* 68(11): 1707-1716.

Brightwell JJ, Taylor BK (2009). Noradrenergic neurons in the locus coeruleus contribute to neuropathic pain. *Neuroscience* 160(1): 174-185.

Bruinstroop E, Cano G, Vanderhorst VG, Cavalcante JC, Wirth J, Sena-Esteves M*, et al.* (2012). Spinal projections of the A5, A6 (locus coeruleus), and A7 noradrenergic cell groups in rats. *The Journal of comparative neurology* 520(9): 1985-2001.

Buffalari DM, Grace AA (2009a). Anxiogenic modulation of spontaneous and evoked neuronal activity in the basolateral amygdala. *Neuroscience* 163(4): 1069-1077.

Buffalari DM, Grace AA (2009b). Chronic cold stress increases excitatory effects of norepinephrine on spontaneous and evoked activity of basolateral amygdala neurons. *The international journal of neuropsychopharmacology* 12(1): 95-107.

Buffalari DM, Grace AA (2007). Noradrenergic modulation of basolateral amygdala neuronal activity: opposing influences of alpha-2 and beta receptor activation. *The Journal of neuroscience : the official journal of the Society for Neuroscience* 27(45): 12358-12366.

Bushnell MC, Ceko M, Low LA (2013). Cognitive and emotional control of pain and its disruption in chronic pain. *Nature reviews. Neuroscience* 14(7): 502-511.

Bushnell MC, Duncan GH, Hofbauer RK, Ha B, Chen JI, Carrier B (1999). Pain perception: is there a role for primary somatosensory cortex? *Proceedings of the National Academy of Sciences of the United States of America* 96(14): 7705-7709.

C

Calati R, Laglaoui Bakhiyi C, Artero S, Ilgen M, Courtet P (2015). The impact of physical pain on suicidal thoughts and behaviors: Meta-analyses. *Journal of psychiatric research* 71: 16-32.

Calejesan AA, Kim SJ, Zhuo M (2000). Descending facilitatory modulation of a behavioral nociceptive response by stimulation in the adult rat anterior cingulate cortex. *European journal of pain* 4(1): 83-96.

Campbell LC, Clauw DJ, Keefe FJ (2003). Persistent pain and depression: a biopsychosocial perspective. *Biological psychiatry* 54(3): 399-409.

Cao X, Mercaldo V, Li P, Wu LJ, Zhuo M (2010). Facilitation of the inhibitory transmission by gastrin-releasing peptide in the anterior cingulate cortex. *Molecular pain* 6: 52.

Carr FB, Zachariou V (2014). Nociception and pain: lessons from optogenetics. *Frontiers in behavioral neuroscience* 8: 69.

Carter ME, Yizhar O, Chikahisa S, Nguyen H, Adamantidis A, Nishino S*, et al.* (2010). Tuning arousal with optogenetic modulation of locus coeruleus neurons. *Nature neuroscience* 13(12): 1526-1533.

Catala E, Reig E, Artes M, Aliaga L, Lopez JS, Segu JL (2002). Prevalence of pain in the Spanish population: telephone survey in 5000 homes. *European journal of pain* 6(2): 133-140.

Cavalli E, Mammana S, Nicoletti F, Bramanti P, Mazzon E (2019). The neuropathic pain: An overview of the current treatment and future therapeutic approaches. *International journal of immunopathology and pharmacology* 33: 2058738419838383.

Clark FM, Yeomans DC, Proudfit HK (1991). The noradrenergic innervation of the spinal cord: differences between two substrains of Sprague-Dawley rats determined using retrograde tracers combined with immunocytochemistry. *Neuroscience letters* 125(2): 155-158.

Condes-Lara M (1998). Different direct pathways of locus coeruleus to medial prefrontal cortex and centrolateral thalamic nucleus: electrical stimulation effects on the evoked responses to nociceptive peripheral stimulation. *European journal of pain* 2(1): 15-23.

Cordeiro Matos S, Zhang Z, Seguela P (2015). Peripheral Neuropathy Induces HCN Channel Dysfunction in Pyramidal Neurons of the Medial Prefrontal Cortex. *The Journal of neuroscience : the official journal of the Society for Neuroscience* 35(38): 13244-13256.

Corder G, Ahanonu B, Grewe BF, Wang D, Schnitzer MJ, Scherrer G (2019). An amygdalar neural ensemble that encodes the unpleasantness of pain. *Science* 363(6424): 276-281.

Cotter D, Mackay D, Landau S, Kerwin R, Everall I (2001). Reduced glial cell density and neuronal size in the anterior cingulate cortex in major depressive disorder. *Archives of general psychiatry* 58(6): 545-553.

Cryan JF, Markou A, Lucki I (2002). Assessing antidepressant activity in rodents: recent developments and future needs. *Trends in pharmacological sciences* 23(5): 238-245.

Cryan JF, Valentino RJ, Lucki I (2005). Assessing substrates underlying the behavioral effects of antidepressants using the modified rat forced swimming test. *Neuroscience and biobehavioral reviews* 29(4-5): 547-569.

Chandler DJ, Gao WJ, Waterhouse BD (2014). Heterogeneous organization of the locus coeruleus projections to prefrontal and motor cortices. *Proceedings of the National Academy of Sciences of the United States of America* 111(18): 6816-6821.

Chandler DJ, Jensen P, McCall JG, Pickering AE, Schwarz LA, Totah NK (2019). Redefining Noradrenergic Neuromodulation of Behavior: Impacts of a Modular Locus Coeruleus Architecture. *The Journal of neuroscience : the official journal of the Society for Neuroscience* 39(42): 8239-8249.

Chang CH, Grace AA (2013). Amygdala beta-noradrenergic receptors modulate delayed downregulation of dopamine activity following restraint. *The Journal of neuroscience : the official journal of the Society for Neuroscience* 33(4): 1441-1450.

Chen X, Choo H, Huang XP, Yang X, Stone O, Roth BL*, et al.* (2015). The first structure-activity relationship studies for designer receptors exclusively activated by designer drugs. *ACS chemical neuroscience* 6(3): 476-484.

Chopra K, Arora V (2014). An intricate relationship between pain and depression: clinical correlates, coactivation factors and therapeutic targets. *Expert opinion on therapeutic targets* 18(2): 159-176.

Chu KL, Xu J, Frost J, Li L, Gomez E, Dart MJ*, et al.* (2015). A selective alpha2 B adrenoceptor agonist (A-1262543) and duloxetine modulate nociceptive neurones in the medial prefrontal cortex, but not in the spinal cord of neuropathic rats. *European journal of pain* 19(5): 649-660.

D

Dahlstrom A, Fuxe K (1964). Localization of monoamines in the lower brain stem. *Experientia* 20(7): 398-399.

David-Pereira A, Sagalajev B, Wei H, Almeida A, Pertovaara A, Pinto-Ribeiro F (2017). The medullary dorsal reticular nucleus as a relay for descending pronociception induced by the mGluR5 in the rat infralimbic cortex. *Neuroscience* 349: 341-354.

De Felice M, Sanoja R, Wang R, Vera-Portocarrero L, Oyarzo J, King T*, et al.* (2011). Engagement of descending inhibition from the rostral ventromedial medulla protects against chronic neuropathic pain. *Pain* 152(12): 2701-2709.

de Sola H, Salazar A, Duenas M, Ojeda B, Failde I (2016). Nationwide cross-sectional study of the impact of chronic pain on an individual's employment: relationship with the family and the social support. *BMJ open* 6(12): e012246.

Detke MJ, Lucki I (1996). Detection of serotonergic and noradrenergic antidepressants in the rat forced swimming test: the effects of water depth. *Behavioural brain research* 73(1-2): 43-46.

Detke MJ, Rickels M, Lucki I (1995). Active behaviors in the rat forced swimming test differentially produced by serotonergic and noradrenergic antidepressants. *Psychopharmacology* 121(1): 66-72.

Dobrzanski G, Kossut M (2017). Application of the DREADD technique in biomedical brain research. *Pharmacological reports : PR* 69(2): 213-221.

Drevets WC (2001). Neuroimaging and neuropathological studies of depression: implications for the cognitive-emotional features of mood disorders. *Current opinion in neurobiology* 11(2): 240-249.

Drevets WC, Savitz J, Trimble M (2008). The subgenual anterior cingulate cortex in mood disorders. *CNS spectrums* 13(8): 663-681.

Duman, R. S., & Nestler, E.J. (1995). Signal transduction pathways for catecholamines receptors. In F. E. Bloom, & D.J. Kupfer (Eds), Psychopharmacology: The Fourth Generation of Progress (pp 303-320). N.Y.: Raven Press.

Duenas M, Ojeda B, Salazar A, Mico JA, Failde I (2016). A review of chronic pain impact on patients, their social environment and the health care system. *Journal of pain research* 9: 457-467.

Duenas M, Salazar A, Ojeda B, Fernandez-Palacin F, Mico JA, Torres LM*, et al.* (2015). A nationwide study of chronic pain prevalence in the general spanish population: identifying clinical subgroups through cluster analysis. *Pain medicine* 16(4): 811-822.

Duflo F, Li X, Bantel C, Pancaro C, Vincler M, Eisenach JC (2002). Peripheral nerve injury alters the alpha2 adrenoceptor subtype activated by clonidine for analgesia. *Anesthesiology* 97(3): 636-641.

Dugast C, Almeida A, Lima D (2003). The medullary dorsal reticular nucleus enhances the responsiveness of spinal nociceptive neurons to peripheral stimulation in the rat. *The European journal of neuroscience* 18(3): 580-588.

Duvarci S, Pare D (2014). Amygdala microcircuits controlling learned fear. *Neuron* 82(5): 966-980.

Dworkin RH, Backonja M, Rowbotham MC, Allen RR, Argoff CR, Bennett GJ*, et al.* (2003). Advances in neuropathic pain: diagnosis, mechanisms, and treatment recommendations. *Archives of neurology* 60(11): 1524-1534.

Dworkin RH, O'Connor AB, Backonja M, Farrar JT, Finnerup NB, Jensen TS*, et al.* (2007). Pharmacologic management of neuropathic pain: evidence-based recommendations. *Pain* 132(3): 237-251.

E

El-Tallawy SN, Nalamasu R, Pergolizzi JV, Gharibo C (2020). Pain Management During the COVID-19 Pandemic. *Pain and therapy* 9(2): 453-466.

F

Fairbanks CA, Stone LS, Kitto KF, Nguyen HO, Posthumus IJ, Wilcox GL (2002). alpha(2C)-Adrenergic receptors mediate spinal analgesia and adrenergic-opioid synergy. *The Journal of pharmacology and experimental therapeutics* 300(1): 282-290.

Fields HL, Heinricher MM, Mason P (1991). Neurotransmitters in nociceptive modulatory circuits. *Annual review of neuroscience* 14: 219-245.

Finnerup NB, Attal N, Haroutounian S, McNicol E, Baron R, Dworkin RH*, et al.* (2015). Pharmacotherapy for neuropathic pain in adults: a systematic review and meta-analysis. *The Lancet. Neurology* 14(2): 162-173.

Fortress AM, Hamlett ED, Vazey EM, Aston-Jones G, Cass WA, Boger HA*, et al.* (2015). Designer receptors enhance memory in a mouse model of Down syndrome. *The Journal of neuroscience : the official journal of the Society for Neuroscience* 35(4): 1343-1353.

Fuxe K, Dahlstrom AB, Jonsson G, Marcellino D, Guescini M, Dam M*, et al.* (2010). The discovery of central monoamine neurons gave volume transmission to the wired brain. *Progress in neurobiology* 90(2): 82-100.

G

Goldman-Rakic PS, Lidow MS, Gallager DW (1990). Overlap of dopaminergic, adrenergic, and serotoninergic receptors and complementarity of their subtypes in primate prefrontal cortex. *The Journal of neuroscience : the official journal of the Society for Neuroscience* 10(7): 2125-2138.

Gomez JL, Bonaventura J, Lesniak W, Mathews WB, Sysa-Shah P, Rodriguez LA*, et al.* (2017). Chemogenetics revealed: DREADD occupancy and activation via converted clozapine. *Science* 357(6350): 503-507.

Grissom NM, Bhatnagar S (2011). The basolateral amygdala regulates adaptation to stress via beta-adrenergic receptor-mediated reductions in phosphorylated extracellular signal-regulated kinase. *Neuroscience* 178: 108-122.

Grzanna R, Molliver ME (1980). The locus coeruleus in the rat: an immunohistochemical delineation. *Neuroscience* 5(1): 21-40.

Gureje O, Von Korff M, Simon GE, Gater R (1998). Persistent pain and well-being: a World Health Organization Study in Primary Care. *Jama* 280(2): 147-151.

Guyenet PG (1980). The coeruleospinal noradrenergic neurons: anatomical and electrophysiological studies in the rat. *Brain research* 189(1): 121-133.

H

Haanpaa M, Attal N, Backonja M, Baron R, Bennett M, Bouhassira D*, et al.* (2011). NeuPSIG guidelines on neuropathic pain assessment. *Pain* 152(1): 14-27.

Hassett AL, Clauw DJ (2010). The role of stress in rheumatic diseases. *Arthritis research & therapy* 12(3): 123.

Hayashida K, DeGoes S, Curry R, Eisenach JC (2007a). Gabapentin activates spinal noradrenergic activity in rats and humans and reduces hypersensitivity after surgery. *Anesthesiology* 106(3): 557-562.

Hayashida K, Obata H, Nakajima K, Eisenach JC (2008a). Gabapentin acts within the locus coeruleus to alleviate neuropathic pain. *Anesthesiology* 109(6): 1077-1084.

Hayashida K, Parker R, Eisenach JC (2007b). Oral gabapentin activates spinal cholinergic circuits to reduce hypersensitivity after peripheral nerve injury and interacts synergistically with oral donepezil. *Anesthesiology* 106(6): 1213-1219.

Hayashida K, Peters CM, Gutierrez S, Eisenach JC (2012). Depletion of endogenous noradrenaline does not prevent spinal cord plasticity following peripheral nerve injury. *The journal of pain* 13(1): 49-57.

Hayashida KI, Clayton BA, Johnson JE, Eisenach JC (2008b). Brain derived nerve growth factor induces spinal noradrenergic fiber sprouting and enhances clonidine analgesia following nerve injury in rats. *Pain* 136(3): 348-355.

Hickey L, Li Y, Fyson SJ, Watson TC, Perrins R, Hewinson J*, et al.* (2014). Optoactivation of locus ceruleus neurons evokes bidirectional changes in thermal nociception in rats. *The Journal of neuroscience : the official journal of the Society for Neuroscience* 34(12): 4148-4160.

Hirschberg S, Li Y, Randall A, Kremer EJ, Pickering AE (2017). Functional dichotomy in spinal- vs prefrontal-projecting locus coeruleus modules splits descending noradrenergic analgesia from ascending aversion and anxiety in rats. *eLife* 6.

Hooley JM, Franklin JC, Nock MK (2014). Chronic pain and suicide: understanding the association. *Current pain and headache reports* 18(8): 435.

Howorth PW, Teschemacher AG, Pickering AE (2009a). Retrograde adenoviral vector targeting of nociresponsive pontospinal noradrenergic neurons in the rat in vivo. *The Journal of comparative neurology* 512(2): 141-157.

Howorth PW, Thornton SR, O'Brien V, Smith WD, Nikiforova N, Teschemacher AG*, et al.* (2009b). Retrograde viral vector-mediated inhibition of pontospinal noradrenergic neurons causes hyperalgesia in rats. *The Journal of neuroscience : the official journal of the Society for Neuroscience* 29(41): 12855-12864.

Hsieh JC, Belfrage M, Stone-Elander S, Hansson P, Ingvar M (1995). Central representation of chronic ongoing neuropathic pain studied by positron emission tomography. *Pain* 63(2): 225-236.

Hughes S, Hickey L, Donaldson LF, Lumb BM, Pickering AE (2015). Intrathecal reboxetine suppresses evoked and ongoing neuropathic pain behaviours by restoring spinal noradrenergic inhibitory tone. *Pain* 156(2): 328-334.

Hughes SW, Hickey L, Hulse RP, Lumb BM, Pickering AE (2013). Endogenous analgesic action of the pontospinal noradrenergic system spatially restricts and temporally delays the progression of neuropathic pain following tibial nerve injury. *Pain* 154(9): 1680-1690.

Humo M, Lu H, Yalcin I (2019). The molecular neurobiology of chronic pain-induced depression. *Cell and tissue research* 377(1): 21-43.

Hwang DY, Carlezon WA, Jr., Isacson O, Kim KS (2001). A high-efficiency synthetic promoter that drives transgene expression selectively in noradrenergic neurons. *Human gene therapy* 12(14): 1731-1740.

I

Isingrini E, Perret L, Rainer Q, Amilhon B, Guma E, Tanti A*, et al.* (2016). Resilience to chronic stress is mediated by noradrenergic regulation of dopamine neurons. *Nature neuroscience* 19(4): 560-563.

J

Jasmin L, Boudah A, Ohara PT (2003). Long-term effects of decreased noradrenergic central nervous system innervation on pain behavior and opioid antinociception. *The Journal of comparative neurology* 460(1): 38-55.

Jasmin L, Tien D, Weinshenker D, Palmiter RD, Green PG, Janni G*, et al.* (2002). The NK1 receptor mediates both the hyperalgesia and the resistance to morphine in mice lacking noradrenaline. *Proceedings of the National Academy of Sciences of the United States of America* 99(2): 1029-1034.

Johansen JP, Fields HL, Manning BH (2001). The affective component of pain in rodents: direct evidence for a contribution of the anterior cingulate cortex. *Proceedings of the National Academy of Sciences of the United States of America* 98(14): 8077-8082.

Jones BE (2003). Arousal systems. *Frontiers in bioscience : a journal and virtual library* 8: s438-451.

Jones BE, Halaris AE, McIlhany M, Moore RY (1977a). Ascending projections of the locus coeruleus in the rat. I. Axonal transport in central noradrenaline neurons. *Brain research* 127(1): 1-21.

Jones BE, Moore RY (1977b). Ascending projections of the locus coeruleus in the rat. II. Autoradiographic study. *Brain research* 127(1): 25-53.

Jones SL, Gebhart GF (1986). Quantitative characterization of ceruleospinal inhibition of nociceptive transmission in the rat. *Journal of neurophysiology* 56(5): 1397-1410.

Jones SL, Gebhart GF (1987). Spinal pathways mediating tonic, coeruleospinal, and raphe-spinal descending inhibition in the rat. *Journal of neurophysiology* 58(1): 138-159.

K

Kandel ER (2013) Principles of neural sciences, Ed 5. New York: McGraw-Hill.

Kang SJ, Kwak C, Lee J, Sim SE, Shim J, Choi T*, et al.* (2015). Bidirectional modulation of hyperalgesia via the specific control of excitatory and inhibitory neuronal activity in the ACC. *Molecular brain* 8(1): 81.

Karunarathne WK, Giri L, Kalyanaraman V, Gautam N (2013). Optically triggering spatiotemporally confined GPCR activity in a cell and programming neurite initiation and extension. *Proceedings of the National Academy of Sciences of the United States of America* 110(17): E1565-1574.

Kaushal R, Taylor BK, Jamal AB, Zhang L, Ma F, Donahue R*, et al.* (2016). GABA-A receptor activity in the noradrenergic locus coeruleus drives trigeminal neuropathic pain in the rat; contribution of NAalpha1 receptors in the medial prefrontal cortex. *Neuroscience* 334: 148-159.

Kawasaki Y, Kumamoto E, Furue H, Yoshimura M (2003). Alpha 2 adrenoceptor-mediated presynaptic inhibition of primary afferent glutamatergic transmission in rat substantia gelatinosa neurons. *Anesthesiology* 98(3): 682-689.

Kimura M, Eisenach JC, Hayashida KI (2016). Gabapentin loses efficacy over time after nerve injury in rats: role of glutamate transporter-1 in the locus coeruleus. *Pain* 157(9): 2024-2032.

Kimura M, Suto T, Morado-Urbina CE, Peters CM, Eisenach JC, Hayashida K (2015). Impaired Pain-evoked Analgesia after Nerve Injury in Rats Reflects Altered Glutamate Regulation in the Locus Coeruleus. *Anesthesiology* 123(4): 899-908.

King T, Vera-Portocarrero L, Gutierrez T, Vanderah TW, Dussor G, Lai J*, et al.* (2009). Unmasking the tonic-aversive state in neuropathic pain. *Nature neuroscience* 12(11): 1364-1366.

Koga K, Shimoyama S, Yamada A, Furukawa T, Nikaido Y, Furue H*, et al.* (2018). Chronic inflammatory pain induced GABAergic synaptic plasticity in the adult mouse anterior cingulate cortex. *Molecular pain* 14: 1744806918783478.

Koga K, Yamada A, Song Q, Li XH, Chen QY, Liu RH*, et al.* (2020). Ascending noradrenergic excitation from the locus coeruleus to the anterior cingulate cortex. *Molecular brain* 13(1): 49.

Kremer M, Becker LJ, Barrot M, Yalcin I (2021). How to study anxiety and depression in rodent models of chronic pain? *The European journal of neuroscience* 53(1): 236-270.

Kremer M, Salvat E, Muller A, Yalcin I, Barrot M (2016). Antidepressants and gabapentinoids in neuropathic pain: Mechanistic insights. *Neuroscience* 338: 183-206.

Kummer KK, Mitric M, Kalpachidou T, Kress M (2020). The Medial Prefrontal Cortex as a Central Hub for Mental Comorbidities Associated with Chronic Pain. *International journal of molecular sciences* 21(10).

Kwiat GC, Basbaum AI (1992). The origin of brainstem noradrenergic and serotonergic projections to the spinal cord dorsal horn in the rat. *Somatosensory & motor research* 9(2): 157-173.

L

LaBuda CJ, Fuchs PN (2005). Attenuation of negative pain affect produced by unilateral spinal nerve injury in the rat following anterior cingulate cortex activation. *Neuroscience* 136(1): 311-322.

LaGraize SC, Labuda CJ, Rutledge MA, Jackson RL, Fuchs PN (2004). Differential effect of anterior cingulate cortex lesion on mechanical hypersensitivity and escape/avoidance behavior in an animal model of neuropathic pain. *Experimental neurology* 188(1): 139-148.

Latremoliere A, Woolf CJ (2009). Central sensitization: a generator of pain hypersensitivity by central neural plasticity. *The journal of pain* 10(9): 895-926.

Leanza G, Pellitteri R, Russo A, Stanzani S (1989). Branching projections from subcoeruleus area neurons to medial preoptic area and cervical spinal cord revealed by double retrograde neuronal labeling. *Neuroscience letters* 103(1): 11-16.

LeDoux JE (2000). Emotion circuits in the brain. *Annual review of neuroscience* 23: 155-184.

Lee GI, Neumeister MW (2020). Pain: Pathways and Physiology. *Clinics in plastic surgery* 47(2): 173-180.

Leite-Almeida H, Pinto-Ribeiro F, Almeida A (2015). Animal Models for the Study of Comorbid Pain and Psychiatric Disorders. *Modern trends in pharmacopsychiatry* 30: 1-21.

Li XY, Ko HG, Chen T, Descalzi G, Koga K, Wang H*, et al.* (2010). Alleviating neuropathic pain hypersensitivity by inhibiting PKMzeta in the anterior cingulate cortex. *Science* 330(6009): 1400-1404.

Liedgens H, Obradovic M, De Courcy J, Holbrook T, Jakubanis R (2016). A burden of illness study for neuropathic pain in Europe. *ClinicoEconomics and outcomes research : CEOR* 8: 113-126.

Lima D (1990). A spinomedullary projection terminating in the dorsal reticular nucleus of the rat. *Neuroscience* 34(3): 577-589.

Lima D, Almeida A (2002). The medullary dorsal reticular nucleus as a pronociceptive centre of the pain control system. *Progress in neurobiology* 66(2): 81-108.

Lonergan T, Teschemacher AG, Hwang DY, Kim KS, Pickering AE, Kasparov S (2005). Targeting brain stem centers of cardiovascular control using adenoviral vectors: impact of promoters on transgene expression. *Physiological genomics* 20(2): 165-172.

Loughlin SE, Foote SL, Grzanna R (1986). Efferent projections of nucleus locus coeruleus: morphologic subpopulations have different efferent targets. *Neuroscience* 18(2): 307-319.

Lucki I (1997). The forced swimming test as a model for core and component behavioral effects of antidepressant drugs. *Behavioural pharmacology* 8(6-7): 523-532.

Llorca-Torralba M, Borges G, Neto F, Mico JA, Berrocoso E (2016). Noradrenergic Locus Coeruleus pathways in pain modulation. *Neuroscience* 338: 93-113.

Llorca-Torralba M, Pilar-Cuellar F, Bravo L, Bruzos-Cidon C, Torrecilla M, Mico JA*, et al.* (2019a). Opioid Activity in the Locus Coeruleus Is Modulated by Chronic Neuropathic Pain. *Molecular neurobiology* 56(6): 4135-4150.

Llorca-Torralba M, Suarez-Pereira I, Bravo L, Camarena-Delgado C, Garcia-Partida JA, Mico JA*, et al.* (2019b). Chemogenetic Silencing of the Locus Coeruleus-Basolateral Amygdala Pathway Abolishes Pain-Induced Anxiety and Enhanced Aversive Learning in Rats. *Biological psychiatry* 85(12): 1021-1035.

M

MacLaren DA, Browne RW, Shaw JK, Krishnan Radhakrishnan S, Khare P, Espana RA*, et al.* (2016). Clozapine N-Oxide Administration Produces Behavioral Effects in Long-Evans Rats: Implications for Designing DREADD Experiments. *eNeuro* 3(5).

Mana MJ, Grace AA (1997). Chronic cold stress alters the basal and evoked electrophysiological activity of rat locus coeruleus neurons. *Neuroscience* 81(4): 1055-1064.

Maren S, Holmes A (2016). Stress and Fear Extinction. *Neuropsychopharmacology : official publication of the American College of Neuropsychopharmacology* 41(1): 58-79.

Martin WJ, Gupta NK, Loo CM, Rohde DS, Basbaum AI (1999). Differential effects of neurotoxic destruction of descending noradrenergic pathways on acute and persistent nociceptive processing. *Pain* 80(1-2): 57-65.

Martins I, Carvalho P, de Vries MG, Teixeira-Pinto A, Wilson SP, Westerink BH*, et al.* (2015). Increased noradrenergic neurotransmission to a pain facilitatory area of the brain is implicated in facilitation of chronic pain. *Anesthesiology* 123(3): 642-653.

Martins I, Costa-Araujo S, Fadel J, Wilson SP, Lima D, Tavares I (2010). Reversal of neuropathic pain by HSV-1-mediated decrease of noradrenaline in a pain facilitatory area of the brain. *Pain* 151(1): 137-145.

Martins I, de Vries MG, Teixeira-Pinto A, Fadel J, Wilson SP, Westerink BH*, et al.* (2013). Noradrenaline increases pain facilitation from the brain during inflammatory pain. *Neuropharmacology* 71: 299-307.

Martins I, Tavares I (2017). Reticular Formation and Pain: The Past and the Future. *Frontiers in neuroanatomy* 11: 51.

Marzo A, Totah NK, Neves RM, Logothetis NK, Eschenko O (2014). Unilateral electrical stimulation of rat locus coeruleus elicits bilateral response of norepinephrine neurons and sustained activation of medial prefrontal cortex. *Journal of neurophysiology* 111(12): 2570-2588.

Mason ST, Fibiger HC (1979). Regional topography within noradrenergic locus coeruleus as revealed by retrograde transport of horseradish peroxidase. *The Journal of comparative neurology* 187(4): 703-724.

Mayberg HS, Liotti M, Brannan SK, McGinnis S, Mahurin RK, Jerabek PA*, et al.* (1999). Reciprocal limbic-cortical function and negative mood: converging PET findings in depression and normal sadness. *The American journal of psychiatry* 156(5): 675-682.

McCall JG, Al-Hasani R, Siuda ER, Hong DY, Norris AJ, Ford CP*, et al.* (2015). CRH Engagement of the Locus Coeruleus Noradrenergic System Mediates Stress-Induced Anxiety. *Neuron* 87(3): 605-620.

McCall JG, Siuda ER, Bhatti DL, Lawson LA, McElligott ZA, Stuber GD*, et al.* (2017). Locus coeruleus to basolateral amygdala noradrenergic projections promote anxiety-like behavior. *eLife* 6.

McWilliams LA, Cox BJ, Enns MW (2003). Mood and anxiety disorders associated with chronic pain: an examination in a nationally representative sample. *Pain* 106(1-2): 127-133.

Metz AE, Yau HJ, Centeno MV, Apkarian AV, Martina M (2009). Morphological and functional reorganization of rat medial prefrontal cortex in neuropathic pain. *Proceedings of the National Academy of Sciences of the United States of America* 106(7): 2423-2428.

Mico JA, Ardid D, Berrocoso E, Eschalier A (2006). Antidepressants and pain. *Trends in pharmacological sciences* 27(7): 348-354.

Millan MJ (2002). Descending control of pain. *Progress in neurobiology* 66(6): 355-474.

Millan MJ (1999). The induction of pain: an integrative review. *Progress in neurobiology* 57(1): 1-164.

Miranda MA, Ferry B, Ferreira G (2007). Basolateral amygdala noradrenergic activity is involved in the acquisition of conditioned odor aversion in the rat. *Neurobiology of learning and memory* 88(2): 260-263.

Miyoshi K, Narita M, Narita M, Suzuki T (2006). Involvement of mGluR5 in the ethanol-induced neuropathic pain-like state in the rat. *Neuroscience letters* 410(2): 105-109.

Mogil JS (2009). Animal models of pain: progress and challenges. *Nature reviews. Neuroscience* 10(4): 283-294.

N

Nakajima K, Obata H, Iriuchijima N, Saito S (2012). An increase in spinal cord noradrenaline is a major contributor to the antihyperalgesic effect of antidepressants after peripheral nerve injury in the rat. *Pain* 153(5): 990-997.

Narita M, Kaneko C, Miyoshi K, Nagumo Y, Kuzumaki N, Nakajima M*, et al.* (2006). Chronic pain induces anxiety with concomitant changes in opioidergic function in the amygdala. *Neuropsychopharmacology : official publication of the American College of Neuropsychopharmacology* 31(4): 739-750.

Ning L, Ma LQ, Wang ZR, Wang YW (2013). Chronic constriction injury induced long-term changes in spontaneous membrane-potential oscillations in anterior cingulate cortical neurons in vivo. *Pain physician* 16(5): E577-589.

O

Ordway GA, Smith KS, Haycock JW (1994). Elevated tyrosine hydroxylase in the locus coeruleus of suicide victims. *Journal of neurochemistry* 62(2): 680-685.

Ortiz JP, Heinricher MM, Selden NR (2007). Noradrenergic agonist administration into the central nucleus of the amygdala increases the tail-flick latency in lightly anesthetized rats. *Neuroscience* 148(3): 737-743.

P

Panneton WM, Gan Q, Livergood RS (2011). A trigeminoreticular pathway: implications in pain. *PloS one* 6(9): e24499.

Paulson PE, Casey KL, Morrow TJ (2002). Long-term changes in behavior and regional cerebral blood flow associated with painful peripheral mononeuropathy in the rat. *Pain* 95(1-2): 31-40.

Pereira-Silva R, Costa-Pereira JT, Alonso R, Serrao P, Martins I, Neto FL (2020). Attenuation of the Diffuse Noxious Inhibitory Controls in Chronic Joint Inflammatory Pain Is Accompanied by Anxiodepressive-Like Behaviors and Impairment of the Descending Noradrenergic Modulation. *International journal of molecular sciences* 21(8).

Pertovaara A (2006). Noradrenergic pain modulation. *Progress in neurobiology* 80(2): 53-83.

Pertovaara A (2013). The noradrenergic pain regulation system: a potential target for pain therapy. *European journal of pharmacology* 716(1-3): 2-7.

Ploner M, Gross J, Timmermann L, Schnitzler A (2002). Cortical representation of first and second pain sensation in humans. *Proceedings of the National Academy of Sciences of the United States of America* 99(19): 12444-12448.

Poe GR, Foote S, Eschenko O, Johansen JP, Bouret S, Aston-Jones G*, et al.* (2020). Locus coeruleus: a new look at the blue spot. *Nature reviews. Neuroscience* 21(11): 644-659.

Porsolt RD, Anton G, Blavet N, Jalfre M (1978). Behavioural despair in rats: a new model sensitive to antidepressant treatments. *European journal of pharmacology* 47(4): 379-391.

Price DD (2000). Psychological and neural mechanisms of the affective dimension of pain. *Science* 288(5472): 1769-1772.

Price DD, Barrell JJ, Gracely RH (1980). A psychophysical analysis of experimential factors that selectively influence the affective dimension of pain. *Pain* 8(2): 137-149.

Proudfit HK, Clark FM (1991). The projections of locus coeruleus neurons to the spinal cord. *Progress in brain research* 88: 123-141.

Q

Qu C, King T, Okun A, Lai J, Fields HL, Porreca F (2011). Lesion of the rostral anterior cingulate cortex eliminates the aversiveness of spontaneous neuropathic pain following partial or complete axotomy. *Pain* 152(7): 1641-1648.

R

Rahman W, D'Mello R, Dickenson AH (2008). Peripheral nerve injury-induced changes in spinal alpha(2)-adrenoceptor-mediated modulation of mechanically evoked dorsal horn neuronal responses. *The journal of pain* 9(4): 350-359.

Rainville P, Duncan GH, Price DD, Carrier B, Bushnell MC (1997). Pain affect encoded in human anterior cingulate but not somatosensory cortex. *Science* 277(5328): 968-971.

Raja SN, Carr DB, Cohen M, Finnerup NB, Flor H, Gibson S*, et al.* (2020). The revised International Association for the Study of Pain definition of pain: concepts, challenges, and compromises. *Pain* 161(9): 1976-1982.

Ramos BP, Arnsten AF (2007). Adrenergic pharmacology and cognition: focus on the prefrontal cortex. *Pharmacology & therapeutics* 113(3): 523-536.

Ramos BP, Stark D, Verduzco L, van Dyck CH, Arnsten AF (2006). Alpha2A-adrenoceptor stimulation improves prefrontal cortical regulation of behavior through inhibition of cAMP signaling in aging animals. *Learning & memory* 13(6): 770-776.

Randall LO, Selitto JJ (1957). A method for measurement of analgesic activity on inflamed tissue. *Archives internationales de pharmacodynamie et de therapie* 111(4): 409-419.

Robertson SD, Plummer NW, de Marchena J, Jensen P (2013). Developmental origins of central norepinephrine neuron diversity. *Nature neuroscience* 16(8): 1016-1023.

Roozendaal B, Castello NA, Vedana G, Barsegyan A, McGaugh JL (2008). Noradrenergic activation of the basolateral amygdala modulates consolidation of object recognition memory. *Neurobiology of learning and memory* 90(3): 576-579.

Roozendaal B, Okuda S, de Quervain DJ, McGaugh JL (2006). Glucocorticoids interact with emotion-induced noradrenergic activation in influencing different memory functions. *Neuroscience* 138(3): 901-910.

Rouwette T, Vanelderen P, Roubos EW, Kozicz T, Vissers K (2012). The amygdala, a relay station for switching on and off pain. *European journal of pain* 16(6): 782-792.

S

Safari MS, Haghparast A, Semnanian S (2009). Effect of lidocaine administration at the nucleus locus coeruleus level on lateral hypothalamus-induced antinociception in the rat. *Pharmacology, biochemistry, and behavior* 92(4): 629-634.

Saloman JL, Scheff NN, Snyder LM, Ross SE, Davis BM, Gold MS (2016). Gi-DREADD Expression in Peripheral Nerves Produces Ligand-Dependent Analgesia, as well as Ligand-Independent Functional Changes in Sensory Neurons. *The Journal of neuroscience : the official journal of the Society for Neuroscience* 36(42): 10769-10781.

Sara SJ (2009). The locus coeruleus and noradrenergic modulation of cognition. *Nature reviews. Neuroscience* 10(3): 211-223.

Sara SJ, Bouret S (2012). Orienting and reorienting: the locus coeruleus mediates cognition through arousal. *Neuron* 76(1): 130-141.

Sawangjit A, Oyanedel CN, Niethard N, Salazar C, Born J, Inostroza M (2018). The hippocampus is crucial for forming non-hippocampal long-term memory during sleep. *Nature* 564(7734): 109-113.

Sciolino NR, Plummer NW, Chen YW, Alexander GM, Robertson SD, Dudek SM*, et al.* (2016). Recombinase-Dependent Mouse Lines for Chemogenetic Activation of Genetically Defined Cell Types. *Cell reports* 15(11): 2563-2573.

Schabel FM, Jr. (1978). Fundamentals in cancer chemotherapy: introduction. *Antibiotics and chemotherapy* 23: 1-3.

Scholz J, Finnerup NB, Attal N, Aziz Q, Baron R, Bennett MI*, et al.* (2019). The IASP classification of chronic pain for ICD-11: chronic neuropathic pain. *Pain* 160(1): 53-59.

Schwarz LA, Luo L (2015). Organization of the locus coeruleus-norepinephrine system. *Current biology : CB* 25(21): R1051-R1056.

Sears RM, Fink AE, Wigestrand MB, Farb CR, de Lecea L, Ledoux JE (2013). Orexin/hypocretin system modulates amygdala-dependent threat learning through the locus coeruleus. *Proceedings of the National Academy of Sciences of the United States of America* 110(50): 20260-20265.

Sellmeijer J, Mathis V, Hugel S, Li XH, Song Q, Chen QY*, et al.* (2018). Hyperactivity of Anterior Cingulate Cortex Areas 24a/24b Drives Chronic Pain-Induced Anxiodepressive-like Consequences. *The Journal of neuroscience : the official journal of the Society for Neuroscience* 38(12): 3102-3115.

Seminowicz DA, Laferriere AL, Millecamps M, Yu JS, Coderre TJ, Bushnell MC (2009). MRI structural brain changes associated with sensory and emotional function in a rat model of long-term neuropathic pain. *NeuroImage* 47(3): 1007-1014.

Seno MDJ, Assis DV, Gouveia F, Antunes GF, Kuroki M, Oliveira CC*, et al.* (2018). The critical role of amygdala subnuclei in nociceptive and depressive-like behaviors in peripheral neuropathy. *Scientific reports* 8(1): 13608.

Shackman AJ, Salomons TV, Slagter HA, Fox AS, Winter JJ, Davidson RJ (2011). The integration of negative affect, pain and cognitive control in the cingulate cortex. *Nature reviews. Neuroscience* 12(3): 154-167.

Shanthanna H, Strand NH, Provenzano DA, Lobo CA, Eldabe S, Bhatia A*, et al.* (2020). Caring for patients with pain during the COVID-19 pandemic: consensus recommendations from an international expert panel. *Anaesthesia* 75(7): 935-944.

Sheng J, Liu S, Wang Y, Cui R, Zhang X (2017). The Link between Depression and Chronic Pain: Neural Mechanisms in the Brain. *Neural plasticity* 2017: 9724371.

Shi TJ, Winzer-Serhan U, Leslie F, Hokfelt T (1999). Distribution of alpha2-adrenoceptor mRNAs in the rat lumbar spinal cord in normal and axotomized rats. *Neuroreport* 10(13): 2835-2839.

Sindrup SH, Otto M, Finnerup NB, Jensen TS (2005). Antidepressants in the treatment of neuropathic pain. *Basic & clinical pharmacology & toxicology* 96(6): 399-409.

Singer T, Seymour B, O'Doherty J, Kaube H, Dolan RJ, Frith CD (2004). Empathy for pain involves the affective but not sensory components of pain. *Science* 303(5661): 1157-1162.

Siuda ER, Al-Hasani R, McCall JG, Bhatti DL, Bruchas MR (2016). Chemogenetic and Optogenetic Activation of Galphas Signaling in the Basolateral Amygdala Induces Acute and Social Anxiety-Like States. *Neuropsychopharmacology : official publication of the American College of Neuropsychopharmacology* 41(8): 2011-2023.

Sluka KA, Westlund KN (1992). Spinal projections of the locus coeruleus and the nucleus subcoeruleus in the Harlan and the Sasco Sprague-Dawley rat. *Brain research* 579(1): 67-73.

Smith BH, Elliott AM, Chambers WA, Smith WC, Hannaford PC, Penny K (2001). The impact of chronic pain in the community. *Family practice* 18(3): 292-299.

Smith BH, Torrance N (2011). Management of chronic pain in primary care. *Current opinion in supportive and palliative care* 5(2): 137-142.

Smith LJ, Shih A, Miletic G, Miletic V (2002). Continual systemic infusion of lidocaine provides analgesia in an animal model of neuropathic pain. *Pain* 97(3): 267-273.

Song Z, Ansah OB, Meyerson BA, Pertovaara A, Linderoth B (2013). Exploration of supraspinal mechanisms in effects of spinal cord stimulation: role of the locus coeruleus. *Neuroscience* 253: 426-434.

Sotgiu ML, Valente M, Storchi R, Caramenti G, Mario Biella GE (2008). Contribution by DRt descending facilitatory pathways to maintenance of spinal neuron sensitization in rats. *Brain research* 1188: 69-75.

Spangler SM, Bruchas MR (2017). Optogenetic approaches for dissecting neuromodulation and GPCR signaling in neural circuits. *Current opinion in pharmacology* 32: 56-70.

Suto T, Eisenach JC, Hayashida K (2014). Peripheral nerve injury and gabapentin, but not their combination, impair attentional behavior via direct effects on noradrenergic signaling in the brain. *Pain* 155(10): 1935-1942.

T

Tang NK, Crane C (2006). Suicidality in chronic pain: a review of the prevalence, risk factors and psychological links. *Psychological medicine* 36(5): 575-586.

Tavares I, Lima D (2002). The caudal ventrolateral medulla as an important inhibitory modulator of pain transmission in the spinal cord. *The journal of pain* 3(5): 337-346.

Taylor BK (2009). Spinal inhibitory neurotransmission in neuropathic pain. *Current pain and headache reports* 13(3): 208-214.

Taylor BK, Roderick RE, Basbaum AI (2000). Brainstem noradrenergic control of nociception is abnormal in the spontaneously hypertensive rat. *Neuroscience letters* 291(3): 139-142.

Taylor BK, Westlund KN (2017). The noradrenergic locus coeruleus as a chronic pain generator. *Journal of neuroscience research* 95(6): 1336-1346.

Torralba A MA, Darba J (2014). Situación actual del dolor crónico en España: iniciativa" Pain Proposal". . *Revista de la Sociedad Española del Dolor* 21(1): 16-22.

Treede RD, Rief W, Barke A, Aziz Q, Bennett MI, Benoliel R*, et al.* (2019). Chronic pain as a symptom or a disease: the IASP Classification of Chronic Pain for the International Classification of Diseases (ICD-11). *Pain* 160(1): 19-27.

Truini A, Cruccu G (2006). Pathophysiological mechanisms of neuropathic pain. *Neurological sciences : official journal of the Italian Neurological Society and of the Italian Society of Clinical Neurophysiology* 27 Suppl 2: S179-182.

Tsuruoka M, Matsutani K, Inoue T (2003). Coeruleospinal inhibition of nociceptive processing in the dorsal horn during unilateral hindpaw inflammation in the rat. *Pain* 104(1-2): 353-361.

Tsuruoka M, Willis WD (1996a). Descending modulation from the region of the locus coeruleus on nociceptive sensitivity in a rat model of inflammatory hyperalgesia. *Brain research* 743(1-2): 86-92.

Tsuruoka M, Willis WD, Jr. (1996b). Bilateral lesions in the area of the nucleus locus coeruleus affect the development of hyperalgesia during carrageenan-induced inflammation. *Brain research* 726(1-2): 233-236.

U

Uematsu A, Tan BZ, Ycu EA, Cuevas JS, Koivumaa J, Junyent F*, et al.* (2017). Modular organization of the brainstem noradrenaline system coordinates opposing learning states. *Nature neuroscience* 20(11): 1602-1611.

Ulrich-Lai YM, Xie W, Meij JT, Dolgas CM, Yu L, Herman JP (2006). Limbic and HPA axis function in an animal model of chronic neuropathic pain. *Physiology & behavior* 88(1-2): 67-76.

V

Valentino RJ, Van Bockstaele E (2008). Convergent regulation of locus coeruleus activity as an adaptive response to stress. *European journal of pharmacology* 583(2-3): 194-203.

van Hecke O, Torrance N, Smith BH (2013). Chronic pain epidemiology and its clinical relevance. *British journal of anaesthesia* 111(1): 13-18.

Vartiainen N, Kirveskari E, Kallio-Laine K, Kalso E, Forss N (2009). Cortical reorganization in primary somatosensory cortex in patients with unilateral chronic pain. *The journal of pain* 10(8): 854-859.

Veinante P, Yalcin I, Barrot M (2013). The amygdala between sensation and affect: a role in pain. *Journal of molecular psychiatry* 1(1): 9.

Verdejo-Garcia A, Bechara A, Recknor EC, Perez-Garcia M (2006). Executive dysfunction in substance dependent individuals during drug use and abstinence: an examination of the behavioral, cognitive and emotional correlates of addiction. *Journal of the International Neuropsychological Society : JINS* 12(3): 405-415.

Viisanen H, Pertovaara A (2007). Influence of peripheral nerve injury on response properties of locus coeruleus neurons and coeruleospinal antinociception in the rat. *Neuroscience* 146(4): 1785-1794.

Villanueva L, Bing Z, Bouhassira D, Le Bars D (1991). Depressive effects of mu and delta opioid receptor agonists on activities of dorsal horn neurones are enhanced by dibencozide. *The Journal of pharmacology and experimental therapeutics* 257(3): 1198-1202.

Villanueva L, Bing Z, Bouhassira D, Le Bars D (1989). Encoding of electrical, thermal, and mechanical noxious stimuli by subnucleus reticularis dorsalis neurons in the rat medulla. *Journal of neurophysiology* 61(2): 391-402.

Villanueva L, Bouhassira D, Bing Z, Le Bars D (1988). Convergence of heterotopic nociceptive information onto subnucleus reticularis dorsalis neurons in the rat medulla. *Journal of neurophysiology* 60(3): 980-1009.

Vogt BA (2005). Pain and emotion interactions in subregions of the cingulate gyrus. *Nature reviews. Neuroscience* 6(7): 533-544.

Vranken JH (2012). Elucidation of pathophysiology and treatment of neuropathic pain. *Central nervous system agents in medicinal chemistry* 12(4): 304-314.

W

Wang J, Tu J, Cao B, Mu L, Yang X, Cong M*, et al.* (2017a). Astrocytic l-Lactate Signaling Facilitates Amygdala-Anterior Cingulate Cortex Synchrony and Decision Making in Rats. *Cell reports* 21(9): 2407-2418.

Wang YJ, Zuo ZX, Wu C, Liu L, Feng ZH, Li XY (2017b). Cingulate Alpha-2A Adrenoceptors Mediate the Effects of Clonidine on Spontaneous Pain Induced by Peripheral Nerve Injury. *Frontiers in molecular neuroscience* 10: 289.

Wei, H., Viisanen, H., You, H. J., & Pertovaara, A. (2016). Spinal histamine in attenuation of mechanical hypersensitivity in the spinal nerve ligation-induced model of experimental neuropathy. *European journal of pharmacology*, *772*, 1-10.

Wei F, Dubner R, Ren K (1999). Nucleus reticularis gigantocellularis and nucleus raphe magnus in the brain stem exert opposite effects on behavioral hyperalgesia and spinal Fos protein expression after peripheral inflammation. *Pain* 80(1-2): 127-141.

Wei H, Pertovaara A (2006). Spinal and pontine alpha2-adrenoceptors have opposite effects on pain-related behavior in the neuropathic rat. *European journal of pharmacology* 551(1-3): 41-49.

Wei H, Viisanen H, You HJ, Pertovaara A (2016). Spinal histamine in attenuation of mechanical hypersensitivity in the spinal nerve ligation-induced model of experimental neuropathy. *European journal of pharmacology* 772: 1-10.

Weinshenker D (2018). Long Road to Ruin: Noradrenergic Dysfunction in Neurodegenerative Disease. *Trends in neurosciences* 41(4): 211-223.

Westlund KN, Bowker RM, Ziegler MG, Coulter JD (1983). Noradrenergic projections to the spinal cord of the rat. *Brain research* 263(1): 15-31.

Westlund KN, Coulter JD (1980). Descending projections of the locus coeruleus and subcoeruleus/medial parabrachial nuclei in monkey: axonal transport studies and dopamine-beta-hydroxylase immunocytochemistry. *Brain research* 2(3): 235-264.

Westlund KN, Craig AD (1996). Association of spinal lamina I projections with brainstem catecholamine neurons in the monkey. *Experimental brain research* 110(2): 151-162.

Westlund KN, Sorkin LS, Ferrington DG, Carlton SM, Willcockson HH, Willis WD (1990). Serotoninergic and noradrenergic projections to the ventral posterolateral nucleus of the monkey thalamus. *The Journal of comparative neurology* 295(2): 197-207.

Wiech K, Tracey I (2009). The influence of negative emotions on pain: behavioral effects and neural mechanisms. *NeuroImage* 47(3): 987-994.

Wilkinson LO, Abercrombie ED, Rasmussen K, Jacobs BL (1987). Effect of buspirone on single unit activity in locus coeruleus and dorsal raphe nucleus in behaving cats. *European journal of pharmacology* 136(1): 123-127.

Wilson KG, Mikail SF, D'Eon JL, Minns JE (2001). Alternative diagnostic criteria for major depressive disorder in patients with chronic pain. *Pain* 91(3): 227-234.

X

Xiao X, Zhang YQ (2018). A new perspective on the anterior cingulate cortex and affective pain. *Neuroscience and biobehavioral reviews* 90: 200-211.

Xu M, Kontinen VK, Kalso E (1999). Endogenous noradrenergic tone controls symptoms of allodynia in the spinal nerve ligation model of neuropathic pain. *European journal of pharmacology* 366(1): 41-45.

Y

Yalcin I, Bohren Y, Waltisperger E, Sage-Ciocca D, Yin JC, Freund-Mercier MJ*, et al.* (2011). A time-dependent history of mood disorders in a murine model of neuropathic pain. *Biological psychiatry* 70(10): 946-953.

Yoshizumi M, Parker RA, Eisenach JC, Hayashida K (2012). Gabapentin inhibits gamma-amino butyric acid release in the locus coeruleus but not in the spinal dorsal horn after peripheral nerve injury in rats. *Anesthesiology* 116(6): 1347-1353.

Z

Zaletel I, Filipovic D, Puskas N (2016). Chronic stress, hippocampus and parvalbumin-positive interneurons: what do we know so far? *Reviews in the neurosciences* 27(4): 397-409.

Zerbi V, Floriou-Servou A, Markicevic M, Vermeiren Y, Sturman O, Privitera M*, et al.* (2019). Rapid Reconfiguration of the Functional Connectome after Chemogenetic Locus Coeruleus Activation. *Neuron* 103(4): 702-718 e705.

Zhang J, Li X, Ren Y, Zhao Y, Xing A, Jiang C*, et al.* (2018). Intermittent Fasting Alleviates the Increase of Lipoprotein Lipase Expression in Brain of a Mouse Model of Alzheimer's Disease: Possibly Mediated by beta-hydroxybutyrate. *Frontiers in cellular neuroscience* 12: 1.

Zhang Z, Cordeiro Matos S, Jego S, Adamantidis A, Seguela P (2013). Norepinephrine drives persistent activity in prefrontal cortex via synergistic alpha1 and alpha2 adrenoceptors. *PloS one* 8(6): e66122.

Zimmermann M (1983). Ethical guidelines for investigations of experimental pain in conscious animals. *Pain* 16(2): 109-110.

Zhu, H., & Roth, B. L. (2015). DREADD: a chemogenetic GPCR signaling platform. *International Journal of Neuropsychopharmacology*, *18*(1).

Progress in Neuro-Psychopharmacology & Biological Psychiatry 70 (2016) 57–67

Contents lists available at ScienceDirect

Progress in Neuro-Psychopharmacology & Biological Psychiatry

journal homepage: www.elsevier.com/locate/pnp

Effect of DSP4 and desipramine in the sensorial and affective component of neuropathic pain in rats

Lidia Bravo [a,b,c], Juan A. Mico [a,b,d], Raquel Rey-Brea [a], Carmen Camarena-Delgado [a], Esther Berrocoso [a,b,c,*]

[a] Neuropsychopharmacology & Psychobiology Research Group, University of Cádiz, Spain
[b] Centro de Investigación Biomédica en Red de Salud Mental (CIBERSAM), Instituto de Salud Carlos III, 28007 Madrid, Spain
[c] Psychobiology Area, Department of Psychology, University of Cadiz, Spain
[d] Department of Neuroscience, University of Cádiz, Spain

ARTICLE INFO

Article history:
Received 13 October 2015
Received in revised form 8 May 2016
Accepted 9 May 2016
Available online 12 May 2016

Chemical compounds studied in this article:
Acetone (PubChem CID: 180)
Chloral hydrate (PubChem CID: 270)
Desipramine (PubChem CID: 2995)
DSP4, [N-(2-chloroethyl)-N-ethyl-2-bromobenzylamine hydrochloride] (PubChem CID: 3172)
Ketamine Hydrochloride (PubChem CID:15851)
Sodium chloride (PubChem CID: 5234)
Xylazine: (PubChem CID: 5707)

ABSTRACT

Previous findings suggest that neuropathic pain induces characteristic changes in the noradrenergic system that may modify the sensorial and affective dimensions of pain. We raise the hypothesis that different drugs that manipulate the noradrenergic system can modify specific domains of pain. In the chronic constriction injury (CCI) model of neuropathic pain, the sensorial (von Frey and acetone tests) and the affective (place escape/avoidance paradigm) domains of pain were evaluated in rats 1 and 2 weeks after administering the noradrenergic neurotoxin [N-(2-chloroethyl)-N-ethyl-2-bromobenzylamine hydrochloride] (DSP4, 50 mg/kg). In other animals, we evaluated the effect of enhancing noradrenergic tone in the 2 weeks after injury by administering the antidepressant desipramine (10 mg/kg/day, delivered by osmotic minipumps) during this period, a noradrenaline reuptake inhibitor. Moreover, the phosphorylation of the extracellular signal regulated kinases (p-ERK) in the anterior cingulate cortex (ACC) was also assessed. The ACC receives direct inputs from the main noradrenergic nucleus, the locus coeruleus, and ERK activation has been related with the expression of pain-related negative affect. These studies revealed that DSP4 almost depleted noradrenergic axons in the ACC and halved noradrenergic neurons in the locus coeruleus along with a decrease in the affective dimension and an increased of p-ERK in the ACC. However, it did not modify sensorial pain perception. By contrast, desipramine reduced pain hypersensitivity, while completely impeding the reduction of the affective pain dimension and without modifying the amount of p-ERK. Together results suggest that the noradrenergic system may regulate the sensorial and affective sphere of neuropathic pain independently.

Keywords:
Neuropathic pain
DSP4 [N-(2-chloroethyl)-N-ethyl-2-bromobenzylamine hydrochloride]
Antidepressant
Affective component of pain
Sensory component of pain
Anterior cingulate cortex

1. Introduction

Neuropathic pain is a complex multifaceted experience that mainly involves two different dimensions: sensorial and affective. At present, it is accepted that sensory pain provides us with information about the location, quality and intensity of a noxious stimulus. However, the affective dimension of the pain experience is comprised of unpleasant emotional aspects and salient fear of the noxious stimulus, which has been correlated with the complex behaviors of escape and avoidance (Price, 2000; Price et al., 1980). While the existence of both dimensions has been extensively reported, the biological mechanisms underlying the sensory and specially the so called "affective pain" are still poorly understood. We previously demonstrated that when rats suffering neuropathic pain were subjected to chronic stress for 2 weeks, the affective component of pain worsened without any relevant accompanying changes in the sensorial pain dimension (Bravo et al., 2013). That is, one dimension can deteriorate without affecting the other, which suggests that emotional aversive situations are processed independently of the sensorial perception. Furthermore, we found that a worsening in the affective component was associated with a disruption of the

* Corresponding author at: Department of Psychology, University of Cadiz, Campus Universitario Río San Pedro s/n, 11510 Puerto Real, Cadiz, Spain.
E-mail address: esther.berrocoso@uca.es (E. Berrocoso).

http://dx.doi.org/10.1016/j.pnpbp.2016.05.002
0278-5846/

locus coeruleus (LC) nucleus, the main source of noradrenaline in the central nervous system (CNS) (Bravo et al., 2013). Thus, it is likely that the noradrenergic system may be implicated in this dimension of pain.

The LC projects widely to all cortical areas (Jones et al., 1977) and it has been proposed that the LC-ACC (anterior cingulate cortex) neuronal circuit is involved in the behavioral strategies activated in the face of salient sensory stimuli (Aston-Jones and Cohen, 2005; Chandler et al., 2013). Furthermore, the affective component of pain seems to be largely processed in the ACC (Johansen et al., 2001; Rainville et al., 1997; Wager et al., 2004) and might be reflected by the accumulation of the phosphorylated form of the extracellular signal-regulated kinases 1/2 (p-ERK) (Borges et al., 2015; Cao et al., 2009; Han et al., 2014). Thus, in the present study we explored the role of the noradrenergic system in the sensory and affective component of pain in rats, in association with possible changes to the activation of ERK in the ACC. To this end, after inducing nerve injury, rats were administered a potent neurotoxin that preferentially destroys noradrenergic projections (N-(2-chloroethyl)-N-ethyl-2-bromobenzylamine [DSP4]: (Fritschy and Grzanna, 1989). Both pain components were then evaluated 1 and 2 weeks after surgery. In parallel, and in order to enhance noradrenergic tone, we also explored how early inhibition of noradrenaline reuptake affected these components by administering desipramine (DMI) instead of DSP4. DMI is a tricyclic antidepressant with demonstrated clinical analgesia in neuropathic pain (Finnerup, 2010; Gilron et al., 2015; Sindrup et al., 1990). In this way, we set out to study the overall implication of the noradrenergic system in the sensorial and/or affective sphere of pain after nerve injury.

2. Materials and methods

2.1. Experimental design

Adult male Harlan Sprague-Dawley rats initially weighing 200–250 g were provided by the Experimental Unit of the University of Cádiz (registration number ES110120000210). The experimental protocols were approved by the Committee for Animal Experimentation at the University of Cádiz and they complied with the ethical guidelines of the International Association for the Study of Pain (Zimmermann, 1983). The procedures for animal care and use conformed to the European Commission's directive 2010/63/EU and current Spanish Law (RD 1201/2005) regarding the care and use of laboratory animals. The experimental design (Fig. 2A) commenced with a habituation period in which the animals (four per cage) were kept under standard laboratory conditions: water and food ad libitum, constant room temperature (22 ± 1 °C), a 12 h light/dark cycle). After 3 weeks of habituation the animals were subjected to chronic constriction injury (CCI) surgery to induce neuropathic pain. On the same day of surgery, an external experimenter randomly allocated into six experimental groups according to the treatment (to assure the blinding conditions of the experimenter): *i*) sham-control (control animals, $n = 15$: sham-operated); *ii*) CCI-control (neuropathic pain control animals, $n = 15$); *iii*) Sham-[DSP4] (sham-operated and administered the noradrenergic neurotoxin, $n = 15$); iv) CCI-[DSP4] (neuropathic pain animals administered the noradrenergic neurotoxin, $n = 15$); v) sham-[DMI] (sham-operated animals administered the inhibitor of noradrenaline reuptake, $n = 15$); vi) CCI-[DMI] (neuropathic pain animals administered the inhibitor of the noradrenaline reuptake, $n = 15$). These six experimental groups were housed by the external experimenter in groups of 4 according to their condition, that is, animals of the same cage belonged to the same group (sham/CCI with or without treatment). 10 animals per group were randomly assigned to the behavioral evaluation (von Frey, cold plate and place/escape avoidance tests) and 4 animals from sham-[DSP-4] and CCI-[DSP4] groups were later selected for immunohistochemistry. The von Frey and cold plate tests were performed the same day (6 and 13 days after nerve injury), maintaining an interval of 30 to 60 min between the testing procedures. The place escape/avoidance test was performed 1 day later. The place escape/avoidance test was also performed in the absence of paw stimulation in a parallel group of sham-control ($n = 11$), CCI-control ($n = 11$), sham-[DSP-4] ($n = 11$) and CCI-[DSP4] ($n = 10$). Furthermore, an independent set of animals ($n = 5$ rats per group) were used for western blotting studies. These animals were submitted to the von Frey test 1 week after surgery to check their nociceptive thresholds.

2.2. Neuropathic pain model: chronic constriction injury

CCI was induced as described previously (Bennett and Xie, 1988; Bravo et al., 2012). Rats were anaesthetized with an intraperitoneal (ip) injection of 100 mg/kg ketamine and 20 mg/kg xylazine, and the common left sciatic nerve was exposed at the mid-thigh level proximal to the sciatic trifurcation and separated from the adjacent tissue. Four loose ligatures were tied around the dissected nerve using chromic catgut sutures (4–0) with a 1.5 mm interval between each pair of ligatures. The overlying muscle was closed in layers with synthetic absorbable surgical suture (4–0) and the skin was sutured with silk thread (2–0). An identical dissection was performed on sham-operated animals but the sciatic nerve was not ligated. After the surgery, 1 CCI animal (belonging to CCI-[DMI] group) was excluded from the study because it showed autotomy of the distal phalanges. Furthermore, 5 sham animals did not survive to the surgery (1 sham-control, 3 sham-[DSP4] and 1 sham-[DMI]).

2.3. Treatment

Once the animals had recovered from the CCI surgery, one group of animals received N-(2-chloroethyl)-N-ethyl-2-bromobenzylamine (DSP4), a noradrenergic neurotoxin (50 mg/kg ip; Sigma, St. Louis, MO, USA) or the vehicle alone (Grzanna et al., 1989; Hormigo et al., 2012). In another set of animals, desipramine (DMI, 10 mg/kg/day; Sigma-Aldrich Chemicals, Madrid, Spain) or the vehicle was administered subcutaneously (sc) for two weeks. To this end, osmotic minipumps (Alzet Corp., Model 2ML2, California, USA) were implanted subcutaneously during CCI surgery through an incision of 1.5 times the diameter of the pump and perpendicular to the pump's long axis(Alba-Delgado et al., 2012b). DMI dose was chosen on the basis of pilot studies performed in our laboratory and on the data available in the literature regarding its analgesic effect in neuropathic animals (Alba-Delgado et al., 2012b; Jett et al., 1997; Ortega-Alvaro et al., 1997; Yalcin et al., 2009). All the drugs were dissolved in isotonic saline solution (NaCl 0.9%).

2.4. Sensorial dimension of pain

2.4.1. Mechanical allodynia (von Frey test)

In order to study sensory pain, mechanical allodynia was measured in rats using an automatic von Frey apparatus (Dynamic Plantar Anesthesiometer Cat. No.37400-002, Ugo Basile, Italy: (Bravo et al., 2013). Animals were randomly placed in plastic cages with an operable metal grid to which they had been habituated for 30 min prior to the test. A vertical force was applied to the hind paw that increased from 0 to 50 g over a period of 20 s, and the threshold was determined as the average of two values that induced a withdrawal response (with a 50 g cut-off). Mechanical allodynia was determined once a week during the habituation (H3) and experimentation phases (E1 and E2: Fig. 2A).

2.4.2. Cold allodynia (acetone test)

Cold allodynia was studied in the same plastic cages as those described above for the von Frey test, allowing the rats to adapt to the testing environment for at least 15 min before placing a drop (100 μl) of acetone to the centre of the hindpaw with a pipette. Acetone was applied alternately five times to each hindpaw, with a 5 min delay between each successive application. Responses were monitored for

1 min after acetone application and they were graded on a 4-point scale, as described previously (Flatters and Bennett, 2004): 0, no response; 1, quick withdrawal, flick or stamp of the paw; 2, prolonged withdrawal or repeated flicking of the paw; 3, repeated flicking of the paw with persistent licking directed at the ventral side of the paw. The cumulative scores were then obtained by summing the four scores for each rat and dividing by 5 (the number of assays). Cold allodynia was determined once a week during the habituation (H3) and experimentation phases (E1 and E2: Fig. 2A).

2.5. Affective component of pain

2.5.1. Place escape/avoidance paradigm testing

To assess the emotional component of pain processing, place escape/avoidance testing was performed once a week during the experimental period (E1 and E2: Fig. 2A), in accordance with previously described protocols (Bravo et al., 2013, 2012; LaBuda and Fuchs, 2000). Animals were randomly placed in one half of a 60 × 30 × 30 cm Plexigas chamber divided into a light and dark area, and raised on an elevated metal grid. Once placed in the chamber, the animals were mechanically stimulated with a von Frey monofilament (60 g) on the plantar surface of the hindpaws at 15 s intervals for 30 min. If the animals were in the dark area the injured hindpaw was stimulated, whereas the non-injured hindpaw of the animals was stimulated in the light area. Thus, animals have to "choose" what they considered to be the least aversive side of the chamber: a dark-non-anxiogenic place in which the injured paw is stimulated or a bright mildly anxiogenic place in which the non-injured paw is stimulated. In order to rule out a possible anxiolytic effect of DSP4 in the test, another set of animals were submitted to the place escape avoidance apparatus without paw stimulation. Each test session was recorded and subsequently analyzed with Spontaneous Motor Activity Recording and Tracking software (Panlab S.L.U., Barcelona, Spain). The percentage time spent in the light area was scored at 5 min intervals.

2.6. Western blotting

At the end of the experimental phase, fresh tissue samples from the ipsilateral and contralateral ACC regions were collected. Animals were sacrificed with an overdose of chloral hydrate. The tissue was stored at 80 °C before analyzing all the samples in western blots. The tissue lysate (50 μg) was resolved on 10% polyacrylamide gels and the proteins transferred to a polyvinylidene difluoride membrane (PVDF; BioRad, Spain). After washing in TBST (Tris buffer saline with 0.1% Tween-20), the blots were blocked with 5% Bovine Serum Albumin (BSA; Sigma, Spain) in TBST and incubated overnight at 4 °C with a mixture of primary antibodies diluted in TBST plus 5% BSA: rabbit anti-phospho-ERK1/2 (1:5000; Neuromics (RA15002), USA), mouse anti-total-ERK1/2 (1:2000; Cell Signaling (L34F12), Izasa, Spain), and mouse anti-Tubulin (1:250,000; Sigma (T8203), Spain). After thorough washing, these primary antibodies were detected for 1 h at room temperature with IRDye 800CW goat anti-rabbit (green) or IRDye 680LT goat anti-mouse (red) secondary antibodies (1:10,000; Bonsai Advanced Technologies, Spain), and after 3 final washes with TBST the bound antibodies were visualized with a LI-COR Odyssey® two-channel quantitative fluorescence imaging system (Bonsai Advanced Technologies, Spain). Digital images of Western-blots were analyzed by densitometry using the free access ImageJ software.

2.7. Immunohistochemistry

One set of animals which were submitted to the behavioral tests from sham-control and sham-[DSP4] groups were perfused with paraformaldehyde (4%) at the end of the behavioral experiments (Alba-Delgado et al., 2012a). In order to test the efficacy of DSP4, tyrosine hydroxylase (TH) in the LC and A5 and dopamine beta hydroxylase (DβH) expression in the ACC were evaluated. For TH one in every four sequential sections (30 μm) was incubated, free-floating, with a sheep anti-tyrosine hydroxylase (1:1000; Abcam (ab113), UK). Subsequently, the sections were incubated, with an Alexa Fluor 568 donkey anti-sheep secondary antibody (1:1000; Invitrogen, Spain) before they were washed and coverslipped in fluoro-gel aqueous mounting medium.

For the expression of DβH, one in every six sequential section of the ACC (40 μm) were submitted to an inactivation of endogenous peroxidase with PBS containing 0.3% hydrogen peroxide (30 min) prior to the incubation with a mouse anti-dopamine beta hydroxylase (1:1000 Millipore (MAB308), USA) for 48 h at 4 °C. Subsequently, the sections were incubated 1 h and 30 min with a biotinylated donkey anti-mouse (1:200, Jackson Immunoresearch Europe). Afterwards, sections were incubated for another hour in avidin–biotin complex (ABC) conjugated with horseradish peroxidase (1:200). Visualization of the immunostaining was achieved using the 3.3′-diaminobenzidine tetrahydrochloride (DAB) reaction (5 min in 0.05 M Tris buffer containing 0.05% DAB and 0.003% hydrogen peroxide). Sections were mounted on gelatine-coated slides, cleared in xylene and coverslipped with Eukitt.

TH-immunoreactivity (TH-IR) and DβH-immunoreactivity (DβH-IR) were visualized on an Olympus BX60 microscope equipped with a U-MNU filter system. An experimenter blind to the conditions manually counted the labeled cell bodies (TH-IR) in an average of 6 sections per animal containing both LC and A5. The average number of TH-IR cells in each region was used to determine the effect of DSP4 on noradrenergic neurons. An experimenter blind to the conditions visualized the presence or absence of noradrenergic fibers in the ACC for each animal.

2.8. Statistical analysis

The data represent the means ± SEM and all the results were analyzed using STATISTICA 10.0 software (StatSoft, Tulsa, OK, USA), using either two or three-way analysis of variance (ANOVA), with or without repeated measures, as appropriate. The factors of variance were: CCI (between-groups), treatment (DSP4 or DMI, between-groups) and time (within-groups) (see Table 1 for detailed statistical analysis). Further analyses were carried out using a Bonferroni post-hoc test. A Student *t*-test was used in order to compare the expression of TH between two groups (sham-control vs sham-[DSP4]). As no differences were found between the ipsi- and contralateral sides in western blotting studies these data were pooled for the analyses. The level of significance considered was $p < 0.05$. Additionally a summary of the global effects of DSP4 and DMI treatment on chronic neuropathic pain is shown in the Table 2.

3. Results

3.1. Effect of DSP4 on noradrenergic neurons

To induce noradrenergic neuronal damage, a single intraperitoneal dose of DSP4 (50 mg/kg) was administered to control and CCI rats, as described previously (Fritschy and Grzanna, 1989, 1991). Fewer noradrenergic neurons were evident per section in the LC of rats that received DSP4 when compared with control group (26.96 vs 45.25 TH-IR neurons) 2 weeks after treatment ($p < 0.001$: Fig. 1A-C). However, DSP4 did not change the number of TH-IR cells in A5 (Fig. 1D-F). Furthermore, DSP4 almost depleted DβH immunoreative axons in the ipsi- and contralateral ACC (Fig. 1H and Fig. 1J), consistent with previous reports about the effect of DSP4 in the cortex (Cohen et al., 1997; Fritschy and Grzanna, 1989; Gonzalez and Aston-Jones, 2006; Gonzalez et al., 1998).

3.2. Effect of DSP4 and DMI administration on mechanical allodynia

The effect of noradrenergic disruption and increased noradrenaline availability on mechanical allodynia, induced by DSP4 and DMI,

Table 1
Summary of the statistical analysis. Data were analyzed by two-way or three-way analysis of variance (ANOVA), with or without repeated measures, as appropriate: $^{*}p < 0.05$, $^{**}p < 0.01$, $^{***}p < 0.001$.

Three-way ANOVA for surgery (CCI), treatment (DSP4) and time factors								
		CCI	DSP4	CCI*DSP4	Time	Time*CCI	Time*DSP4	Time*CCI*DSP4
von Frey test	I	$\mathbf{F_{(1.32)} = 75.61^{***}}$	$\mathbf{F_{(1.32)} = 3.34^{*}}$	$F_{(1.32)} = 0.02$	$\mathbf{F_{(2.64)} = 95.94^{***}}$	$\mathbf{F_{(2.64)} = 53.06^{***}}$	$F_{(2.64)} = 0.13$	$F_{(2.64)} = 1.37$
	C	$F_{(1.32)} = 0.46$	$F_{(1.32)} = 0.22$	$F_{(1.32)} = 0.00$	$F_{(2.64)} = 0.63$	$F_{(2.64)} = 0.66$	$F_{(2.64)} = 1.24$	$F_{(2.64)} = 0.60$
Acetone test	I	$\mathbf{F_{(1.32)} = 265.47^{***}}$	$F_{(1.32)} = 0.10$	$F_{(1.32)} = 1.52$	$\mathbf{F_{(2.64)} = 90.68^{***}}$	$\mathbf{F_{(2.64)} = 89.90^{***}}$	$F_{(2.64)} = 0.96$	$\mathbf{F_{(2.64)} = 5.95^{**}}$
	C	$F_{(1.32)} = 0.17$	$F_{(1.32)} = 0.00$	$F_{(1.32)} = 0.04$	$F_{(2.64)} = 0.84$	$F_{(2.64)} = 1.46$	$\mathbf{F_{(2.64)} = 5.66^{**}}$	$F_{(2.64)} = 2.36$
Place escape/avoidance test	First	$\mathbf{F_{(1.32)} = 6.97^{*}}$	$F_{(1.32)} = 0.10$	$F_{(1.32)} = 0.00$	$F_{(5.160)} = 0.82$	$F_{(5.160)} = 2.44$	$F_{(5.160)} = 1.78$	$F_{(5.160)} = 1.90$
	Second	$\mathbf{F_{(1.32)} = 37.86^{***}}$	$\mathbf{F_{(1.32)} = 6.20^{*}}$	$\mathbf{F_{(1.32)} = 4.95^{*}}$	$F_{(5.160)} = 1.07$	$\mathbf{F_{(5.160)} = 12.88^{***}}$	$F_{(5.160)} = 0.82$	$F_{(5.160)} = 0.90$
Place escape/avoidance test without stimulation	First	$\mathbf{F_{(1,39)} = 14.18^{***}}$	$\mathbf{F_{(1,39)} = 5.80^{*}}$	$F_{(1,39)} = 0.09$	$F_{(5195)} = 1.50$	$F_{(5195)} = 0.25$	$F_{(5195)} = 1.17$	$F_{(5195)} = 0.39$
	Second	$\mathbf{F_{(1,39)} = 9.56^{**}}$	$\mathbf{F_{(1,39)} = 4.27^{*}}$	$F_{(1,39)} = 0.29$	$F_{(5195)} = 13.76$	$F_{(5195)} = 1.84$	$F_{(5195)} = 2.04$	$F_{(5195)} = 0.41$
p-ERK		$F_{(1.16)} = 3.37$	$\mathbf{F_{(1.16)} = 14.50^{**}}$	$F_{(1.16)} = 2.74$				
t-ERK		$F_{(1.16)} = 3.59$	$F_{(1.16)} = 0.76$	$F_{(1.16)} = 0.59$				
Three-way ANOVA for surgery (CCI), treatment (DMI) and time factors								
		CCI	DMI	CCI*DMI	Time	Time*CCI	Time*DMI	Time*CCI*DMI
von Frey test	I	$\mathbf{F_{(1.33)} = 53.97^{***}}$	$\mathbf{F_{(1.33)} = 7.56^{**}}$	$F_{(1.33)} = 2.15$	$\mathbf{F_{(2.66)} = 56.80^{***}}$	$\mathbf{F_{(2.66)} = 35.01^{***}}$	$F_{(2.66)} = 0.88$	$F_{(2.66)} = 0.99$
	C	$F_{(1.33)} = 0.25$	$F_{(1.33)} = 3.22$	$F_{(1.33)} = 0.12$	$F_{(2.66)} = 0.27$	$F_{(2.66)} = 0.36$	$F_{(2.66)} = 0.39$	$F_{(2.66)} = 0.26$
Acetone test	I	$\mathbf{F_{(1.33)} = 58.74^{***}}$	$\mathbf{F_{(1.33)} = 16.84^{***}}$	$\mathbf{F_{(1.33)} = 13.17^{***}}$	$\mathbf{F_{(2.66)} = 32.91^{***}}$	$\mathbf{F_{(2.66)} = 39.13^{***}}$	$\mathbf{F_{(2.66)} = 8.68^{***}}$	$\mathbf{F_{(2.66)} = 4.44^{*}}$
	C	$F_{(1.33)} = 0.18$	$F_{(1.33)} = 0.65$	$F_{(1.33)} = 0.04$	$F_{(2.66)} = 1.32$	$F_{(2.66)} = 0.45$	$\mathbf{F_{(2.66)} = 5.39^{**}}$	$F_{(2.66)} = 0.09$
Place escape/avoidance test	First	$F_{(1.33)} = 0.44$	$F_{(1.33)} = 2.05$	$F_{(1.33)} = 3.98$	$F_{(5.165)} = 2.00$	$\mathbf{F_{(5.165)} = 3.76^{**}}$	$F_{(5.165)} = 0.60$	$F_{(5.165)} = 1.98$
	Second	$F_{(1.33)} = 3.57$	$\mathbf{F_{(1.33)} = 4.27^{*}}$	$\mathbf{F_{(1.33)} = 6.87^{*}}$	$\mathbf{F_{(5.165)} = 4.00^{**}}$	$F_{(5.165)} = 2.08$	$F_{(5.165)} = 1.59$	$\mathbf{F_{(5.165)} = 2.47^{*}}$
p-ERK		$F_{(1.16)} = 0.07$	$F_{(1.16)} = 0.91$	$F_{(1.16)} = 0.00$				
t-ERK		$F_{(1.16)} = 1.00$	$F_{(1.16)} = 1.00$	$F_{(1.16)} = 0.99$				

Abbreviations: CCI, chronic constriction injury; DMI, desipramine; DSP4, N-(2-chloroethyl)-N-ethyl-2-bromobenzylamine; I, ipsilateral; C, contralateral.

respectively, was evaluated weekly during the experimental phase with the von Frey test (Fig. 2A and Table 1). A three-way repeated measures ANOVA for the ipsilateral hindpaw revealed a significant effect of CCI, Time and the Time*CCI interaction ($p < 0.001$) after DSP4 administration, and a significant effect of DSP4 treatment ($p < 0.05$). Subsequently, a Bonferroni post-hoc test revealed significant differences for CCI-control versus sham-control rats ($p < 0.001$) and versus sham-[DSP4] animals ($p < 0.01$: Fig. 2B) in the first and second week ($p < 0.001$: Fig. 2B). Likewise, the sensorial threshold was lower in CCI-[DSP4] than in sham-control and sham-[DSP4] animals (E1 and E2, $p < 0.001$: Fig 2B). However, DSP4 administration to control or CCI rats did not modify the nociceptive mechanical threshold relative to the respective control and CCI animals (Fig. 2B). Thus, although DSP4 treatment revealed a statistically significant effect in the three way repeated measures ANOVA, this effect did not seem to be biologically relevant. By contrast, a three way repeated measures ANOVA for the contralateral hindpaw did not show any significant effect of CCI or DSP4 administration (Table 1 and Fig. 2C).

In terms of the effect of DMI on mechanical allodynia, the three-way repeated measures ANOVA for the ipsilateral hindpaw revealed a significant effect of DMI ($p < 0.01$). The post-hoc test revealed that CCI-[DMI] rats developed mechanical allodynia after one week of surgery, although the severity of mechanical allodynia was weaker than that shown by CCI-control rats after two weeks of surgery ($p < 0.001$: Fig. 2D). Similar analysis of the contralateral hindpaw failed to reveal a significant effect of DMI (Fig. 2E). Overall, the sensorial responses of the ipsilateral hindpaw to mechanical stimulation were similar in the CCI rats irrespective of whether they received DSP4, while DMI reduced mechanical allodynia in neuropathic rats. No effect in the mechanical pain threshold was observed in the sham-[DSP4] or sham-[DMI] rats (ipsilateral or contralateral).

3.3. Effect of DSP4 and DMI administration on cold allodynia

The effect of DSP4 and DMI on cold allodynia was evaluated in a similar manner, once weekly during the experimental phase (Fig. 2A and Table 1). After DSP4 administration, the three-way repeated measures ANOVA of the ipsilateral hindpaw revealed a significant effect of CCI, Time and Time*CCI ($p < 0.001$), as well as an effect of the Time*CCI*DSP4 interaction ($p < 0.01$). However, the post-hoc analysis revealed that CCI-control and CCI-[DSP4] rats had similar pronounced cold allodynia compared with the sham-control and sham-[DSP4] animals ($p < 0.001$: Fig. 3A). The three-way repeated measures ANOVA for the contralateral hindpaw showed a significant effect for Time*DSP4 ($p < 0.01$), yet post hoc analysis did not show any differences between these groups.

Regarding DMI administration, there was a significant effect for all the variables when a three-way repeated measures ANOVA was performed for the ipsilateral hindpaw. After one week of surgery, CCI-control rats developed cold allodynia and Bonferroni post-hoc test revealed a significant effect relative to the sham-control and sham-[DMI] rats ($p < 0.001$ respectively: Fig. 3C). Conversely, while CCI-[DMI] animals had a lower pain hypersensitivity than CCI-control rats ($p < 0.001$), they still displayed more pronounced allodynia after one week than the sham-control ($p < 0.01$), sham-[DMI] rats ($p < 0.05$: Fig. 3C). However, after two weeks of DMI treatment, CCI-[DMI] rats scored similarly in the cold allodynia test than sham-control and sham-[DMI] rats, with differences only evident when comparing them with the CCI-control animals ($p < 0.001$: Fig. 3C). Therefore, the sensorial responses of the ipsilateral hindpaw to acetone were similar in CCI rats irrespective of DSP4 administration, while DMI reduced cold allodynia in neuropathic rats. No significant effect was observed in the sham-[DSP4] or sham-[DMI] animals.

3.4. Effect of DSP4 and DMI administration in the place escape/avoidance test

The affective-emotional component of pain was evaluated once weekly during the experimental phase (Fig. 2A and Table 1). In order

Table 2
Summary of the global effects of DSP4 and DMI treatment on chronic neuropathic pain.

		Sham-control	CCI-control	Sham-[DSP4]	CCI-[DSP4]	Sham-[DMI]	CCI-[DMI]
Sensory pain							
Mechanical allodynia	I	0	+++	0	+++	0	+
	C	0	0	0	0	0	0
Cold allodynia	I	0	+++	0	+++	0	+
	C	0	0	0	0	0	0
Affective pain							
First week		0	+	0	+	0	0
Second week		0	++	0	+++	0	0
Anterior Cingulate Cortex							
pERK		0	0	0	++	0	0
tERK		0	0	0	0	0	0

Global effect vs sham-control group: 0, no effect; +, slight effect; ++, medium effect; +++, strong effect.
Abbreviations: CCI, chronic constriction injury; C, contralateral; I, ipsilateral.

to rule out any anxiolytic effect of DSP4, a set of animals were submitted to the place escape/avoidance apparatus without paw stimulation. For this group, the three-way repeated measure ANOVA for the percentage of time within light area revealed a significant effect of CCI and DSP4 after one week ($p < 0.001$ and $p < 0.05$, respectively) and two weeks ($p < 0.01$ and $p < 0.05$, respectively) of surgery and treatment (Table 1). Subsequently, Bonferroni post-hoc analysis revealed that CCI-control rats spent less time in the light area at 15 min than sham-control rats, one and two weeks after surgery ($p < 0.05$: Fig. 4A). The same analysis revealed that CCI-[DSP4] rats spent less time in the light area than sham-control after one week of experimentation at 15 and 25 min ($p < 0.01$ and $p < 0.05$: Fig. 4A) and after two weeks at 15 and 20 min ($p < 0.05$: Fig. 4B). However, no differences were found between CCI-control and CCI-[DSP4] groups.

Regarding to the affective-emotional component of pain, the three-way repeated measure ANOVA for the place escape/avoidance test revealed a significant effect of CCI after one week of neuropathic pain and DSP4 administration ($p < 0.01$), but no significant effects for the others factors. After two weeks, the same analysis revealed a significant effect of CCI ($p < 0.001$), DSP4 ($p < 0.05$), CCI*DSP4 ($p < 0.05$) and Time*CCI ($p < 0.001$). The comparison among the groups revealed that the CCI-control rats spent more time in the light area over 30 min than sham-control rats one and two weeks after surgery ($p < 0.01$ and $p < 0.001$ respectively: Fig. 4C and D. Bravo et al., 2012). There was a significant effect in CCI-[DSP4] animals after 20 min compared with sham-control rats ($p < 0.05$: Fig. 4C). Interestingly, this behavior was more evident in the CCI-[DSP4] group two weeks after surgery and DSP4 administration, which was significant from 10 min after the beginning of the test when compared with sham-control rats, and from 15 min when compared with the sham-[DSP4] animals ($p < 0.001$: Fig. 4D). Furthermore, the escape behavior of CCI-[DSP4] rats was significantly stronger than that in CCI-control animals 10 and 30 min into the test ($p < 0.05$ and $p < 0.001$, respectively: Fig. 4D), suggesting a worsening of the affective pain in the CCI-[DSP4] animals.

For the rats that received DMI, there were significant differences for Time*CCI in the three-way repeated measures ANOVA one week after surgery ($p < 0.01$). After two weeks, the same analysis revealed a significant effect of DMI and CCI*DMI ($p < 0.05$), as well as an effect of Time ($p < 0.01$) and Time*CCI*DMI ($p < 0.05$). Subsequent post-hoc analysis revealed that one week after surgery and DMI administration, the CCI-control rats spent more time in the light area than the CCI-[DMI] rats 25 and 30 min into the test ($p < 0.05$: Fig. 4E). Since this effect persisted

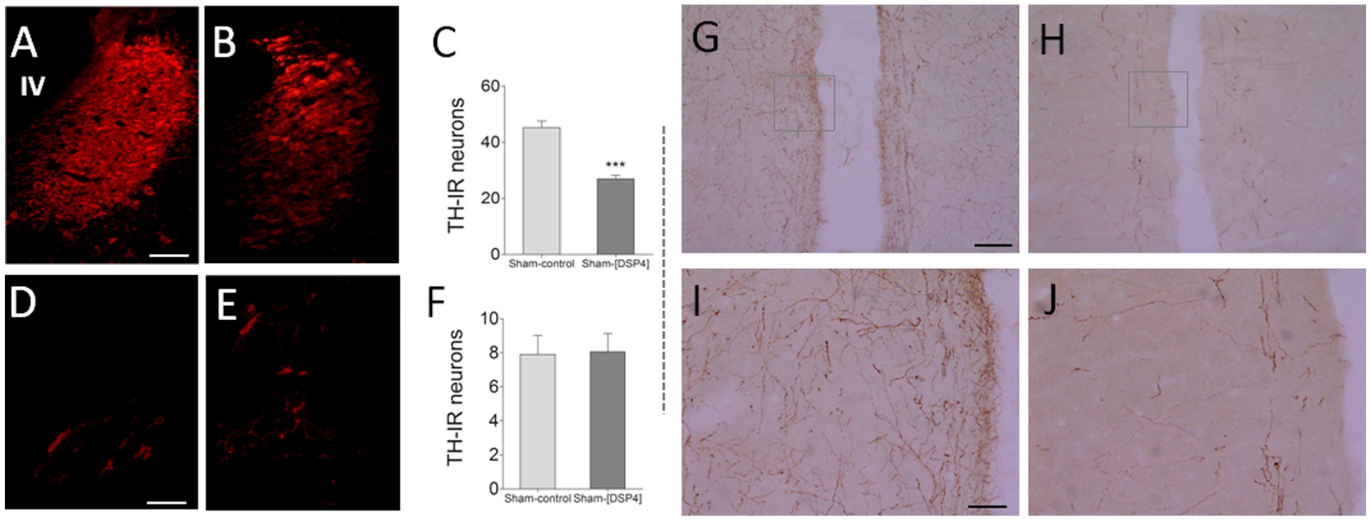

Fig. 1. Expression of TH-IR neurons in LC and A5 (A-F) and DβH-IR axons in the ACC (G–J) after DSP4 administration. (A–C) Representative photomicrographs of the LC showing TH-IR neurons in (A) sham-control and (B) sham-[DSP4] rats: scale bar: 100 μm. (C) Graph showing the decrease in the number of TH-IR neurons in the LC nucleus of sham-[DSP4] ($n = 4$): ***$p < 0.001$ vs sham-control. (D–F) Representative photomicrographs of the A5 showing the TH-IR neurons in (D) sham-control and (E) sham-[DSP4] rats: scale bar: 100 μm. (F) Graph showing similar TH-IR neurons in the A5 nucleus of sham-control rats and sham-[DSP4]. (G–J) Representative photomicrographs of the ACC showing a decrease of DβH-IR axons in (H and J) sham-[DSP4] rats vs (G and I) sham-control rats: scale bar: 100 μm (G-H) and 50 μm (I-J). Abbreviations: TH-IR, tyrosine hydroxylase-immunoreactivity; LC, locus coeruleus; DβH-IR, dopamine beta hydroxylase-immunoreactivity; DSP4, N-(2-chloroethyl)-N-ethyl-2-bromo-benzylamine.

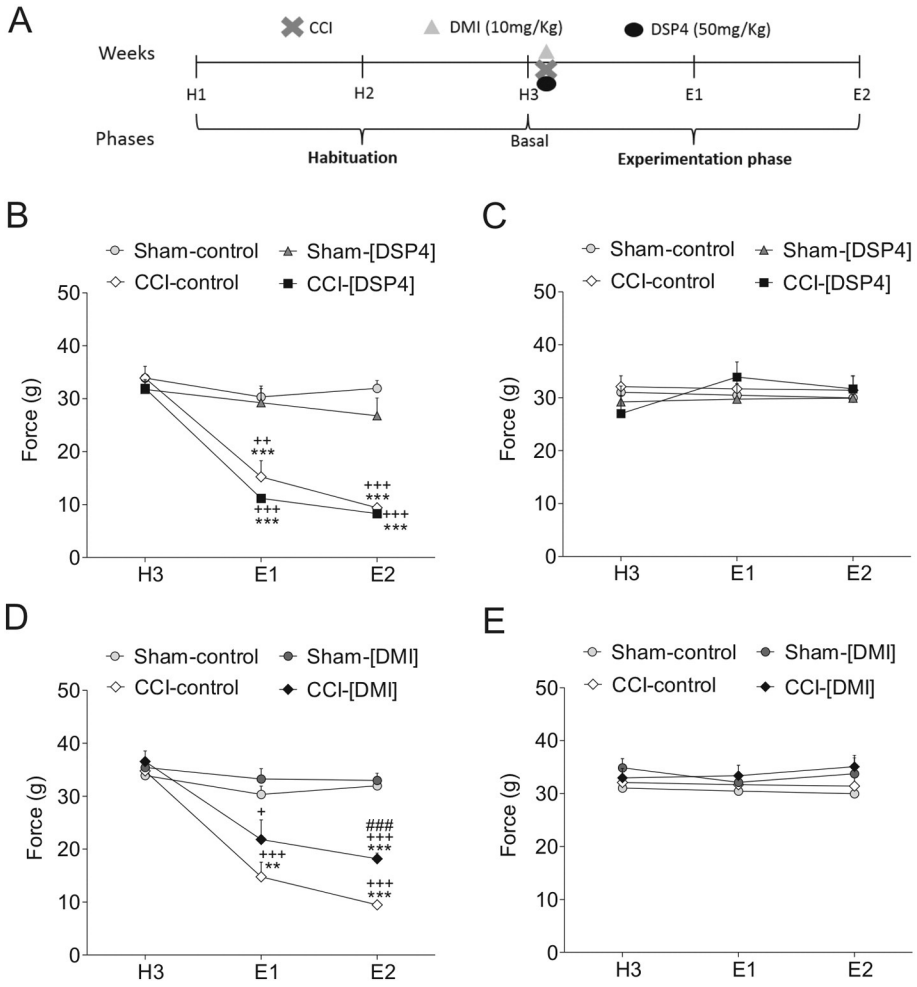

Fig. 2. Effect of DSP4 and DMI treatment on mechanical allodynia assessed with the von Frey test. (A) Experimental design. (B–C) Withdrawal threshold of the ipsilateral (B) and contralateral hindpaw (C) one or two weeks after CCI surgery and DSP4 administration. (D–E) Withdrawal threshold of the ipsilateral (D) and contralateral hindpaw (E) one or two weeks after CCI surgery and DMI administration. Note that sensorial responses of the hindpaw to mechanical stimulation were similar in the CCI groups irrespective of whether they received DSP4, while DMI reduced pain hypersensitivity. Each symbol represents the mean + SEM of 7–10 rats per group: $^{**}p < 0.01$ and $^{***}p < 0.001$ vs sham-control; $^{###}p < 0.001$ vs CCI-control; $+p < 0.05$, $++p < 0.01$ and $+++p < 0.001$ vs sham-[DSP4] (A–B) or sham-[DMI] (C-D). Abbreviations: CCI, chronic constriction injury; DMI, desipramine; DSP4, N-(2-chloroethyl)-N-ethyl-2-bromobenzylamine; E1 and E2, first and second week of the experimentation phase; H3, third week of habituation.

for two weeks (Fig. 4F), the administration of the antidepressant DMI appeared to reverse the escape behavior observed in rats experiencing neuropathic pain.

3.5. Effect of DSP4 and DMI administration on the activation of ERK in the ACC

The activation of ERK in the ACC was evaluated in western blots at the end of the experimental phase (Table 1) and the two-way ANOVA revealed a significant effect of DSP4 ($p < 0.01$) but not for DMI. Interestingly, a Bonferroni post-hoc analysis showed an increase in the activation of ERK in the ACC of CCI-[DSP4] rats compared to their sham-control and CCI-control groups ($p < 0.01$ respectively: Fig. 5A and C). No significant differences were detected for ERK activation in the ACC after DMI administration by two-way ANOVA, and no differences were detected in the overall expression of ERK in the ACC between each group (Fig. 5B–C).

4. Discussion

The present study demonstrates that administration of the noradrenergic neurotoxin DSP4 to rats experiencing neuropathic pain accentuates their escape behavior in response to a noxious stimulus in the place escape/avoidance test, without producing changes in sensory pain. These changes were accompanied by enhanced ERK activation in the ACC, where affective pain seems to be processed. In parallel, the administration of DMI in association with nerve injury improved sensory pain and prevented the accentuation of escape behavior in the place escape/avoidance test, as well as ERK activation in the ACC.

To study the influence of the noradrenergic system on pain domains, we disrupted this system by administering DSP4, a noradrenergic toxin. DSP4 did not induce any effect on sensory pain in control animals as the response to a mechanical or cold stimulus was not altered in these rats. This is an interesting finding as the administration of DSP4 to naïve rats has been proposed as a model of central neuropathic pain (Kudo et al., 2010, 2011). In these earlier studies, rats exhibited a dampened paw withdrawal latency when compared to control groups, which may reflect the type of stimuli used, non-noxious as opposed to a noxious one (the hot plate sensory test: (Kudo et al., 2010, 2011)). Furthermore, our data are consistent with previous finding showing that lesions of the LC, pharmacological inhibition of α2-adrenoceptors in the spinal cord, noradrenergic denervation (induced by intrathecal injection of dopamine beta-hydroxylase antibodies conjugated to the toxin saporin (DβH-saporin)), or gene ablation of any α2-adrenoceptor subtype do not change the basal withdrawal responses to nociceptive stimuli (Jasmin et al., 2003; Malmberg et al., 2001; Takano and Yaksh, 1992;

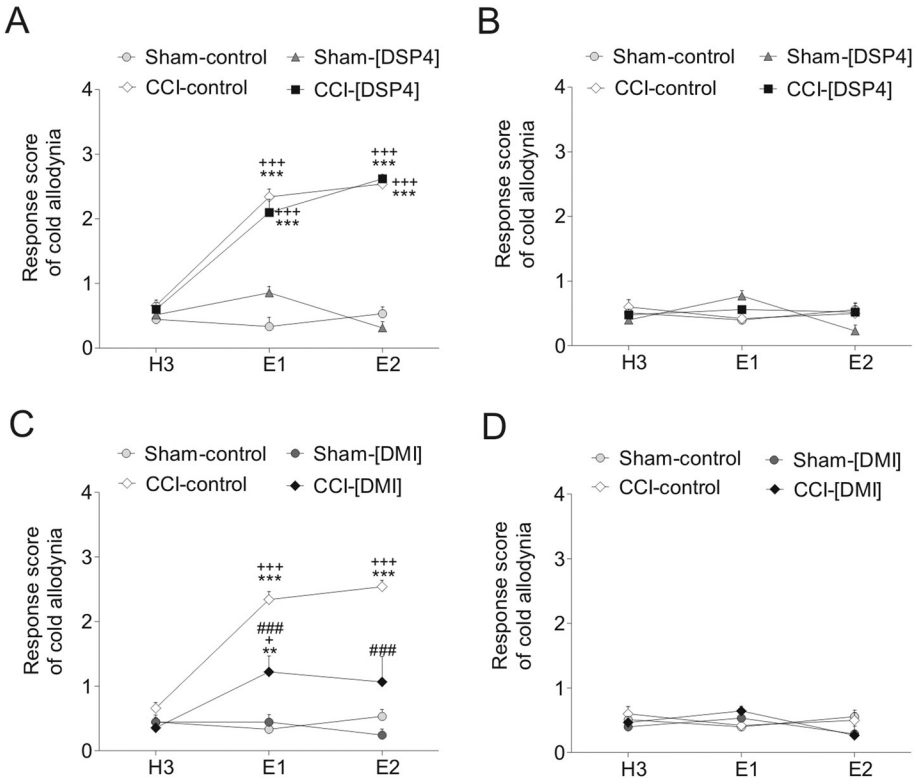

Fig. 3. Effect of DSP4 and DMI treatment on cold allodynia in the acetone test. (A–B) Response of the ipsilateral (A) and contralateral hindpaw (B) one or two weeks after CCI surgery and DSP4 administration. (C-D) Response of the ipsilateral (C) and contralateral hindpaw (D) one or two weeks after CCI surgery and DMI administration. Note that DSP4 did not modify and DMI treatment reduced cold allodynia in the ipsilateral hindpaw of neuropathic rats. Each symbol represents the mean + SEM of 7–10 rats per group: $^{**}p < 0.01$ and $^{***}p < 0.001$ *vs* sham-control; ###$p < 0.001$ *vs* CCI-control; +$p < 0.05$ and +++$p < 0.001$ vs sham-[DSP4] (A-B) or sham-[DMI] (C–D). Abbreviations: CCI, chronic constriction injury; DMI, desipramine; DSP4, N-(2-chloroethyl)-N-ethyl-2-bromobenzylamine; E1 and E2, first and second week of experimentation; H3, third week of the habituation phase.

Tsuruoka and Willis, 1996). Therefore, it appears that the intrinsic noradrenergic pain regulatory system has weak basal activity in animals without sustained pain.

Similarly, DSP4 did not modify sensorial pain responses in neuropathic animals 2 weeks after the induction of CCI in agreement with previous data showing that inhibition of the descending noradrenergic system is ineffective once neuropathic pain has developed (Howorth et al., 2009; Jasmin et al., 2003). For example, intrathecal blockade of α_2-adrenoceptors with yohimbine revealed earlier ipsilateral pain in the rat tibial nerve transection model. However, when allodynia was fully established (by week 3) yohimbine no longer had any sensitizing effect (Hughes et al., 2013). Along similar lines, intrathecal administration of either yohimbine or idazoxan (both α_2-adrenoceptors antagonists) does not modify pain hypersensitivity after 1 or 2 weeks in the CCI rat model (Muto et al., 2012; Roh et al., 2008). This suggests that when neuropathic pain is established, the endogenous noradrenergic analgesic system is unable to correct the neuropathic pain phenotype. Thus, it is likely that DSP4 does not modify the sensory component of pain because the activity of the intrinsic descending noradrenergic analgesic system is already diminished 2 weeks after induction of neuropathic pain. Thus, it would be interesting to evaluate the effect of DSP4 administration over shorter timescales (e.g., 2 days after nerve injury). On the other hand, it is remarkable to note that DSP4 was administered at the same time that nerve injury was done. Previous studies have also shown that mechanical hypersensitivity did not change following intrathecal DβH-saporin treatment (Li et al., 2002). However, changes in mechanical hyperalgesia were detected when this toxin was i.t. or i.c.v. administered before the induction of neuropathic pain (Brightwell and Taylor, 2009; Hayashida et al., 2012; Jasmin et al., 2003), suggesting the importance of an intact noradrenergic system for sensory pain when injury occurs.

Contralateral neuropathic sensitization has been found neither in CCI-control nor CCI-[DSP4] animals. Contralateral hypersensitivity has been sometimes reported in animal models of neuropathic pain (Decosterd and Woolf, 2000; Paulson et al., 2000). The different behavioural outcome in spite of being submitted to apparently the same nerve injury is thought to be dependent on the degree of activation of the inhibitory descending noradrenergic system. In line with this, it has been reported in the tibial nerve transection model that contralateral hypersensitivity can be unmasked by intrathecal yohimbine which would block the activity of the inhibitory α_2-adrenoceptors that are being activated by the descending noradrenergic tone (Hughes et al., 2013). Therefore, this lack of effect of DSP4 in the contralateral paw may reinforce the idea that noradrenergic neurons are not actively opposing to the sensitization at a spinal level at the studied time point of our work.

Other possibility concerns possible noradrenergic compensatory mechanisms. Previous studies have shown that the high selectivity of DSP4 for noradrenergic axons originated from the LC Fritschy and Grzanna (Fritschy and Grzanna, 1989). Additionally, Lyons et al. (Lyons et al., 1989) demonstrated by using a retrograde tracing (True Blue) injected into spinal cord, that DSP4 blocked the transport to the LC but not to the A5 and A7 groups indicating a selective degeneration of the LC. These data are in agreement with ours because we have not found a decrease in the number of TH-inmunoreactive cells in A5. Thus, having in mind that the stimulation of the A5 and A7 produces spinal antinociception (Burnett and Gebhart, 1991; Yeomans et al., 1992), we could infer that DSP4 was affecting selectively LC and other nuclei (A5 and A7) could compensate the noradrenergic disruption at the spinal cord level. The result of this noradrenergic compensatory mechanism could mask the "no effect" on the sensorial dimension.

Human's emotional component of pain cannot be objectively and quantitatively evaluated currently and it is usually assessed using

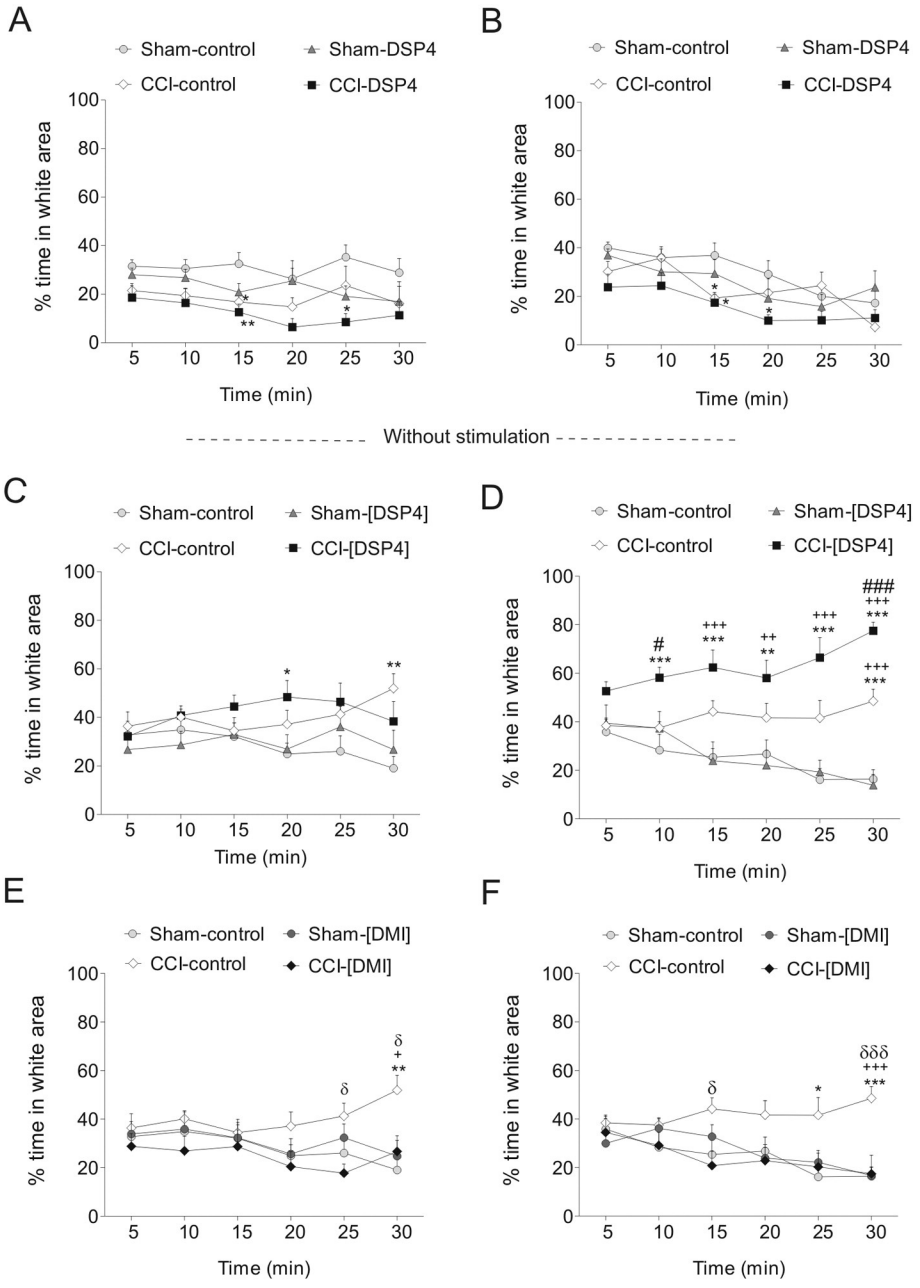

Fig. 4. Effect of DSP4 and DMI treatment on the affective component of pain in the place escape/avoidance test. (A–B) The time spent in the light area one (A) and two weeks (B) after CCI surgery and DSP4 administration without paw stimulation. (C–D) The time spent in the light area one (C) and two weeks (D) after CCI surgery and DSP4 administration with paw stimulation. (E–F) Percentage time spent in the light area one (E) and two weeks (F) after CCI surgery and DMI administration with paw stimulation. Note that both CCI-control and CCI-[DSP4] showed a decrease of the time spent in white area in the first and second week of experimentation without paw stimulation. CCI-[DSP4] increased the escape behavior to an aversive stimulus in the second week of experimentation. CCI-[DMI] group decreased the escape behavior to an aversive stimulus from the first week. Each symbol represents the mean + SEM of 7–11 rats per group: $^{*}p < 0.05$, $^{**}p < 0.01$ and $^{***}p < 0.001$ *vs* sham-control; $\#p < 0.01$ and $\#\#\#p < 0.001$ *vs* CCI-control; $+p < 0.05$ $++p < 0.01$ and $+++p < 0.001$ vs sham-[DSP4] (C–D) or sham-[DMI] (E–F) and $\delta p < 0.05$ and $\delta\delta\delta p < 0.001$ *vs* CCI-[DMI]. Abbreviations: CCI, chronic constriction injury; DMI, desipramine; DSP4, N-(2-chloroethyl)-N-ethyl-2-bromobenzylamine.

standardized questionnaires about subjective and personal experiences. Assessment of analogous affective aspects of pain in rodents is still challenging (Navratilova and Porreca, 2014). Several preclinical paradigms have been developed to study the affective component of pain in last years (Johansen et al., 2001; LaBuda and Fuchs, 2000). These paradigms focus on the ability of an animal to discriminate a noxious stimulus associated with an environment or compartment. As expected, animals with neuropathic pain display accentuated escape behavior 1 week after surgery (reflected by their permanence in the light area). Furthermore, this behavior was reinforced 2 weeks after surgery, confirming our previous data (Bravo et al., 2012) and highlighting the importance of pain aversion while neuropathy develops. Furthermore, it has been suggested that activity of the ACC is necessary to induce the affective component of pain (Cao et al., 2009; Johansen et al., 2001; Qu et al., 2011) and that ERK activation in the ACC might be necessary for neuropathic pain-evoked aversion in rats (Han et al., 2014). However, we did not detect any change in p-ERK in the ACC of CCI animals 2 weeks after lesion, a difference that was also reflected by a preference for the light compartment, close to 50% in these animals, which was far from the 90% for CCI animals detected previously (Han et al., 2014). Thus, it is likely that ERK activation in the ACC is related with a high degree of pain-evoked aversion.

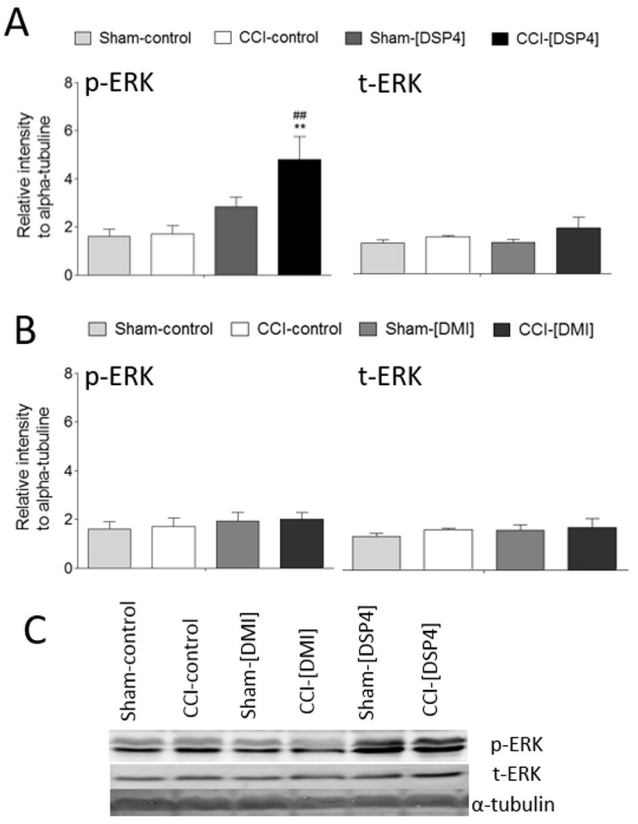

Fig. 5. Expression of ERK in the ACC after DSP4 and DMI administration (A–C). Graphs showing the quantitative analysis of activated ERK (p-ERK) and total unphosphorilated ERK (t-ERK) relative to α-tubulin in (A) animals treated with DSP4 and (B) animals treated with DMI. (C) Representative western blot to show the accumulation of *p*-ERK, t-ERK and α-tubulin in the ACC. The data represent the mean + SEM of 5 assays performed on ACC samples ($n = 5$ rats): $^{**}p < 0.01$ vs sham-control; $\#\#p < 0.01$ vs CCI-control. Abbreviations: ACC, anterior cingulate cortex; DSP4, N-(2-chloroethyl)-N-ethyl-2-bromobenzylamine; DMI, desipramine.

In order to rule out a possible anxiolytic effect of DSP4, animals were submitted to 30 min of free movement in the place escape/avoidance apparatus without paw stimulation. Interestingly, both CCI-control and CCI-[DSP4] spent less time in the white area compared to sham-control group in some experimental points but no differences were found between them. This might suggest that nerve injury is contributing to develop an anxiety-like behavior, as it has been reported at longer time points (Alba-Delgado et al., 2012c), but DSP4 did not potentiate it. However, when animals were submitted to the place escape/avoidance test with paw stimulation, CCI-[DSP4] showed a stronger escape response to a noxious stimulus than that of CCI-control rats. Additionally, the higher escape behavior was correlated with an enhancement of ERK in the ACC of CCI-[DSP4] animals.

As it has been shown that DSP4 preferentially lesions LC neurons (Fritschy and Grzanna, 1991) and this is the site of the majority of noradrenergic projections innervating all cortical areas (Jones et al., 1977), this might indicate the importance of the ascending pain projections from the LC to the ACC in the processing of affective pain (Aston-Jones and Cohen, 2005). Interestingly, these data are similar to those we presented previously showing that ERK is more strongly activated in the ACC of animals with neuropathic pain that are submitted to a model of depression model for 2 weeks. This response in the ACC is accompanied by an accentuated escape response to a noxious stimulus (Bravo et al., 2012). Thus, the noradrenergic disruption induced by DSP4 administration might mimic the effect of a depression model in terms of the emotional component of pain. However, studies evaluating the effect of DSP4 on depressive-like behavior indicate that DSP4 does not induce depressive-like behavior *per se* but rather, it enhances the antidepressant effect of the selective norepinephrine reuptake inhibitor (reboxetine:(Cryan et al., 2002; Ku et al., 2012). This is obviously a counterintuitive result given the large body of data demonstrating that antidepressant drugs affect LC function (Valentino et al., 1990), raising the question as to the actions of DSP4 in the pathway ascending from the LC (such as modifications to α2 adrenoreceptor, noradrenaline transporter expression or noradrenaline availability: (Ross and Stenfors, 2015). Thus, an alternative interpretation could be that the DSP4 is actually increasing the amount of noradrenaline being released in the cortex which may be aversive, having in mind the emerging literature on the aversive effects of the LC stimulation and also noradrenergic re-uptake inhibitors in the context of pain (Brightwell and Taylor, 2009; Hughes et al., 2015). Therefore, further studies using more selective methods of neuronal perturbation (local drug administration, opto- or chemogenetic experimental approaches) will be necessary to better understand the role of the LC in neuropathic pain. Overall, our current data clearly shows that perturbation of the noradrenergic system for 2 weeks after nerve injury does not modify either mechanical or cold allodynia but rather, it exacerbates the escape and avoidance response to a painful stimulus. This might suggest that in the long term, LC activity is more closely implicated in the processing of affective pain than in the sensorial aspect of pain.

In the second part of our study, we administered the antidepressant DMI to CCI rats for 2 weeks in order to enhance noradrenergic tone. We found that mechanical and cold allodynia was less severe in these rats than in the CCI-control animals, reflecting the well-known antinociceptive effect of DMI in neuropathic pain (Alba-Delgado et al., 2012b; Jones et al., 2009, Mico et al., 2006). This finding supports the idea that nerve injury dampens the descending noradrenergic tone, which can be effectively reversed with noradrenaline reuptake inhibitors. In addition, the administration of DMI to CCI rats completely attenuated the place escape/avoidance behavior and no changes in ERK activity were found at ACC level. Thus, the noradrenergic plasticity caused by nerve injury in the sensorial and affective sphere over time is counteracted by the antidepressant DMI. Increasing evidences have shown that antidepressants may normalize altered ERK phosporilation. Indeed, it has been reported that imipramine ameliorated increased pERK-immunopositive cells in the ACC in animals with long-term neuropathy (21 days) that had also developed a pro-depressive behavior (Yasuda et al., 2014). Furthermore, other authors have shown that chronic treatment with fluoxetine, a selective serotonin reuptake inhibitor, reduced ERK phosphorylation in the hippocampus, frontal cortex and striatum. This suggests that a decreased activity of this signaling pathway might occur as a result of antidepressant activity (Fumagalli et al., 2005). However, it is important to note that there also evidences suggesting that ERK activation in the prefrontal cortex may potentiate and/or underlie the pharmacological action of antidepressants (see review in (Borges et al., 2015). Therefore, further studies comparing the expression of ERK signaling cascade or other biomarkers (c-fos) at spinal cord and ACC level after DSP4 and DMI treatment would help to know if these treatments are having a differential effect at spinal and supraspinal level that may explain the behavioral outcome found. Furthermore, DMI, as tricyclic antidepressant, has affinity for other receptors and channels (e.g: sodium channels (Dick et al., 2007). Thus, we cannot exclude that other mechanisms different to those related with the noradrenergic system might explain the apparent difference with DSP4 action.

It is interesting to note that the dose of DMI used more effectively reverses the affective component of pain than the sensorial component (a reflex based measure of pain). Similar data was found in rats administered morphine, gabapentin and duloxetine in relation to neuropathic pain (Pedersen and Blackburn-Munro, 2006), and in rats with inflammatory pain administered celecoxib and diclofenac (Boyce-Rustay et

al., 2010). It was suggested that the doses effective in rodent models of pain reflexes are higher than the doses needed to achieve clinical pain relief (Whiteside et al., 2008). Thus, the doses that significantly reduce the affective component of pain could be more relevant to predict efficacy in the clinical setting. These data support the use of tests to evaluate the affective component of pain in order to accelerate analgesic drug discovery, in addition to those based on reflex pain reactions, such as operant tests.

Overall, the data presented here allow us to conclude that alterations to noradrenergic neurotransmission by DSP4 deteriorate the emotional component of pain independently of sensorial pain perception within two weeks of neuropathic pain induction. These changes are presumably due to the impaired activity of noradrenergic inputs from the LC to the ACC, without excluding the possible influence of other areas not evaluated in this study (e.g., the amygdala). The antidepressant DMI could reduce pain hypersensitivity and prevent a deterioration of the emotional pain dimension. In conclusion, the observations from this study suggest that the noradrenergic system may regulate the affective and sensorial sphere of neuropathic pain independently and in a distinct manner.

Acknowledgements

We are very grateful for the excellent help provided by José Antonio García Partida, Jesus Gallego-Gamo, Paula Reyes Perez and Santiago Muñoz. This work was carried out using funds from: the Instituto de Salud Carlos III (Madrid, Spain) and FEDER (European Union), co-financed by the Fondo Europeo de Desarrollo Regional ("Una manera de hacer Europa" PI13/02659); the Ministerio de Economía y Competitividad (SAF2015-68647-R); the "Centro de Investigación Biomédica en Red de Salud Mental", Madrid, Spain (G18); the "Consejería de Economía, Innovación, Ciencia y Empleo de la Junta de Andalucía", Seville, Spain (CTS-510 and Proyectos de Excelencia: CTS-4303 and CTS-7748); 2015 NARSAD Young Investigator Grant from the Brain & Behavior Research Foundation (23982); Travel Grant and Project from Fundación Española de Dolor (FED-1632 and PI2015-FED-007) and the "Cátedra Externa del Dolor Fundación Grünenthal-Universidad de Cádiz" Cádiz, Spain.

References

Alba-Delgado, C., Borges, G., Sanchez-Blazquez, P., Ortega, J.E., Horrillo, I., Mico, J.A., et al., 2012a. The function of alpha-2-adrenoceptors in the rat locus coeruleus is preserved in the chronic constriction injury model of neuropathic pain. Psychopharmacology 221, 53–65.

Alba-Delgado, C., Mico, J.A., Sanchez-Blazquez, P., Berrocoso, E., 2012b. Analgesic antidepressants promote the responsiveness of locus coeruleus neurons to noxious stimulation: implications for neuropathic pain. Pain 153, 1438–1449.

Alba-Delgado, C., Llorca-Torralba, M., Horrillo, I., Ortega, J.E., Mico, J.A., Sanchez-Blazquez, P., et al., 2012c. Chronic pain leads to concomitant noradrenergic impairment and mood disorders. Biol. Psychiatry 73, 54–62.

Aston-Jones, G., Cohen, J.D., 2005. Adaptive gain and the role of the locus coeruleus-norepinephrine system in optimal performance. J. Comp. Neurol. 493, 99–110.

Bennett, G.J., Xie, Y.K., 1988. A peripheral mononeuropathy in rat that produces disorders of pain sensation like those seen in man. Pain 33, 87–107.

Borges, G., Berrocoso, E., Mico, J.A., Neto, F., 2015. ERK1/2: function, signaling and implication in pain and pain-related anxio-depressive disorders. Prog. Neuro-Psychopharmacol. Biol. Psychiatry 60, 77–92.

Boyce-Rustay, J.M., Zhong, C., Kohnken, R., Baker, S.J., Simler, G.H., Wensink, E.J., et al., 2010. Comparison of mechanical allodynia and the affective component of inflammatory pain in rats. Neuropharmacology 58, 537–543.

Bravo, L., Mico, J.A., Rey-Brea, R., Perez-Nievas, B., Leza, J.C., Berrocoso, E., 2012. Depressive-like states heighten the aversion to painful stimuli in a rat model of comorbid chronic pain and depression. Anesthesiology 117, 613–625.

Bravo, L., Alba-Delgado, C., Torres-Sanchez, S., Mico, J.A., Neto, F.L., Berrocoso, E., 2013. Social stress exacerbates the aversion to painful experiences in rats exposed to chronic pain: the role of the locus coeruleus. Pain 154, 2014–2023.

Brightwell, J.J., Taylor, B.K., 2009. Noradrenergic neurons in the locus coeruleus contribute to neuropathic pain. Neuroscience 160, 174–185.

Burnett, A., Gebhart, G.F., 1991. Characterization of descending modulation of nociception from the A5 cell group. Brain Res. 546, 271–281.

Cao, H., Cui, Y.H., Zhao, Z.Q., Cao, X.H., Zhang, Y.Q., 2009. Activation of extracellular signal-regulated kinase in the anterior cingulate cortex contributes to the induction of long-term potentiation in rats. Neurosci. Bull. 25, 301–308.

Chandler, D.J., Lamperski, C.S., Waterhouse, B.D., 2013. Identification and distribution of projections from monoaminergic and cholinergic nuclei to functionally differentiated subregions of prefrontal cortex. Brain Res. 1522, 38–58.

Cohen, Z., Molinatti, G., Hamel, E., 1997. Astroglial and vascular interactions of noradrenaline terminals in the rat cerebral cortex. J. Cereb. Blood Flow Metab. 17, 894–904.

Cryan, J.F., Page, M.E., Lucki, I., 2002. Noradrenergic lesions differentially alter the antidepressant-like effects of reboxetine in a modified forced swim test. Eur. J. Pharmacol. 436, 197–205.

Decosterd, I., Woolf, C.J., 2000. Spared nerve injury: an animal model of persistent peripheral neuropathic pain. Pain 87, 149–158.

Dick, I.E., Brochu, R.M., Purohit, Y., Kaczorowski, G.J., Martin, W.J., Priest, B.T., 2007. Sodium channel blockade may contribute to the analgesic efficacy of antidepressants. J. Pain 8, 315–324.

Finnerup NAaNB, 2010. Pharmacological management of neuropathic pain. In: IASP (Ed.), Pain Clinical Updates.

Flatters, S.J., Bennett, G.J., 2004. Ethosuximide reverses paclitaxel- and vincristine-induced painful peripheral neuropathy. Pain 109, 150–161.

Fritschy, J.M., Grzanna, R., 1989. Immunohistochemical analysis of the neurotoxic effects of DSP-4 identifies two populations of noradrenergic axon terminals. Neuroscience 30, 181–197.

Fritschy, J.M., Grzanna, R., 1991. Selective effects of DSP-4 on locus coeruleus axons: are there pharmacologically different types of noradrenergic axons in the central nervous system? Prog. Brain Res. 88, 257–268.

Fumagalli, F., Molteni, R., Calabrese, F., Frasca, A., Racagni, G., Riva, M.A., 2005. Chronic fluoxetine administration inhibits extracellular signal-regulated kinase 1/2 phosphorylation in rat brain. J. Neurochem. 93, 1551–1560.

Gilron, I., Baron, R., Jensen, T., 2015. Neuropathic pain: principles of diagnosis and treatment. Mayo Clin. Proc. 90, 532–545.

Gonzalez, M.M., Aston-Jones, G., 2006. Circadian regulation of arousal: role of the noradrenergic locus coeruleus system and light exposure. Sleep 29, 1327–1336.

Gonzalez, M.M., Debilly, G., Valatx, J.L., 1998. Noradrenaline neurotoxin DSP-4 effects on sleep and brain temperature in the rat. Neurosci. Lett. 248, 93–96.

Grzanna, R., Berger, U., Fritschy, J.M., Geffard, M., 1989. Acute action of DSP-4 on central norepinephrine axons: biochemical and immunohistochemical evidence for differential effects. J. Histochem. Cytochem. 37 (9), 1435–1442.

Han, M., Xiao, X., Yang, Y., Huang, R.Y., Cao, H., Zhao, Z.Q., et al., 2014. SIP30 is required for neuropathic pain-evoked aversion in rats. J. Neurosci. 34, 346–355.

Hayashida, K., Peters, C.M., Gutierrez, S., Eisenach, J.C., 2012. Depletion of endogenous noradrenaline does not prevent spinal cord plasticity following peripheral nerve injury. J. Pain 13, 49–57.

Hormigo, S., Horta Junior Jde, A., Gomez-Nieto, R., Lopez, D.E., 2012. The selective neurotoxin DSP-4 impairs the noradrenergic projections from the locus coeruleus to the inferior colliculus in rats. Front. Neural Circuits 6 (41), 1–14.

Howorth, P.W., Teschemacher, A.G., Pickering, A.E., 2009. Retrograde adenoviral vector targeting of nociresponsive pontospinal noradrenergic neurons in the rat in vivo. J. Comp. Neurol. 512, 141–157.

Hughes, S.W., Hickey, L., Hulse, R.P., Lumb, B.M., Pickering, A.E., 2013. Endogenous analgesic action of the pontospinal noradrenergic system spatially restricts and temporally delays the progression of neuropathic pain following tibial nerve injury. Pain 154, 1680–1690.

Hughes, S., Hickey, L., Donaldson, L.F., Lumb, B.M., Pickering, A.E., 2015. Intrathecal reboxetine suppresses evoked and ongoing neuropathic pain behaviours by restoring spinal noradrenergic inhibitory tone. Pain 156, 328–334.

Jasmin, L., Boudah, A., Ohara, P.T., 2003. Long-term effects of decreased noradrenergic central nervous system innervation on pain behavior and opioid antinociception. J. Comp. Neurol. 460, 38–55.

Jett, M.F., McGuirk, J., Waligora, D., Hunter, J.C., 1997. The effects of mexiletine, desipramine and fluoxetine in rat models involving central sensitization. Pain 69, 161–169.

Johansen, J.P., Fields, H.L., Manning, B.H., 2001. The affective component of pain in rodents: direct evidence for a contribution of the anterior cingulate cortex. Proc. Natl. Acad. Sci. U. S. A. 98, 8077–8082.

Jones, B.E., Halaris, A.E., McIlhany, M., Moore, R.Y., 1977. Ascending projections of the locus coeruleus in the rat. I. Axonal transport in central noradrenaline neurons. Brain Res. 127, 1–21.

Jones, K.L., Finn, D.P., Governo, R.J., Prior, M.J., Morris, P.G., Kendall, D.A., et al., 2009. Identification of discrete sites of action of chronic treatment with desipramine in a model of neuropathic pain. Neuropharmacology 56, 405–413.

Ku, Y.C., Tsai, Y.J., Tung, C.S., Fang, T.H., Lo, S.M., Liu, Y.P., 2012. Different involvement of ventral and dorsal norepinephrine pathways on norepinephrine reuptake inhibitor-induced locomotion and antidepressant-like effects in rats. Neurosci. Lett. 514, 179–184.

Kudo, T., Kushikata, T., Kudo, M., Hirota, K., 2010. A central neuropathic pain model by DSP-4 induced lesion of noradrenergic neurons: preliminary report. Neurosci. Lett. 481, 102–104.

Kudo, T., Kushikata, T., Kudo, M., Hirota, K., 2011. Antinociceptive effects of neurotropin in a rat model of central neuropathic pain: DSP-4 induced noradrenergic lesion. Neurosci. Lett. 503, 20–22.

LaBuda, C.J., Fuchs, P.N., 2000. A behavioral test paradigm to measure the aversive quality of inflammatory and neuropathic pain in rats. Exp. Neurol. 163, 490–494.

Li, X., Conklin, D., Ma, W., Zhu, X., Eisenach, J.C., 2002. Spinal noradrenergic activation mediates allodynia reduction from an allosteric adenosine modulator in a rat model of neuropathic pain. Pain 97, 117–125.

Lyons, W.E., Fritschy, J.M., Grzanna, R., 1989. The noradrenergic neurotoxin DSP-4 eliminates the coeruleospinal projection but spares projections of the A5 and A7 groups to the ventral horn of the rat spinal cord. J. Neurosci. 9, 1481–1489.
Malmberg, A.B., Hedley, L.R., Jasper, J.R., Hunter, J.C., Basbaum, A.I., 2001. Contribution of alpha(2) receptor subtypes to nerve injury-induced pain and its regulation by dexmedetomidine. Br. J. Pharmacol. 132, 1827–1836.
Mico, J.A., Ardid, D., Berrocoso, E., Eschalier, A., 2006. Antidepressants and pain. Trends Pharmacol. Sci. 27, 348–354.
Muto, Y., Sakai, A., Sakamoto, A., Suzuki, H., 2012. Activation of NK(1) receptors in the locus coeruleus induces analgesia through noradrenergic-mediated descending inhibition in a rat model of neuropathic pain. Br. J. Pharmacol. 166, 1047–1057.
Navratilova, E., Porreca, F., 2014. Reward and motivation in pain and pain relief. Nat. Neurosci. 17, 1304–1312.
Ortega-Alvaro, A., Gibert-Rahola, J., Mellado-Fernandez, M.L., Chover, A.J., Mico, J.A., 1997. The effects of different monoaminergic antidepressants on the analgesia induced by spinal cord adrenal medullary transplants in the formalin test in rats. Anesth. Analg. 84, 816–820.
Paulson, P.E., Morrow, T.J., Casey, K.L., 2000. Bilateral behavioral and regional cerebral blood flow changes during painful peripheral mononeuropathy in the rat. Pain 84, 233–245.
Pedersen, L.H., Blackburn-Munro, G., 2006. Pharmacological characterisation of place escape/avoidance behaviour in the rat chronic constriction injury model of neuropathic pain. Psychopharmacology 185, 208–217.
Price, D.D., 2000. Psychological and neural mechanisms of the affective dimension of pain. Science 288, 1769–1772.
Price, D.D., Barrell, J.J., Gracely, R.H., 1980. A psychophysical analysis of experimential factors that selectively influence the affective dimension of pain. Pain 8, 137–149.
Qu, C., King, T., Okun, A., Lai, J., Fields, H.L., Porreca, F., 2011. Lesion of the rostral anterior cingulate cortex eliminates the aversiveness of spontaneous neuropathic pain following partial or complete axotomy. Pain 152, 1641–1648.
Rainville, P., Duncan, G.H., Price, D.D., Carrier, B., Bushnell, M.C., 1997. Pain affect encoded in human anterior cingulate but not somatosensory cortex. Science 277, 968–971.
Roh, D.H., Kim, H.W., Yoon, S.Y., Seo, H.S., Kwon, Y.B., Han, H.J., et al., 2008. Intrathecal clonidine suppresses phosphorylation of the N-methyl-D-aspartate receptor NR1 subunit in spinal dorsal horn neurons of rats with neuropathic pain. Anesth. Analg. 107, 693–700.
Ross, S.B., Stenfors, C., 2015. DSP4, a selective neurotoxin for the locus coeruleus noradrenergic system. A review of its mode of action. Neurotox. Res. 27, 15–30.
Sindrup, S.H., Gram, L.F., Skjold, T., Grodum, E., Brosen, K., Beck-Nielsen, H., 1990. Clomipramine vs desipramine vs placebo in the treatment of diabetic neuropathy symptoms. A double-blind cross-over study. Br. J. Clin. Pharmacol. 30, 683–691.
Takano, Y., Yaksh, T.L., 1992. Characterization of the pharmacology of intrathecally administered alpha-2 agonists and antagonists in rats. J. Pharmacol. Exp. Ther. 261, 764–772.
Tsuruoka, M., Willis Jr., W.D., 1996. Bilateral lesions in the area of the nucleus locus coeruleus affect the development of hyperalgesia during carrageenan-induced inflammation. Brain Res. 726, 233–236.
Valentino, R.J., Curtis, A.L., Parris, D.G., Wehby, R.G., 1990. Antidepressant actions on brain noradrenergic neurons. J. Pharmacol. Exp. Ther. 253, 833–840.
Wager, T.D., Rilling, J.K., Smith, E.E., Sokolik, A., Casey, K.L., Davidson, R.J., et al., 2004. Placebo-induced changes in fMRI in the anticipation and experience of pain. Science 303, 1162–1167.
Whiteside, G.T., Adedoyin, A., Leventhal, L., 2008. Predictive validity of animal pain models? A comparison of the pharmacokinetic–pharmacodynamic relationship for pain drugs in rats and humans. Neuropharmacology 54, 767–775.
Yalcin, I., Tessier, L.H., Petit-Demouliere, N., Doridot, S., Hein, L., Freund-Mercier, M.J., et al., 2009. Beta2-adrenoceptors are essential for desipramine, venlafaxine or reboxetine action in neuropathic pain. Neurobiol. Dis. 33, 386–394.
Yasuda, S., Yoshida, M., Yamagata, H., Iwanaga, Y., Suenaga, H., Ishikawa, K., et al., 2014. Imipramine ameliorates pain-related negative emotion via induction of brain-derived neurotrophic factor. Cell. Mol. Neurobiol. 34, 1199–1208.
Yeomans, D.C., Clark, F.M., Paice, J.A., Proudfit, H.K., 1992. Antinociception induced by electrical stimulation of spinally projecting noradrenergic neurons in the A7 catecholamine cell group of the rat. Pain 48, 449–461.
Zimmermann, M., 1983. Ethical guidelines for investigations of experimental pain in conscious animals. Pain 16, 109–110.

Archival Report

Biological Psychiatry: Celebrating 50 Years

Chemogenetic Silencing of the Locus Coeruleus–Basolateral Amygdala Pathway Abolishes Pain-Induced Anxiety and Enhanced Aversive Learning in Rats

Meritxell Llorca-Torralba, Irene Suárez-Pereira, Lidia Bravo, Carmen Camarena-Delgado, Jose Antonio Garcia-Partida, Juan Antonio Mico, and Esther Berrocoso

ABSTRACT

BACKGROUND: Pain affects both sensory and emotional aversive responses, often provoking anxiety-related diseases when chronic. However, the neural mechanisms underlying the interactions between anxiety and chronic pain remain unclear.

METHODS: We characterized the sensory, emotional, and cognitive consequences of neuropathic pain (chronic constriction injury) in a rat model. Moreover, we determined the role of the locus coeruleus (LC) neurons that project to the basolateral amygdala (BLA) using a DREADD (designer receptor exclusively activated by designer drugs).

RESULTS: Chronic constriction injury led to sensorial hypersensitivity in both the short term and long term. Otherwise, long-term pain led to an anxiety-like profile (in the elevated zero maze and open field tests), as well as increased responses to learn aversive situations (in the passive avoidance and fear conditioning tests) and an impairment of nonemotional cognitive tasks (in the novel object recognition and object pattern of separation tests). Chemogenetic blockade of the LC-BLA pathway and intra-BLA or systemic antagonism of beta-adrenergic receptors abolished both long-term pain-induced anxiety and enhanced fear learning. By contrast, chemogenetic activation of this pathway induced anxiety-like behaviors and enhanced the aversive learning and memory index in sham animals, although it had little effect on short- and long-term chronic constriction injury animals. Interestingly, modulation of LC-BLA activity did not modify sensorial perception or episodic memory.

CONCLUSIONS: Our results indicate that dimensions associated with pain are processed by independent pathways and that there is an overactivation of the LC-BLA pathway when anxiety and chronic pain are comorbid, which involves the activity of beta-adrenergic receptors.

Keywords: Anxiety, Aversive memory, Basolateral amygdala, Cognition, Locus coeruleus, Neuropathic pain

https://doi.org/10.1016/j.biopsych.2019.02.018

The positive interaction between negative emotions (fear, anxiety, sadness, or depression) and pain has been well established. Epidemiological studies estimate that chronic pain affects more than 20% of the population in Europe and the United States (1–4) and that 20% to 30% of those individuals also suffer anxiety-related disorders (5,6). While this comorbidity is apparently clear, few studies have directly explored the interaction between pain and anxiety at the network level.

Current theories suggest that long-term (LT) pain triggers functional changes that would be responsible for affective and cognitive alterations (anxiety, depression, emotional decision making, and working memory). The locus coeruleus (LC) is a region that might be implicated in these changes (7–17). Indeed, we reported increased electrophysiological activity, tyrosine hydroxylase, and noradrenaline transporter expression in the LC and enhanced alpha2-adrenoceptor expression and sensitivity, which temporally coincides with the onset of anxiodepressive behavior in LT nerve-injured rats (8). Interestingly, new LC projection mapping data revealed that the LC noradrenaline system is anatomically and functionally heterogeneous and that its responses can be modulated by sensory inputs (18). Indeed, specific LC projections would appear to be modulated by painful input (18,19). One neural target of the LC is the basolateral amygdala (BLA), which integrates sensory information to encode and drive diverse and, at times opposing, affective behaviors, including anxiety, aversion, and reward behaviors (20). In fact, it was recently shown that the neuromodulatory LC system utilizes the BLA output to promote acute anxiety (21,22) and aversive learning (23). Together, these data suggest that LC-BLA projections are involved in mediating acute negative affective

SEE COMMENTARY ON PAGE 983

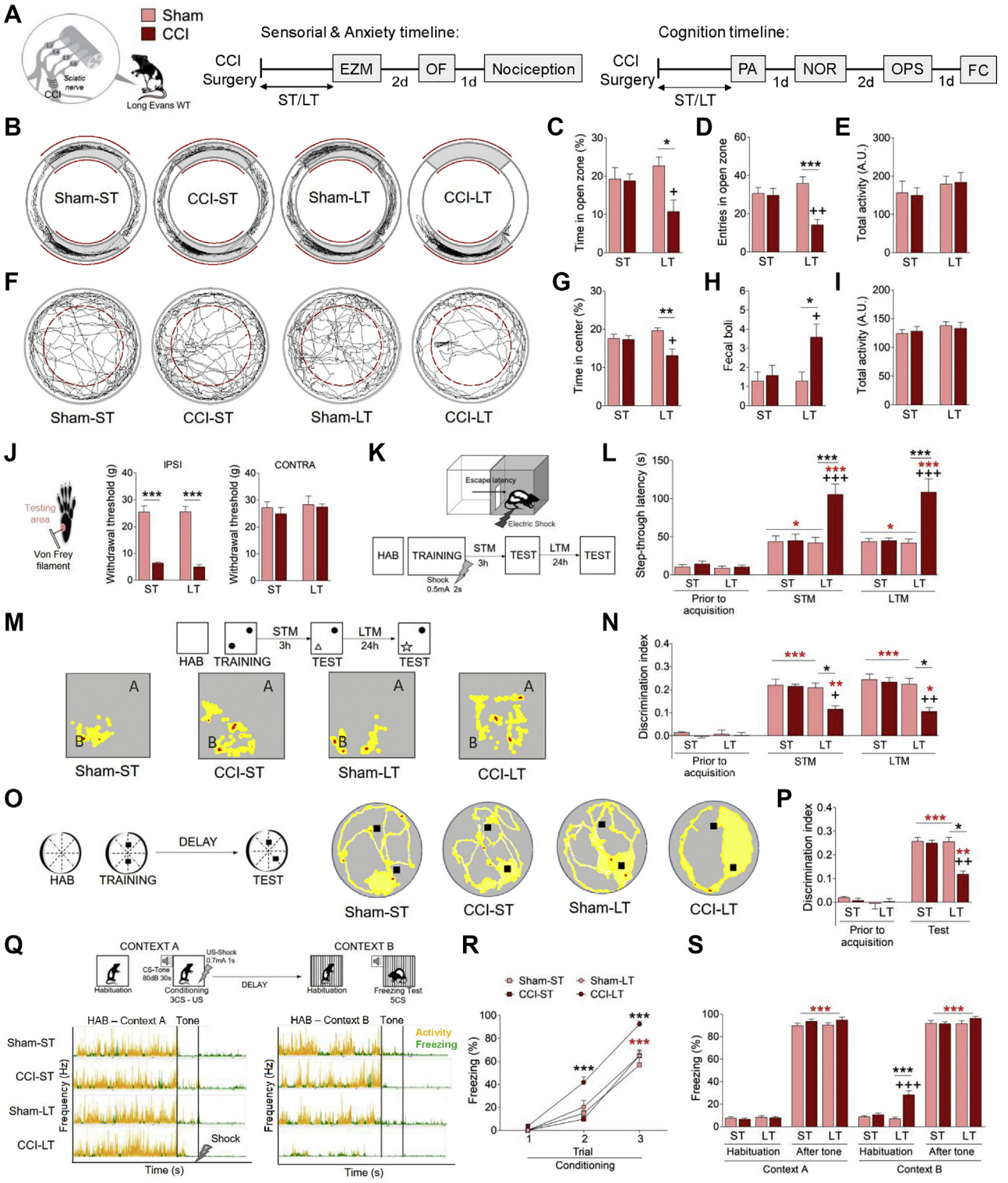

Figure 1. Sensory, affective, and cognitive characterization of the development of neuropathic pain. **(A)** Experimental timeline and schematic representation of chronic constriction injury (CCI) surgery for the behavioral experiments in male Long-Evans wild-type (WT) rats. Rats were tested 2–3 weeks (short-term [ST]) or 5–6 weeks (long-term [LT]) after surgery. **(B–E)** Effects of neuropathic pain on the elevated zero maze (EZM). **(B)** Representative activity traces, the graphs representing **(C)** the relative time spent in the open zone and **(D)** the number of entries into the open zone, and **(E)** the locomotor activity. **(F–I)** The effects of

behavior, although less is unknown about sustained aversive situations like chronic pain.

In the light of this situation, we hypothesized that noradrenergic LC projections to the BLA may be hyperactivate in chronic pain, driving processes like anxiety and increased aversive emotional learning. As such, we characterized the evolution of hypersensitivity and that of the anxiety and cognitive capacity in Long-Evans rats submitted to chronic constriction injury (CCI) of the sciatic nerve. These phenotypes where subsequently evaluated when the LC noradrenergic terminals in the BLA were chemogenetically modulated.

METHODS AND MATERIALS

Additional details of the materials and methods can be found in the figure legends and in the Supplement.

Animals

Male wild-type or tyrosine hydroxylase–Cre transgenic Long-Evans rats (350–450 g) were produced and maintained under standard laboratory conditions (University of Cádiz). All animal handling and use was carried out in accordance with the guidelines of the European Commission's directive (2010/63/EC) and Spanish law (RD 53/2013).

Surgical Procedures

Neuropathic Pain. CCI was used as a model of neuropathic pain (24,25), and short-term (ST) (2–3 weeks postsurgery) and LT (5–6 weeks postsurgery) experiments were performed.

Stereotaxic Surgery. Surgery was performed under ketamine (100 mg/kg) and xylazine (20 mg/kg) anesthesia. Rats were injected with a DREADD (designer receptor exclusively activated by designer drug). A DREADD adeno-associated virus 2 (AAV2)/hSyn-DIO-hM4D(Gi)-mCherry, AAV2/hSyn-DIO-rM3D(Gs)-mCherry or AAV2/hSyn-DIO-mCherry virus (Virus Vector Core, Gene Therapy Center Vector Core, University of North Carolina at Chapel Hill, Chapel Hill, NC) was injected unilaterally or bilaterally into the LC [1.4 μL/side (26): −3.2 anteroposterior from lambda, ±1.3 mediolateral, and 6.2 dorsoventral]. Unilateral administration was performed for testing the rM3D(Gs)-DREADD–mediated activation of LC neurons (c-Fos+ neurons). Alternatively, the BLA of rats (−2.9 anteroposterior from bregma, ±4.8 mediolateral, and −8.4 dorsoventral) was injected with the Fluoro-Gold retrograde tracer (4% w/v, 0.2 μL) (Fluorochrome, Denver, CO). The rats were allowed to recover for 3 weeks (DREADD virus) or 4 days (Fluoro-Gold tracer) before the behavioral studies were carried out, favoring robust expression in the target regions. A metal cannula was then implanted bilaterally into BLA 4 days before performing the behavioral studies.

Drug Administration

Clozapine-*N*-oxide (CNO) [3 μM/0.5 μL intra-BLA (27) or 1 mg/kg intraperitoneal (26)] (Enzo Life Sciences, Farmingdale, NY), propranolol [a beta-adrenergic receptor (β-AR) antagonist; 1 μg/0.5 μL intra-BLA (21) or 3 mg/kg intraperitoneal] (Sigma-Aldrich, Madrid, Spain), isoproterenol (a β-AR agonist; 30 μg/0.5 μL intra-BLA) (Sigma-Aldrich), or saline (ss) 0.9% was administered 20 minutes before behavioral testing. When administering both CNO and propranolol, CNO was injected 20 minutes before propranolol or saline.

Behavioral Assessment

Anxiety. For the elevated zero maze (EZM), the time spent in the open zones and the number of entries into these areas, as well as the total activity, were monitored during a 5-minute test (28,29).

For the open field test, the time spent in the central area, the total activity, and the number of fecal boluses was recorded.

Nociception. In the von Frey test, the withdrawal threshold (grams) of a hindpaw when subjected to a force increasing from 0 to 50 g over a period of 20 seconds was used as a measure of mechanical hypersensitivity (30).

The acetone test involves applying a drop of acetone (100 μL) to the surface in the middle of a hindpaw with a pipette (31).

In the cold plate test (4 ± 1°C), the times the animal briskly lifted its ipsilateral hindpaw was measured over a period of 2 minutes (32) as a measure of thermal hypersensitivity.

For dynamic weight bearing, spontaneous nociceptive behavior was measured as the weight (grams) or area (mm^2) of the hindpaw for 5 minutes (33).

neuropathic pain on the open field (OF) test. **(F)** Representative activity traces and graphs representing **(G)** the relative time spent in the central zone, **(H)** the number of fecal boluses, and **(I)** the locomotor activity. **(J)** Study of mechanical sensitivity of pain model. The graphs represent the withdrawal threshold (grams) of the ipsilateral (IPSI) and contralateral (CONTRA) hindpaw in response to von Frey hair stimulation (0–50 g, 20 seconds). **(K, L)** The effects of neuropathic pain on passive avoidance (PA). **(K)** Schematic representation of the PA procedure and the graph represents **(L)** the latency to enter the dark compartment (seconds) in the different phases of the paradigm: training (prior to acquisition), ST memory (STM) test (as learning index) and LT memory (LTM) test (as memory index). **(M, N)** The effects of neuropathic pain on the novel object recognition (NOR) test. **(M)** Schematic representation of the NOR procedure and representative heatmaps showing activity (yellow = low activity, and red = high activity) around the objects in memory tests (A = familiar object, B = novel object) and **(N)** the graph representing the discrimination index between objects in the different phases of the paradigm: training, STM, and LTM. **(O, P)** The effects of neuropathic pain on object pattern separation (OPS). **(O)** Schematic representation of the OPS procedure and representative heatmaps showing activity (yellow = low activity, red = high activity) around the columns in the OPS test session; **(P)** the graph representing the discrimination index between objects in the different phases of the paradigm: training and test. **(Q–S)** The effects of neuropathic pain on fear conditioning (FC). **(Q)** Schematic representation of the FC procedure and representative activity (yellow) and freezing (green) traces in the different phases of the FC test: habituation (HAB), during tone, and after tone in both contexts. The graphs represent **(R)** the relative freezing during conditioned stimulus (CS)–unconditioned stimulus (US) paired in context A over the trials (learning index) and **(S)** the relative freezing during HAB and after the tone sessions in contexts A and B. The data are represented as the mean ± SEM (n = 8 per group): $^{*}p < .05$, $^{**}p < .01$, $^{***}p < .001$ vs. sham; $+p < .05$, $++p < .01$, $+++p < .001$ vs. CCI as assessed by two-way analysis of variance followed by Newman-Keuls post hoc test. $^{*}p < .05$, $^{**}p < .01$, $^{***}p < .001$ vs. prior to acquisition in each group as assessed by two-way analysis of variance with repeated measures followed by Newman-Keuls post hoc test. A.U., arbitrary units.

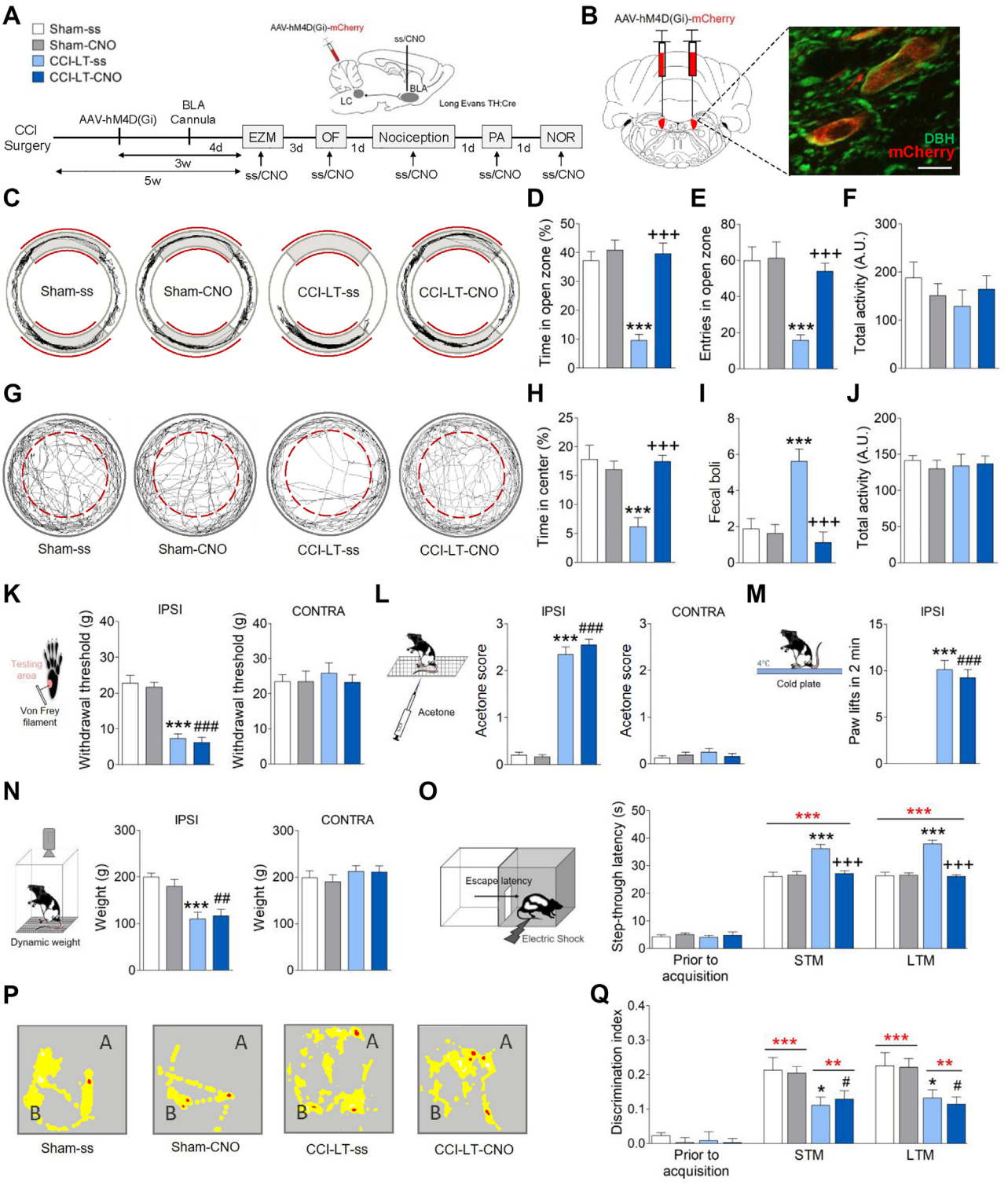

Figure 2. Selective inhibition of the locus coeruleus–basolateral amygdala (LC-BLA) pathway. **(A)** Experimental timeline and schematic representation of the hM4D(Gi)-DREADD (designer receptor exclusively activated by designer drugs) viral and cannula delivery in the behavioral experiments on male Long-Evans tyrosine hydroxylase–Cre (TH-Cre) rats. A Cre-dependent adeno-associated virus (AAV) fluorescently tagged with mCherry [AAV-hM4D(Gi)-mCherry] (1.4 μL/side) was injected bilaterally into the TH neurons of the LC of TH-Cre rats 2 weeks after chronic constriction injury (CCI). The rats were allowed to recover for 3 weeks and to achieve a robust expression of DREADD, and they were implanted bilaterally with metal cannulae into the BLA 4 days before the behavioral

Cognition. In the step-through passive avoidance (PA) test, electric shocks were applied via the grid floor in the dark chamber (2 seconds and 0.5-mA intensity), and the number of chamber changes in the habituation period and the latency of the animal to move into the dark chamber (step-through latency) were recorded in training session and two test sessions, 3 (ST memory [STM]) and 24 (LT memory [LTM]) hours after training (34).

In the novel object recognition test, the time spent exploring each object over 10 minutes was recorded, expressing the relative exploration of the novel object as a discrimination index [discrimination index = $(t_{novel} - t_{familiar})/(t_{novel} + t_{familiar})$, where t is time] (35). The task included a habituation session, training session, and two memory tests, 3 (STM as a learning index) and 24 (LTM as a memory index) hours after training.

The object pattern separation task is a modified version of the novel object recognition test and it was analyzed in the same way (36).

In fear conditioning, a tone (30 seconds, 5 kHz, 80 dB) was used as a conditioned stimulus, and a foot shock (1 second, 0.7 mA) was used as an unconditioned stimulus. The conditioned rats were tested for fear responses (freezing), defined as the absence of all movement except that necessary for respiration (37), and it was monitored throughout the procedure and represented as the percent freezing in each phase.

All behavioral assessments were monitored and analyzed using the SMART video 3.0 software (Panlab, Cornellà de Llobregat, Spain).

Histology and Immunohistochemistry

Immunohistochemistry was performed (12) to evaluate the expression of DREADD-mCherry, Fluoro-Gold tracer, and c-Fos in the LC. The cannula placement and CNO spread in the BLA was also verified.

Statistical Analysis

Data distribution was assumed to be normal and our analytic approaches were based on previously published work (8,19,23), but normality was not formally tested. The data are presented as the mean ± SEM and analyzed with the GraphPad Prism 5.0 software (GraphPad San Diego, CA) and Statistica 10.0 (StatSoft, Tulsa, OK). An unpaired Student *t* test was used to compare the values between the two groups. One- or two-way analyses of variance (with/without repeated measures) were followed by Newman-Keuls post hoc tests. In all cases, $p < .05$ was considered significant (Supplemental Tables S1–10).

RESULTS

Temporal Characterization of the Symptoms Produced by Pain

In these experiments, anxiety-like behaviors, nociceptive responses, and the cognitive capacity of CCI rats were evaluated at two time points after nerve injury, ST (2–3 weeks) and LT (5–6 weeks) (Figure 1A; Supplemental Figure S1A). As expected, anxiety was observed only in the CCI-LT animals (Figure 1B–I), with these rats spending less time in the open quadrant ($p < .05$) and entering the EZM fewer times ($p < .001$), as well as spending less time in the center of the open field ($p < .01$) and producing more fecal boluses ($p < .05$) in that test relative to the sham rats. By contrast, both CCI-ST and CCI-LT rats developed mechanical hypersensitivity in the ipsilateral hindpaw compared with the sham animals ($p < .001$) (Figure 1J), suggesting that pain arises after nerve injury and that it remains constant over time.

We next investigated whether the cognitive sphere is affected by the development of neuropathic pain, using strong emotional arousing (PA test) and weak nonemotional arousing (novel object recognition test) cognitive paradigms. Learning and memory involve two separate events, acquisition and storage, and thus STM was used as an index of learning and LTM as an index of memory. Step-through latencies in the PA test were significantly longer for CCI-LT rats than in the sham animals (STM $p < .001$; LTM $p < .001$) (Figure 1K–L), suggesting hypersensitivity to aversive experiences. By contrast, CCI-LT rats displayed poor discrimination in both novel object recognition tests relative to the sham rats (STM and LTM $p < .05$) (Figure 1M, N). These results were corroborated using the object pattern separation (nonemotional) and fear conditioning (emotional) paradigms. A cognitive deficit was evident in the CCI-LT animals with respect to the sham rats in the object pattern separation task ($p < .05$) (Figure 1O, P), and in the fear conditioning test (Figure 1Q), freezing behavior progressed more significantly during the conditioning phase in the CCI-LT

studies were carried out. Clozapine-*N*-oxide (CNO) (3 μM/0.5 μL) was administered 20 minutes before performing the behavioral tests. **(B)** Representative immunohistofluorescence images (scale bar = 10 μm) of hM4D(Gi)-mCherry expression in noradrenergic LC neurons (red = mCherry, green = dopamine beta hydroxylase). The rats were tested 5–6 weeks (long-term [LT]) after surgery. **(C–F)** The effects of inhibiting the LC-BLA pathway in the elevated zero maze (EZM). **(C)** The representative activity traces and the graphs represent **(D)** the relative time spent in the open zone and **(E)** the number of entries into that zone, or **(F)** the locomotor activity. **(G–J)** The effects of inhibiting the LC-BLA pathway in the open field (OF) test. **(G)** The representative activity traces and the graphs represent **(H)** the relative time spent in the center zone, **(I)** the number of fecal boluses, and **(J)** the locomotor activity. **(K–N)** Sensorial evaluation. The graphs represent **(K)** the withdrawal threshold (grams) of the ipsilateral (IPSI) and contralateral (CONTRA) hindpaws in response to von Frey hair stimulation (0–50 g, 20 seconds), **(L)** the response of IPSI and CONTRA hindpaws to acetone application (100 μL), **(M)** the number of lifts of the IPSI hindpaw in the cold plate test (2 minutes, 4°C), and **(N)** the weight distributed on the IPSI and CONTRA hindpaws in the dynamic weight-bearing test (5 minutes). **(O)** The effects of the inhibition of the LC-BLA pathway on passive avoidance (PA). The graph represents the latency to enter the dark compartment (seconds) in the different phases of the paradigm: training (prior to acquisition), short-term memory (STM) test (as learning index), and long-term memory (LTM) test (as memory index). **(P, Q)** The effects of inhibiting the LC-BLA pathway on the novel object recognition (NOR) test. **(P)** The representative heatmaps showing activity (yellow = low activity, red = high activity) around the objects in the memory tests (A = familiar object, B = novel object) and **(Q)** the graph represents the discrimination index between objects in the different phases of the paradigm: training, STM, and LTM. The data represent the mean ± SEM ($n = 8$ per group): $^{*}p < .05$,$^{***}p < .001$ vs. sham-saline (ss); $+++p < .001$ vs. CCI-LT-ss; $\#p < .05$, $\#\#p < .01$, $\#\#\#p < .001$ vs. sham-CNO; $^{**}p < .01$, $^{***}p < .001$ (red asterisks) vs. prior to acquisition of each group as assessed by two-way analysis of variance followed by Newman-Keuls post hoc test. A.U., arbitrary units.

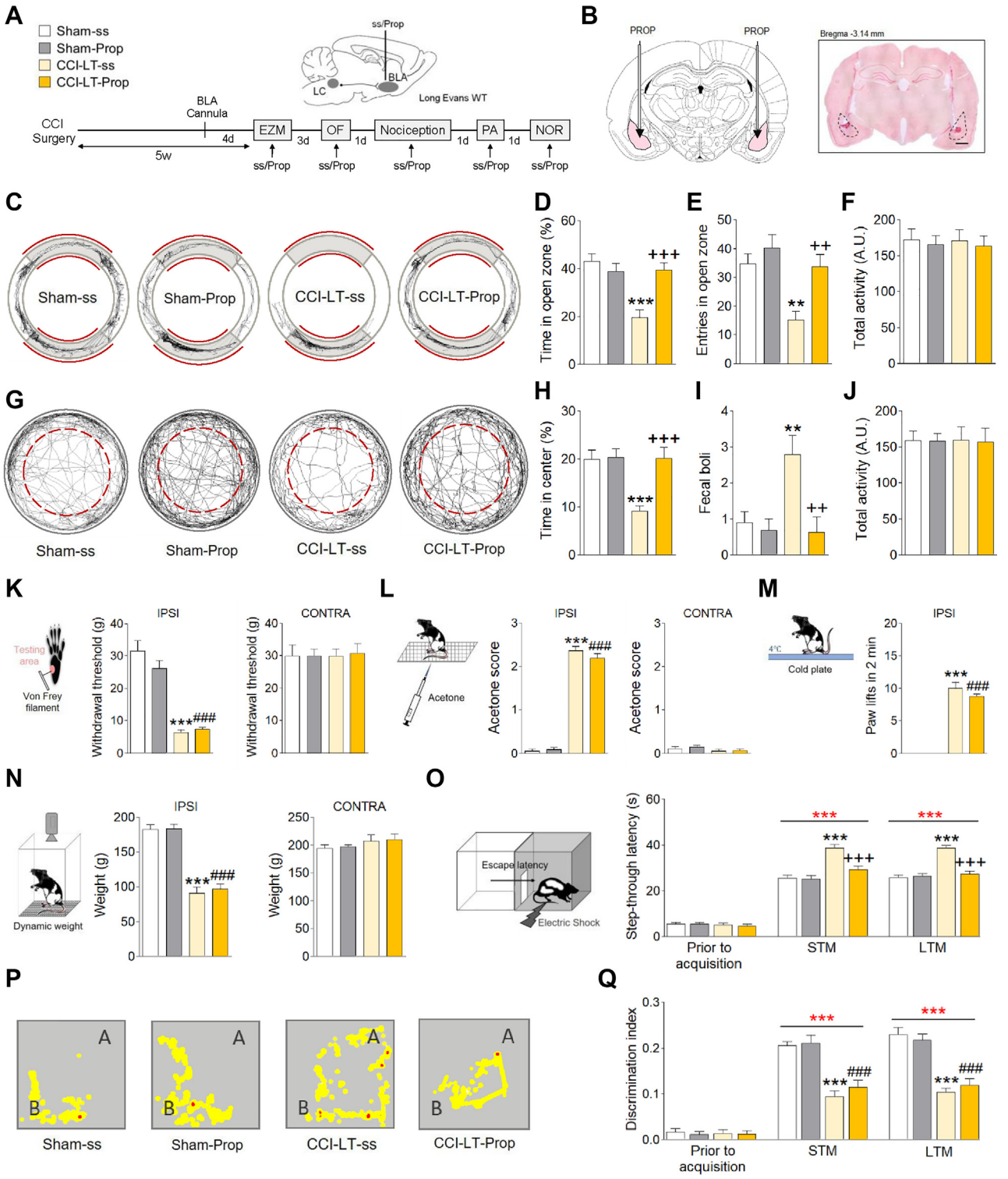

Figure 3. Pharmacological inhibition of beta-adrenergic receptors (β-ARs) in the basolateral amygdala (BLA). **(A)** Experimental timeline and schematic representation of cannula delivery for the behavioral experiments in male Long-Evans wild-type (WT) rats. A metal cannula was implanted bilaterally into the BLA 4 days before performing the behavioral studies. Propranolol (Prop) (1 μg/0.5 μL) was administered 20 minutes before behavioral testing. **(B)** Photomicrograph of a coronal section (neutral red stain) of the rat brainstem showing the tract of the cannula in the BLA (scale bar = 500 μm). The rats were tested 5–6 weeks (long-term [LT]) after chronic constriction injury (CCI). **(C–F)** The effects of inhibiting the β-ARs in the BLA in the elevated zero maze (EZM). **(C)** The representative activity traces and the graphs represent **(D)** the relative time spent in the open zone and **(E)** the number of entries into that zone, as well as **(F)**

rats than in the sham animals ($p < .001$) (Figure 1R). Surprisingly, CCI-LT animals also showed freezing behavior when habituating in another context (context B) ($p < .001$) (Figure 1S), while the rest of the groups remained unaffected. Finally, no significant differences were evident in the cognitive capacities between the CCI-ST and sham rats in any of the tests performed, and none of the behaviors evaluated were affected by any locomotor dysfunction (Figure 1E, I; Supplemental Figure S1B–G). These data show that neuropathy leads to ST and LT sensorial hypersensitivity, whereas anxiety and cognitive impairment develop only when nerve injury persists for long periods of time.

Selective Inhibition of the LC-BLA Pathway Relieves Pain-Induced Anxiety and Aversive Processing

We previously demonstrated in Sprague Dawley rats that c-Fos expression in the LC augments in LT neuropathic pain (38). Accordingly, there was a significant increase in the number of neurons labeled for c-Fos in the LC of CCI-LT with respect to the sham rats ($p < .05$) (Supplemental Figure S2A–F), confirming that LT nerve injury provokes LC hyperactivity.

One brain area innervated by LC neurons is the BLA, as seen by Fluoro-Gold tracing (Supplemental Figure S3A–L). Thus, to explore whether the activity of the LC-BLA pathway is involved in the phenotype observed in CCI-LT rats, we examined hM4D(Gi)-DREADD–mediated inhibition of this pathway (Figure 2A, B; Supplemental Figures S4A–M, S5A, S6A–D, S7, S8A–P, and S9A–H). CCI-LT-CNO animals exhibited a significant increase in the time spent and in the number of entries into the open zones relative to the CCI-LT-ss animals in the EZM ($p < .001$) (Figure 2C–E). Furthermore, more time was spent in the center of the open field, and there were fewer fecal boluses compared with CCI-LT-ss rats in this test ($p < .001$) (Figure 2G–I). Thus, inhibition of LC neurons projecting to the BLA appears to reverse anxiety in CCI-LT animals, reaching similar values to those found in sham-ss rats. Importantly, the hM4D(Gi) manipulation had no effect on the baseline anxiety of sham animals, and none of the manipulations affected locomotor activity (Figure 2F, J).

Subsequently, pain hypersensitivity was evaluated after CNO-mediated inhibition of the LC-BLA pathway in the von Frey, acetone, cold plate, and dynamic weight bearing tests. CNO administration did not produce any change in hypersensitivity-related responses in the CCI-LT-CNO with respect to CCI-LT-ss rats (Figure 2K–N; Supplemental Figure S5B–E). However, there was a significant decrease in the step-through latency of CCI-LT-CNO rats relative to CCI-LT-ss in the PA test (STM and LTM $p < .001$) (Figure 2O; Supplemental Figure S5F). Nevertheless, no differences were found in the novel object recognition test between CCI-LT-CNO and CCI-LT-ss rats (Figure 2P, Q; Supplemental Figure S5G–I). Moreover, inhibition of the LC-BLA pathway had no effect on the sham animals in any of the tests used. Hence, LT pain appears to activate the LC-BLA pathway, leading to anxiety and alterations in the processing of aversive information.

BLA β-ARs Are Involved in Pain-Induced Anxiety and Aversive Processing

To test whether blocking β-AR activity in the BLA would reverse the behaviors associated with LT pain, the effects of intra-BLA administration of the nonselective β-AR antagonist propranolol were tested (Figure 3A, B; Supplemental Figure S10A). Propranolol administration increased the time CCI-LT animals spent in the open zones of the EZM ($p < .001$) and their number of entries into this zone ($p < .01$) (Figure 3C–E). In addition, it also increased the time CCI-LT-propranolol animals spent in the center of the open field ($p < .001$), in conjunction with a decrease in the number of fecal boluses in this test ($p < .01$) relative to the CCI-LT-ss rats (Figure 3G–I). However, in terms of their sensorial evaluation, CCI-LT-propranolol rats performed similarly to CCI-LT-ss animals (Figure 3K–N; Supplemental Figure S10B–E). Propranolol did induce a significant decrease in the step-through latency of CCI-LT rats relative to the controls in the PA test ($p < .001$) (Figure 3O; Supplemental Figure S10F), although their performance in the novel object recognition test was no different (Figure 3P, Q; and Supplemental Figure S10G–I). We next determined the effect of intraperitoneal propranolol administration in the same tests. Interestingly, the systemic antagonism of β-ARs mimicked the effect of intra-BLA blockade of those receptors (Figure 4A–P; Supplemental Figure S11A–H). At the doses studied, propranolol also had no effect on baseline anxiety, nociception, and cognition in the sham animals, and none of the manipulations affected locomotor activity (Figures 3F, J and 4E, I; Supplemental Figures S10F, H–I and S11E, G, H). These data show that blocking β-ARs produced relief from pain-induced anxiety and that it reduced hypersensitivity to aversive experiences.

the locomotor activity. **(G–J)** The effects of β-ARs in the BLA in the open field (OF) test. **(G)** The representative activity traces and the graphs represent **(H)** the relative time spent in the central zone, **(I)** the number of fecal boluses, and **(J)** the locomotor activity. **(K–N)** Sensorial evaluation. The graphs represent **(K)** the withdrawal threshold (grams) of the ipsilateral (IPSI) and contralateral (CONTRA) hindpaws in response to von Frey hair stimulation (0–50 g, 20 seconds), **(L)** the response of the IPSI and CONTRA hindpaws to acetone application (100 μL), **(M)** the number of lifts of the ipsilateral hindpaw in the cold plate test (2 minutes, 4°C), and **(N)** the weight distributed on the IPSI and CONTRA hindpaws in the dynamic weight bearing test (5 minutes). **(O)** The effects of β-ARs in the BLA on passive avoidance (PA). The graph represents the latency to enter the dark compartment (seconds) in the different phases of the paradigm: training (prior to acquisition), short-term memory (STM) test (as learning index), and long-term memory (LTM) test (as memory index). **(P–Q)** The effects of β-ARs in the BLA in the novel object recognition (NOR) test. **(P)** The representative heatmaps showing activity (yellow = low activity, red = high activity) around the objects in the memory tests (A = familiar object, B = novel object) and **(Q)** the graph represents the discrimination index between objects in the different phases of the paradigm: training, STM, and LTM. The data represent the mean ± SEM (n = 8–9 per group): $^{**}p < .01$,$^{***}p < .001$ vs. sham-saline (ss); $++p < .01$, $+++p < .001$ vs. CCI-LT-ss; $###p < .001$ vs. sham-Prop as assessed by two-way analysis of variance followed by Newman-Keuls post hoc test. $^{***}p < .001$ (red asterisks) vs. prior to acquisition of each group as assessed by two-way analysis of variance with repeated measures followed by Newman-Keuls post hoc test. A.U., arbitrary units.

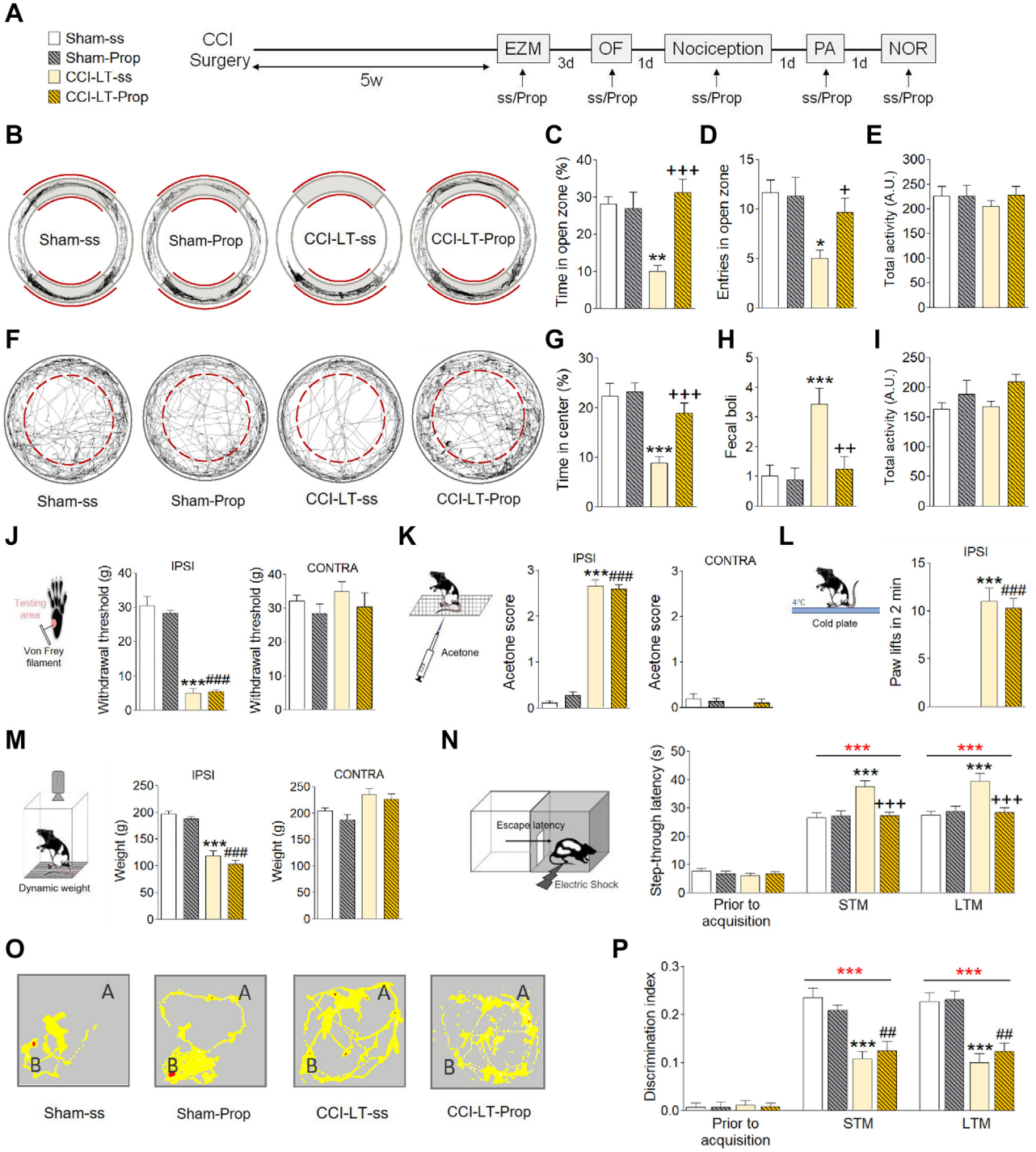

Figure 4. Systemic pharmacological inhibition of beta-adrenergic receptors (β-ARs). **(A)** Experimental timeline for the behavioral experiments in male Long-Evans wild-type rats. Propranolol (Prop) (3 mg/kg intraperitoneal) was administered 20 minutes before behavioral testing. The rats were tested 5–6 weeks (long-term [LT]) after chronic constriction injury (CCI). **(B–E)** The effects of the systemic inhibition of the β-ARs in the elevated zero maze (EZM). **(B)** The representative activity traces and the graphs represent **(C)** the relative time spent in the open zone and **(D)** number of entries into that zone, as well as **(E)** the locomotor activity. **(F–I)** The effects of the systemic inhibition of the β-ARs in the open field (OF) test. **(F)** The representative activity traces and the graphs represent **(G)** the relative time spent in the central zone, **(H)** the number of fecal boluses, and **(I)** the locomotor activity. **(J–M)** Sensorial evaluation. The graphs represent **(J)** the withdrawal threshold (grams) of the ipsilateral (IPSI) and contralateral (CONTRA) hindpaws in response to von Frey hair stimulation (0–50 g, 20 seconds), **(K)** the response of the IPSI and CONTRA hindpaws to acetone application (100 μL), **(L)** the number of lifts of the IPSI hindpaw in the cold plate test (2 minutes, 4°C), and **(M)** the weight distributed on the IPSI and CONTRA hindpaws in the dynamic weight-bearing test (5 minutes). **(N)** The effects of the

Selective Activation of the LC-BLA Pathway Induces Anxiety and Aversive Learning

To assess whether activation of the LC-BLA pathway would induce pain-related phenotypes, we examined the effects of rM3D(Gs)-DREADD–mediated activation of this pathway in sham and CCI-ST animals (Figure 5A, B; Supplemental Figures S12A–E, I–O, S13A). CNO-activated sham animals spent significantly less time in the open zones of the EZM and entered this zone less often than sham-ss rats ($p < .05$) (Figure 5C–F). This effect was significantly blocked by intra-BLA administration of propranolol ($p < .01$) (Supplemental Figure S14A–E). Moreover, similar results were obtained in the open field test (Figure 5G–J). Subsequent evaluation of the animal's cognitive abilities showed a significant increase in the step-through latency of sham-CNO rats relative to the sham-ss animals after STM ($p < .05$) and LTM ($p < .01$) (Figure 5O; Supplemental Figure S13F), which was significantly blocked by intra-BLA propranolol ($p < .05$) (Supplemental Figure S14A, F, G). Hence, LC-BLA activation appears to provoke an anxiogenic-like profile mediated by local β-AR activation, in agreement with previous optogenetic data (21). Strikingly, LC-BLA activation did not modify the parameters of CCI-ST rats, except that CNO decreased the number of entries into the open zones of the EZM relative to the CCI-ST-ss rats ($p < .05$) (Figure 5E). Furthermore, no significant change was observed between CCI-ST-CNO and CCI-ST-ss rats in the step-through latency (Figure 5O). We next explored the local effect of the nonselective β-AR agonist isoproterenol (Supplemental Figures S15A and S16A). At the dose studied, isoproterenol significantly reduced the time spent by CCI-ST animals in the open zone in the EZM ($p < .05$ vs. CCI-ST-ss) (Supplemental Figure S15B–E) but not in the open field test ($p = .06$ vs. CCI-ST-ss) (Supplemental Figure S15F–I). No significant change was observed in the step-through latency (Supplemental Figures S15N and S16F).

We also evaluated the activation of this LC-BLA pathway in LT pain (CCI-LT) (Figure 6A; Supplemental Figure S17A). While in these experiments sham-CNO animals performed similarly to those tested previously, CNO did not modify the pain-induced anxiety and aversive learning and memory of CCI-LT-CNO animals relative to the CCI-LT-ss rats (Figure 6B–I, N; Supplemental Figure S17F), although it did increase the number of fecal boluses recorded in the open field test (CCI-LT-CNO vs. CCI-LT-ss, $p < .01$) (Figure 6H). Importantly, CNO-activated CCI-LT rats did not further increase the already elevated expression of c-Fos neurons in the LC of CCI-LT-ss animals ($p < .05$ vs. sham-ss) (Supplemental Figure S12F–H).

No differences were found between groups in the sensorial evaluation (Figures 5K–N, 6J–M; Supplemental Figures S13B–E, M, S16B–E, and S17B–E) and novel object recognition test (Figures 5P–Q, 6O, P; Supplemental Figures S13G–I, S15O, P, S16G–I, and S17G–I). Thus, activation of the LC-BLA pathway through β-ARs promotes an anxiogenic-like state, as well as an increase in aversive learning and in the memory index in pain-free animals (sham), whereas minor changes are produced in ST and LT nerve-injured animals.

DISCUSSION

Unlike ST pain, LT neuropathic pain leads to an anxiety-like profile and cognitive alterations. Notably, chemogenetic blockade of LC neurons that project to the BLA can reverse such pain-induced anxiety, as well as enhancing PA learning and memory, suggesting that overactivity of this pathway involves β-AR. While activation of LC-BLA neurons leads to anxiety and to enhanced aversive learning and memory in pain-free animals, minor changes are produced in nerve-injured animals. Furthermore, LC-BLA neurons do not seem to modulate sensorial sensitivity or episodic memory.

It has been reported that sensorial hypersensitivity appears immediately in rodents following nerve injury and that after several weeks (3–8 weeks depending on the species and animal model), anxiodepressive and cognitive symptoms arise (7,39,40). Indeed, ST and LT nerve injury in Long-Evans rats lowers sensory thresholds, while only LT injury provokes an anxiogenic-like profile. An evaluation of aversive learning and memory performance shows that only CCI-LT enhances PA learning, as occurs in rodents previously submitted to acute distress, a process involving BLA activity (41). Alternatively, all animals demonstrate similar fear-conditioned acquisition in the fear conditioning test, as indicated previously (42), although the high rate of acquisition (around 90%) might limit the differences between the groups. Interestingly, CCI-LT animals display a higher percentage of freezing in the conditioning phase, developing stronger and earlier fear behavior when faced with an aversive stimulus. Furthermore, and somewhat surprisingly, CCI-LT animals freeze in the habituation phase in a different context (context B). Thus, it would appear that CCI-LT animals do not recognize context B to be different from context A and consequently do not extinguish contextual fear. Indeed, CCI-LT animals show deficits in visual attention, as well as in visuospatial recognition learning and memory, in the novel object recognition test (a nonemotional related test), as reported previously (43). Furthermore, CCI-LT rats also show a deficit in the object pattern separation test that aims to measure spatial pattern separation. Therefore, LT neuropathic pain appears to produce a cognitive bias affecting the processing of aversive stimuli rather than neutral stimuli, probably provoking and maintaining a state of anxiety as appears to occur in human disease-related anxiety (44).

systemic inhibition of the β-ARs on passive avoidance (PA). The graph represents the latency to enter the dark compartment (seconds) in the different phases of the paradigm: training (prior to acquisition), short-term memory (STM) test (as learning index), and long-term memory (LTM) test (as memory index). **(O–P)** The effects of the systemic inhibition of the β-ARs in the novel object recognition (NOR) test. **(O)** The representative heatmaps showing activity (yellow = low activity, red = high activity) around the objects in the memory tests (A = familiar object, B = novel object) and **(P)** the graph represents the discrimination index between objects in the different phases of the paradigm: training, STM, and LTM. The data represent the mean ± SEM ($n = 7–8$ per group): $^{*}p < .05$, $^{**}p < .01$, $^{***}p < .001$ vs. sham-saline (ss); $+p < .05$, $++p < .01$, $+++p < .001$ vs. CCI-LT-ss; $\#\#p < .01$, $\#\#\#p < .001$ vs. sham-Prop as assessed by two-way analysis of variance followed by Newman-Keuls post hoc test. $^{***}p < .001$ (red asterisks) vs. prior to acquisition of each group as assessed by two-way analysis of variance with repeated measures followed by Newman-Keuls post hoc test. A.U., arbitrary units.

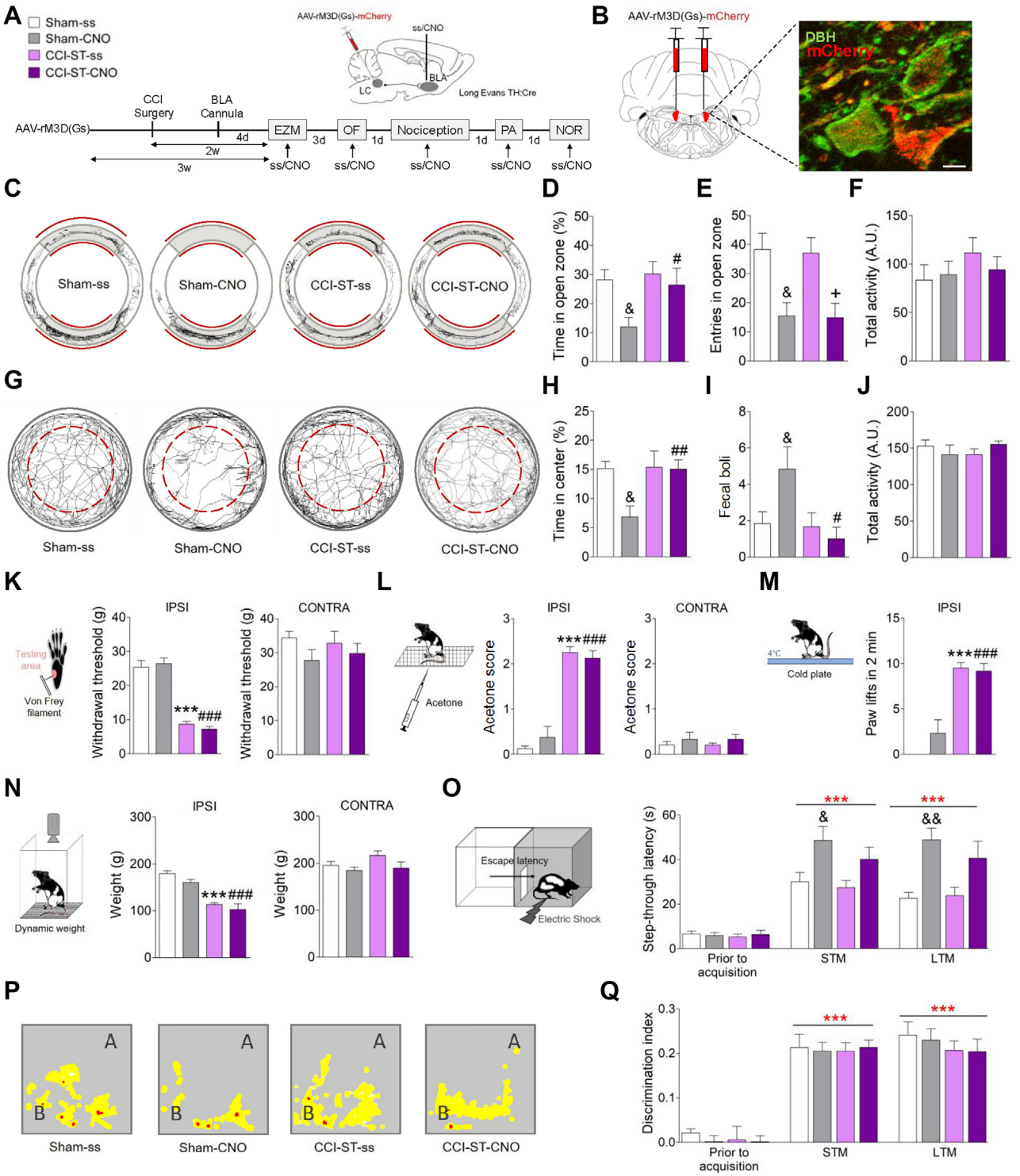

Figure 5. Selective activation of the locus coeruleus–basolateral amygdala (LC-BLA) pathway (short-term [ST] neuropathic pain). **(A)** Experimental timeline and schematic representation of the viral and cannula delivery of rM3D(Gs)-DREADD (designer receptor exclusively activated by designer drugs) for behavioral experiments in male Long-Evans tyrosine hydroxylase (TH)–Cre rats. A Cre-dependent adeno-associated virus (AAV), fluorescently tagged with mCherry [AAV-rM3D(Gs)-mCherry] (1.4 μL/side), was injected bilaterally into the TH neurons of the LC of TH-Cre rats 1 week before inducing chronic constriction injury (CCI). The rats were implanted bilaterally with a metal cannula into the BLA 4 days before the behavioral studies were performed. Clozapine-*N*-oxide (CNO) (3 μM/0.5 μL) was administered 20 minutes before performing the behavioral tests. **(B)** Representative immunofluorescence images (scale bar = 10 μm) of

The activity of LC-noradrenergic neurons is required to elicit acute stress-induced anxiety, and optogenetic/chemogenetic activation of LC neurons itself is anxiogenic (45,46). One of the LC-related networks involved in the expression of emotions is the BLA. Stress augments the noradrenaline in the BLA (47,48), this noradrenaline coming from the LC and from other structures (20). Later studies showed that photostimulation of LC-noradrenergic fibers in the BLA evokes noradrenaline release in this structure, altering BLA neuronal activity and condition aversion, and increasing anxiety-like behavior in control animals (45). Accordingly, selective chemogenetic activation of tyrosine hydroxylase–positive LC neurons that project to the BLA elicits anxiety-like behavior and aversive memory in sham animals, specifically linking the LC-BLA network with negative emotions in pain free animals. Furthermore, it is notable that LC-BLA inhibition does not modify any of the parameters evaluated in sham, suggesting that inhibition of the LC-noradrenergic system is not necessarily anxiolytic.

In the light of these findings, we hypothesize that pain-induced overactivation of the LC-BLA pathway increases the salience of aversive sensory events in LT nerve-injured animals. Blocking this pathway produces robust recovery of the anxiogenic and cognitive-aversive thresholds, which is mediated by beta-adrenergic activity in the BLA. In fact, site-specific pharmacological blockade indicates that β-ARs within the BLA are necessary for this behavior and that they mediate the anxiety-like phenotype associated with increased noradrenaline release in the BLA (21). Furthermore, systemic administration of a β-AR antagonist also reverses the anxiogenic phenotype of animals experiencing LT pain. This effect may have translational value, opening the possibility to treat pain-induced anxiety with brain penetrant beta-blockers. By contrast, chemogenetic LC-BLA inhibition had no effect on a low-arousing behavioral task (novel object recognition test). Previous studies revealed that noradrenergic activation of BLA modulates hippocampal consolidation in the novel object recognition test, although emotional arousal was enhanced in this test and the role of the BLA was potentiated in all these studies (49–52). By contrast, our protocol produces little emotional arousal, minimizing the influence of the LC-BLA pathway in this paradigm. Indeed, if this nonemotional task only includes strong novelty-related emotional arousal, plastic changes in the hippocampus are mediated by the BLA (53). Furthermore, deficits evident in the novel object recognition test have been ascribed to enhanced noradrenergic input to the prefrontal cortex following nerve injury (54). This suggests that other LC brain targets (the hippocampus or prefrontal cortex) might be involved in the novel object recognition test deficits in CCI-LT animals. Alternatively, no change in sensorial hypersensitivity arises when the LC-BLA noradrenergic pathway is inhibited, suggesting that this pathway is not directly related to nociception itself.

We also wondered about the consequences of activating LC-BLA neurons in nerve-injured animals. As expected, stronger activity of this pathway leads to an anxiogenic profile and, consequently, to an increase in the processing of aversive information mediated by β-AR in pain-free animals. Strikingly, nerve injured animals that do not develop secondary anxiety-related symptoms do not display a robust enhancement of their anxiety-related profile when LC-BLA neurons are chemogenetically activated. However, the pharmacological activation of β-AR in the BLA with isoproterenol did intensify the anxiogenic phenotype of these animals to some extent. This was unexpected and might be due to changes in AR expression, with opposing effects of β-ARs and β_2-ARs (55,56). Alternatively, these behavioral manifestations may be counteracted by the activity of other pathways that impede the noradrenergic activation of the BLA after ST injury. Perhaps, these opposing effects are overridden after a period of time, leading to the anxiogenic phenotype and the stronger aversive memory performance evident in CCI-LT rats. Further studies into the different ARs and the expression of c-Fos–mediated rM3D(Gs)-DREADD will be necessary to determine what plastic changes take place in this phase of pain. Interestingly, it was recently shown that the chemogenetic activation of LC neurons projecting to the prefrontal cortex provokes anxiety and aversion in naïve animals, as well as anxiety, aversion, and spontaneous pain in animals with neuropathic pain but without comorbid anxiety (19). This demonstrates that LC neurons can produce distinct responses and that prefrontal cortex–projecting ensemble is susceptible to full activation in conjunction with pain, provoking anxiety. rM3D(Gs)-DREADD was not able to further intensify anxiety or the already elevated c-Fos expression in LT nerve-injured animals, suggesting that LT pain leads to maximal activation of the LC-BLA pathway. Bearing in mind previous findings (19), it would be

rM3D(Gs)-mCherry expression in noradrenergic LC neurons (red = mCherry; green = dopamine beta hydroxylase). The rats were tested 2–3 weeks (ST) after surgery. **(C–F)** The effects of activating the LC-BLA pathway in the elevated zero maze (EZM). **(C)** The representative activity traces and the graphs represent **(D)** the relative time spent in the open zone and **(E)** the number of entries into that zone, as well as **(F)** the locomotor activity. **(G–J)** The effects of activating the LC-BLA pathway in the open field (OF) test. **(G)** The representative activity traces and the graphs represent **(H)** the relative time spent in the central zone, **(I)** the number of fecal boluses, and **(J)** the locomotor activity. **(K–N)** Sensorial evaluation. The graphs represent **(K)** the withdrawal threshold (grams) of the ipsilateral (IPSI) and contralateral (CONTRA) hindpaws in response to von Frey hair stimulation (0–50 g, 20 seconds), **(L)** the response of the IPSI and CONTRA hindpaws to acetone application (100 μL), **(M)** the number of lifts of the ipsilateral hindpaw in the cold plate test (2 minutes, 4°C), and **(N)** the weight distributed on the IPSI and CONTRA hindpaws in the dynamic weight bearing test (5 minutes). **(O)** The effects of activating the LC-BLA pathway on passive avoidance (PA). The graph represents the latency to enter the dark compartment (seconds) in the different phases of the paradigm: training (prior to acquisition), short-term memory (STM) test (as learning index), and long-term memory (LTM) test (as memory index). **(P–Q)** The effects of activating the LC-BLA pathway on the novel object recognition (NOR) test. **(P)** The representative heatmaps showing activity (yellow = low activity, red = high activity) around the objects in the memory tests (A = familiar object, B = novel object) and **(Q)** the graph represents the discrimination index between objects in the different phases of the paradigm: training, STM, and LTM. The data represent the mean ± SEM (n = 5–6 per group): $^{**}p < .01$, $^{***}p < .001$ vs. sham-saline (ss); $+p < .05$ vs. CCI-ST-ss; $\#p < .05$, $\#\#p < .01$, $\#\#\#p < .001$ vs. sham-CNO; $\&p < .05$, $\&\&\ p < .01$ vs. sham-ss as assessed by two-way analysis of variance followed by Newman-Keuls post hoc test. $^{***}p < .001$ (red asterisks) vs. prior to acquisition of each group as assessed by two-way analysis of variance with repeated measures followed by Newman-Keuls post hoc test. A.U., arbitrary units.

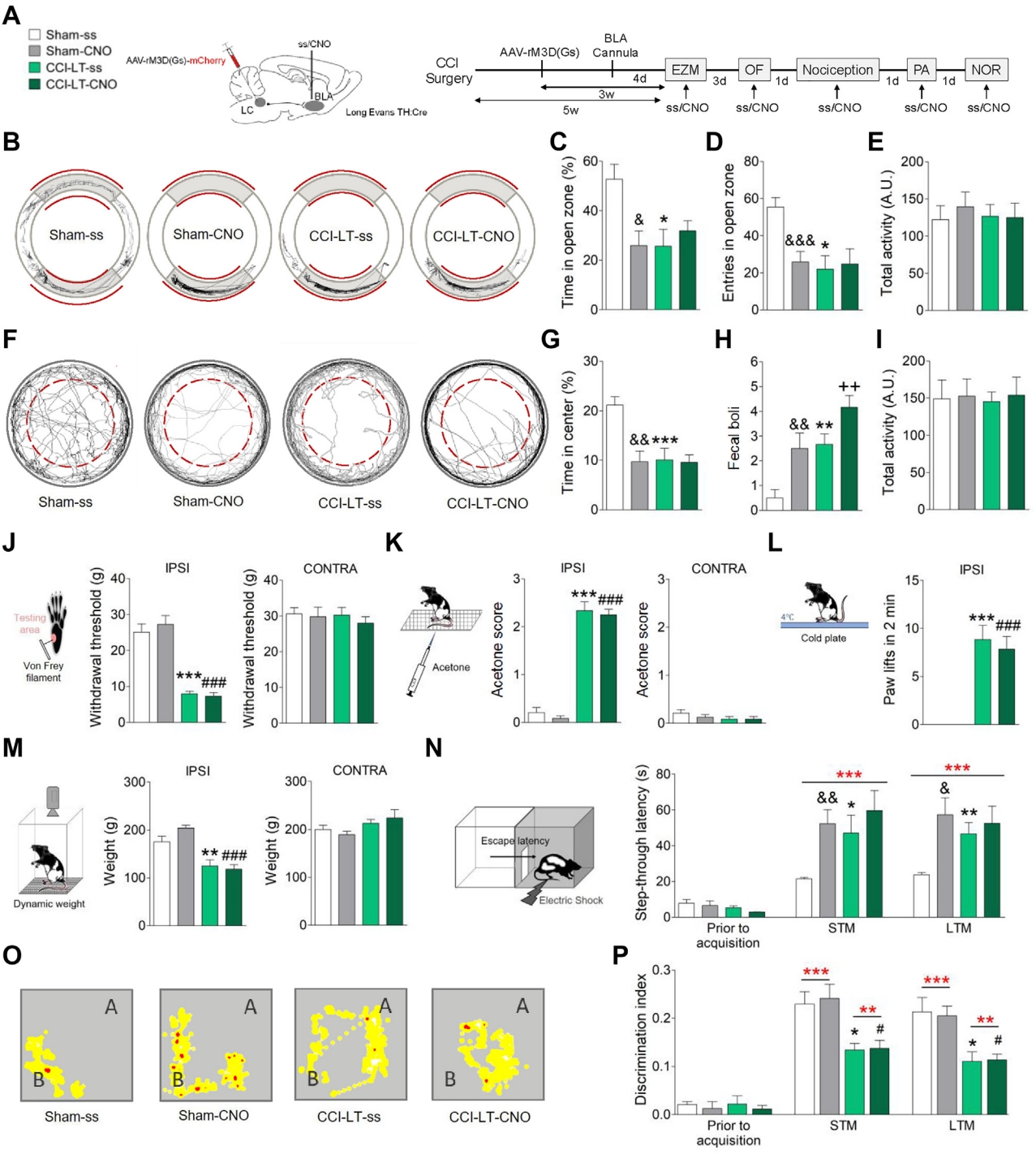

Figure 6. Selective activation of the locus coeruleus–basolateral amygdala (LC-BLA) pathway (long-term [LT] neuropathic pain). **(A)** Experimental timeline and schematic representation of viral and cannula delivery of rM3D(Gs)-DREADD (designer receptor exclusively activated by designer drugs) for behavioral experiments in male Long-Evans tyrosine hydroxylase (TH)–Cre rats. A Cre-dependent adeno-associated virus (AAV), fluorescently tagged with mCherry [AAV-rM3D(Gs)-mCherry] (1.4 μL/side), was injected bilaterally into the TH neurons of locus coeruleus (LC) of TH-Cre rats 2 weeks after chronic constriction injury (CCI). The rats were allowed to recover for 3 weeks to achieve robust expression of DREADD, and a metal cannula was implanted bilaterally into the BLA 4 days before carrying out the behavioral studies. Clozapine-*N*-oxide (CNO) (3 μM/0.5 μL) was administered 20 minutes before the behavioral testing. The rats were tested 5–6 weeks (LT) after surgery. **(B–E)** The effects of activating the LC-BLA pathway in the elevated zero maze (EZM). **(B)** The representative activity traces

very interesting to explore the LC–prefrontal cortex activity in animals experiencing neuropathic pain in conjunction with comorbid anxiety. Stronger activity of the LC–medial prefrontal cortex projecting neurons is required during extinction of aversive learning (23). Weaker activity in this circuit may underlie the inability to achieve extinction of aversive experiences described in LT pain animals that also display anxiety (57). Finally, neither mechanical sensory nor low-arousal task behavior is modified in these animals, indicating that the sensorial, affective, and cognitive dimensions are independent. Accordingly, one dimension can deteriorate without affecting the other.

Using ethological tests and models that involve learned/punished responses, the data presented here show that overactivation of the LC-BLA pathway provoked by chronic pain leads to anxiety and enhanced processing of aversive stimuli, which in turn might exaggerate vulnerability when confronted by stress. Specifically, pain would augment the noradrenaline in the BLA, enhancing the memorization of negative events. The inhibition of this projection, or that of the local blockade of β-ARs, inhibits pain-induced anxiety. This beneficial effect on anxiety was also found when beta-blockers were administered systemically, which may open new interventional options for the treatment of comorbid pain and anxiety. Finally, our study builds on previous work showing the circuit-selective modular organization of the LC system and its role in regulating brain function in the healthy and disease states (19,21,23).

ACKNOWLEDGMENTS AND DISCLOSURES

This study was supported by grants cofinanced by "Fondo Europeo de Desarrollo Regional" (FEDER)-UE "A way to build Europe" from the "Ministerio de Economía y Competitividad" (MINECO) (SAF2015-68647-R) and "Ministerio de Salud-Instituto de Salud Carlos III (PI18/01691); the "Consejería de Salud de la Junta de Andalucía" (PI-0134-2018); the "Programa Operativo de Andalucía FEDER, Iniciativa Territorial Integrada ITI 2014-2020 Consejería Salud, Junta de Andalucía" (PI-0080-2017); the "Consejería de Economía, Innovación, Ciencia y Empleo de la Junta de Andalucía" (CTS-510); the "Centro de Investigación Biomédica en Red de Salud Mental-CIBERSAM" (CB/07/09/0033); a Young Investigator Grant from the Brain Behavior Research Foundation (NARSAD23982).

We thank Mr. Muñoz, Mrs. Reyes, and Mrs. Verges-Castillo for their skilled technical assistance; the Central Services for Scientific and Technological Research, Health Sciences, and Animal Research from the University of Cádiz; the Rat Resource and Research Center and Dr. K. Deisseroth for providing the tyrosine hydroxylase–Cre rat transgenic line; and Dr. J. Nacher for providing the cFos antibody (BIOTECMED, Universitat de València).

The authors report no biomedical financial interests or potential conflicts of interest.

ARTICLE INFORMATION

From the Neuropsychopharmacology and Psychobiology Research Group (ML-T, IS-P, LB, JAG-P, JAM), Department of Neuroscience; Biomedical Research and Innovation Institute of Cádiz (INiBICA) Research Unit (ML-T, IS-P, LB, CC-D, JAG-P, JAM, EB), Puerta del Mar University Hospital; Biomedical Research Foundation of Cadiz (ML-T), Puerta del Mar University Hospital; and Neuropsychopharmacology and Psychobiology Research Group (CC-D, EB), Department of Psychology, University of Cádiz, Cádiz; and Biomedical Research Networking Center for Mental Health Network (CIBERSAM) (ML-T, IS-P, LB, JAM, EB), Institute of Health Carlos III, Madrid, Spain.

ML-T and IS-P contributed equally to this work.

Address correspondence to Esther Berrocoso, Ph.D., Neuropsychopharmacology and Psychobiology Research Group, Psychobiology Area, Department of Psychology, University of Cádiz, 11510 Puerto Real, Cádiz, Spain; E-mail: esther.berrocoso@uca.es.

Received Jun 21, 2018; revised and accepted Feb 19, 2019.

Supplementary material cited in this article is available online at https://doi.org/10.1016/j.biopsych.2019.02.018.

REFERENCES

1. Reid KJ, Harker J, Bala MM, Truyers C, Kellen E, Bekkering GE, *et al.* (2011): Epidemiology of chronic non-cancer pain in Europe: Narrative review of prevalence, pain treatments and pain impact. Curr Med Res Opin 27:449–462.
2. Goldberg DS, McGee SJ (2011): Pain as a global public health priority. BMC Public Health 11:770.
3. Johannes CB, Le TK, Zhou X, Johnston JA, Dworkin RH (2010): The prevalence of chronic pain in United States adults: Results of an Internet-based survey. J Pain 11:1230–1239.
4. Breivik H, Collett B, Ventafridda V, Cohen R, Gallacher D (2006): Survey of chronic pain in Europe: Prevalence, impact on daily life, and treatment. Eur J Pain 10:287–333.
5. Maletic V, Raison CL (2009): Neurobiology of depression, fibromyalgia and neuropathic pain. Front Biosci (Landmark Ed) 14:5291–5338.
6. McWilliams LA, Cox BJ, Enns MW (2003): Mood and anxiety disorders associated with chronic pain: An examination in a nationally representative sample. Pain 106:127–133.
7. Alba-Delgado C, Cebada-Aleu A, Mico JA, Berrocoso E (2016): Comorbid anxiety-like behavior and locus coeruleus impairment in diabetic peripheral neuropathy: A comparative study with the chronic constriction injury model. Prog Neuropsychopharmacol Biol Psychiatry 71:45–56.

and the graphs represent **(C)** the relative time spent in the open zone and **(D)** the number of entries into that zone, as well as **(E)** the locomotor activity. **(F–I)** The effects of activating the LC-BLA pathway in the open field (OF) test. **(F)** The representative activity traces and the graphs represent **(G)** the relative time spent in the central zone, **(H)** the number of fecal boluses, and **(I)** the locomotor activity. **(J–M)** Sensorial evaluation. The graphs represent **(J)** the withdrawal threshold (grams) of the ipsilateral (IPSI) and contralateral (CONTRA) hindpaws in response to von Frey hair stimulation (0–50 g, 20 seconds), **(K)** the response of the IPSI and CONTRA hindpaws to acetone application (100 μL), **(L)** the number of lifts of the ipsilateral hindpaw in the cold plate test (2 minutes, 4°C), and **(M)** the weight distributed on the IPSI and CONTRA hindpaws in the dynamic weight bearing test (5 minutes). **(N)** The effects of activating the LC-BLA pathway on passive avoidance (PA). The graph represents the latency to enter the dark compartment (seconds) in the different phases of the paradigm: training (prior to acquisition), short-term memory (STM) test (as learning index), and long-term memory (LTM) test (as memory index). **(O, P)** The effects of activating the LC-BLA pathway on the novel object recognition (NOR) test. **(O)** The representative heatmaps showing activity (yellow = low activity, red = high activity) around the objects in the memory tests (A = familiar object, B = novel object) and **(P)** the graph represents the discrimination index between objects in the different phases of the paradigm: training, STM, and LTM. The data represent the mean ± SEM (n = 5–6 per group): $^{*}p < .05$, $^{**}p < .01$, $^{***}p < .001$ vs. sham-saline (ss); $++p <$ .01 vs. CCI-LT-ss; $\#p < .05$, $\#\#\#p < .001$ vs. sham-CNO; $\&p < .05$, $\&\&p < .01$, $\&\&\&p < .001$ vs. sham-ss as assessed by two-way analysis of variance followed by Newman-Keuls post hoc test. $^{**}p < .01$, $^{***}p < .001$ (red asterisks) vs. prior to acquisition of each group as assessed by two-way analysis of variance with repeated measures followed by Newman-Keuls post hoc test. A.U., arbitrary units.

8. Alba-Delgado C, Llorca-Torralba M, Horrillo I, Ortega JE, Mico JA, Sanchez-Blazquez P, *et al.* (2013): Chronic pain leads to concomitant noradrenergic impairment and mood disorders. Biol Psychiatry 73:54–62.
9. Alba-Delgado C, Mico JA, Sanchez-Blazquez P, Berrocoso E (2012): Analgesic antidepressants promote the responsiveness of locus coeruleus neurons to noxious stimulation: Implications for neuropathic pain. Pain 153:1438–1449.
10. Borges G, Miguelez C, Neto F, Mico JA, Ugedo L, Berrocoso E (2017): Activation of extracellular signal-regulated kinases (ERK 1/2) in the locus coeruleus contributes to pain-related anxiety in arthritic male rats. Int J Neuropsychopharmacol 20:463.
11. Borges GP, Mico JA, Neto FL, Berrocoso E (2015): Corticotropin-releasing factor mediates pain-induced anxiety through the ERK1/2 signaling cascade in locus coeruleus neurons. Int J Neuropsychopharmacol 18:pyv019.
12. Bravo L, Alba-Delgado C, Torres-Sanchez S, Mico JA, Neto FL, Berrocoso E (2013): Social stress exacerbates the aversion to painful experiences in rats exposed to chronic pain: The role of the locus coeruleus. Pain 154:2014–2023.
13. Bravo L, Mico JA, Rey-Brea R, Camarena-Delgado C, Berrocoso E (2016): Effect of DSP4 and desipramine in the sensorial and affective component of neuropathic pain in rats. Prog Neuropsychopharmacol Biol Psychiatry 70:57–67.
14. Bravo L, Torres-Sanchez S, Alba-Delgado C, Mico JA, Berrocoso E (2014): Pain exacerbates chronic mild stress-induced changes in noradrenergic transmission in rats. Eur Neuropsychopharmacol 24:996–1003.
15. Llorca-Torralba M, Borges G, Neto F, Mico JA, Berrocoso E (2016): Noradrenergic Locus Coeruleus pathways in pain modulation. Neuroscience 338:93–113.
16. Llorca-Torralba M, Mico JA, Berrocoso E (2018): Behavioral effects of combined morphine and MK-801 administration to the locus coeruleus of a rat neuropathic pain model. Prog Neuropsychopharmacol Biol Psychiatry 84:257–266.
17. Torres-Sanchez S, Borges GDS, Mico JA, Berrocoso E (2018): Opioid and noradrenergic contributions of tapentadol to the inhibition of locus coeruleus neurons in the streptozotocin rat model of polyneuropathic pain. Neuropharmacology 135:202–210.
18. Martins AR, Froemke RC (2015): Coordinated forms of noradrenergic plasticity in the locus coeruleus and primary auditory cortex. Nat Neurosci 18:1483–1492.
19. Hirschberg S, Li Y, Randall A, Kremer EJ, Pickering AE (2017): Functional dichotomy in spinal- vs. prefrontal-projecting locus coeruleus modules splits descending noradrenergic analgesia from ascending aversion and anxiety in rats. Elife 6:e29808.
20. Robertson SD, Plummer NW, de Marchena J, Jensen P (2013): Developmental origins of central norepinephrine neuron diversity. Nat Neurosci 16:1016–1023.
21. McCall JG, Siuda ER, Bhatti DL, Lawson LA, McElligott ZA, Stuber GD, *et al.* (2017): Locus coeruleus to basolateral amygdala noradrenergic projections promote anxiety-like behavior. Elife 6:e18247.
22. Siuda ER, Al-Hasani R, McCall JG, Bhatti DL, Bruchas MR (2016): Chemogenetic and optogenetic activation of galphas signaling in the basolateral amygdala induces acute and social anxiety-like states. Neuropsychopharmacology 41:2011–2023.
23. Uematsu A, Tan BZ, Ycu EA, Cuevas JS, Koivumaa J, Junyent F, *et al.* (2017): Modular organization of the brainstem noradrenaline system coordinates opposing learning states. Nat Neurosci 20:1602–1611.
24. Bennett GJ, Xie YK (1988): A peripheral mononeuropathy in rat that produces disorders of pain sensation like those seen in man. Pain 33:87–107.
25. Berrocoso E, De Benito MD, Mico JA (2007): Role of serotonin 5-HT1A and opioid receptors in the antiallodynic effect of tramadol in the chronic constriction injury model of neuropathic pain in rats. Psychopharmacology (Berl) 193:97–105.
26. Vazey EM, Aston-Jones G (2014): Designer receptor manipulations reveal a role of the locus coeruleus noradrenergic system in isoflurane general anesthesia. Proc Natl Acad Sci U S A 111:3859–3864.
27. Tervo DGR, Proskurin M, Manakov M, Kabra M, Vollmer A, Branson K, *et al.* (2014): Behavioral variability through stochastic choice and its gating by anterior cingulate cortex. Cell 159:21–32.
28. Cryan JF, Kelly PH, Chaperon F, Gentsch C, Mombereau C, Lingenhoehl K, *et al.* (2004): Behavioral characterization of the novel GABAB receptor-positive modulator GS39783 (N,N'-dicyclopentyl-2-methylsulfanyl-5-nitro-pyrimidine-4,6-diamine): Anxiolytic-like activity without side effects associated with baclofen or benzodiazepines. J Pharmacol Exp Ther 310:952–963.
29. Bleickardt CJ, Mullins DE, Macsweeney CP, Werner BJ, Pond AJ, Guzzi MF, *et al.* (2009): Characterization of the V1a antagonist, JNJ-17308616, in rodent models of anxiety-like behavior. Psychopharmacology (Berl) 202:711–718.
30. Berrocoso E, Mico JA, Vitton O, Ladure P, Newman-Tancredi A, Depoortere R, *et al.* (2011): Evaluation of milnacipran, in comparison with amitriptyline, on cold and mechanical allodynia in a rat model of neuropathic pain. Eur J Pharmacol 655:46–51.
31. Bravo L, Mico JA, Rey-Brea R, Perez-Nievas B, Leza JC, Berrocoso E (2012): Depressive-like states heighten the aversion to painful stimuli in a rat model of comorbid chronic pain and depression. Anesthesiology 117:613–625.
32. Jasmin L, Kohan L, Franssen M, Janni G, Goff JR (1998): The cold plate as a test of nociceptive behaviors: Description and application to the study of chronic neuropathic and inflammatory pain models. Pain 75:367–382.
33. Tetreault P, Dansereau MA, Dore-Savard L, Beaudet N, Sarret P (2011): Weight bearing evaluation in inflammatory, neuropathic and cancer chronic pain in freely moving rats. Physiol Behav 104:495–502.
34. Suarez-Pereira I, Canals S, Carrion AM (2015): Adult newborn neurons are involved in learning acquisition and long-term memory formation: The distinct demands on temporal neurogenesis of different cognitive tasks. Hippocampus 25:51–61.
35. Romero-Granados R, Fontan-Lozano A, Delgado-Garcia JM, Carrion AM (2010): From learning to forgetting: Behavioral, circuitry, and molecular properties define the different functional states of the recognition memory trace. Hippocampus 20:584–595.
36. van Hagen BT, van Goethem NP, Lagatta DC, Prickaerts J (2015): The object pattern separation (OPS) task: A behavioral paradigm derived from the object recognition task. Behav Brain Res 285:44–52.
37. Fanselow MS (1980): Conditioned and unconditional components of post-shock freezing. Pavlov J Biol Sci 15:177–182.
38. Llorca-Torralba M, Pilar-Cuéllar F, Bravo L, Bruzos-Cidon C, Torrecilla M, Mico JA, *et al.* (2019): Opioid activity in the locus coeruleus is modulated by chronic neuropathic pain. Mol Neurobiol 56:4135–4150.
39. Barthas F, Sellmeijer J, Hugel S, Waltisperger E, Barrot M, Yalcin I (2015): The anterior cingulate cortex is a critical hub for pain-induced depression. Biol Psychiatry 77:236–245.
40. Yalcin I, Barthas F, Barrot M (2014): Emotional consequences of neuropathic pain: Insight from preclinical studies. Neurosci Biobehav Rev 47:154–164.
41. Ito W, Erisir A, Morozov A (2015): Observation of distressed conspecific as a model of emotional trauma generates silent synapses in the prefrontal-amygdala pathway and enhances fear learning, but ketamine abolishes those effects. Neuropsychopharmacology 40:2536–2545.
42. Moriarty O, Roche M, McGuire BE, Finn DP (2012): Validation of an air-puff passive-avoidance paradigm for assessment of aversive learning and memory in rat models of chronic pain. J Neurosci Methods 204:1–8.
43. Kodama D, Ono H, Tanabe M (2011): Increased hippocampal glycine uptake and cognitive dysfunction after peripheral nerve injury. Pain 152:809–817.
44. Burman OH, Parker RM, Paul ES, Mendl MT (2009): Anxiety-induced cognitive bias in non-human animals. Physiol Behav 98:345–350.
45. McCall JG, Al-Hasani R, Siuda ER, Hong DY, Norris AJ, Ford CP, *et al.* (2015): CRH engagement of the locus coeruleus noradrenergic system mediates stress-induced anxiety. Neuron 87:605–620.
46. Sciolino NR, Plummer NW, Chen YW, Alexander GM, Robertson SD, Dudek SM, *et al.* (2016): Recombinase-dependent mouse lines for

chemogenetic activation of genetically defined cell types. Cell Rep 15:2563–2573.
47. Galvez R, Mesches MH, McGaugh JL (1996): Norepinephrine release in the amygdala in response to footshock stimulation. Neurobiol Learn Mem 66:253–257.
48. Hatfield T, Spanis C, McGaugh JL (1999): Response of amygdalar norepinephrine to footshock and GABAergic drugs using in vivo microdialysis and HPLC. Brain Res 835:340–345.
49. Mello-Carpes PB, da Silva de Vargas L, Gayer MC, Roehrs R, Izquierdo I (2016): Hippocampal noradrenergic activation is necessary for object recognition memory consolidation and can promote BDNF increase and memory persistence. Neurobiol Learn Mem 127:84–92.
50. Mello-Carpes PB, Izquierdo I (2013): The nucleus of the solitary tract–> nucleus paragigantocellularis–> locus coeruleus–> CA1 region of dorsal hippocampus pathway is important for consolidation of object recognition memory. Neurobiol Learn Mem 100:56–63.
51. Barsegyan A, McGaugh JL, Roozendaal B (2014): Noradrenergic activation of the basolateral amygdala modulates the consolidation of object-in-context recognition memory. Front Behav Neurosci 8:160.
52. Roozendaal B, Castello NA, Vedana G, Barsegyan A, McGaugh JL (2008): Noradrenergic activation of the basolateral amygdala modulates consolidation of object recognition memory. Neurobiol Learn Mem 90:576–579.
53. McReynolds JR, Anderson KM, Donowho KM, McIntyre CK (2014): Noradrenergic actions in the basolateral complex of the amygdala modulate Arc expression in hippocampal synapses and consolidation of aversive and non-aversive memory. Neurobiol Learn Mem 115:49–57.
54. Suto T, Eisenach JC, Hayashida K (2014): Peripheral nerve injury and gabapentin, but not their combination, impair attentional behavior via direct effects on noradrenergic signaling in the brain. Pain 155:1935–1942.
55. Bashiri H, Rezayof A, Sahebgharani M, Tavangar SM, Zarrindast MR (2016): Modulatory effects of the basolateral amygdala alpha2-adrenoceptors on nicotine-induced anxiogenic-like behaviours of rats in the elevated plus maze. Neuropharmacology 105:478–486.
56. Buffalari DM, Grace AA (2007): Noradrenergic modulation of basolateral amygdala neuronal activity: Opposing influences of alpha-2 and beta receptor activation. J Neurosci 27:12358–12366.
57. Mutso AA, Radzicki D, Baliki MN, Huang L, Banisadr G, Centeno MV, *et al.* (2012): Abnormalities in hippocampal functioning with persistent pain. J Neurosci 32:5747–5756.

Chemogenetic Silencing of the Locus Coeruleus-Basolateral Amygdala Pathway Abolishes Pain-Induced Anxiety and Enhanced Aversive Learning in Rats

Supplemental Information

Supplemental Methods and Materials

Animals

Males rats were obtained by crosses hemizygous tyrosine hydroxylase-Cre (TH:Cre) transgenic and wild-type Long Evans rats. The breeding was done at the University of Cadiz, from founders provided by Rat Resource and Research Center (RRCC, USA), which were donated by K. Deisseroth. Experiments were carried out on male wildtype or TH-Cre rats, weighing 350-450 g, that were maintained under standard laboratory conditions (22 ºC, 12 h light/dark cycle, lights on at 08:00 AM, food and water *ad libitum*). Animal handling and procedures were carried out in accordance with the guidelines of the European Commission's directive (2010/63/EC) and Spanish Law (RD 53/2013) regulating animal research. Furthermore, all experimental protocols were approved by the Committee for Animal Experimentation at the University of Cadiz (Spain).

Neuropathic pain model

Chronic constriction injury (CCI) was produced after anesthetizing the rats with isoflurane (the induction with 3%-4% and the maintenance with 1.5%-2.5%), and the left sciatic nerve was then exposed at the mid-thigh level, proximal to the sciatic trifurcation. Four chrome gut (4–0) ligatures were tied loosely around the nerve, separated by 1.0 –1.5 mm so as not to compromise the vascular supply. The overlying layers of muscle were closed with 4–0 non-absorbable silk thread and the skin was sutured with a 2–0 silk thread. Sham operations were performed in the same manner but without nerve ligation.

DREADD virus injection

Rats were anesthetized with an i.p. injection of ketamine (100 mg/kg) and xylazine (20 mg/kg), placed in a stereotaxic frame with the head oriented at a 15º angle to the horizontal plane (nose down) and a Designer Receptor Exclusively Activated by Designer Drugs DREADD virus was injected unilateral or bilaterally (1.4 µl/side) into the LC (coordinates to lambda: -3.2 anterior-posterior [AP], ± 1.3 medial-lateral [ML], and 6.2 dorsal-ventral [DV]). DREADDs virus were: AAV2/hSyn-DIO-hM4D(Gi)-mCherry (Inhibitor virus; titer 3 x 10^12 vg/ml), AAV2/hSyn-DIO-rM3D(Gs)-mCherry (Activator virus; titer 3 x 10^12 vg/ml) and AAV2/hSyn-DIO-

mCherry (control virus; titer 5.6 x 10^12 vg/ml) from Virus Vector Core, Gene Therapy Center Vector Core at the University of North Caroline, USA. The control vector contained a mCherry reporter protein only. Alternatively, the Fluoro-Gold retrograde tracer (4 % w/v, 0.2 µl; FG: Fluorocrome, USA) was injected unilateral or bilaterally into the BLA of rats placed in a stereotaxic frame with the head oriented at a 0º angle to the horizontal plane using a syringe pump at a rate of 0.1 µl/min (coordinates to bregma: -2.9 AP, ± 4.8 ML, and -8.4 DV). The infuser was left in place for an additional 3 minutes following each injection before it was slowly removed. Following surgery, rats were allowed to recover for 4 days (FG tracer) or 3 weeks (DREADD virus) before behavioral studies were performed to allow for robust tracer or gene expression in the target regions.

BLA cannula implantation

Rats were anesthetized with an i.p. injection of ketamine (100 mg/kg) and xylazine (20 mg/kg) and placed in a stereotaxic frame with the head oriented at a 0º angle to the horizontal plane. A cannula was implanted bilaterally into the BLA (coordinates to bregma: -2.9 AP, ± 4.8 ML, and -8.4 DV), and fixed in place with dental cement and four anchor screws. Following surgery, the rats were allowed to recover for 4 days before performing the behavioral experiments and the cannula was maintained closed until the test session by inserting a stainless steel wire.

Drug administration

CNO, propranolol, isoproterenol or saline 0.9 % were administered into the BLA 20 minutes before testing through a stainless steel injection cannula connected to the 5 µl Hamilton syringe by a length of polyethylene tubing. The efficacy of injection was evaluated by watching the movement of a small air bubble through the tubing. The solutions were injected over 30 seconds and the injection cannula was left in place for an additional 30 seconds to minimize the reflux of the drug solution back up the injector tract. When administering both CNO and propanolol, CNO was injected 20 min before propanolol or saline. Additionally, propanolol or saline 0.9% were administered intraperitoneally 20 minutes before testing.

Behavioral assessment

Elevated zero maze (EZM)

Rats were placed in a black, 10 cm wide circular track (120 cm in diameter) elevated 70 cm above the ground, with two opposing enclosed quadrants and two open ones, and with a 7 mm high edge to prevent falls. The time spent in the open quadrants (a measure of anxiety) and the total distance travelled (total activity, A.U.) was monitored over a 5 min test period using the SMART video software (Spontaneous Motor Activity Recording and Tracking: Panlab, S.L.,

Barcelona, Spain). In addition, the number of entries into the open quadrants was recorded manually as a measure of anxiety.

Open field test (OFT)

The open field test (OFT) was performed in a 7,850 cm^2 enclosure over 10 min, the center of which was defined as a circle that covered 50% of the total OF area. The time spent in the central area and the total distance travelled (total activity, A.U.) was monitored over a 10 min test period using the SMART video software. In addition, the number of fecal boluses was recorded manually as a measure of anxiety.

Pain behavior assessment

Responses to thermal and mechanical stimuli were tested in all groups. Mechanical hypersensitivity was measured through the von Frey test (Dynamic Plantar Aesthesiometer, Ugo Basile, Italy), applying an increasing vertical force from 0 to 50 g to the ipsilateral and contralateral hind paws over a period of 20 s. Mechanical hypersensitivity was indicated by a reduction in the force that provokes paw withdrawal. Thermal hypersensitivity was tested using the acetone test, applying a drop of acetone (100 μl) to the surface in the center of the ipsilateral and contralateral hind paws with a pipette. The responses were recorded over a 1 min period after application according to the scale: 0, no response; 1, quick withdrawal, flick or stamp of the paw; 2, prolonged withdrawal or repeated flicking of the paw; 3, repeated flicking of the paw with persistent licking directed at the ventral side of the paw. The cumulative scores were obtained by summing the scores for each rat and dividing by the number of assays. The rats were also placed on a cold metal plate maintained at 4 ± 1 °C, and the number of times the animal briskly lifted its ipsilateral hind paw was measured over a period of 2 min. Thermal hypersensitivity is indicated by an increase in the response of paw withdrawal. Mechanical and thermal hypersensitivity were evaluated before and after the drug administration.

Spontaneous nociceptive behavior was measured for 5 min using the dynamic weight bearing device (Bioseb, France). Briefly, the device consisted of a Plexiglas enclosure (22 × 22 × 30 cm) with floor sensors containing pressure transducers. The system uses software that records the average weight that each limb exerts on the floor, in grams, without any interference. A camera was directed towards the side of the enclosure to assist with the data analysis. All movements were filmed and validated by the experimenter in accordance with the position of the rat on the device. This dynamic weight bearing software provides data about the weight (in grams) and surface (in mm^2) of the hindpaws that touch the floor. The rat's testicles and tail were excluded from the analysis. The animals were subjected to the test without prior adaptation since exploratory movements improve data capture. The results were expressed as the weight or

area of the ipsilateral and contralateral hindpaw. This test was evaluated only after drug administration.

A 15–20-min interval was maintained between all the testing procedures.

Step-through passive avoidance test (PA)

The PA apparatus (Shuttle Box; Panlab, Spain) (51 × 25 × 24 cm) involved a dark chamber and a bright one that were separated by a guillotine door. Electric shocks in the dark chamber were provided by a standard stimulator via the grid floor (2 s and 0.5 mA intensity). In the habituation phase, the rats were allowed to move freely in both compartments (the guillotine door was open) for 1 min. In the training phase, the rats were briefly confined to the light compartment and the door was then opened 30 s later. Once the rats entered the dark compartment (to a maximum of 300 sec; cut-off latency), the door closed automatically and they received an electric shock. The animal was then tested again as in the training session but without shock in the two test sessions, 3 hours (Short-term memory [STM]) and 24 hours (Long-term memory [LTM]) after the training session. The parameter recorded was the latency of the animal to move into the dark chamber (step-through latency).

Novel Object Recognition

Rats were tested in a rectangular arena (2,025 cm^2) located in a room with dim lighting and with constant background noise. The plastic objects used were of different shapes, colors and textures, and they were thoroughly cleansed with 70% ethanol between trials to ensure the absence of olfactory cues. The rats did not show preference for any of the selected objects. Briefly, two identical objects were placed in the arena during the training phase and subsequently, novel object recognition memory was evaluated in two test sessions one with a familiar object and one with a novel object, 3 (STM) and 24 hours (LTM) after the training session. The time spent exploring each object was recorded and the relative exploration of the novel object was expressed as a discrimination index: $DI = (tnovel - tfamiliar)/(tnovel + tfamiliar)$. The criteria for exploration were based strictly on active exploration, circling or sitting on the object was not considered exploratory behavior. The exploration times in each session of the novel object recognition test were 10 min and all trials were performed by an experimenter blind to the drug treatments and/or manipulations. The total distance travelled (total activity, A.U.) was also monitored over a 10 min test period using the SMART video software.

Object Pattern Separation

Rats were tested in a circular arena (7,850 cm^2) located in a room with dim lighting and constant background noise. The front of the arena (facing the experimenter) was colored white and the

other half black. In this task, two identical columns were used per trial (5.7cm × 5.7cm × 10cm). The task consisted of one habituation session (10 min) of free exploration and two 10 min trials, performed with an interval of 3 h. The first trial was a training session in which two identical objects were placed symmetrically on a horizontal line in the arena, approximately 15 cm apart. The second trial was a test, in which one of the objects was displaced along a straight line to a position away from the previous location (maximum change). The object pattern separation task is a modified version of the novel object recognition and it was analyzed in the same way as the novel object recognition test.

Fear conditioning

Animals were fear conditioned and context tested in (Startfear Box; Panlab, Spain) (25 × 25 × 25 cm) using two context options: Context A involves a black chamber with white light and scented with a 1% ammoniac solution; Context B involves a black/white chamber with red light and scented with 1% acetic acid. Prior to conditioning, rats were habituated to the apparatus for a minimum of 5 min. On the day of conditioning, the rats were given 3 CS-US pairings, consisted of a tone of 30 s, 5 kHz, 80 dB (conditioned stimulus, CS) that terminated with a 1 s, 0.7 mA foot shock (unconditioned stimulus, US) in context A. The inter-trial interval (ITI) was 120 s. The conditioned rats were testing for fear responses (freezing) with a 5 trials 24 h after conditioning. For this test, the rats were assessed in Context B and exposed to 5 CS with a 120 s delay between the tones. Freezing, defined as the absence of all movement except that required for respiration, was calculated automatically via the load cell coupler weight transducer requiring activity to be below the activity threshold for 2s to record a freezing event (software calibration established activity threshold allowing to discriminate non-awake or rest body posture) (PACKWIN v2 software). It was monitored throughout the protocol, representing the % time spent frozen in each phase.

Histology and immunohistochemistry

Animals were perfused with paraformaldehyde (4%) at the end of the experiments. In order to verify the mCherry expression into the LC and BLA, all animals were evaluated in blind conditions using the fluorescent Olympus BX60 microscope. Additionally, to estimate the percentage of mCherry expression in the noradrenergic LC neurons, 6 sections per animal (1 in every 4 sequential sections of 30 μm, n= 3 animal/group) were incubated with anti-red fluorescent protein antibody [5F8] (RFP, 1:500, chromotek, Germany) and mouse anti-dopamine beta hydroxylase (DBH, 1:1000, Merck Chemicals & Life Science S.A., Spain) 48 hours at 4ºC. Subsequently, sections were revealed with biotinylated donkey anti-rat (1:200, Jackson ImmunoResearch Europe) followed by Alexa Fluor 546 streptavidin and donkey anti-

mouse Alexa Fluor 488 (1:000, Invitrogen™, USA), before they were washed and coverslipped in fluoro-gel aqueous mounting medium and the images were acquired with Zeiss LSM 880 Confocal with FAST Airyscan (Carl Zeiss Microscopy GmbH, Germany). In order to test the selective expression of DREADD in LC, both A5 noradrenergic nucleus and ventral tegmental area (in this case incubated with primary rabbit tirosine hydroxylase (TH, 1:1000, Invitrogen™, USA) followed by goat anti-rabbit Alexa Fluor 488) were also included in this immunohistochemistry experiment. The images were acquired on a fluorescent Olympus BX60 microscope and the number of DBH, mCherry and the percentage of mCherry in DBH total neurons in both –ipsi and contralateral LC were counted.

For c-fos inmunodetection, DREADD-expressing rats were injected with the saline or CNO (1 mg/kg i.p.) and perfused 120 min later. Thus, LC sections (3 animals per group) were incubated with a rabbit anti c-fos (1:1000, abcam, Spain) overnight at 4ºC. Subsequently, the sections were incubated with a biotinylated donkey anti-rabbit (1:200, Jackson ImmunoResearch Europe). Immunodetection was achieved using ABC kit (1:200, vectorLabs, Spain) and by reaction with using the 3,3'-diaminobenzidine tetrahydrochloride (DAB). Sections were mounted on gelatine-coated slides, cleared in xylene and coverslipped with Eukitt. The images were acquired on an Olympus BX60 microscope and the number of c-fos positive neurons in both –ipsi and contralateral LC were manually counted.

For c-fos, mCherry and DBH inmunodetection, sections containing LC with rM3D(Gs) bilateral injection and perfused 120 min after CNO administration (intra-BLA (3 µM/0.5 µl)) were incubated with anti-red fluorescent protein antibody [5F8] (1:500), mouse anti-dopamine beta hydroxylase (1:1000) and rabbit anti c-fos (1:1000, Synaptic System, Germany) 48 hours at 4ºC. Subsequently, sections were revealed with biotinylated donkey anti-rat (1:200, Jackson ImmunoResearch Europe) followed by Alexa Fluor 546 streptavidin, donkey anti-rabbit Alexa Fluor 488 (1:000) and donkey anti-mouse Alexa 647 (1:000, Invitrogen™, USA) before they were washed and coverslipped in fluoro-gel aqueous mounting medium and the images were acquired with Zeiss LSM 880 Confocal with FAST Airyscan. For c-fos cell counting, the images were acquired on an Olympus BX60 microscope and the number of c-fos positive neurons in both ipsi- and contralateral LC were manually counted.

In order to evaluate the ipsi- and contralateral projections from LC to BLA nucleus, animals were perfused 4 days after unilateral or bilateral administration of Fluoro-Gold (FG, Fluorochrome, USA). Sections from several noradrenergic areas (A1/C1, A2/C2, A3, A5, A6) (6 animals per group) were incubated with a rabbit anti-FG (1:1000, Merck Chemicals & Life Science S.A., Spain) and mouse anti-DBH (1:1000) 24 hours at 4ºC, and subsequently were incubated with a goat anti-rabbit Alexa Fluor 488 (1:1000) and a donkey anti-mouse Alexa Fluor 546 (1:1000). To visualize DBH+ fibers in BLA, the above mentioned mouse anti-DBH and goat anti-rabbit Alexa Fluor 488 antibodies were used. Representative images were

acquired with a Zeiss LSM 880 Confocal with FAST Airyscan and the number of FG-positive in both –ipsi and contralateral LC were manually counted on a fluorescent Olympus BX60 microscope.

Cannula placement intra-BLA was verified by injection of 0.5 µl of Pontamine Sky Blue in the injection side just before the animals were perfused. Sections (1 in every 6 sequential sections of 30 µm) were stained with neutral red and they were visualized on an optical microscope (Olympus BX60, Center Valley, USA). The location of the injection site was verified as being within the BLA in all the animals studied.

CNO spread intra-BLA was estimated by the injection of 0.5 µl of DAPI 20 min before the animals were perfused and brain sections were visualized on a fluorescent Olympus BX60 microscope.

Supplementary figures

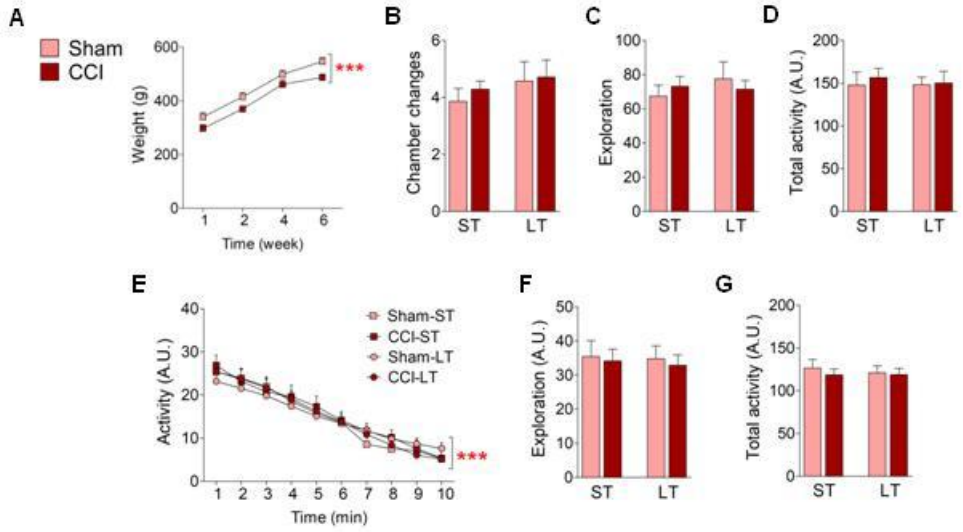

Figure S1. Supplemental information of Fig.1.

(A) Effects of neuropathic pain on weight (g). **(B)** The effects of neuropathic pain on passive avoidance: the graph represents the number of chamber changes during the habituation session. **(C-E)** The effects of neuropathic pain on novel object recognition: the graphs represent **(C)** the exploration (A.U.) in the training phase, and **(D)** the locomotor activity and **(E)** activity per minute (A.U.) in the habituation phase of the paradigm. **(F-G)** The effects of neuropathic pain on object pattern separation: the graphs represent **(F)** the exploration (A.U.) in the training phase and **(G)** the locomotor activity (A.U.) in the habituation phase of the paradigm. The data are represented as the mean + SEM (n=8 per group): ***$p<0.001$ versus week 1 or min 1, as assessed by two-way ANOVA with repeated measures followed by Newman-Keuls post hoc test. CCI, chronic constriction injury; ST, short-term; LT, long-term; A.U., arbitrary units.

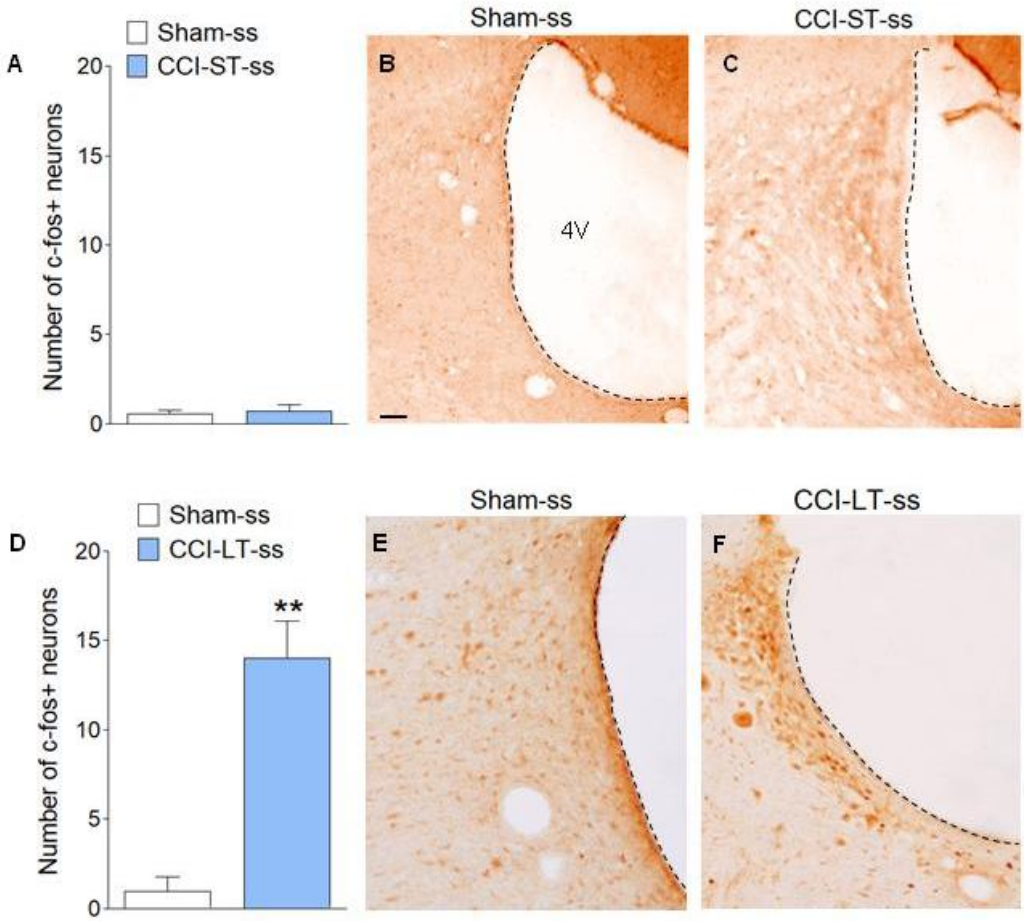

Figure S2. C-fos expression in nerve injured animals.

(A-C) Short-term pain does not modify the expression of c-fos in the LC. **(A)** Quantification of c-fos positive neurons in the LC and representative immunohistochemistry for **(B)** sham-ss and **(C)** CCI-ST-ss animals. **(D-F)** Long-term pain increases c-fos expression in the LC. **(D)** Quantification of c-fos positive neurons in the LC and representative immunohistochemistry for **(E)** sham-ss and **(F)** CCI-LT-ss animals. The data are represented as the mean + SEM per slice (n=4 slices from 3 animals/group): **p<0.001, as assessed by Student's t-test. Scale bar=50 µm. CCI, chronic constriction injury; ST, short-term; LT, long-term; ss, saline; LC, locus coeruleus; 4V, fourth ventricle.

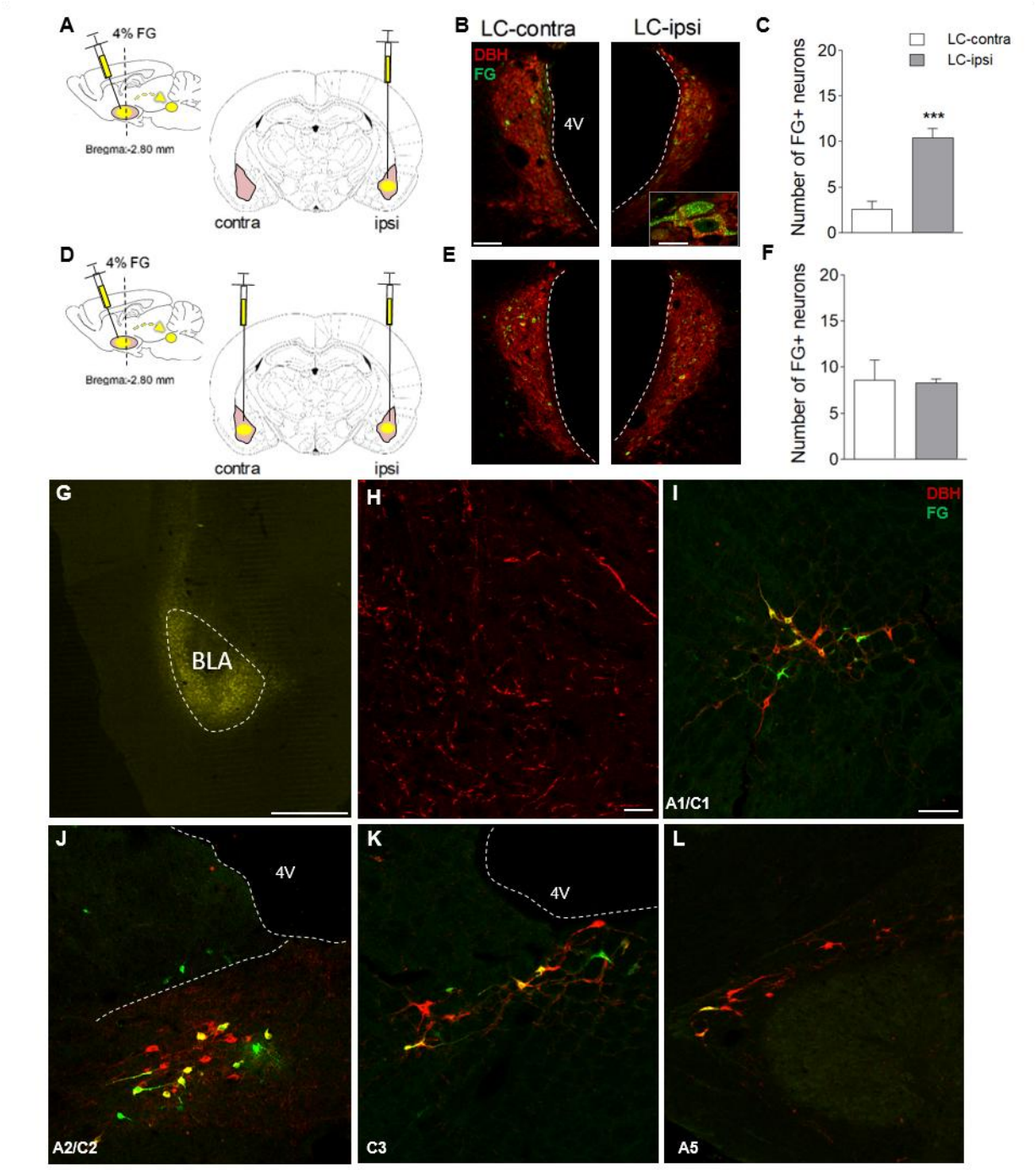

Figure S3. Identifying noradrenergic inputs to the BLA.

(**A-C**) Unilateral injection of FG intra-BLA in naïve animals: (**A**) cartoon depicting FG tracing strategy, (**B**) representative immunofluorescence and (**C**) quantification shows ipsilateral prominent projection from LC to BLA. (**D-F**) Bilateral injection of FG intra-BLA in naïve animals: (**D**) cartoon depicting FG tracing strategy, (**E**) representative immunofluorescence and (**F**) quantification shows bilateral prominent projection from LC to BLA (scale bar=100 µm). Magnification indicates an example of co-localization (scale bar=20 µm). Data represented as mean + SEM neurons per slice, n=8-10 slices from 6 animals/group: ***p<0.001 versus LC-contra, as assessed by Student t-test. (**G**) Histological verification of FG administration intra-BLA (scale bar=200 µm). Yellow, FG. **(H)** Representative immunofluorescence of DBH+

fibers in BLA (scale bar= 50 µm). (**I-L**) Noradrenergic projections (A1/C1, A2/C2, C3 and A5) to BLA (scale bar=100 µm). Red, DBH; green, FG and yellow, FG/DBH merge. Ipsi/contra nomenclature is referred to the site of administration of FG intra-BLA. DBH: dopamine beta hydroxylase; FG, Fluoro-Gold; LC, locus coeruleus; contra, contralateral; ipsi, ipsilateral; 4V, fourth ventricle, BLA, basolateral amygdala.

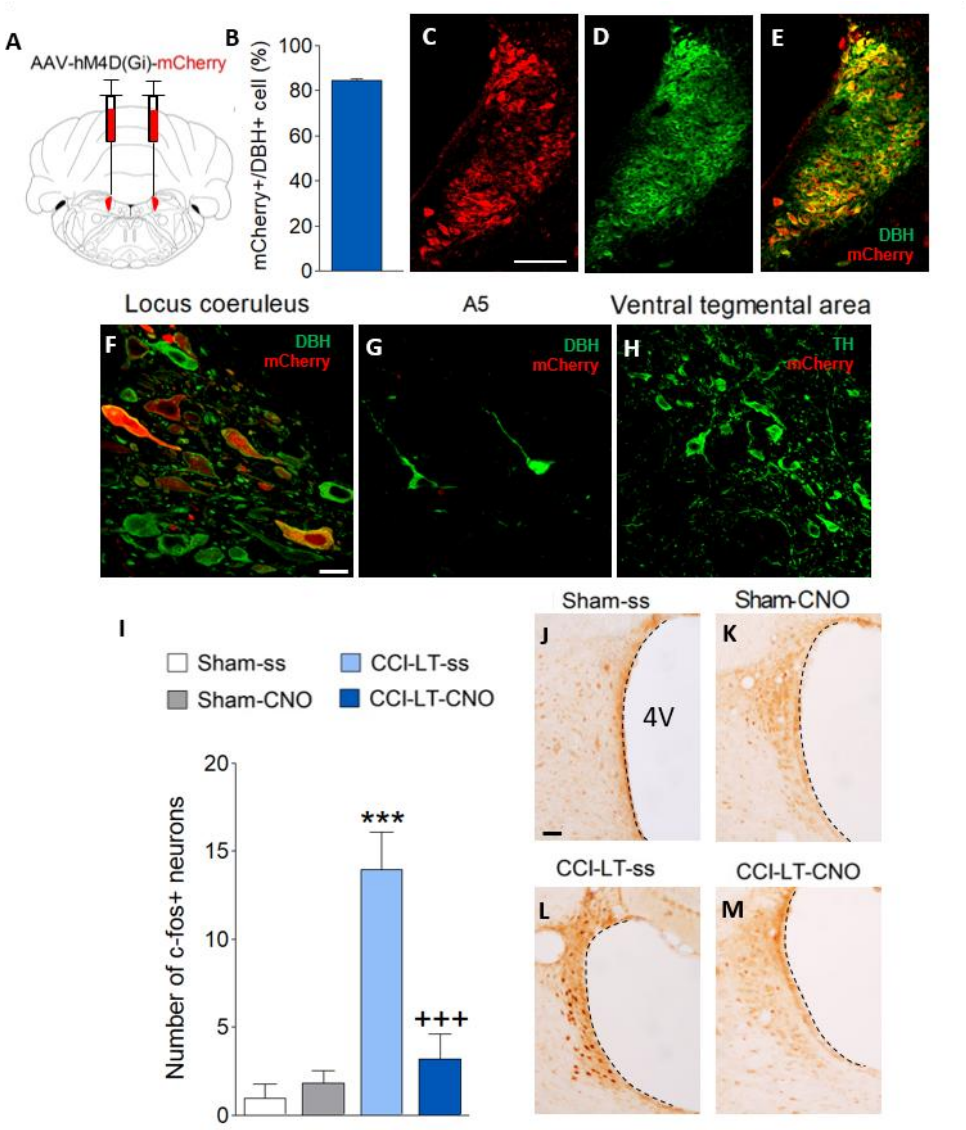

Figure S4. Selective hM4D(Gi)-DREADD expression and locus coeruleus inhibition DREADD-mediated.

(**A**) Cartoon hM4D(Gi) bilateral injection intra-LC. **(B-E)** Quantification and representative immunohistochemistry of mCherry expression in LC neurons (scale bar=100 µm). (**F-H**) High power confocal images of mCherry expression in **(F)** LC noradrenergic neurons. No expression of mCherry was observed in **(G)** A5 noradrenergic neurons and **(H)** ventral tegmental area dopamine neurons (scale bar=20 µm). **(I-M)** Quantification and representative immunohistochemistry show inhibition of LC neurons decrease the number of c-fos in both ipsi- and contralateral LC in CCI-LT-CNO group (scale bar=50 µm). Data represented as mean + SEM neurons per slice, n=4-6 slices from 3 animals/group. ***p<0.001 versus sham-ss;

+++p<0.001 versus CCI-LT-ss, as assessed by two-way ANOVA followed by Newman-Keuls post hoc test. Green, DBH/TH and red, mCherry. DBH, dopamine beta hydroxylase; TH, tyrosine hydroxylase; contra, contralateral; ipsi, ipsilateral; 4V, fourth ventricle; CCI, chronic constriction injury; LT, long-term; ss, saline.

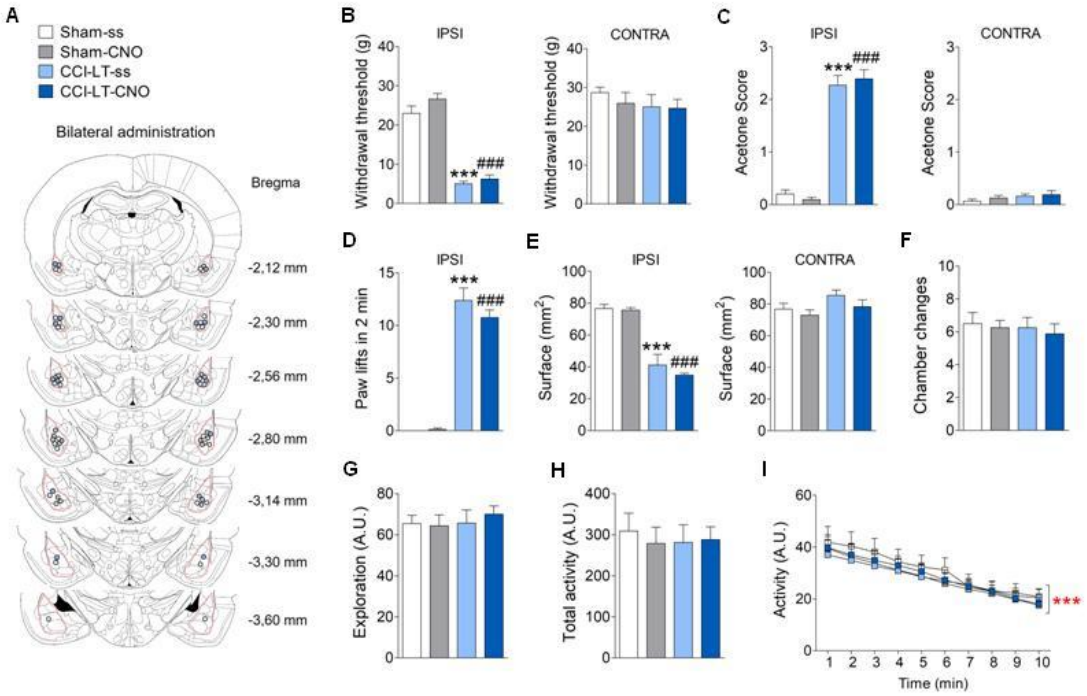

Figure S5. Supplemental information of Fig.2.

(A) Schematic diagrams adapted from the atlas of Paxinos and Watson (Paxinos and Watson, 2007) showing the sites of the microinjection into the BLA. Each color represents a different treatment and each dot corresponds to an infusion focus in a 30 µm section. (**B-D**) Sensorial evaluation before inhibition of the LC-BLA pathway: the graphs represent **(B)** the withdrawal threshold (g) of the ipsilateral and contralateral hind paws to von Frey hair stimulation (0 to 50 g, 20 sec), **(C)** the response of the ipsilateral and contralateral hind paws to acetone application (100 ul), **(D)** the number of lifts of the ipsilateral hind paw in the cold plate test (2 min, 4 ºC). **(E)** The surface of the ipsilateral and contralateral hind paws supported in the dynamic weight bearing test (5 min) after inhibition of the LC-BLA pathway. **(F)** The effects of inhibiting the LC-BLA pathway on passive avoidance, the graph represents the number of chamber changes during the habituation session. **(G-I)** The effects of inhibiting the LC-BLA pathway on novel object recognition: the graphs represent **(G)** exploration (A.U.) in the training phase, and **(H)** locomotor activity (A.U.) and **(I)** activity per minute (A.U.) in the habituation phase of the paradigm. The data are represented as the mean + SEM (n=8 per group): ***p<0.001 versus sham-ss and ###p<0.001 versus sham-CNO as assessed by two-way ANOVA followed by Newman-Keuls post hoc test; ***p<0.001 versus min 1 as assessed by two-way ANOVA with repeated measures followed by Newman-Keuls post hoc test. CCI, chronic constriction injury; LC, locus coeruleus; BLA, basolateral amygdala; CNO, clozapine-N-oxide; ss, saline.

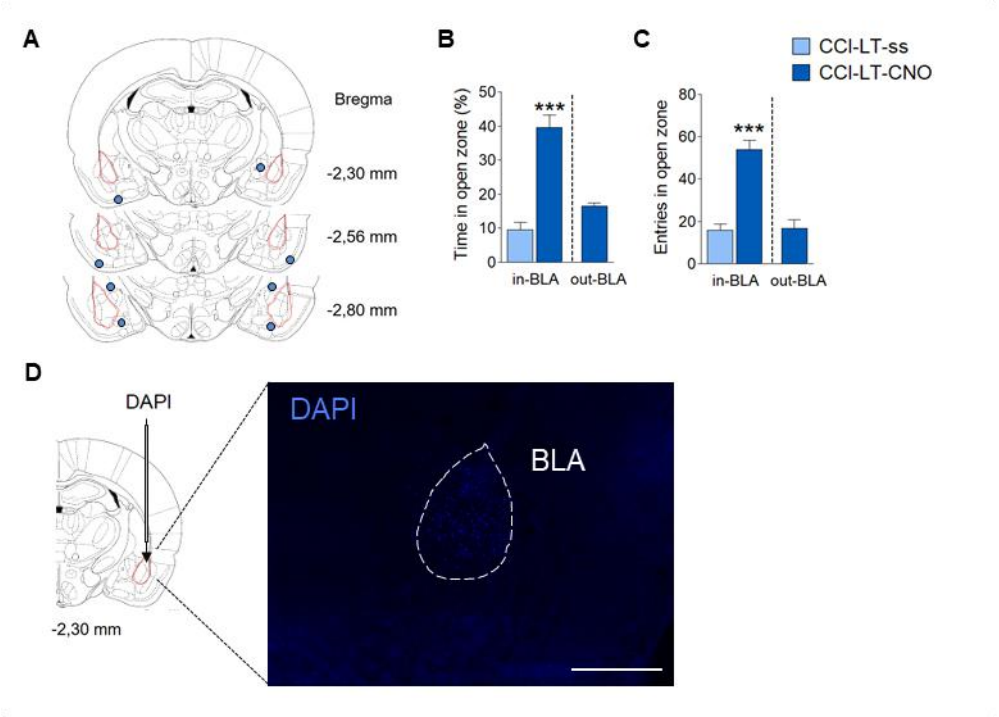

Figure S6.

(A) Schematic diagrams adapted from the atlas of Paxinos and Watson (Paxinos and Watson, 2007) showing the sites of CNO microinjection outside the BLA in the CCI-LT animals treated with the inhibitor virus (hM4D(Gi)-DREADD). Animals show anxiogenic-like behavior in the elevated zero maze when the microinjection of CNO was outside the BLA. **(B)** The relative time spent in the open zone and **(C)** the number of entries into that zone. The data represent the mean + SEM (n=8, CCI-LT-ss in-BLA; n=8, CCI-LT-CNO in-BLA; n=4, CCI-LT-CNO out-BLA): ***p<0.001 versus CCI-LT-ss in-BLA as assessed by Student's t-test. Methodological approach to validate the diffusion of the CNO. **(D)** Schematic diagram and photomicrograph showing the spread of DAPI after its administration into the BLA (0.5µl) (scale bar=500 µm). CCI, chronic constriction injury; BLA, basolateral amygdala; ss, saline; CNO, clozapine-N-oxide; LT, long-term.

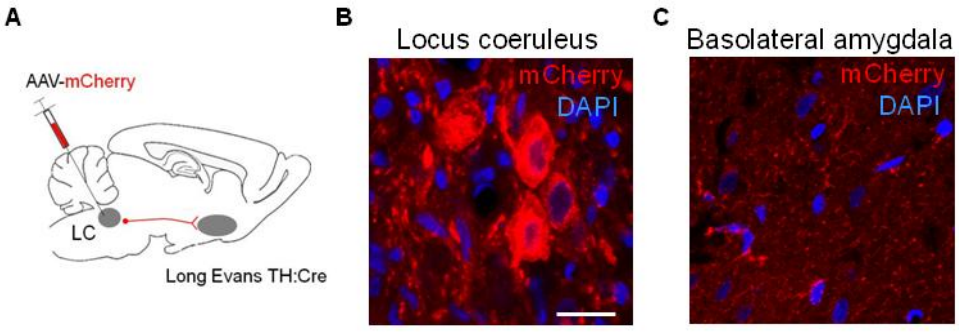

Figure S7. Identification of LC input to the BLA.

(A) Cartoon control-DREADD bilateral injection intra-LC (1.4µl/side) in naïve Long-Evans TH:Cre rats. The rats were allowed to recover for 3weeks to achieve robust expression of mCherry. **(B-C)** High power confocal images of mCherry expression and DAPI in **(B)** LC noradrenergic neurons and **(C)** fibers of LC in BLA (scale bars=20 µm). red, mCherry and blue, DAPI. TH, tyrosine hydroxylase; LC, locus coeruleus.

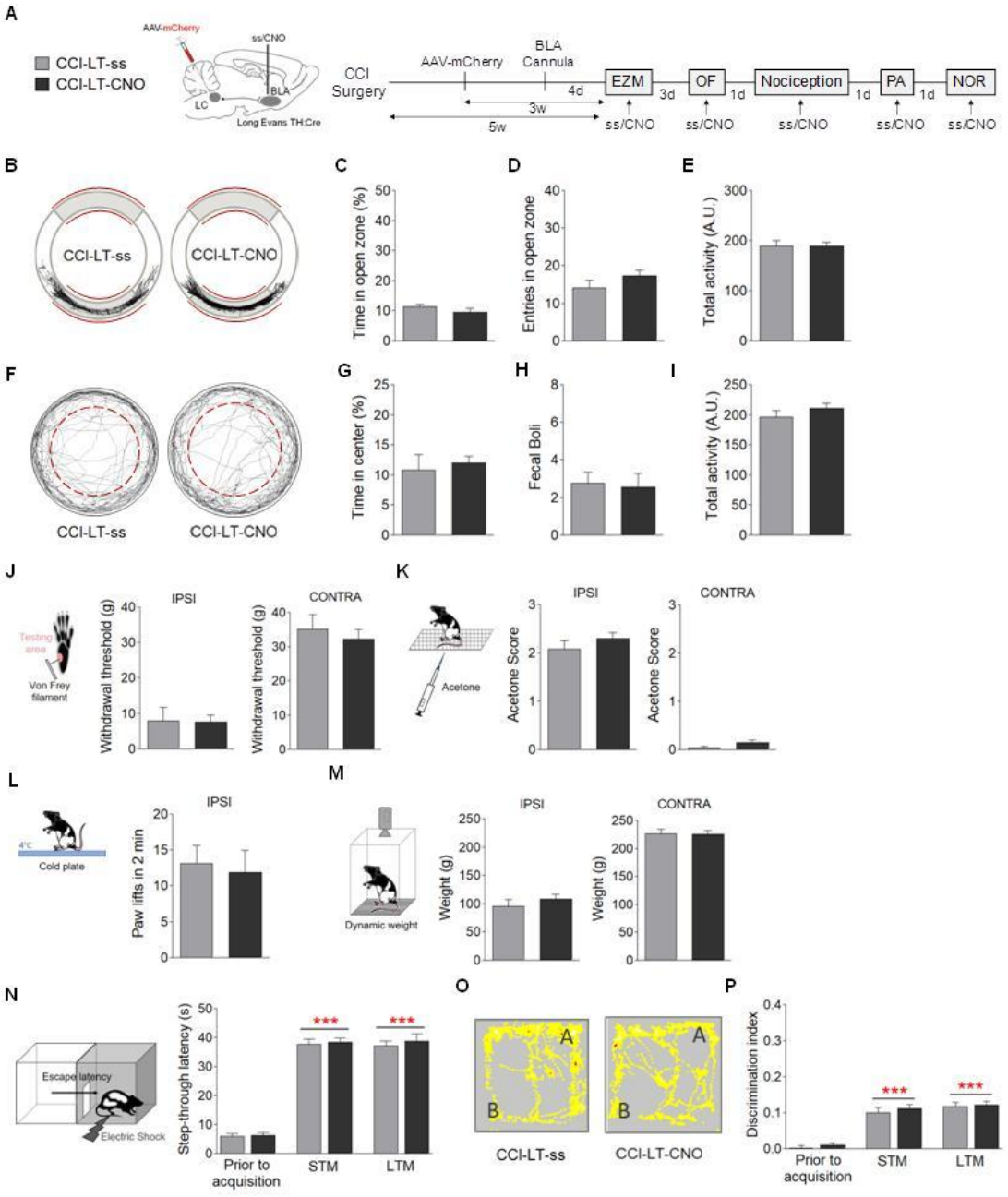

Figure S8. CNO does not elicit changes in the behavioral testing with control-DREADD.

A) Experimental timeline and schematic representation of control virus (control-DREADD) and cannula delivery for the behavioral experiments in male Long-Evans TH:Cre rats. A control Cre-dependent AAV, fluorescently tagged with mCherry (1.4µl/side), was injected bilaterally into TH neurons of LC of TH-Cre rats 2 weeks after chronic constriction injury. The rats were allowed to recover for 3weeks to achieve robust expression of mCherry and a metal cannula was implanted bilaterally into the BLA 4 days before carrying out the behavioral studies. The rats were tested 5-6 weeks (long-term: LT) after surgery. CNO (3 µM/ 0.5 µl) was administered twenty minutes before performing the behavioral tests. (**B-E**) The effects of CNO with control-DREADD in the elevated zero maze. (**B**) The representative activity traces and the graphs represent (**C**) the relative time spent in the open zone and (**D**) number of entries into that zone, as well as (**E**) the locomotor activity (A.U.: arbitrary units). (**F-I**) The effects of CNO with control-DREADD in the open field test. (**F**) The representative activity traces and the graphs represent (**G**) the relative time spent in the central zone, (**H**) the number of fecal boluses and (**I**) the locomotor activity (A.U.). (**J-M**) Sensorial evaluation. The graphs represent (**J**) the

withdrawal threshold (g) of the ipsilateral and contralateral hind paws in response to von Frey hair stimulation (0 to 50 g, 20 sec), (**K**) the response of the ipsilateral and contralateral hind paws to acetone application (100 ul), (**L**) the number of lifts of the ipsilateral hind paw in the cold plate test (2 min, 4°C), and (**M**) the weight distributed on the ipsilateral and contralateral hind paws in the dynamic weight bearing test (5 min). (**N**) The effects of CNO with control-DREADD on passive avoidance. The graph represents the latency to enter the dark compartment (s) in the different phases of the paradigm: training (prior to acquisition), short-term memory test (STM as learning index) and long-term memory test (LTM as memory index). (**O**-**P**) The effects of CNO with control-DREADD in the novel object recognition test. (**O**) The representative heatmaps showing activity (Yellow=low and Red=high activity) around the objects in the memory test session (A=familiar and B=novel object) and the graph represent (**P**) the discrimination index between objects in the different phases of the paradigm: training, STM and LTM. The data represent the mean + SEM (n=8-9 per group): CCI-LT-CNO vs CCI-LT-ss as assessed by Student's t-test (non-significant); ***$p<0.01$ versus prior to acquisition of each group as assessed by one-way ANOVA with repeated measures followed by Newman-Keuls post hoc. CCI, chronic constriction injury; d, days; w, weeks; CNO, clozapine-N-oxide; ss, saline.

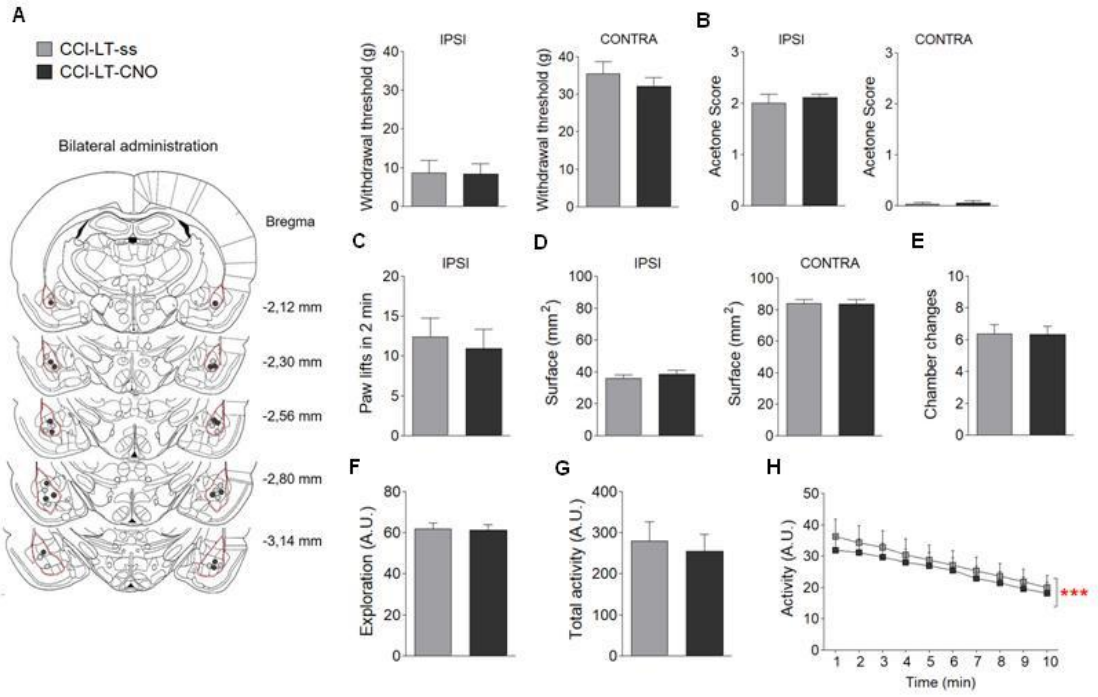

Figure S9. Supplemental information of Figure S8.

(A) Schematic diagrams adapted from the atlas of Paxinos and Watson (Paxinos and Watson, 2007) showing the sites of the microinjection into the BLA. Each color represents a different treatment and each dot corresponds to an infusion focus in a 30 µm section. (**B-D**) Sensorial evaluation before CNO administration: the graphs represent **(B)** the withdrawal threshold (g) of the ipsilateral and contralateral hind paws to von Frey hair stimulation (0 to 50 g, 20 sec), **(C)** the response of the ipsilateral and contralateral hind paws to acetone application (100 ul), **(D)** the number of lifts of the ipsilateral hind paw in the cold plate test (2 min, 4 ºC). **(E)** The surface of the ipsilateral and contralateral hind paws supported in the dynamic weight bearing test (5 min) after inhibition of the LC-BLA pathway. **(F)** The effects of CNO with control-DREADD on passive avoidance, the graph represents the number of chamber changes during the habituation session. **(G-I)** The effects of CNO with control-DREADD on novel object recognition: the graphs represent **(G)** exploration (A.U.) in the training phase, and **(H)** locomotor activity (A.U.) and **(I)** activity per minute (A.U.) in the habituation phase of the paradigm. The data are represented as the mean + SEM (n=8-9 per group): CCI-LT-CNO vs CCI-LT-ss as assessed by Student's t-test (non-significant). ***$p<0.001$ versus min 1 as assessed by two-way ANOVA with repeated measures followed by Newman-Keuls post hoc test. CCI, chronic constriction injury; LC, locus coeruleus; BLA, basolateral amygdala; CNO, clozapine-N-oxide; ss, saline.

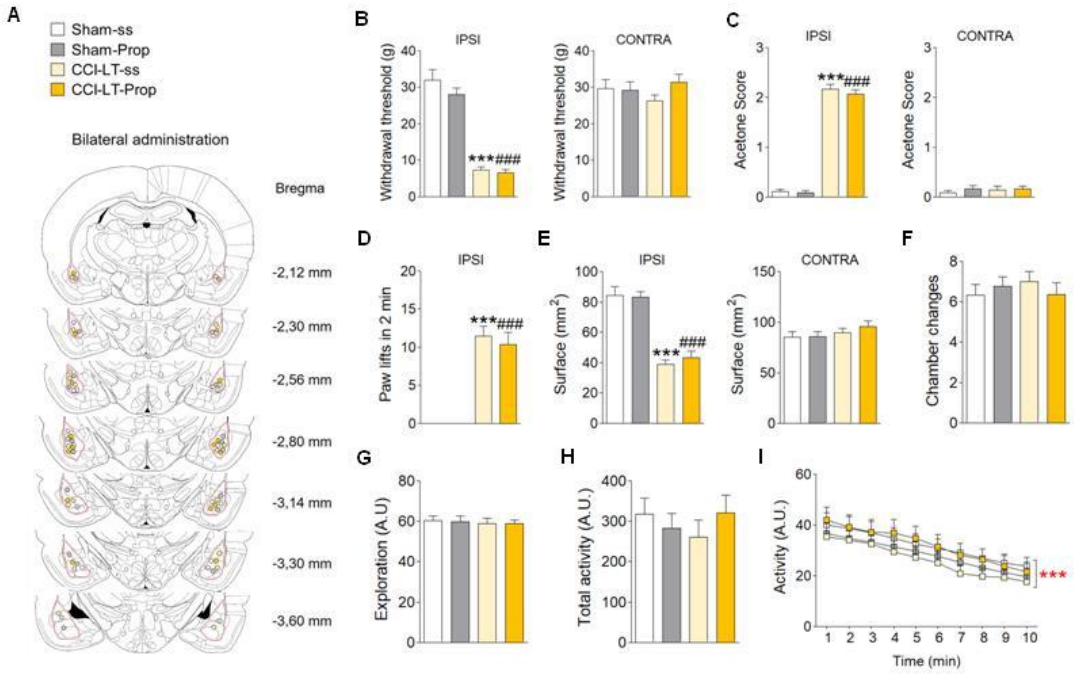

Figure S10. Supplemental information of Fig.3.

(A) Schematic diagrams adapted from the atlas of Paxinos and Watson (Paxinos and Watson, 2007) showing the locations of the microinjection sites in the BLA. Each color represents a different treatment and each dot corresponds to an infusion focus in a 30 µm section. (**B-D**) Sensorial evaluation before the inhibition of beta-adrenoceptors (b-AR) of BLA. The graphs represent **(B)** withdrawal threshold (g) of the ipsilateral and contralateral hind paws to von Frey hair stimulation (0 to 50 g, 20 sec), **(C)** the response of ipsilateral and contralateral hind paws to acetone applied (100 ul), and **(D)** the number of lifts of the ipsilateral hind paw in the cold plate test (2 min, 4ºC). **(E)** The surface of ipsilateral and contralateral hind paws supported in the dynamic weight bearing test (5 min) after inhibition of the b-AR in the BLA. **(F)** The effects of inhibiting the b-AR in the BLA on passive avoidance, the graph represents the number of chamber changes during the habituation session. **(G-I)** The effects of inhibiting the b-AR in the BLA on novel object recognition, the graphs represent **(G)** exploration (A.U.) in the training phase and **(H)** locomotor activity (A.U.) and **(I)** activity per minute (A.U.) in the habituation of the paradigm. The data are represented as the mean + SEM (n=8-9 per group): ***p<0.001 versus sham-ss; ###p<0.001 versus sham-CNO as assessed by two-way ANOVA followed by Newman-Keuls post hoc test. *** p<0.001 versus min 1 as assessed by two-way ANOVA with repeated measures followed by Newman-Keuls post hoc test. CCI, chronic constriction injury; BLA, basolateral amygdala; Prop, propanolol; ss, saline.

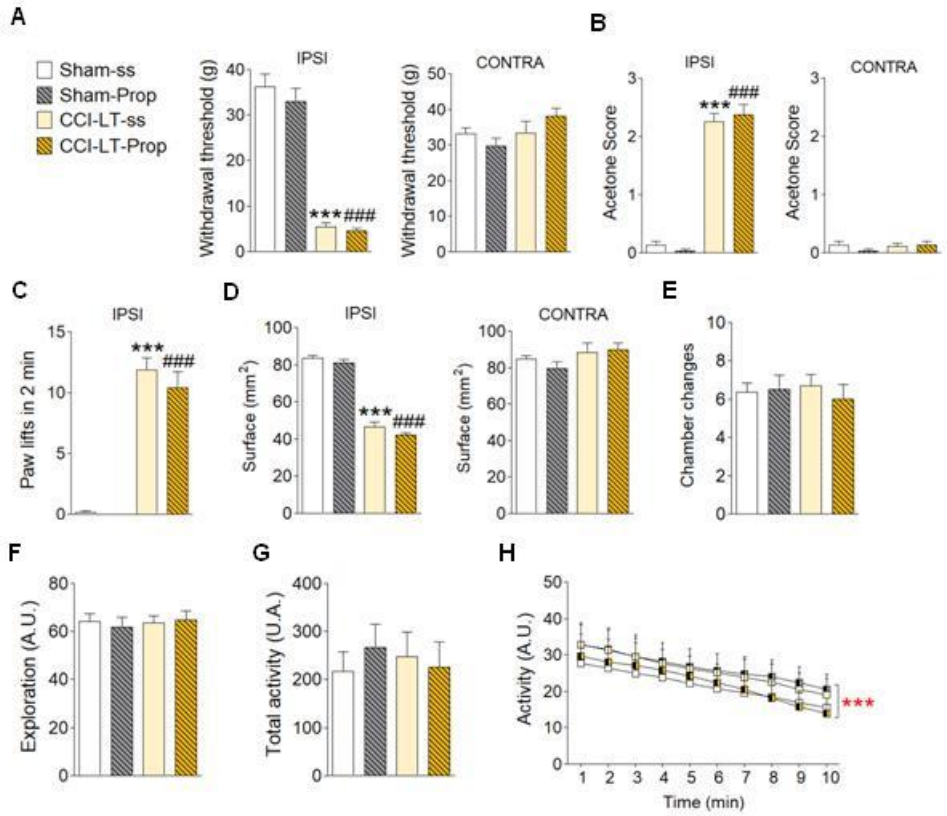

Figure S11. Supplemental information of Fig.4.

(**A-C**) Sensorial evaluation before the systemic inhibition of beta-adrenoceptors (b-AR). The graphs represent **(A)** withdrawal threshold (g) of the ipsilateral and contralateral hind paws to von Frey hair stimulation (0 to 50 g, 20 sec), **(B)** the response of ipsilateral and contralateral hind paws to acetone applied (100 ul), and **(C)** the number of lifts of the ipsilateral hind paw in the cold plate test (2 min, 4ºC). **(D)** The surface of ipsilateral and contralateral hind paws supported in the dynamic weight bearing test (5 min) after inhibition of the b-AR. **(E)** The effects of systemic inhibiting the b-AR on passive avoidance, the graph represents the number of chamber changes during the habituation session. **(F-H)** The effects of systemic inhibiting the b-AR on novel object recognition, the graphs represent **(F)** exploration (A.U.) in the training phase and **(G)** locomotor activity (A.U.) and **(H)** activity per minute (A.U.) in the habituation of the paradigm. The data are represented as the mean + SEM (n=6-8 per group): ***p<0.001 versus sham-ss; ###p<0.001 versus sham-CNO as assessed by two-way ANOVA followed by Newman-Keuls post hoc test. *** p<0.001 versus min 1 as assessed by two-way ANOVA with repeated measures followed by Newman-Keuls post hoc test. CCI, chronic constriction injury; Prop, propanolol; ss, saline.

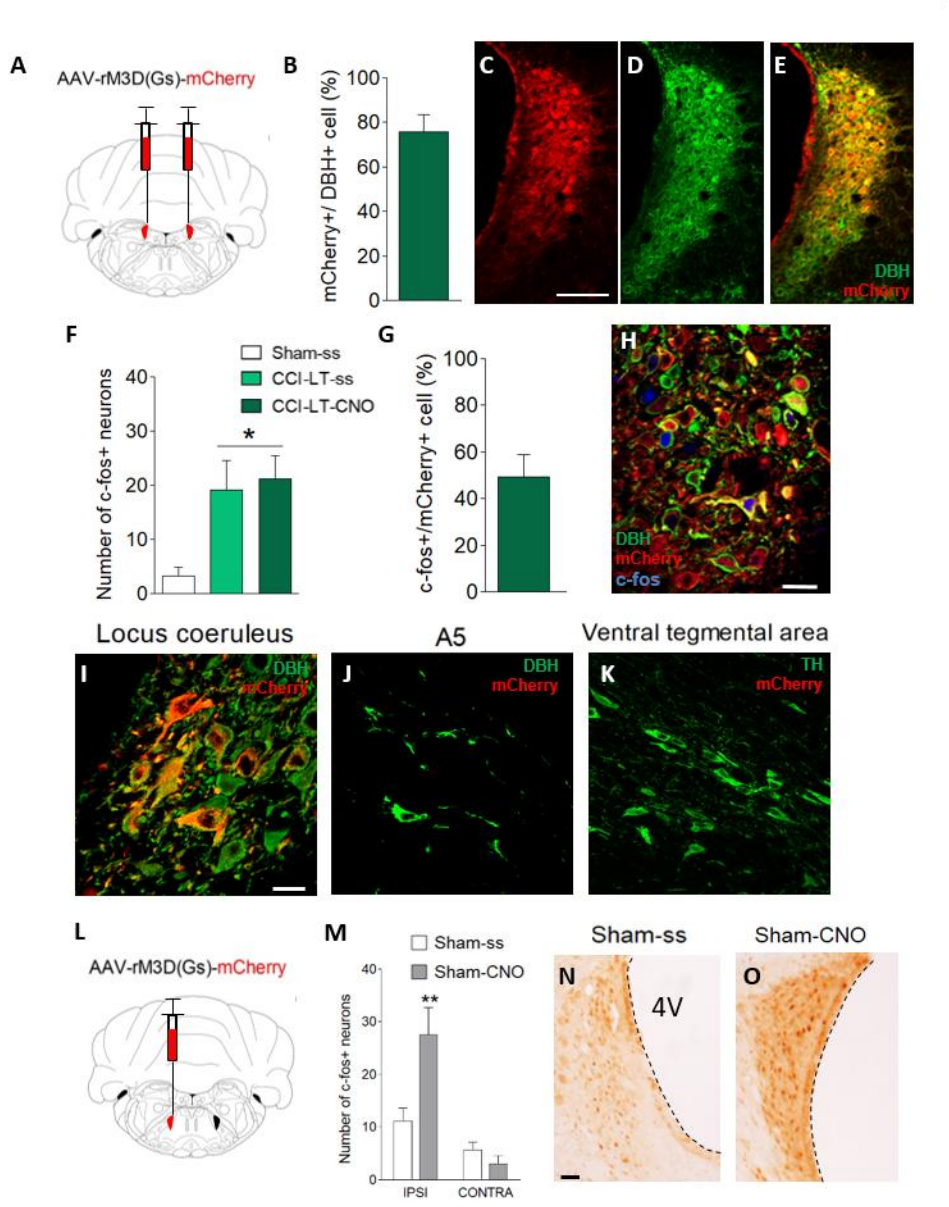

Figure S12. Selective rM3D(Gs)-DREADD expression and locus coeruleus activation DREADD-mediated.

(A) Cartoon rM3D(Gs) bilateral injection intra-LC. (**B-E**) Quantification and representative immunohistochemistry of mCherry expression in LC neurons (scale bar=100 µm). Quantification of c-fos and/or mCherry positive neurons show (**F**) DREADD-mediated activation of LC neurons does not modify the number of c-fos+ neurons already enhanced by CCI-LT and (**G**) mCherry positive neurons merged with c-fos and (H) representative merge of c-fos, mCherry and DBH positive neurons (scale bar=20µm). CNO was administered intra-BLA (3 µM/0.5 µl) 120 min prior to the perfusion. (**I-K**) High power confocal images of mCherry expression in (**I**) LC noradrenergic neurons. No expression of mCherry was observed in (**J**) A5 noradrenergic neurons and (**K**) ventral tegmental area dopamine neurons (scale bars=20µm). (**L**) Cartoon rM3D(Gs) unilateral injection intra-LC. (**M-O**) Quantification and representative immunohistochemistry show activation of LC neurons increases the number of c-fos in ipsilateral LC in Sham-CNO group (scale bar=50 µm). CNO (1 mg/kg i.p.) was administered 120 min prior to the perfusion. Data represented as mean + SEM neurons per slice, n=4-6 slices from 3 animals/group: *p<0.05, **p<0.01 versus sham-ss; as assessed by a Student t-test.

Green, DBH, red, mCherry and blue, c-fos. DBH, dopamine beta hydroxylase; TH, tyrosine hydroxylase; contra, contralateral; ipsi, ipsilateral; 4V, fourth ventricle; CCI, chronic constriction injury; LT, long-term; ss, saline.

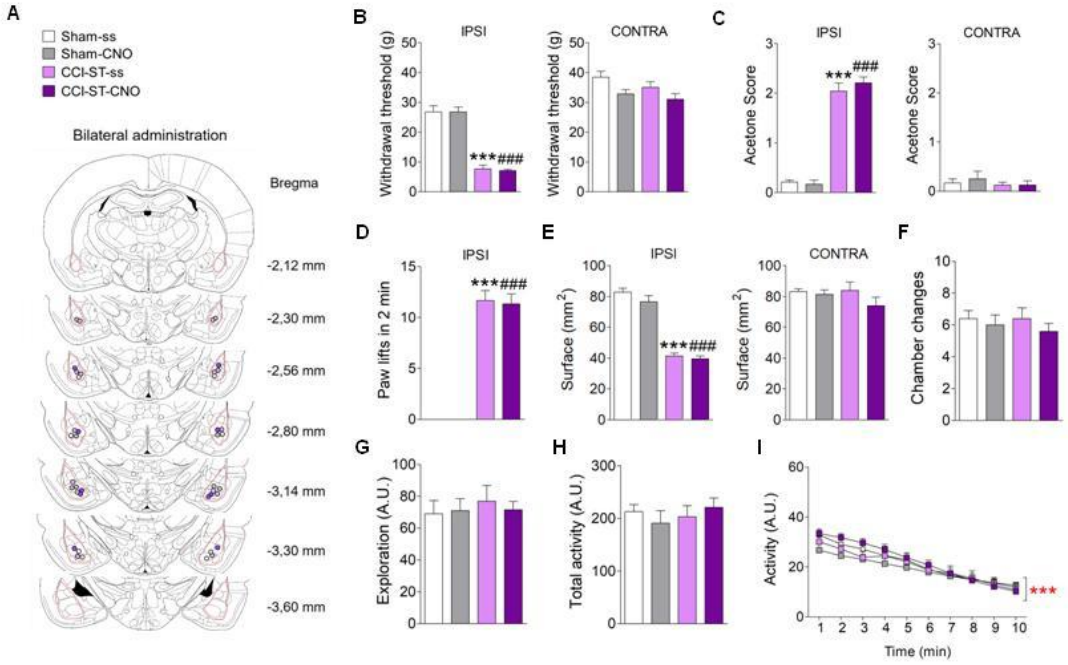

Figure S13. Supplemental information of Fig.5.

(A) Schematic diagrams adapted from the atlas of Paxinos and Watson (Paxinos and Watson, 2007) showing the locations of the microinjection sites in the BLA. Each color represents a different treatment and each dot corresponds to an infusion focus in a 30 µm section. (**B-D**) Sensorial evaluation before activation of the LC-BLA pathway. The graphs represent **(B)** the withdrawal threshold (g) of the ipsilateral and contralateral hindpaws to von Frey hair stimulation (0 to 50 g, 20 sec), **(C)** the response of the ipsilateral and contralateral hind paws to acetone application (100 ul), **(D)** the number of lifts of the ipsilateral hind paw in the cold plate test (2 min, 4ºC). **(E)** The surface of the ipsilateral and contralateral hindpaws supported in the dynamic weight bearing test (5 min) after activation of the LC-BLA pathway. **(F)** The effects of activating the LC-BLA pathway on passive avoidance, the graph represents the number of chamber changes during the habituation session. **(G-I)** The effects of activating the LC-BLA pathway on novel object recognition, the graphs represent **(G)** exploration (A.U.) in the training phase, and **(H)** the locomotor activity (A.U.) and **(I)** activity per minute (A.U.) in the habituation of the paradigm. The data are the mean + SEM (n=5-6 per group): ***p<0.001 versus sham-ss; ###p<0.001 versus sham-CNO as assessed by two-way ANOVA followed by Newman-Keuls post hoc test; *** p<0.001 versus min 1 as assessed by two-way ANOVA with repeated measures followed by Newman-Keuls post hoc test. CCI, chronic constriction injury; LC, locus coeruleus; BLA, basolateral amygdala; CNO, clozapine-N-oxide; ss, saline.

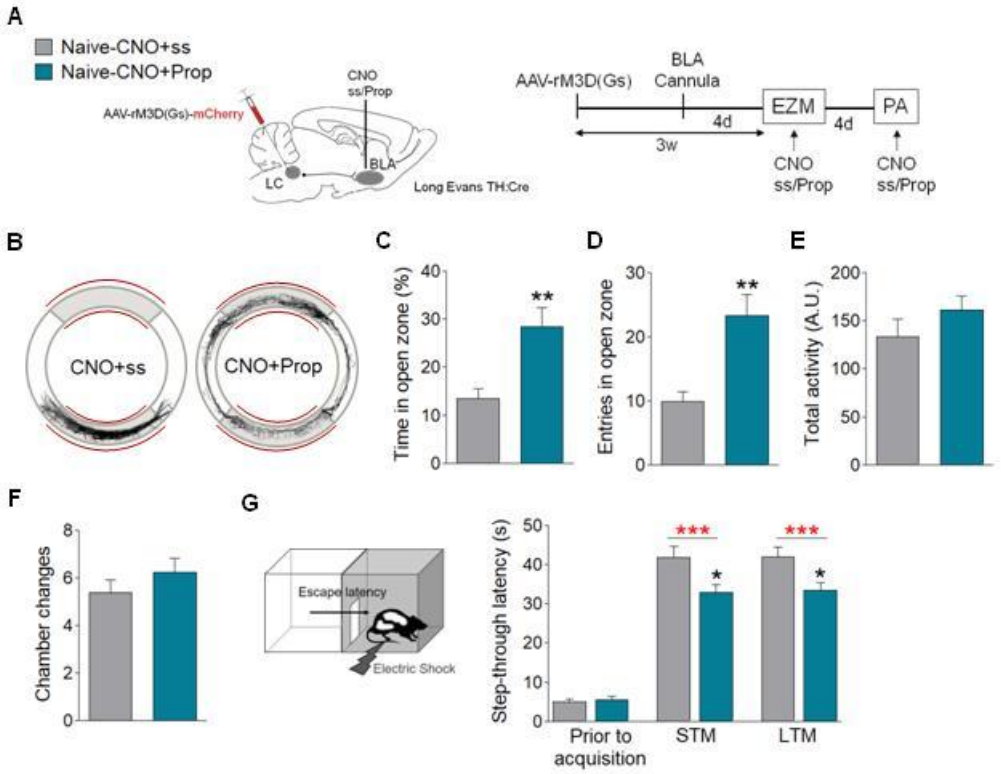

Figure S14. Chemogenetic activation of LC-BLA pathway promotes anxiety-like behavior and enhanced aversive learning through beta-adrenoceptors (b-AR).

(**A**) Experimental timeline and schematic representation of viral (rM3D(Gs)-DREADD) and cannula delivery for behavioral experiments in male Long-Evans TH:Cre rats. A Cre-dependent AAV, fluorescently tagged with mCherry (AAV-rM3D(Gs)-mCherry: 1.4µl/side), was injected bilaterally into TH neurons of LC of naive TH-Cre rats. The rats were allowed to recover for 3 weeks to achieve robust expression of DREADD and a metal cannula was implanted bilaterally into the BLA 4 days before carrying out the behavioral studies. CNO (3µM/0.5µl) and Propanolol (1µg/0.5µl) were administered forty minutes and twenty minutes before behavioral testing, respectively. (**B-E**) The effects of inhibiting the b-AR over induced anxiety by activation of the LC-BLA pathway in the elevated zero maze. (**B**) The representative activity traces and the graphs represent (**C**) the relative time spent in the open zone and (**D**) number of entries into that zone, as well as (**E**) the locomotor activity (A.U.: arbitrary units). (**F-G**) The effects of b-AR in the BLA in combination with the activation of the LC-BLA pathway on passive avoidance. The graphs represent (**F**) the number of chamber changes during the habituation session and (**G**) the latency to enter the dark compartment (s) in the different phases of the paradigm: training (prior to acquisition), short-term memory test (STM as learning index) and long-term memory test (LTM as memory index). The data represent the mean + SEM (n=8 per group): *p<0.05, **p<0.01 versus naive-CNO-ss as assessed by Student's t-test; *** p<0.001 versus prior to acquisition by one-way ANOVA with repeated measures followed by Newman-Keuls post hoc test. CCI, chronic constriction injury; d, days; BLA, basolateral amygdala; Prop, propanolol; ss, saline; CNO, Clozapine-N-oxide.

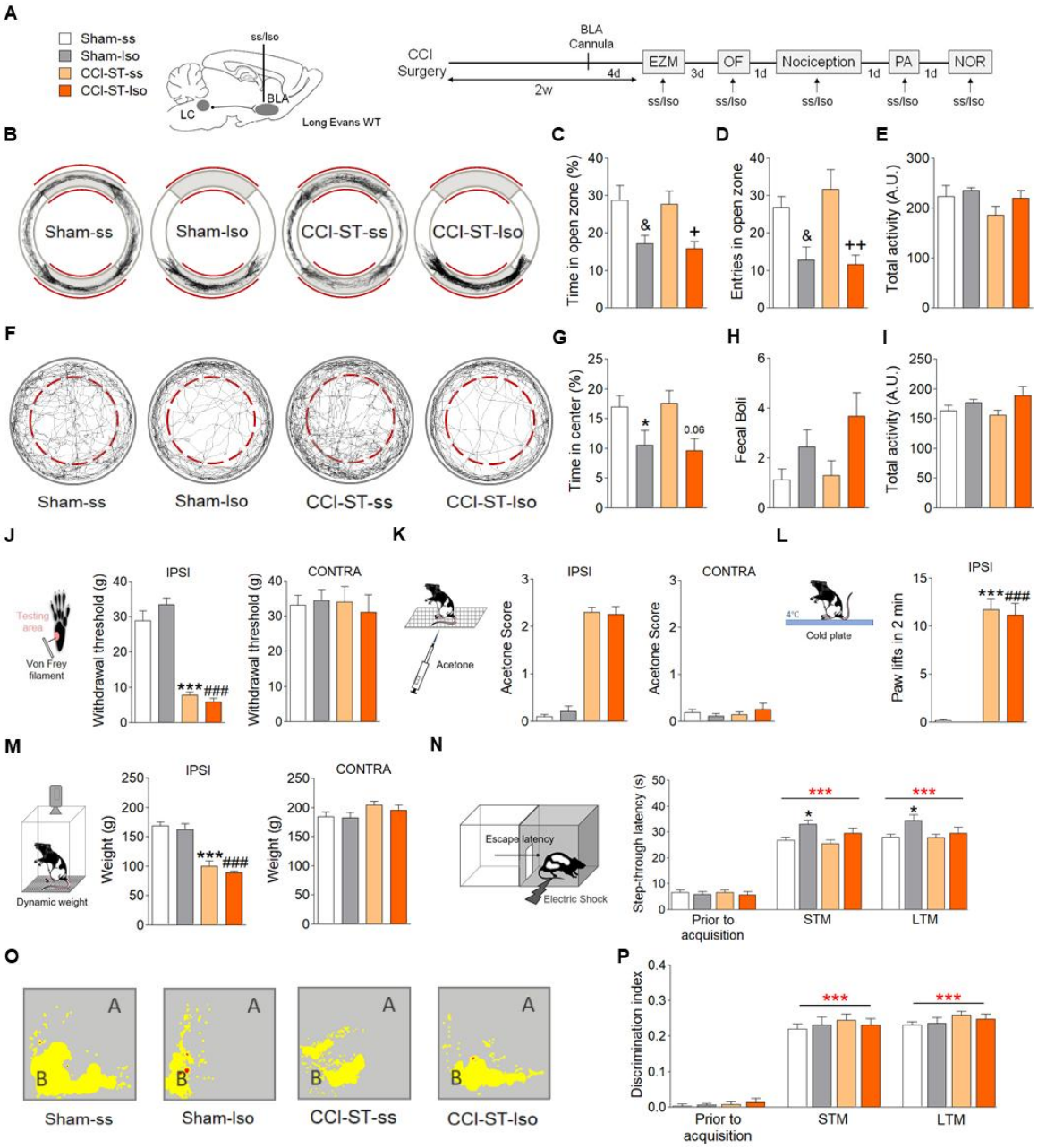

Figure S15. Pharmacological activation of beta-adrenoceptors (b-AR) in BLA.

A) Experimental timeline and schematic representation of cannula delivery for the behavioral experiments in male Long-Evans wild-type rats. Isoproterenol (30µg /0.5 ul) was administered twenty minutes before behavioral testing. The rats were tested 2-3 weeks (short-term: ST) after surgery. (**B-E**) The effects of activating the beta-adrenoceptors (b-AR) in the elevated zero maze. (**B**) The representative activity traces and the graphs represent (**C**) the relative time spent in the open zone and (**D**) number of entries into that zone, as well as (**E**) the locomotor activity (A.U.: arbitrary units). (**F-I**) The effects of activating b-AR in the open field test. (**F**) The representative activity traces and the graphs represent (**G**) the relative time spent in the central zone, (**H**) the number of fecal boluses and (**I**) the locomotor activity (A.U.). (**J-M**) Sensorial evaluation. The graphs represent (**J**) the withdrawal threshold (g) of the ipsilateral and contralateral hind paws in response to von Frey hair stimulation (0 to 50 g, 20 sec), (**K**) the response of the ipsilateral and contralateral hind paws to acetone application (100 ul), (**L**) the number of lifts of the ipsilateral hind paw in the cold plate test (2 min, 4°C), and (**M**) the weight

distributed on the ipsilateral and contralateral hind paws in the dynamic weight bearing test (5 min). (**N**) The effects of activating b-AR on passive avoidance. The graph represents the latency to enter the dark compartment (s) in the different phases of the paradigm: training (prior to acquisition), short-term memory test (STM as learning index) and long-term memory test (LTM as memory index). (**O**-**P**) The effects of activating b-AR in the novel object recognition test. (**O**) The representative heatmaps showing activity (Yellow=low and Red=high activity) around the objects in the memory test session (A=familiar and B=novel object) and the graph represent (**P**) the discrimination index between objects in the different phases of the paradigm: training, STM and LTM. The data represent the mean + SEM (n=6-8 per group): *p<0.05, ***p<0.001 versus sham-ss; &p<0.05 versus sham-ss; +p<0.05, ++p<0.01 versus CCI-ST-ss; ###p<0.001 versus sham-Iso as assessed by two-way ANOVA followed by Newman-Keuls post hoc. ***p<0.001 versus prior to acquisition of each group as assessed by two-way ANOVA with repeated measures followed by Newman-Keuls post hoc. CCI, chronic constriction injury; d, days; w, weeks; Iso, isoproterenol; ss, saline.

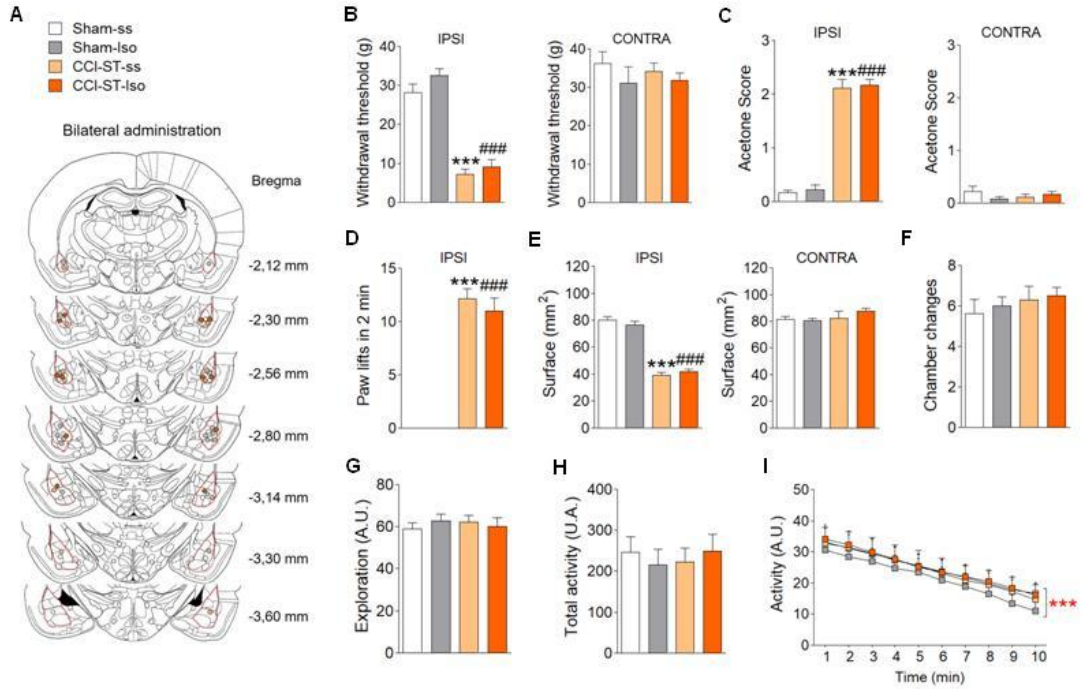

Figure S16. **Supplemental information of Figure S15.**

(**A-C**) Sensorial evaluation before the systemic inhibition of beta-adrenoceptors (b-AR). The graphs represent **(A)** withdrawal threshold (g) of the ipsilateral and contralateral hind paws to von Frey hair stimulation (0 to 50 g, 20 sec), **(B)** the response of ipsilateral and contralateral hind paws to acetone applied (100 ul), and **(C)** the number of lifts of the ipsilateral hind paw in the cold plate test (2 min, 4ºC). **(D)** The surface of ipsilateral and contralateral hind paws supported in the dynamic weight bearing test (5 min) after inhibition of the b-AR. **(E)** The effects of systemic inhibiting the b-AR on passive avoidance, the graph represents the number of chamber changes during the habituation session. **(F-H)** The effects of systemic inhibiting the b-AR on novel object recognition, the graphs represent **(F)** exploration (A.U.) in the training phase and **(G)** locomotor activity (A.U.) and **(H)** activity per minute (A.U.) in the habituation of the paradigm. The data are represented as the mean + SEM (n=6-8 per group): ***p<0.001 versus sham-ss; ###p<0.001 versus sham-CNO as assessed by two-way ANOVA followed by Newman-Keuls post hoc test. *** p<0.001 versus min 1 as assessed by two-way ANOVA with repeated measures followed by Newman-Keuls post hoc test. CCI, chronic constriction injury; Iso, isoproterenol; ss, saline.

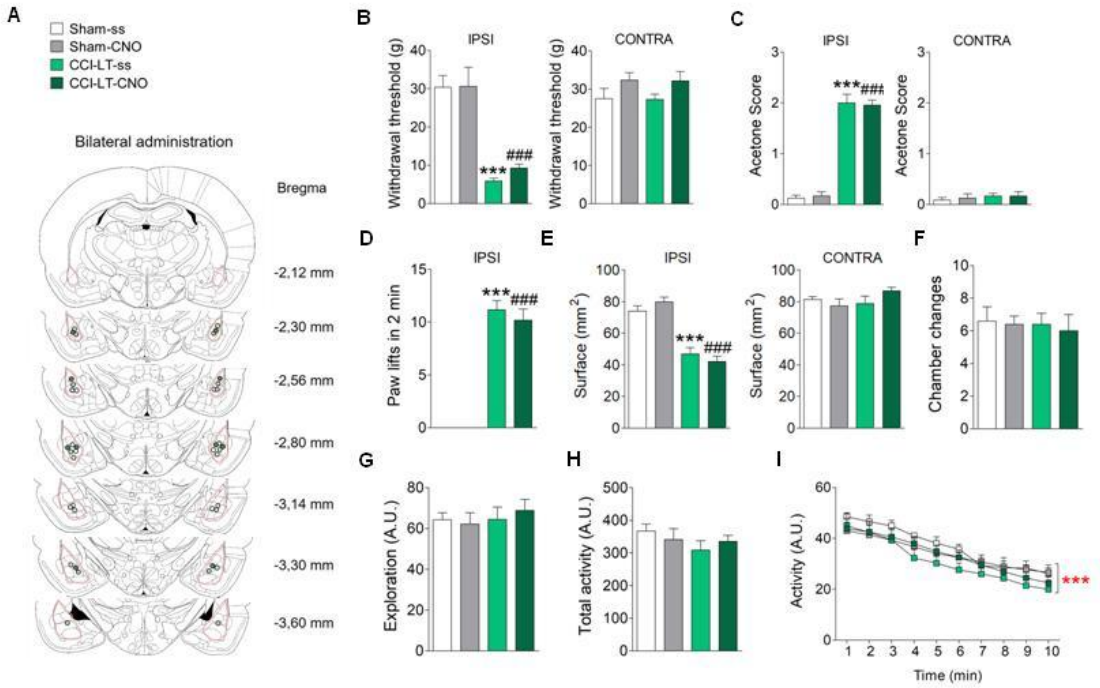

Figure S17. Supplemental information of Fig.6.

(A) Schematic diagrams adapted from the atlas of Paxinos and Watson (Paxinos and Watson, 2007) showing the locations of the microinjection sites in the BLA. Each color represents a different treatment and each dot corresponds to an infusion focus in a 30 µm section. (**B-D**) Sensorial evaluation before activation of the LC-BLA pathway. The graphs represent **(B)** the withdrawal threshold (g) of the ipsilateral and contralateral hind paws to von Frey hair stimulation (0 to 50 g, 20 sec), **(C)** the response of the ipsilateral hind paw to acetone application (100 ul), **(D)** the number of lifts of the ipsilateral and contralateral hind paws in the cold plate test (2 min, 4ºC). **(E)** The surface of ipsilateral and contralateral hind paws supported in the dynamic weight bearing test (5 min) after activation of the LC-BLA pathway. **(F)** The effects of activating the LC-BLA pathway on the passive avoidance test, the graph representing the number of chamber changes during the habituation session. **(G-I)** The effects of activating the LC-BLA pathway on novel object recognition, the graphs representing **(G)** the exploration (A.U.) in the training phase and **(H)** the locomotor activity (A.U.) and **(I)** activity per minute (A.U.) in the habituation of the paradigm. The data are represented as the mean + SEM (n=5-6 per group): ***p<0.001 versus sham-ss; ###p<0.001 versus sham-CNO as assessed by two-way ANOVA followed by Newman-Keuls post hoc test; ***p<0.001 versus min 1 as assessed by two-way ANOVA with repeated measures followed by Newman-Keuls post hoc test. CCI, chronic constriction injury; LC, locus coeruleus; BLA, basolateral amygdala; CNO, clozapine-N-oxide; ss, saline.

Table S1. Summary of statistical analysis of Fig.1 and S1.

	Two-way ANOVA without repeated measures			
	Surgery	*Time*	*Interaction*	
- Elevated zero maze test				
% time in open zone	**$F_{1,24}$ = 5.6***	$F_{1,24}$= 0.8	**$F_{1,24}$= 5.0***	
Entry number in open zone	**$F_{1,24}$ = 11.2****	$F_{1,24}$= 2.3	**$F_{1,24}$= 9.6****	
Total activity (A.U.)	$F_{1,24}$ = 0.0	$F_{1,24}$= 1.3	$F_{1,24}$= 0.1	
- Open field test				
% time in center	**$F_{1,24}$ = 7.9****	$F_{1,24}$= 0.8	**$F_{1,24}$= 6.7***	
Fecal boli number	**$F_{1,24}$ = 5.5***	$F_{1,24}$= 3.3	$F_{1,24}$= 3.3	
Total activity (A.U.)	$F_{1,24}$ = 0.0	$F_{1,24}$= 1.3	$F_{1,24}$ = 0.3	
- Von Frey test (g)				
ipsilateral hind paw	**$F_{1,24}$ = 158.1*****	$F_{1,24}$= 0.2	$F_{1,24}$= 0.2	
contralateral hind paw	$F_{1,24}$ = 0.5	$F_{1,24}$= 0.6	$F_{1,24}$= 0.1	
- Passive avoidance				
Chamber changes number	$F_{1,24}$ = 0.3	$F_{1,24}$= 1.2	$F_{1,24}$= 0.1	
Training latency	$F_{1,24}$ = 0.7	$F_{1,24}$= 0.8	$F_{1,24}$= 0.1	
STM latency	**$F_{1,24}$ = 10.9****	**$F_{1,24}$= 9.1****	**$F_{1,24}$ = 10.0****	
LTM latency	**$F_{1,24}$ = 12.3****	**$F_{1,24}$= 10.3****	**$F_{1,24}$= 11.4****	
- Novel object recognition test				
Exploration	$F_{1,24}$ = 0.0	$F_{1,24}$= 1.3	$F_{1,24}$ = 0.3	
Activity (A.U.)	$F_{1,24}$ = 0.1	$F_{1,24}$= 0.8	$F_{1,24}$= 0.0	
Training Discrimination Index	$F_{1,24}$ = 0.5	$F_{1,24}$= 0.4	$F_{1,24}$= 0.0	
STM Discrimination Index	**$F_{1,24}$ = 7.4****	**$F_{1,24}$= 5.3***	**$F_{1,24}$ = 7.0****	
LTM Discrimination Index	**$F_{1,24}$ = 5.4***	**$F_{1,24}$= 5.0***	**$F_{1,24}$ = 5.2***	
- Object pattern separation				
Exploration	$F_{1,24}$ = 0.1	$F_{1,24}$= 1.0	$F_{1,24}$ = 0.2	
Activity (A.U.)	$F_{1,24}$ = 0.3	$F_{1,24}$= 1.3	$F_{1,24}$ = 0.1	
Training Discrimination Index	$F_{1,24}$ = 0.0	$F_{1,24}$= 1.0	$F_{1,24}$ = 0.3	
Test Discrimination Index	**$F_{1,24}$ = 10.5****	**$F_{1,24}$= 9.3****	**$F_{1,24}$ = 10.2****	
- Fear conditioning				
Habituation ContextA	$F_{1,24}$ = 0.4	$F_{1,24}$= 0.7	$F_{1,24}$ = 0.0	
After Tone ContextA	$F_{1,24}$ = 3.1	$F_{1,24}$= 0.1	$F_{1,24}$ = 0.0	
Habituation ContextB	**$F_{1,24}$ = 26.6*****	**$F_{1,24}$= 12.6****	**$F_{1,24}$ = 18.7*****	
After Tone ContextB	$F_{1,24}$ = 0.9	$F_{1,24}$= 1.1	$F_{1,24}$ = 1.3	
	One-way ANOVA with repeated measures			
	Surgery		*Time*	*Interaction*
- Weight (g)	$F_{1,12}$ = 3.4		**$F_{3.36}$= 643.4*****	$F_{3.36}$= 1.8
	Two-way ANOVA with repeated measures			
	Surgery	*Time 1*	*Interaction*	*Time 2*	*Interaction*
- Passive avoidance (Latency)	**$F_{1,24}$ = 15.3*****	**$F_{1,24}$= 10.7****	**$F_{1,24}$= 12.5****	**$F_{2,48}$= 65.8*****	**$F_{2,48}$= 7.6****
- Novel object recognition test					
Activity (A.U.)	$F_{1,24}$ = 0.0	$F_{1,24}$= 0.1	$F_{1,24}$= 0.0	**$F_{9,216}$= 180.9*****	$F_{9,216}$= 0.6
Discrimination Index	**$F_{1,24}$ = 15.4*****	**$F_{1,24}$= 8.1****	**$F_{1,24}$= 11.4****	**$F_{2,48}$= 80.6*****	$F_{2,48}$= 0.4
- Object pattern separation					
Discrimination Index	**$F_{1,24}$ = 13.2*****	**$F_{1,24}$= 9.2****	**$F_{1,24}$= 10.1****	**$F_{2,48}$= 101.4*****	$F_{2,48}$= 0.4
- Fear conditioning					

Freezing (Conditioning)	**$F_{1,24}$ = 17.7*****	**$F_{1,24}$= 33.4*****	**$F_{1,24}$= 12.2*****	**$F_{2,48}$= 484.7*****	**$F_{2,48}$= 3.0***
Freezing (ContextA)	$F_{1,24}$ = 1.4	$F_{1,24}$= 0.5	$F_{1,24}$= 1.0	**$F_{2,48}$= 4523.7*****	$F_{2,48}$= 0.0
Freezing (ContextB)	**$F_{1,24}$ = 28.7*****	**$F_{1,24}$= 16.1*****	**$F_{1,24}$= 23.0*****	**$F_{2,48}$= 1895.0*****	$F_{2,48}$= 3.8

Non-repeated two-way ANOVA compares data from all groups (Sham-ST, Sham-LT, CCI-ST and CCI-LT) in the different behavioural test; Repeated measures two-way ANOVA compares data from all groups between different trials in cognition evaluation (passive avoidance, novel object recognition, object pattern separation and fear conditioning tests) and the activity over time in the habituation session in novel object recognition test. The F values were expressed with their associated degrees of freedom. Time 1, time of neuropathy; Time 2, different trials; A.U., arbitrary unit; STM, short-term memory; LTM, long-term memory. *p<0.05, **p<0.01 and ***p<0.001.

Table S2. Summary of statistical analysis of Fig.2, S5 and S6.

	Two-way ANOVA without repeated measures		
	Surgery	*Treatment*	*Interaction*
- Elevated zero maze test			
% time in open zone	**$F_{1,28}$ = 20.6*****	**$F_{1,28}$= 27.9*****	**$F_{1,28}$= 17.1*****
Entry number in open zone	**$F_{1,28}$ = 15,4*****	**$F_{1,28}$= 9,1*****	**$F_{1,28}$= 8,0*****
Total activity (A.U.)	$F_{1,28}$ = 0.6	$F_{1,28}$= 0,0	$F_{1,28}$= 1.4
- Open field test			
% time in center	**$F_{1,28}$ = 9.3****	**$F_{1,28}$= 7.9****	**$F_{1,28}$= 14.9*****
Fecal boli number	**$F_{1,28}$ = 7.6****	**$F_{1,28}$= 16.3*****	**$F_{1,28}$= 13.0*****
Total activity (A.U.)	$F_{1,28}$ = 0.0	$F_{1,28}$= 0,1	$F_{1,28}$= 0.4
- Von Frey test (g)			
ipsilateral hind paw (before inhibition)	**$F_{1,28}$ = 210.9*****	$F_{1,28}$= 3.4	$F_{1,28}$= 0.9
ipsilateral hind paw (after inhibition)	**$F_{1,28}$ =90.8*****	$F_{1,28}$= 0.5	$F_{1,28}$= 0.0
contralateral hind paw (before inhibition)	$F_{1,28}$ = 1.1	$F_{1,28}$= 0.4	$F_{1,28}$= 0.3
contralateral hind paw (after inhibition)	$F_{1,28}$ = 0.2	$F_{1,28}$= 0.3	$F_{1,28}$= 0.3
- Acetone test (score)			
ipsilateral hind paw (before inhibition)	**$F_{1,28}$ = 250.9*****	$F_{1,28}$= 0.0	$F_{1,28}$= 0.6
ipsilateral hind paw (after inhibition)	**$F_{1,28}$ = 436.7*****	$F_{1,28}$= 0.5	$F_{1,28}$= 1.0
contralateral hind paw (before inhibition)	$F_{1,28}$ = 2.0	$F_{1,28}$= 0.7	$F_{1,28}$= 0.1
contralateral hind paw (after inhibition)	$F_{1,28}$ = 0.5	$F_{1,28}$= 0.1	$F_{1,28}$= 1.4
- Cold plate test (paw lifts in 2min)			
ipsilateral hind paw (before inhibition)	**$F_{1,28}$ = 273.7*****	$F_{1,28}$= 1.2	$F_{1,28}$= 1.6
ipsilateral hind paw (after inhibition)	**$F_{1,28}$ = 222.7*****	$F_{1,28}$= 0.5	$F_{1,28}$= 0.5
- Dynamic weight bearing test			
ipsilateral hind paw (g)	**$F_{1,28}$ = 33.8*****	$F_{1,28}$= 0.3	$F_{1,28}$= 1.0
ipsilateral hind paw (surface)	**$F_{1,28}$ = 104.9*****	$F_{1,28}$= 1.0	$F_{1,28}$= 0.5
contralateral hind paw (g)	$F_{1,28}$ = 1.5	$F_{1,28}$= 0.1	$F_{1,28}$= 0.1
contralateral hind paw (surface)	$F_{1,28}$ = 3.6	$F_{1,28}$= 2.1	$F_{1,28}$= 0.2
- Passive avoidance			
Chamber changes number	$F_{1,28}$ = 0.3	$F_{1,28}$= 0.3	$F_{1,28}$= 0.0
Training latency	$F_{1,28}$ = 0.1	$F_{1,28}$= 0.7	$F_{1,28}$= 0.0
STM latency	**$F_{1,28}$ = 15.6*****	**$F_{1,28}$= 9.9****	**$F_{1,28}$= 12.6****
LTM latency	**$F_{1,28}$ = 25.9*****	**$F_{1,28}$= 27.9*****	**$F_{1,28}$= 30.2*****
- Novel object recognition test			
Exploration	$F_{1,28}$ = 0.3	$F_{1,28}$= 0.1	$F_{1,28}$= 0.3
Activity (A.U.)	$F_{1,28}$ = 0.1	$F_{1,28}$= 0.1	$F_{1,28}$= 0.2
Training Discrimination Index	$F_{1,28}$ = 0.2	$F_{1,28}$= 0.6	$F_{1,28}$= 0.2
STM Discrimination Index	**$F_{1,28}$ = 11.3****	$F_{1,28}$= 0.0	$F_{1,28}$= 0.2

LTM Discrimination Index	**$F_{1,28}$ = 12.9****	$F_{1,28}$= 0.2	$F_{1,28}$= 0.1		
	Two-way ANOVA with repeated measures				
	Surgery	*Treatment*	*Interaction*	*Time*	*Interaction*
- Passive avoidance (Latency)	**$F_{1,28}$ = 17.7*****	**$F_{1,28}$= 13.6*****	**$F_{1,28}$= 17.9*****	**$F_{2,56}$= 1047.2*****	**$F_{2,56}$= 13.3*****
- Novel object recognition test					
Activity (A.U.)	$F_{1,28}$ = 0.0	$F_{1,28}$= 0.1	$F_{1,28}$= 0.2	**$F_{9,252}$= 150.7*****	$F_{9,252}$= 1.2
Discrimination Index	**$F_{1,28}$ = 18.5*****	$F_{1,28}$= 0.2	$F_{1,28}$= 0.1	**$F_{2,56}$= 64.1*****	$F_{2,56}$= 0.2
	Unpaired Student's t-test				
	tdf				
- Elevated zero maze test (Fig.S6)					
% time in open zone					
in-BLA	**t_{14}=6.978*** **				
out-BLA	t_{10}=2.208				
Entry number in open zone					
in-BLA	**t_{14}=7.230*** **				
out-BLA	t_{10}=0.196				

Non-repeated two-way ANOVA compares data from all groups (Sham-ss, Sham-CNO, CCI-LT-ss and CCI-LT-CNO) in the different behavioural test; Repeated measures two-way ANOVA compares data from all groups between different trials in cognition evaluation (passive avoidance and novel object recognition tests) and the activity over time in the habituation session in novel object recognition test. The F values were expressed with their associated degrees of freedom. Unpaired Student's t-test compares data from CCI-LT-ss and CCI-LT-CNO in the different behavioural tests. A.U., arbitrary unit; STM, short-term memory; LTM, long-term memory. **p<0.01 and ***p<0.001.

Table S3. Summary of statistical analysis of Fig.S8 and S9.

	Unpaired Student's t-test	**One-way ANOVA with repeated measures**		
	tdf	*Treatment*	*Time*	*Interaction*
- Elevated zero maze test				
% time in open zone	t_{16} = 1.26			
Entry number in open zone	t_{16} = 1.25			
Total activity (A.U.)	t_{16} = 1.01			
- Open field test				
% time in center	t_{15} = 0.44			
Fecal boli number	t_{15} = 0.21			
Total activity (A.U.)	t_{15} = 1.14			
- Von Frey test (g)				
ipsilateral hind paw (before inhibition)	t_{15} = 0.05			
ipsilateral hind paw (after inhibition)	t_{15} = 0.08			
contralateral hind paw (before inhibition)	t_{15} = 0.85			
contralateral hind paw (after inhibition)	t_{15} = 0.61			
- Acetone test (score)				
ipsilateral hind paw (before inhibition)	t_{15} = 0.62			
ipsilateral hind paw (after inhibition)	t_{15} = 1.04			
contralateral hind paw (before inhibition)	t_{15} = 0.50			
contralateral hind paw (after inhibition)	t_{15} = 1.52			
- Cold plate test (paw lifts in 2min)				
ipsilateral hind paw (before inhibition)	t_{15} = 0.44			
ipsilateral hind paw (after inhibition)	t_{15} = 0.31			
- Dynamic weight bearing test				
ipsilateral hind paw (g)	t_{15} = 0.87			

ipsilateral hind paw (surface)	$t_{15} = 0.09$			
contralateral hind paw (g)	$t_{15} = 0.83$			
contralateral hind paw (surface)	$t_{15} = 0.09$			
- Passive avoidance				
Chamber changes number	$t_{15} = 0.05$			
Training latency	$t_{15} = 0.29$	$F_{1,15} = 0.22$	**$F_{2,30} = 566.61$*** **	$F_{2,30} = 0.16$
STM latency	$t_{15} = 0.37$			
LTM latency	$t_{15} = 0.50$			
- Novel object recognition test				
Exploration	$t_{15} = 0.14$			
Activity (A.U.)	$t_{15} = 0.41$	$F_{1,15} = 0.16$	**$F_{9,135} = 84.06$*** **	$F_{9,135} = 0.57$
Training Discrimination Index	$t_{15} = 0.87$	$F_{1,15} = 0.50$	**$F_{2,30} = 127.82$*** **	$F_{2,30} = 0.11$
STM Discrimination Index	$t_{15} = 0.67$			
LTM Discrimination Index	$t_{15} = 0.27$			

Unpaired Student's t-test compares data from CCI-LT-ss and CCI-LT-CNO in the different behavioural tests; Repeated measures one-way ANOVA compares data from all groups between different trials in cognition evaluation (passive avoidance and novel object recognition tests) and the activity over time in the habituation session in novel object recognition test. The F values were expressed with their associated degrees of freedom. CCI, chronic constriction injury; ss, saline; CNO, clozapine-N-oxide; A.U., arbitrary unit; STM, short-term memory; LTM, long-term memory. ***p<0.001.

Table S4. Summary of statistical analysis of Fig.3 and S10.

	Two-way ANOVA without repeated measures		
	Surgery	*Treatment*	*Interaction*
- Elevated zero maze test			
% time in open zone	**$F_{1,32} = 11.8$****	**$F_{1,32} = 5.7$***	**$F_{1,32} = 13.0$****
Entry number in open zone	**$F_{1,32} = 10.6$****	**$F_{1,32} = 9.2$****	$F_{1,32} = 2.7$
Total activity (A.U.)	$F_{1,32} = 0.0$	$F_{1,32} = 0.3$	$F_{1,32} = 0.0$
- Open field test			
% time in center	**$F_{1,31} = 9.0$****	**$F_{1,31} = 9.7$****	**$F_{1,31} = 8.3$****
Fecal boli number	**$F_{1,31} = 5.0$***	**$F_{1,31} = 8.2$****	**$F_{1,31} = 5.4$***
Total activity (A.U.)	$F_{1,31} = 0.0$	$F_{1,31} = 0.0$	$F_{1,31} = 0.0$
- Von Frey test (g)			
ipsilateral hind paw (before inhibition)	**$F_{1,31} = 154.3$*****	$F_{1,31} = 1.6$	$F_{1,31} = 0.8$
ipsilateral hind paw (after inhibition)	**$F_{1,31} = 96.0$*****	$F_{1,31} = 0.9$	$F_{1,31} = 2.0$
contralateral hind paw (before inhibition)	$F_{1,31} = 0.1$	$F_{1,31} = 1.1$	$F_{1,31} = 1.7$
contralateral hind paw (after inhibition)	$F_{1,31} = 0.0$	$F_{1,31} = 0.0$	$F_{1,31} = 0.0$
- Acetone test (score)			
ipsilateral hind paw (before inhibition)	**$F_{1,31} = 811.0$*****	$F_{1,31} = 0.9$	$F_{1,31} = 0.3$
ipsilateral hind paw (after inhibition)	**$F_{1,31} = 832.5$*****	$F_{1,31} = 0.9$	$F_{1,31} = 1.7$
contralateral hind paw (before inhibition)	$F_{1,31} = 0.1$	$F_{1,31} = 0.7$	$F_{1,31} = 0.3$
contralateral hind paw (after inhibition)	$F_{1,31} = 2.5$	$F_{1,31} = 0.2$	$F_{1,31} = 0.1$
- Cold plate test (paw lifts in 2min)			
ipsilateral hind paw (before inhibition)	**$F_{1,31} = 122.9$*****	$F_{1,31} = 0.3$	$F_{1,31} = 0.3$
ipsilateral hind paw (after inhibition)	**$F_{1,31} = 380.3$*****	$F_{1,31} = 1.2$	$F_{1,31} = 1.2$
- Dynamic weight bearing test			
ipsilateral hind paw (g)	**$F_{1,31} = 147.8$*****	$F_{1,31} = 0.2$	$F_{1,31} = 0.1$
ipsilateral hind paw (surface)	**$F_{1,31} = 93.0$*****	$F_{1,31} = 0.1$	$F_{1,31} = 0.4$
contralateral hind paw (g)	$F_{1,31} = 2.7$	$F_{1,31} = 0.1$	$F_{1,31} = 0.0$

contralateral hind paw (surface)	$F_{1,31}$ = 1.9	$F_{1,31}$= 0.4	$F_{1,31}$= 0.3
- Passive avoidance			
Chamber changes number	$F_{1,31}$ = 0.1	$F_{1,31}$= 0.0	$F_{1,31}$ = 1.1
Training latency	$F_{1,31}$ = 0.5	$F_{1,31}$= 0.1	$F_{1,31}$ = 0.1
STM latency	**$F_{1,31}$ = 33.7*****	**$F_{1,31}$= 10.8****	**$F_{1,31}$ = 8.9****
LTM latency	**$F_{1,31}$ = 37.1****	**$F_{1,31}$= 23.0*****	**F_{131}= 29.3*****
- Novel object recognition test			
Exploration	$F_{1,31}$ = 0.2	$F_{1,31}$= 0.0	$F_{1,31}$= 0.0
Activity (A.U.)	$F_{1,31}$ = 0.0	$F_{1,31}$= 0.1	$F_{1,31}$= 1.4
Training Discrimination Index	$F_{1,31}$ = 0.0	$F_{1,31}$= 0.2	$F_{1,31}$= 0.1
STM Discrimination Index	**$F_{1,31}$ = 55.5*****	$F_{1,31}$= 0.9	$F_{1,31}$= 0.3
LTM Discrimination Index	**$F_{1,31}$ = 75.5*****	$F_{1,31}$= 0.0	$F_{1,31}$= 1.1

	Two-way ANOVA with repeated measures				
	Surgery	*Treatment*	*Interaction*	*Time*	*Interaction*
- Passive avoidance (Latency)	**$F_{1,31}$ = 55.3*****	**$F_{1,31}$= 27.4*****	**$F_{1,31}$= 28.5*****	**$F_{2,62}$= 580.3*****	**$F_{2,62}$= 6.6****
- Novel object recognition test					
Activity (A.U.)	$F_{1,31}$ = 0.0	$F_{1,31}$= 0.1	$F_{1,31}$= 1.3	**$F_{9,279}$= 123.8*****	$F_{9,279}$= 0.2
Discrimination Index	**$F_{1,31}$ = 113.5*****	$F_{1,31}$= 0.3	$F_{1,31}$= 1.3	**$F_{2,62}$= 207.2*****	$F_{2,62}$= 0.2

Non-repeated two-way ANOVA compares data from all groups (Sham-ss, Sham-Prop, CCI-LT-ss and CCI-LT-Prop) in the different behavioural test; Repeated measures two-way ANOVA compares data from all groups between different trials in cognition evaluation (passive avoidance and novel object recognition tests) and the activity over time in the habituation session in novel object recognition test. The F values were expressed with their associated degrees of freedom. A.U., arbitrary unit; STM, short-term memory; LTM, long-term memory. *p<0.05, **p<0.01 and ***p<0.001.

Table S5. Summary of statistical analysis of Fig.4 and S11.

	Two-way ANOVA without repeated measures		
	Surgery	*Treatment*	*Interaction*
- Elevated zero maze test			
% time in open zone	**$F_{1,27}$ = 4.7***	**$F_{1,27}$= 9.9****	**$F_{1,27}$= 12.2****
Entry number in open zone	**$F_{1,27}$ = 7.6***	$F_{1,27}$= 2.0	$F_{1,27}$= 2.8
Total activity (A.U.)	$F_{1,27}$ = 0.2	$F_{1,27}$= 0.4	$F_{1,27}$= 0.3
- Open field test			
% time in center	**$F_{1,27}$ = 18.5*****	**$F_{1,27}$= 7.1***	**$F_{1,27}$= 4.9***
Fecal boli number	**$F_{1,27}$ = 10.8****	**$F_{1,27}$= 7.3***	**$F_{1,27}$= 5.8***
Total activity (A.U.)	$F_{1,27}$ = 0.6	**$F_{1,27}$= 4.5***	$F_{1,27}$= 0.3
- Von Frey test (g)			
ipsilateral hind paw (before inhibition)	**$F_{1,27}$ = 189.8*****	$F_{1,27}$= 0.9	$F_{1,27}$= 0.3
ipsilateral hind paw (after inhibition)	**$F_{1,27}$ =234.2*****	$F_{1,27}$= 0.3	$F_{1,27}$= 0.8
contralateral hind paw (before inhibition)	$F_{1,27}$ = 3.3	$F_{1,27}$= 0.1	$F_{1,27}$= 3.1
contralateral hind paw (after inhibition)	$F_{1,27}$ = 0.6	$F_{1,27}$= 1.8	$F_{1,27}$= 0.0
- Acetone test (score)			
ipsilateral hind paw (before inhibition)	**$F_{1,27}$ = 371.2*****	$F_{1,27}$= 0.0	$F_{1,27}$= 0.9
ipsilateral hind paw (after inhibition)	**$F_{1,27}$ = 742.4*****	$F_{1,27}$= 0.3	$F_{1,27}$= 1.5
contralateral hind paw (before inhibition)	$F_{1,27}$ = 0.4	$F_{1,27}$= 0.4	$F_{1,27}$= 1.0
contralateral hind paw (after inhibition)	$F_{1,27}$ = 2.1	$F_{1,27}$= 0.1	$F_{1,27}$= 1.2
- Cold plate test (paw lifts in 2min)			
ipsilateral hind paw (before inhibition)	**$F_{1,27}$ = 179.9*****	$F_{1,27}$= 0.9	$F_{1,27}$= 0.7
ipsilateral hind paw (after inhibition)	**$F_{1,27}$ = 166.4*****	$F_{1,27}$= 0.2	$F_{1,27}$= 0.2

- Dynamic weight bearing test			
ipsilateral hind paw (g)	**$F_{1,27}$ = 146.8*****	$F_{1,27}$= 3.3	$F_{1,27}$= 0.2
ipsilateral hind paw (surface)	**$F_{1,27}$ = 443.6*****	$F_{1,27}$= 3.7	$F_{1,27}$= 0.2
contralateral hind paw (g)	**$F_{1,27}$ = 13.8*****	$F_{1,27}$= 1.9	$F_{1,27}$= 0.2
contralateral hind paw (surface)	$F_{1,27}$ = 3.8	$F_{1,27}$= 0.2	$F_{1,27}$= 0.9
- Passive avoidance			
Chamber changes number	$F_{1,27}$ = 0.0	$F_{1,27}$= 0.2	$F_{1,27}$ = 0.4
Training latency	$F_{1,27}$ = 0.8	$F_{1,27}$= 0.0	$F_{1,27}$ = 0.8
STM latency	**$F_{1,27}$ = 11.1****	**$F_{1,27}$= 8.3****	**$F_{1,27}$ = 10.4****
LTM latency	**$F_{1,27}$ = 9.8****	**$F_{1,27}$= 6.8***	**$F_{1,27}$= 10.9****
- Novel object recognition test			
Exploration	$F_{1,27}$ = 0.1	$F_{1,2}$= 0.0	$F_{1,27}$= 0.2
Activity (A.U.)	$F_{1,27}$ = 0.0	$F_{1,27}$= 0.1	$F_{1,27}$= 0.1
Training Discrimination Index	$F_{1,27}$ = 0.1	$F_{1,27}$= 0.0	$F_{1,27}$= 0.0
STM Discrimination Index	**$F_{1,27}$ = 37.4*****	$F_{1,27}$= 0.1	$F_{1,27}$= 1.5
LTM Discrimination Index	**$F_{1,27}$ = 40.3*****	$F_{1,27}$= 0.5	$F_{1,27}$= 0.3

	Two-way ANOVA with repeated measures				
	Surgery	*Treatment*	*Interaction*	*Time*	*Interaction*
- Passive avoidance (Latency)	**$F_{1,27}$ = 8.7****	**$F_{1,27}$= 7.3***	**$F_{1,27}$= 8.9****	**$F_{2,54}$= 537.5*****	**$F_{2,54}$= 10.7*****
- Novel object recognition test					
Activity (A.U.)	$F_{1,27}$ = 0.2	$F_{1,27}$= 0.1	$F_{1,27}$= 0.1	**$F_{9,243}$= 124.3*****	$F_{9,243}$= 0.5
Discrimination Index	**$F_{1,27}$ = 61.03*****	$F_{1,27}$= 0.1	$F_{1,27}$= 1.1	**$F_{2,54}$= 150.9*****	$F_{2,54}$= 0.6

Non-repeated two-way ANOVA compares data from all groups (Sham-ss, Sham-Prop, CCI-LT-ss and CCI-LT-Prop) in the different behavioural test; Repeated measures two-way ANOVA compares data from all groups between different trials in cognition evaluation (passive avoidance and novel object recognition tests) and the activity over time in the habituation session in novel object recognition test. The F values were expressed with their associated degrees of freedom. A.U., arbitrary unit; STM, short-term memory; LTM, long-term memory. *p<0.05, **p<0.01 and ***p<0.001.

Table S6. Summary of statistical analysis of Fig.5 and S13.

	Two-way ANOVA without repeated measures		
	Surgery	*Treatment*	*Interaction*
- Elevated zero maze test			
% time in open zone	$F_{1,20}$ = 3.6	**$F_{1,20}$=5.4***	$F_{1,20}$= 2.1
Entry number in open zone	$F_{1,20}$=0.0	**$F_{1,20}$= 19.4*****	$F_{1,20}$= 0.0
Total activity (A.U.)	$F_{1,20}$ = 1.2	$F_{1,20}$= 0.2	$F_{1,20}$= 0.6
- Open field test			
% time in center	$F_{1,20}$ = 3.5	**$F_{1,20}$= 4.9***	$F_{1,20}$= 3.0
Fecal boli number	$F_{1,20}$= 1.8	**$F_{1,20}$= 5.5***	$F_{1,20}$= 2.8
Total activity (A.U.)	$F_{1,20}$ = 0.0	$F_{1,20}$= 0.0	$F_{1,20}$= 2.0
- Von Frey test (g)			
ipsilateral hind paw (before inhibition)	**$F_{1,20}$ = 166.4*****	$F_{1,20}$= 0.0	$F_{1,20}$= 0.3
ipsilateral hind paw (after inhibition)	**$F_{1,20}$ = 166.5*****	$F_{1,20}$= 0.0	$F_{1,20}$= 0.8
contralateral hind paw (before inhibition)	$F_{1,20}$ = 2.0	$F_{1,20}$= 1.0	$F_{1,20}$= 0.2
contralateral hind paw (after inhibition)	$F_{1,20}$ = 10.0	$F_{1,20}$= 2.6	$F_{1,20}$= 0.4
- Acetone test (score)			
ipsilateral hind paw (before inhibition)	**$F_{1,20}$ = 302.4*****	$F_{1,20}$= 0.3	$F_{1,20}$= 0.9
ipsilateral hind paw (after inhibition)	**$F_{1,20}$ = 142.7*****	$F_{1,20}$= 0.1	$F_{1,20}$= 1.3
contralateral hind paw (before inhibition)	$F_{1,20}$ = 0.6	$F_{1,20}$= 0.2	$F_{1,20}$= 0.2

contralateral hind paw (after inhibition)	$F_{1,20} = 0.0$	$F_{1,20} = 1.5$	$F_{1,20} = 0.0$
- Cold plate test (paw lifts in 2min)			
ipsilateral hind paw (before inhibition)	$\mathbf{F_{1,20} = 270.5^{***}}$	$F_{1,20} = 0.1$	$F_{1,20} = 0.1$
ipsilateral hind paw (after inhibition)	$\mathbf{F_{1,20} = 80.3^{***}}$	$F_{1,20} = 1.2$	$F_{1,20} = 2.1$
- Dynamic weight bearing test			
ipsilateral hind paw (g)	$\mathbf{F_{1,20} = 65.8^{***}}$	$F_{1,20} = 3.9$	$F_{1,20} = 0.3$
ipsilateral hind paw (surface)	$\mathbf{F_{1,20} = 194.5^{***}}$	$F_{1,20} = 2.0$	$F_{1,20} = 0.6$
contralateral hind paw (g)	$F_{1,20} = 1.7$	$F_{1,20} = 3.5$	$F_{1,20} = 0.7$
contralateral hind paw (surface)	$F_{1,20} = 0.0$	$F_{1,20} = 1.0$	$F_{1,20} = 0.0$
- Passive avoidance			
Chamber changes number	$F_{1,16} = 0.0$	$F_{1,16} = 0.2$	$F_{1,16} = 0.0$
Training latency	$F_{1,16} = 0.1$	$F_{1,16} = 0.0$	$F_{1,16} = 0.3$
STM latency	$F_{1,16} = 1.2$	$\mathbf{F_{1,16} = 10.0^{**}}$	$F_{1,16} = 0.3$
LTM latency	$F_{1,16} = 0.5$	$\mathbf{F_{1,16} = 17.0^{***}}$	$F_{1,16} = 0.8$
- Novel object recognition test			
Exploration	$F_{1,16} = 0.1$	$F_{1,16} = 0.0$	$F_{1,16} = 0.2$
Activity (A.U.)	$F_{1,16} = 0.0$	$F_{1,16} = 0.1$	$F_{1,16} = 0.1$
Training Discrimination Index	$F_{1,16} = 0.1$	$F_{1,16} = 0.0$	$F_{1,16} = 0.2$
STM Discrimination Index	$F_{1,16} = 0.3$	$F_{1,16} = 0.1$	$F_{1,16} = 0.1$
LTM Discrimination Index	$F_{1,16} = 0.2$	$F_{1,16} = 0.1$	$F_{1,16} = 0.1$

	Two-way ANOVA with repeated measures				
	Surgery	*Treatment*	*Interaction*	*Time*	*Interaction*
- Passive avoidance (Latency)	$F_{1,16} = 1.4$	$\mathbf{F_{1,16} = 22.2^{***}}$	$F_{1,16} = 0.7$	$\mathbf{F_{2,32} = 69.9^{***}}$	$F_{2,32} = 0.5$
- Novel object recognition test					
Activity (A.U.)	$F_{1,16} = 0.2$	$F_{1,16} = 0.1$	$F_{1,16} = 0.1$	$\mathbf{F_{9,144} = 168.4^{***}}$	$F_{9,144} = 0.5$
Discrimination Index	$F_{1,16} = 1.5$	$F_{1,16} = 0.1$	$F_{1,16} = 1.1$	$\mathbf{F_{2,32} = 350.8^{***}}$	$F_{2,32} = 0.6$

Non-repeated two-way ANOVA compares data from all groups (Sham-ss, Sham-CNO, CCI-ST-ss and CCI-ST-CNO) in the different behavioural test; Repeated measures two-way ANOVA compares data from all groups between different trials in cognition evaluation (passive avoidance and novel object recognition tests) and the activity over time in the habituation session in novel object recognition test. The F values were expressed with their associated degrees of freedom. A.U., arbitrary unit; STM, short-term memory; LTM, long-term memory. **p<0.01 and ***p<0.001.

Table S7. Summary of statistical analysis of Fig.S14.

	Unpaired Student's t-test	**One-way ANOVA with repeated measures**		
	tdf	***Treatment***	***Time***	***Interaction***
- Elevated zero maze test				
% time in open zone	$t_{14} = 3.26$			
Entry number in open zone	$t_{14} = 3.61$			
Total activity (A.U.)	$t_{14} = 1.20$			
- Passive avoidance				
Chamber changes number	$t_{14} = 1.10$			
Training latency	$t_{14} = 0.54$	$\mathbf{F_{1,14} = 6.70^{***}}$	$\mathbf{F_{2,28} = 360.47^{***}}$	$\mathbf{F_{2,28} = 7.63^{**}}$
STM latency	$\mathbf{t_{14} = 2.62^{*}}$			
LTM latency	$\mathbf{t_{14} = 2.86^{*}}$			

Unpaired Student's t-test compares data from Naïve-CNO+ss and Naïve-CNO+Prop in the different behavioural tests; Repeated measures one-way ANOVA compares data from all groups between different trials in passive avoidance test. The F values were expressed with their associated degrees of freedom. A.U., arbitrary unit; STM, short-term memory; LTM, long-term memory. *p<0.05, **p<0.01, ***p<0.001.

Table S8. Summary of statistical analysis of Fig.S15 and S16.

	Two-way ANOVA without repeated measures				
	Surgery	*Treatment*	*Interaction*		
- Elevated zero maze test					
% time in open zone	$F_{1,28} = 0.1$	**$F_{1,28} = 15.1^{***}$**	$F_{1,28} = 0.0$		
Entry number in open zone	$F_{1,28} = 0.2$	**$F_{1,28} = 21.0^{***}$**	$F_{1,28} = 0.7$		
Total activity (A.U.)	$F_{1,28} = 2.5$	$F_{1,28} = 2.1$	$F_{1,28} = 0.5$		
- Open field test					
% time in center	$F_{1,24} = 0.0$	**$F_{1,24} = 11.0^{**}$**	$F_{1,24} = 0.1$		
Fecal boli number	**$F_{1,24} = 4.5^{*}$**	$F_{1,24} = 1.4$	$F_{1,24} = 0.3$		
Total activity (A.U.)	$F_{1,24} = 0.0$	**$F_{1,24} = 5.9^{*}$**	$F_{1,24} = 0.9$		
- Von Frey test (g)					
ipsilateral hind paw (before inhibition)	**$F_{1,24} = 145.6^{***}$**	$F_{1,24} = 2.8$	$F_{1,24} = 0.4$		
ipsilateral hind paw (after inhibition)	**$F_{1,24} = 157.1^{***}$**	$F_{1,24} = 0.4$	$F_{1,24} = 2.7$		
contralateral hind paw (before inhibition)	$F_{1,24} = 0.1$	$F_{1,24} = 1.5$	$F_{1,24} = 0.2$		
contralateral hind paw (after inhibition)	$F_{1,24} = 0.1$	$F_{1,24} = 0.0$	$F_{1,24} = 0.3$		
- Acetone test (score)					
ipsilateral hind paw (before inhibition)	**$F_{1,24} = 318.8^{***}$**	$F_{1,24} = 0.3$	$F_{1,24} = 0.0$		
ipsilateral hind paw (after inhibition)	**$F_{1,24} = 360.1^{***}$**	$F_{1,24} = 0.1$	$F_{1,24} = 0.4$		
contralateral hind paw (before inhibition)	$F_{1,24} = 0.0$	$F_{1,24} = 0.4$	$F_{1,24} = 2.0$		
contralateral hind paw (after inhibition)	$F_{1,24} = 0.4$	$F_{1,24} = 0.0$	$F_{1,24} = 1.6$		
- Cold plate test (paw lifts in 2min)					
ipsilateral hind paw (before inhibition)	**$F_{1,24} = 268.7^{***}$**	$F_{1,24} = 0.7$	$F_{1,24} = 0.7$		
ipsilateral hind paw (after inhibition)	**$F_{1,24} = 212.8^{***}$**	$F_{1,24} = 0.2$	$F_{1,24} = 0.1$		
- Dynamic weight bearing test					
ipsilateral hind paw (g)	**$F_{1,24} = 86.5^{***}$**	$F_{1,24} = 1.3$	$F_{1,24} = 0.1$		
ipsilateral hind paw (surface)	**$F_{1,24} = 266.8^{***}$**	$F_{1,24} = 0.1$	$F_{1,24} = 1.7$		
contralateral hind paw (g)	$F_{1,24} = 4.2$	$F_{1,24} = 0.5$	$F_{1,24} = 0.3$		
contralateral hind paw (surface)	$F_{1,24} = 1.5$	$F_{1,24} = 0.4$	$F_{1,24} = 1.0$		
- Passive avoidance					
Chamber changes number	$F_{1,24} = 0.9$	$F_{1,24} = 0.2$	$F_{1,24} = 0.0$		
Training latency	$F_{1,24} = 0.0$	$F_{1,24} = 0.6$	$F_{1,24} = 0.0$		
STM latency	$F_{1,24} = 2.2$	**$F_{1,24} = 10.3^{**}$**	$F_{1,24} = 0.5$		
LTM latency	$F_{1,24} = 2.1$	**$F_{1,24} = 5.4^{*}$**	$F_{1,24} = 1.8$		
- Novel object recognition test					
Exploration	$F_{1,24} = 0.0$	$F_{1,24} = 0.1$	$F_{1,24} = 0.8$		
Activity (A.U.)	$F_{1,24} = 0.0$	$F_{1,24} = 0.0$	$F_{1,24} = 0.6$		
Training Discrimination Index	$F_{1,24} = 0.7$	$F_{1,24} = 0.4$	$F_{1,24} = 0.0$		
STM Discrimination Index	$F_{1,24} = 0.5$	$F_{1,27} = 0.0$	$F_{1,24} = 0.5$		
LTM Discrimination Index	$F_{1,24} = 2.7$	$F_{1,24} = 0.1$	$F_{1,24} = 0.4$		
	Two-way ANOVA with repeated measures				
	Surgery	*Treatment*	*Interaction*	*Time*	*Interaction*
- Passive avoidance (Latency)	$F_{1,24} = 2.3$	**$F_{1,24} = 6.4^{*}$**	$F_{1,24} = 1.1$	**$F_{2,48} = 468.8^{***}$**	$F_{2,48} = 0.9$
- Novel object recognition test					
Activity (A.U.)	$F_{1,24} = 0.1$	$F_{1,24} = 0.1$	$F_{1,24} = 0.2$	**$F_{9,216} = 177.9^{***}$**	$F_{9,216} = 0.7$
Discrimination Index	$F_{1,24} = 1.7$	$F_{1,24} = 0.0$	$F_{1,24} = 1.4$	**$F_{2,48} = 586.6^{***}$**	$F_{2,48} = 0.4$

Non-repeated two-way ANOVA compares data from all groups (Sham-ss, Sham-Iso, CCI-ST-ss and CCI-ST-Iso) in the different behavioural test;

Repeated measures two-way ANOVA compares data from all groups between different trials in cognition evaluation (passive avoidance and novel object recognition tests) and the activity over time in the habituation session in novel object recognition test. The F values were expressed with their associated degrees of freedom. A.U., arbitrary unit; STM, short-term memory; LTM, long-term memory. *p<0.05, **p<0.01 and ***p<0.001.

Table S9. Summary of statistical analysis of Fig.6 and S17.

	Two-way ANOVA without repeated measures				
	Surgery	*Treatment*	*Interaction*		
- Elevated zero maze test					
% time in open zone	**$F_{1,20}$ = 5.3***	**$F_{1,20}$=5.2***	**$F_{1,20}$= 8.2****		
Entry number in open zone	**$F_{1,20}$=6.7***	**$F_{1,20}$= 5.1***	**$F_{1,20}$= 5.9***		
Total activity (A.U.)	$F_{1,20}$ = 0.1	$F_{1,20}$= 0.2	$F_{1,20}$= 0.3		
- Open field test					
% time in center	**$F_{1,20}$ = 8.2****	**$F_{1,20}$= 9.5***	**$F_{1,20}$= 7.9****		
Fecal boli number	**$F_{1,20}$= 16.2*****	**$F_{1,20}$= 13.5****	$F_{1,20}$= 0.2		
Total activity (A.U.)	$F_{1,20}$ = 0.0	$F_{1,20}$= 0.1	$F_{1,20}$= 0.0		
- Von Frey test (g)					
ipsilateral hind paw (before inhibition)	**$F_{1,20}$ = 58.9*****	$F_{1,20}$= 0.4	$F_{1,20}$= 0.3		
ipsilateral hind paw (after inhibition)	**$F_{1,20}$ = 109.2*****	$F_{1,20}$= 0.2	$F_{1,20}$= 0.6		
contralateral hind paw (before inhibition)	$F_{1,20}$ = 0.0	$F_{1,20}$= 0.4	$F_{1,20}$= 0.0		
contralateral hind paw (after inhibition)	$F_{1,20}$ = 0.2	$F_{1,20}$= 0..5	$F_{1,20}$= 0.1		
- Acetone test (score)					
ipsilateral hind paw (before inhibition)	**$F_{1,20}$ = 272.7*****	$F_{1,20}$= 0.0	$F_{1,20}$= 0.1		
ipsilateral hind paw (after inhibition)	**$F_{1,20}$ = 299.7*****	$F_{1,20}$= 0.7	$F_{1,20}$= 0.0		
contralateral hind paw (before inhibition)	$F_{1,20}$ = 0.8	$F_{1,20}$= 0.1	$F_{1,20}$= 0.1		
contralateral hind paw (after inhibition)	$F_{1,20}$ = 1.9	$F_{1,20}$= 0.5	$F_{1,20}$= 0.5		
- Cold plate test (paw lifts in 2min)					
ipsilateral hind paw (before inhibition)	**$F_{1,20}$ = 236.7*****	$F_{1,20}$= 0.5	$F_{1,20}$= 0.5		
ipsilateral hind paw (after inhibition)	**$F_{1,20}$ = 70.82*****	$F_{1,20}$= 0.3	$F_{1,20}$= 0.3		
- Dynamic weight bearing test					
ipsilateral hind paw (g)	**$F_{1,20}$ = 45.5*****	$F_{1,20}$= 1.2	$F_{1,20}$= 3.0		
ipsilateral hind paw (surface)	**$F_{1,20}$ = 93.2*****	$F_{1,20}$= 0.0	$F_{1,20}$= 2.6		
contralateral hind paw (g)	$F_{1,20}$ = 3.6	$F_{1,20}$= 0.0	$F_{1,20}$= 0.9		
contralateral hind paw (surface)	$F_{1,20}$ = 1.0	$F_{1,20}$= 0.3	$F_{1,20}$= 2.8		
- Passive avoidance					
Chamber changes number	$F_{1,16}$ = 0.2	$F_{1,16}$= 0.2	$F_{1,16}$ = 0.0		
Training latency	$F_{1,16}$= 0.1	$F_{1,16}$= 0.3	$F_{1,16}$ = 0.0		
STM latency	**$F_{1,16}$ = 13.4****	**$F_{1,16}$= 9.2****	**$F_{1,16}$ = 11.3****		
LTM latency	**$F_{1,16}$ =13.6****	**$F_{1,16}$= 10.0****	**$F_{1,16}$= 9.3****		
- Novel object recognition test					
Exploration	$F_{1,16}$ = 0.1	$F_{1,16}$= 0.1	$F_{1,16}$= 0.2		
Activity (A.U.)	$F_{1,16}$ = 0.0	$F_{1,16}$= 0.1	$F_{1,16}$= 0.1		
Training Discrimination Index	$F_{1,16}$ = 0.2	$F_{1,16}$= 0.3	$F_{1,16}$= 0.2		
STM Discrimination Index	**$F_{1,16}$ = 10.1****	$F_{1,16}$= 0.0	$F_{1,16}$= 0.1		
LTM Discrimination Index	**$F_{1,16}$ = 11.6****	$F_{1,16}$= 0.1	$F_{1,16}$= 0.1		
	Two-way ANOVA with repeated measures				
	Surgery	*Treatment*	*Interaction*	*Time*	*Interaction*
- Passive avoidance (Latency)	**$F_{1,16}$ = 12.6****	**$F_{1,16}$= 12.2****	**$F_{1,16}$=10.7****	**$F_{2,32}$= 60.8*****	**$F_{2,32}$= 10.5****

- Novel object recognition test					
Activity (A.U.)	$F_{1,16}$ = 0.0	$F_{1,16}$= 0.1	$F_{1,16}$= 0.1	**$F_{9,144}$= 128.1*****	$F_{9,144}$= 1.0
Discrimination Index	**$F_{1,16}$ = 13.5****	$F_{1,16}$= 0.2	$F_{1,16}$= 0.1	**$F_{2,32}$= 80.9*****	$F_{2,32}$= 0.2

Non-repeated two-way ANOVA compares data from all groups (Sham-ss, Sham-CNO, CCI-LT-ss and CCI-LT-CNO) in the different behavioural test; Repeated measures two-way ANOVA compares data from all groups between different trials in cognition evaluation (passive avoidance and novel object recognition tests) and the activity over time in the habituation session in novel object recognition test. The F values were expressed with their associated degrees of freedom. A.U., arbitrary unit; STM, short-term memory; LTM, long-term memory. *p<0.05, **p<0.01 and ***p<0.001.

Table S10. Summary of statistical analysis of Fig. S3, S4, and S12.

	Unpaired Student's t-test	**Two-way ANOVA**		
	tdf	*Surgery*	*Treatment*	*Interaction*
Fluorogold administration (Fig. S3)				
Unilateral (LC contra vs ipsi)	**t_{10}=5.845*** **			
Bilateral (LC contra vs ipsi)	t_{10}=0.1548			
Number of c-fos+ neurons				
hM4D(Gi) (Fig. S4)		**$F_{1,8}$= 27.28*** **	**$F_{1,8}$= 12,78*** **	**$F_{1,8}$= 17,93*** **
rM3D(Gs) (Fig. S11)				
Bilateral administration:				
sham vs CCI-LT	**t_4=2.867***			
sham vs CCI-LT-CNO	**t_4=3.827***			
CCI-LT vs CCI-LT-CNO	t_4=0.2820			
Unilateral administration:				
sham vs sham-CNO	**t_4=2.854***			

The F values were expressed with their associated degrees of freedom. LC, locus coeruleus; CCI, chronic constriction injury; LT, long-term; CNO, clozapine-N-oxide. *p<0.05, ***p<0.001.